



2nd Latin-American Symposium on Physical  
and Chemical Methods in Archaeology, Art and  
Cultural Heritage Conservation

Symposium on Archaeological and  
Arts Issues in Materials Science

IMRC 2009



*Selected Papers*

José Luis Ruvalcaba Sil | Javier Reyes Trujeque | Jesús Arenas Alatorre | Adrián Velázquez Castro



Sociedad  
Mexicana de  
Materiales A.C.





**2<sup>nd</sup> Latin-American Symposium on Physical  
and Chemical Methods in Archaeology, Art and  
Cultural Heritage Conservation**

**Symposium on Archaeological and Arts Issues in  
Materials Science  
IMRC 2009**



**Selected Papers**

José Luis Ruvalcaba Sil  
Javier Reyes Trujeque  
Jesús Arenas Alatorre  
Adrián Velázquez Castro

Editors

2010



INAH



UNAM



UAC

**2nd Latin-American Symposium on Physical and Chemical Methods in  
Archaeology, Art and Cultural Heritage Conservation. Selected Papers  
Archaeological and Arts Issues in Materials Science**

First Edition: 2010

Editors:

José Luis Ruvalcaba Sil / Javier Reyes Trujeque / Jesús A. Arenas Alatorre / Adrián Velázquez Castro

© 2010. Edition:

Universidad Nacional Autónoma de México, UNAM  
Instituto de Física  
Circuito de la Investigación Científica s/n  
Ciudad Universitaria  
Mexico DF C.P. 04510  
MEXICO

Universidad Autónoma de Campeche, UAC  
Centro de Investigación en Corrosión  
Avenida agustín Melgar s/n entre Juan de la Barrera y Calle 20  
Col. Buenavista  
San Francisco de Campeche C.P. 24039  
MEXICO

Instituto Nacional de Antropología e Historia, INAH.  
Museo del Templo Mayor  
Seminario No. 8  
Centro Histórico  
Mexico DF C.P. 06060  
MEXICO

Portada: Dulce María Aguilar Téllez

ISBN: 978-607-02-2017-3

Made and Printed in MEXICO  
December 17, 2010

This publication has been supported by the project:

Fortalecimiento para la consolidación del Cuerpo Académico de Ciencia e  
Ingeniería de Corrosión de la Universidad Autónoma de Campeche.  
Code: CAMP-2007-C01-71800.

and partially by the grants CONACyT Mexico MOVIL U49839-R  
and PAPIIT UNAM IN403210 ANDREAH

## LASMAC 2009 & IMRC09

The 2nd Latin-American Symposium on Physical and Chemical Methods in Archaeology, Art and Cultural Heritage Conservation (LASMAC 2009) and the Archaeological and Arts Issues were carried out jointly during the Materials Science Symposium as part of the International Material Research Congress 2009 in Cancun, Quintana Roo, Mexico from August 16 to 21, 2009. The objective of this meeting was to present and to discuss the most recent and new Latin-American researches for the study of the cultural heritage and the historical past using the most diverse techniques and scientific methodologies, including non destructive methods, nuclear techniques and ion beam accelerators, optical and electronic microscopy, imaging techniques, experimental archaeology, archaeo-magnetism and paleo-magnetism, all kind of chemical methods, dating, deterioration studies and conservation procedures. This forum was open to conservators, physicists, chemists, engineers, archaeologists, art historians and other specialists involved with the scientific study and conservation of the cultural heritage and archaeological and historical collections. This meeting opened a space for the collaborations between different groups and specialists, as well for network and collaboration in the American continent and with European facilities.

The LASMAC 2009 meeting, organized by the first time in Sao Paulo, Brazil in 2007 (LASMAC 2007), was this time integrated to one of the most Mexican outstanding meetings for materials characterization related to archaeology, history, arts and conservation, the Archaeological and Arts Issues in Materials Science Symposium that has been organized since more than ten years ago as part of the International Materials Research Congress. Besides the Latin-American area, the joint meeting was opened to the participation of colleagues from Spain and Portugal in order to provide an Ibero-American frame, as well as to the main research groups in other countries of Europe and the USA working on this field. In the scientific program we had a total of 81 works, 36 of them from Mexico, 27 from South-American countries (Brazil, Argentina, Cuba, Chile, Colombia and Peru), 6 papers from USA, 11 presentations from European countries, mainly Spain and 1 work from Japan. We consider that the meeting was very successful.

The main topics of the meeting considered:

- Methodologies for the characterization of materials for archaeology, history and cultural heritage using physical and chemical techniques.
- Studies on ancient technologies and manufacturing of objects and materials.
- Provenance and sourcing of manufactured and raw materials.
- Dating techniques and their applications.
- Deterioration and conservation of materials and collections.
- Pollution effects on cultural heritage.

The symposium included several invited lectures as well as oral presentations selected by the committee of the symposium. Two sessions of posters were organized and the most relevant works

selected by a jury were awarded: “*Non destructive Study of Teotihuacan Vases with Post-firing Decoration*” by J.L. Ruvalcaba Sil, L. Filloy, et al, “*The manufacturing techniques of the Turquoise Mosaics from the Great Temple of Tenochtitlan*” by E. Melgar & R. Solís, “*Rock Art at Jaguariava Archaeological Site (Parana, Brazil): In Situ Pigments Study by Portable Energy Dispersive X-ray Fluorescence (PXRF)*” by C.R. Appoloni et al., and “*Non destructive Analysis of Handwriting and Colored Drawings of the Printed Book Divina Proportione (1509)*” by V. Aguilar Melo et al..

In this volume, and after a revision process, a set of 36 papers of some of the most outstanding works discussed during the meeting on the main topics is presented. This publication is the results of the efforts of the organizing committee and the Mexican institutions involved in the successful organization of this symposium, as well to the support of different research projects.

Most of the papers are related to methodologies of characterization of cultural heritage materials: Pigments, paintings and stones materials are the most studied, followed by metals, glass and photography. Few work on pottery and manuscripts and were presented. The geographical regions and chronologies cover from mural paintings in Brazil to Colonial and European pigments and paintings. Studies on stone are related to prehistoric raw materials to pre-Hispanic Mesoamerican pieces, but materials from Colonial buildings were also addressed. Metals were represented by technological studies on Volga region and Maya artifacts, while the studied glass was mainly from South America. A comparative work on blue pigments of Chinese porcelain and Portuguese faiences as well as a non-destructive study on *ex-libris*, annotations and drawings of a XVI century book are outstanding examples of the nowadays methods and techniques for cultural heritage studies. Photographic materials were well represented with papers on new methodologies and alternatives for their study.

Manufacturing of pre-Hispanic objects is described in detail on shells and bones pieces by the solid group of research on experimental archaeology of the Templo Mayor Museum of Mexico, leader in this field. Several examples of these technological investigations are presented.

On the other hand, provenance and dating, two of the most archaeometric topics are not missing. Works on Obsidians, Plumbate pottery and slates objects from various Mesoamerican regions are presented including fine methods and alternatives for sourcing. Both papers on dating are related to buidings trought materials characterization.

Finally, in the subject devoted to deterioration and conservation a very complete work on bone characterization for these purposes was presented, but definitely this topic was dominated by the studies of buildings and monuments, showing that the cultural heritage of the historic cities is a main concern for the research groups in Latin-America.

This publication is an example of the collaboration of humanities and sciences research teams for the study and conservation the cultural heritage.

Dr. José Luis Ruvalcaba Sil  
Instituto de Física, UNAM  
México, December, 2010

## Organizing Committee of LASMAC 2009 & IMRC09

- José Luis Ruvalcaba Sil, Instituto de Física, UNAM. *Chairman*
- Jesús Arenas Alatorre, Instituto de Física, UNAM. *Secretary*
- Javier Reyes Trujeque, Universidad Autónoma de Campeche. *Co-chairman*
- Adrián Velázquez Castro, Museo del Templo Mayor, INAH. *Co-chairman*
- Ana Maria Soler Arechalde., Instituto de Geofísica, UNAM.
- Sandra Zetina Ocaña, Instituto de Investigaciones Estéticas, UNAM.
- Manuel Espinosa Pesqueira, Instituto Nacional de Investigaciones Nucleares. ININ.
- Carolusa González Tirado, Escuela Nacional de Conservación, Restauración y Museografía, ENCRyM-INAH.



### Participants of the LASMAC 2009 & IMRC09

**First line from left to right:** Pamela Vandiver, Lourdes Couoh, Ondina Figueiredo, Marian de Egido, José Luis Ruvalcaba, Valentina Aguilar, Verónica Urbina, Naoli Victoria, Elva Castillo, Sandra Zetina, Gabriela Siracusano, Sachiko Sakai, Kaoru Yonekura.

**Second line left to right:** Jessica Curado, María Eugenia Peltzer, Ana María Soler, María Inés Casadas, Thomas Cramer, Roberto Appoloni, Andrea Cavicchioli, Paulo Pascolatti, Emiliano Melgar, Reyna Solís, Javier Reyes.

**Third line left to right:** Marcia Rizzuto, Thomas Calligaro, Manuel Espinosa, Cecilia Valdés, Angel Bustamante, Carlos Lariot, F. Torres, Hector Neff.

## PUBLICATION INDEX

### Methodologies for the Characterization of Materials for Archaeology, History and Cultural Heritage using Physical and Chemical Techniques.

#### *Pigments and Paintings*

1. **Rock Art at Jaguaríaiva 1 Archaeological Site (Paraná, Brazil): In Situ Pigments Study by Portable Energy Dispersive X-Ray Fluorescence (PXRF).** C.R. Appoloni, F.L. Melquiades, F. Lopes, C. I. Parellada, M.H.L.B Morales and G.E.V. de Biasi. 1
2. **Verdigris, a Pigment with Different Hues. Relation between Chemical Composition and Colour.** M. San Andrés, J. M. de la Roja, N. Sancho and V. G. Baonza. 4
3. **Chemical Changes in Pictorial Models: Characterization by FT-IR Spectroscopy.** V. Urbina, T. Pradell, N. Salvadó, S. Buti and J.L. Ruvalcaba. 10
4. **The Mobility of Imitation: An Analysis of 18th Century Chinese Style Furniture with IR-UV Imaging, Portable XRF and SEM.** S. Zetina, E. Arroyo, T. Falcón, E. Hernández, J.L. Ruvalcaba, M.E. Espinosa, V. Aguilar Melo, D. Ramírez, V. Santos and F. Riquelme. 15
5. **The Sky of Salamanca. An Example of Experimental Methodology Applied to a Singular Work of Art.** M.A. García, M. Gómez, D. Juanes and C. Vega. 23
6. **Material Investigation in the Course of the Restoration of a Series of Colonial Paintings.** F. Eisner-Sagüés and C. Ossa-Izquierdo. 29
7. **Images Analysis Coupled With PIXE Technique For Picture Characterization.** E. Kajiya, M. A. Rizzutto, V. Pagliaro, S.I. Finazzo and P. R. Pascholati. 35

#### *Minerals and Stone Materials*

8. **Infrared Reflection Spectrometry Analysis as a Non-destructive Method of Characterizing Minerals and Stone Materials in Geoarchaeological and Archaeometric Applications.** M. Ostrooumov. 40
9. **Preliminary Analysis on Microindentation Hardness of Prehistoric Lithic Raw Materials.** K.Yonekura. 45
10. **Non-Destructive Characterization of Green Stone Pieces from La Joya Site, Veracruz, Mexico.** J. L. Ruvalcaba Sil, A. Daneels, M. Vaggi and M. Aguilar Franco. 49
11. **Chemical Characterization of Mortar from San Roque Church (San Francisco de Campeche, México).** J. Reyes, Y. Espinosa-Morales, P. Maldonado, G. Ancona, P. Bartolo-Pérez and J.A. Azamar-Barrios. 56

#### *Metals*

12. **Warrior's Belt from the Middle Volga Burial Ground X A.D. - Technology and Origin.** I. Saprykina, O. Zelentsova, R. Mitoyan. 62
13. **Microstructural Study of Gilded Copper Artifacts from the Chichén-Itzá Cenote.** J. Arenas Alatorre, J. Contreras and J. L. Ruvalcaba Sil. 67

## **Glass**

14. ***Study of Fragments of Archaeological Glass Objects by Portable Energy Dispersive X-Ray Fluorescence (PXRF).***  
C. R. Appoloni, F. L. Melquiades and F. Lopes. 72
15. ***Implementation of Techniques for the Study of Vitreous and Metallic Materials from the Archaeological Site “Guardia del Monte”, San Miguel del Monte, Buenos Aires Province.***  
L.P. Traversa, M.I. Casadas, M.E. Peltzer and F.H.Lloro. 76

## **Pottery**

16. ***Blue Pigments in XVI-XVII Century Glazes: A Comparative Study between Portuguese Faiences and Chinese Porcelains.***  
M.O. Figueiredo, T.P. Silva, J.P. Veiga, M.I. Prudêncio, M.I. Dias, M.A. Matos and A.M. Pais. 81

## **Manuscripts**

17. ***Non-destructive Analysis of Handwriting and Colored Drawings of the Printed Book Divina Proportione (1509).***  
V. Aguilar Melo, J.L. Ruvalcaba Sil, O. Escamilla Gonzalez, L. Milan, D. Ramírez Miranda and Ma.C. León García. 86

## **Photography**

18. ***The Application of Portable X-Ray Fluorescence Spectrometer in Historical Photography: a Proposal of Experimental Configuration.***  
M. del Egido, D. Juanes. 93
19. ***The Daguerreotype under High Magnification: An Ultra-High Resolution SEM Study of a 19th Century Daguerreotype’s Surface Nanostructure.***  
M. Patrick Ravines, A. West, J. Minter(c) and R.O. Gutierrez Jr. 99

## **Studies on Ancient Technologies and Manufacturing of Objects and Materials.**

20. ***Nerita Shell Objects in the Offerings of the Great Temple of Tenochtitlan.***  
A. Velázquez-Castro, B. Zúñiga-Arellano and Á . González-López 105
21. ***Manufacture of Spondylus princeps Objects in Calica, Quintana Roo.***  
E. A. Castillo Velasco and S. A. Páez Torres. 110
22. ***Manufacturing Techniques of the Pinctada mazatlanica Objects in Tula, Hidalgo, México.*** R. B. Solís Ciriaco and O. Sterpone Canuto. 115
23. ***Manufacturing Techniques of the Turquoise Mosaics from the Great Temple of Tenochtitlan, Mexico.*** E. R. Melgar Tísoc and R. B. Solís Ciriaco 119
24. ***Analysis of Modified Osseous Remains from Monte Alban, Oaxaca, Mexico.***  
N. Valentín Maldonado and G. Pérez Roldán. 125
25. ***Objects Made of Copal, A Glance through the Time.***  
N. Victoria Lona 131

## **Provenance and Sourcing of Manufactured and Raw Materials.**

26. ***ICP-MS Analysis for the Characterization of Obsidian Sub-Sources In Sierra de Pachuca Region, Hidalgo, Mexico***  
D. Argote Espino, J. Solé Viñas, O. Sterpone Canuto and P. López García. 135
27. ***Plumbate Technology Revisited.***  
H. Neff. 140
28. ***Characterization of Slates from Teotihuacan using XRD, PIXE and IOL.***  
J. López Juárez, J.L. Ruvalcaba-Sil and M. Aguilar Franco. 146

## **Dating Techniques and their Applications.**

29. ***Dating Techniques through the Characterization of Materials. XVI Century South Sardinian Coast Defense Towers.*** C. Giannattasio and S.M. Grillo. 152
30. ***Dating Tests, Mineralogical Analysis and Technological Characterization on Building Materials from Archaeological Excavations in Urban Historical Sites.***  
L.P. Traversa, M.I. Casadas, M.E. Peltzer, F. Iloro and A.M. Cesio 159

## **Deterioration and Conservation of Materials and Monuments.**

31. ***Diagnosis of State of Preservation and Quantification of Trace Elements in Ancient Bones from La Laguna, Tlaxcala, Mexico.***  
L. R. Couoh, J. L. Ruvalcaba, L. Bucio and J. Arenas. 165
32. ***Basalt Chemical Weathering at Puebla Historical Buildings.***  
M. Teutli, E. León, J. Cerna and A. C. Ruíz. 172
33. ***Biodeterioration of Mineral Materials in Cultural Heritage, Archaeology and Historical Collections.*** L.E. Rendon, X. Li, M.E. Lara, M. Rendon and S. K. Rendon. 176
34. ***Analysis of Black Crust from a Cuban Historic Building.***  
J. Reyes, F. Corvo, Y. Espinosa-Morales, C. Valdés, P. Bartolo, D. Aguilar, P. Quintana, B. Hermosín and C. Saiz-Jimenez. 181
35. ***Laboratory and In Situ Evaluation of Polysiloxane Hidrofuge Product for Protection of Stone at San Francisco de Asis and Basilica Minor in the Old Havana, Cuba.***  
C. Valdés Clemente, F. Corvo Pérez and C. Lariot Sánchez. 188
36. ***Dissolution of Traditional Mortars under Artificial Rain Conditions: A Laboratory Test.***  
J. Reyes, F. Torres, I. Ché, F. Corvo, T. Pérez, H. Bravo, P. Sánchez, D. Aguilar and P. Quintana. 195

## **Rock Art at Jaguaríaiva 1 Archaeological Site (Paraná, Brazil): *In Situ* Pigments Study by Portable Energy Dispersive X-Ray Fluorescence (PXRF)**

C.R. Appoloni<sup>1</sup>, F.L. Melquiades<sup>2</sup>, F. Lopes<sup>1</sup>, C.I. Parellada<sup>3</sup>,  
M.H.L.B. Morales<sup>3</sup> and G.E.V. de Biasi<sup>2</sup>

<sup>1</sup>*Departamento de Física, Universidade Estadual de Londrina, Caixa Postal 6001, CEP 86051-990, Londrina PR, BRAZIL. e-mail: appoloni@uel.br, bonn@uel.br*

<sup>2</sup>*Departamento de Física, Universidade Estadual Centro Oeste, Caixa Postal 3010, CEP 85015-430, Guarapuava, PR, BRAZIL.*

<sup>3</sup>*Museu Paranaense, Departamento de Arqueologia, Rua Kellers, 289, CEP 80410-100, Curitiba, BRAZIL.*

**Abstract.** Jaguaríaiva 1 rockshelter is located in the Jaguaríaiva city region, Paraná State, Brazil (17x 21x5.20 m size, E 632 454 e N 7 315 244 UTM coordinates and 887 m high). It is a sandstone shelter with paintings from, at least, two different periods. The oldest one is around 7.000 years BP. Measurements were performed *in situ* and non-destructively employing a portable EDXRF system with an X-ray tube (Ag filter and target), a Si-PIN photodiode detector, standard X-ray spectrometry electronic chain and a special designed mechanical system for the detector and X-ray tube positioning, that enables angular and XYZ movements of the excitation-detection system respect to the measurement area. X-Ray Fluorescence spectra were acquired with PMCA software and analyzed using the AXIL-WinQXAS software. Nineteen regions of one wall were analyzed. White sandstone regions without pigment and paintings with red and yellow pigments were measured. Elements from Si to Pb were identified. Both red and yellow pigments have Fe as strong key element, clearly indicating use of raw materials with iron oxides. Sandstone regions presented Ca, Ti, Mn, Fe, Cu, Zn, Sr and Zr.

**Keywords:** Rock Art, PXRF, Pigment, In Situ.

### **INTRODUCTION**

Rock art is a general term that is related to human symbolical marks on rock surfaces, and in this paper it will be specific discussed rock paintings or pictograms, with application of pigments. Survival of ancient paintings is attributable to use of mineral pigments, most commonly manganese, hematite, malachite, gypsum, limonite, clays and various oxides.

In Paraná State, in the south of Brazil, there are known about 100 shelters with paintings [1,2], the majority is in sandstones. The rock art in Paraná could be associated with different groups: at least, the oldest ones are related to “Umbu” hunters and gatherers populations, and the more recent to the Itararé-Taquara ceramist group, of Jê linguistic family.

In this case its is very interesting to test other pigments possibilities than the usual inorganic ones, such as the organic pigments usually employed by these indigenous groups and already know in the literature [3]. However, the majority of the rock art in Paraná are on rocks, which usually does not show this behavior.

In situ sampling is done only in very special situations. So, non-destructive in situ examinations, as performed by PXRF, are very suitable for the conservation and management of rock art sites. The identification of pigments can be done with fragments of the rock with paintings which, in the past, had come off the wall and were recuperated in archaeological digs. That is not as frequent as desirable.

Until now, in Brazil, analyses of the pictograms pigments are made taking samples to the laboratory

both for destructive or non-destructive methodologies. Here it is presented one test-program of the potentialities of a “home made” portable EDXRF for the pictograms in situ characterization, performed at Jaguariaíva 1 rockshelter.

## ANALYTICAL APPROACH

Measurements were performed *in situ* and non-destructively employing a portable EDXRF system [4] with an X-ray tube (Ag filter and target), a Si-PIN photodiode detector (5mm<sup>2</sup>, 680μm, 0.5 mil Be Window, 149eV FWHM for the 5.9keV line of <sup>55</sup>Fe), standard X-ray spectrometry electronic chain and a special designed mechanical system for the detector and X-ray tube positioning, that enables angular and XYZ movements of the excitation-detection system respect to the measurement area. A portable stabilized electric generator sustained the whole system. Excitation-detection time was 300 s for each measurement.

K<sub>α</sub> and L<sub>α</sub> X-rays were employed for the elements detection. Only net areas greater than three sigmas above mean background level were accepted for the analysis. X-Ray Fluorescence spectra were acquired with PMCA software. Spectra analysis was performed with the WinQ-XAS software [5].

## JAGUARIAÍVA 1 ROCKSHELTER

Jaguariaíva 1 rockshelter is located in the Jaguariaíva city region (Figures 1 and 2), Paraná State, Brazil (17x 21x5.20m size, E 632 454 e N 7 315 244 UTM coordinates, SAD 69, and 887m high).

It is a sandstone shelter with paintings from, at least, two different periods. The oldest one is around 7.000 years BP, the next moment of paintings could be around 2.000 years BP, as another dated and related Paraná rock paintings suggests.

Rock art in the Jaguariaíva 1 shelter is on part of the walls and ceilings of two sides: the majority is on the west positioned from 0.5m until 1.90m high, and at north side some geometric signs and barred lines that were placed from 1.80m to 3.60m at north.

The studies started in 2002, and the shelter floor was excavated by Paranaense Museum team. The main documented panel of the rockshelter has a superimposition of paintings of animals and lattice motifs placed over deer figures infilled with red. The more recent are reddish brown outline figures filled by straight lines, which could be related to Jê people.

Figure 1 shows the location of Jaguariaíva city region. Figure 2 presents the Jaguariaíva 1 rockshelter. Figure 3 shows three pictograms of the shelter. Figure 4 shows a pictogram area and the PXRf system positioned for measurement.



FIGURE 1. Location of Jaguariaíva city region.



FIGURE 2. Jaguariaíva 1 rockshelter and detail of the entrance, the west side.



FIGURE 3. Three rock paintings of the Jaguariaíva 1 shelter.



FIGURE 4. A pictogram area and the PXRf system positioned for measurement.

## RESULTS

Nineteen regions of the west side wall were analyzed, with measures in different pictograms, and in some of them, like one infilled deer (measures 1 to 4) in many parts of it: head, neck and two points of the body. Other paintings of Jaguariaíva shelter were also measured: animals with other characteristics, barred lines, lattice motifs, and little circles that form figures.

White sandstone regions without pigment and paintings with red and yellow pigments were measured to have more data about the sandstone composition.

Elements from Si to Pb were identified. The last one could be due to atmospheric pollution of the nearby road. Ni and Cu are contaminants of the system.

Both red and yellow pigments have Fe as strong key element, clearly indicating use of raw materials with iron oxides of these colors. Sandstone regions presented Ca, Ti, Mn, Fe, Cu, Zn, Sr and Zr. Figure 5 shows the energy spectrum (counts x energy keV) of the rock (green line) and of a near red colored pictograph region (lilac line).

Table 1 presents the elements peak areas of the spectra at Figure 5.

Pigment key element is Fe, so, it is an iron oxide based pigment, which raw material also includes other elements currently found in soil as Ti, Mn and Sr.

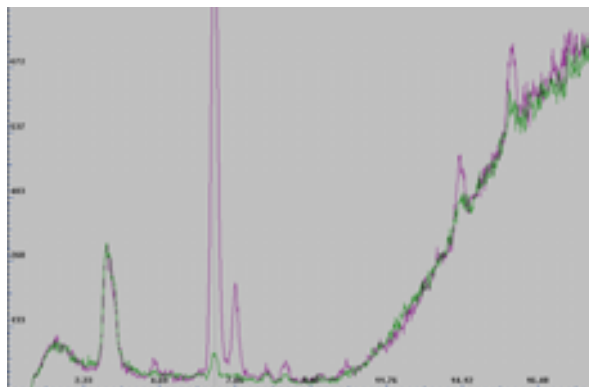


**FIGURE 5.** Energy spectrum (counts versus energy keV) of the rock (green line) and of a near red colored pictograph (lilac line).

**TABLE 1.** Elements peak areas of the same spectra presented at Figure 5.

Element	Rock area			Red figure area		
	Counts	error	background	Counts	error	background
Ar	3771	58	1197	3713	68	1183
Ti	-	-	-	325	39	783
Mn	158	35	714	-	-	-
Fe	890	94	740	15327	129	583
Ni	-	-	613	148	30	611
Cu	284	45	627	230	32	614
Zn	223	40	686	462	35	633
Sr	1118	177	12487	1067	123	675
Zr	1207	519	19119	1062	307	11917
Pb	-	-	-	129	34	967

## CONCLUSIONS

The obtained results indicate that the possibility of an organic pigment, as mentioned before, due to the Itararé-Taquara groups tradition knowledge, can be discarded.

Results strongly indicate that the portable EDXRF equipment used offer a viable alternative for *in situ* rock art analysis.

This is an encouraging result employing a portable equipment and an *in situ* non-destructive analysis, which is a very cheap, easy and fast method compared to the others currently employed in this area.

Other rockshelters in Paraná State with paintings and petroglyphs that have special interest of the Archaeology Department of Paranaense Museum will be studied with this methodology.

## REFERENCES

1. A.G.C.L. Silva, C I. Parellada and M.S. Melo, *Publicatio Ciências Exatas Terra* **13** (2007) 25-33.
2. C.I. Parellada, *Revista Científica FAP* **4** (2009) 1-25.
3. J.L. Fernandes, *Arquivos do Museu Paranaense* **1** (1941) 161-229.
4. C.R. Appoloni, M.S. Blonski, P.S. Parreira, L.A.C. Souza, *Nuclear Physics and Methods in Physics Research A* **580** (2007) 710-713.
5. WinQxas software, 1.40: 32-bit edition, International Atomic Energy Agency, 2002.

## ***Verdigris*, a Pigment with Different Hues. Relation between Chemical Composition and Colour**

M. San Andrés<sup>1</sup>, J. M. de la Roja<sup>1</sup>, N. Sancho<sup>1</sup> and V. G. Baonza<sup>2</sup>

<sup>1</sup> *Dep. de Pintura (Pintura y Restauración), Facultad de Bellas Artes, Universidad Complutense de Madrid, 28040 Madrid, SPAIN. e-mail: msam@art.ucm.es*

<sup>2</sup> *Dep. de Química-Física I, Facultad de Ciencias Químicas, Universidad Complutense de Madrid, 28040 Madrid, SPAIN.*

**Abstract.** Verdigris is a wide term to refer to different compounds derived from the corrosion of copper which have been used as pigments. Among the most important compounds are copper (II) acetate monohydrate and several copper(II) hydroxyacetates hydrated. In this paper, the relationship between the chemical composition of the pigment and its colorimetric characteristics is established. To achieve this goal we have reproduced an old preparation recipe based on the corrosion of a copper plate in contact to acetic acid vapors from vinegar. After six months, we obtained a mixture of compounds with different morphological and colorimetric characteristics. Of course, all the compounds are essentially copper(II) acetates, but differing in basicity and hydration degrees. The characterization and analytical techniques used in this study have been LM, SEM, micro-Raman, ATR- FTIR, XRD and colorimetric measurements.

**Keywords:** Verdigris, Pigments, FTIR, Raman, Colour, Colorimetry.

### **INTRODUCTION**

Artistic pigments are often classified depending on their colours. On the other hand, the chemical compounds derived from selected chemical elements (mostly transition metals) have appealing colours to be used as pigments. One of them is copper whose salts usually exhibit blue or green colours [1]. Verdigris, which belongs to the second class, is an historical synthetic pigment that has been known by different names over the History [2]. Frequently, its primary colour is green or green-bluish [3] and many denominations are related with these chromatic characteristics, for example, green of Montpellier, green of Greece, spanish green, verderame, verdet, etc. However, other names, as cardenillo, are etymologically related with the blue colour. In addition, this pigment was specifically recommended to wash plans and cartographic documents in ancient literature [4]. In this application, verdigris is called sea

green and it is used to represent blue-coloured or green areas (in the second case mixed with yellow dyes).

Verdigris was one of the first synthesized pigments [5]. The different synthetic methods are compiled in some treatises and texts related to the materials and pictorial procedures (from antique to 19<sup>th</sup> century) [6,7]. Its synthesis is affected by different factors, like the nature of the corrosive agent and the time to reaction. Regarding the synthetic time, references span from fifteen days to six months.

In this investigation we have used copper and vinegar as reagents and the time has been six months. The final product was a complex mixture of compounds showing different chemical compositions, morphology and colours. The full characterization of these compounds were been carried out by LM, SEM, ATR-FTIR, micro Raman, XRD and colorimetric measures.

## EXPERIMENTAL

### Synthesis of Pigment

The recipe reproduced here is one of the most frequently reported in ancient and medieval texts. It consists on the corrosion of a copper sheet exposed to acetic acid vapour from vinegar. As already noted, the suggested reaction time varies from fifteen days to six months [Dioscorides (1<sup>st</sup> aC), Pliny (1<sup>st</sup> aC), and in the *Mappae Clavicula*, medieval manuscript of 9<sup>th</sup> century with notes of 11<sup>th</sup> and 12<sup>th</sup> centuries].

The procedure applied in our laboratory consists in introducing a copper plate in a crystal container, together with beaker filled with 50 ml of vinegar. This container is then hermetically closed and maintained at 40 °C for six months. After this time the plate is extracted and exposed to room temperature for 24 h. The final result is a layer of corrosion products formed onto the copper plate, their thicknesses, colours and distribution being quite heterogeneous. Direct optical inspection reveals different regions that differ in both colour and morphology. Figure 1 shows the corroded copper plate and the areas from samples were collected for further study. These samples studied have been labelled as A1, A2 and A4. The samples were carefully scraped off the copper plate surface, grounded in agate mortar, and place in a desiccator.

### Analytical techniques

#### *Light Microscopy*

A stereoscopic light microscope Leica MZ125 was used for morphological examination of the corroded copper plate and to distinguish the different areas of interest. The samples selected were studied by LM with a ZEISS petrographic microscopy, mod. Jenapol. They were studied with transmitted and polarized light.

#### *Scanning electron microscopy (SEM)*

The SEM study was performed on a JEOL JSM 6400 electron microscope with 20 kV accelerating voltage, incorporating a LINK eXL energy dispersion spectrometer with resolution of 138 eV–5.39 keV. The samples were metallized with gold and examined on secondary electron (SE). For this analysis the samples were not grounded.

#### *Infrared spectroscopy*

A Fourier transform infrared spectrometer (Thermo Nicolet 380) with a DTGS (deuterated triglycine

sulphate) temperature-stabilized coated detector was used (4000–400 cm<sup>-1</sup>). It is equipped with an attenuated total reflection diamond crystal accessory (ATR). The spectra were obtained in absorbance mode, from 64 scans at 4 cm<sup>-1</sup> resolution. Spectra were analyzed using Omnic v 7.3 and processed with Origin v 7.0.

#### *Raman spectroscopy*

The samples were analyzed by micro-Raman spectroscopy using the 488 nm line of an ILT argon-ion laser. A 100x Mitutoyo-based microscope was used to select the laser spot. The signal was analyzed in a ISA HR460 spectrograph coupled to a CCD detector (ISA CCD3000). Spectral resolution better than 4cm<sup>-1</sup> is achieved by using a 600 gr/mm diffraction grating. Raman spectra obtained were processed with the Origin 7.0 software package.

#### *X-ray diffraction*

XRD patterns were collected on a Philips X'PERT diffractometer, using a voltage 45 kV and intensity 40 mA. This setup uses two slits, a 18 divergence slit for primary optics and a 18 anti-scatter slit (receiving slit = 0.05 mm) for secondary optics. A curved Cu monochromator was used to eliminate the contribution of the K<sub>β</sub> line.

#### *Colour Measurement*

We used a Konica Minolta CM 2600d spectrophotometer for colour measurements with an spot size of 3mm, SCE mode, CIELAB space, range 400nm to 700nm, step size of 10 nm light source D65, standard observer 10°.

## RESULTS AND DISCUSSION

As shown in Figure 1, the corroded copper plate shows very different areas in relation to morphological and chromatic characteristics. The study performed on samples taken from selected areas of the transformed copper plate allowed us to verify important differences in relation to their physical properties and chemical composition.

Figures 2 and 3 shows the results obtained by LM and SEM(SE). These images reveal three different optical and morphological characteristics corresponding to the samples labeled as A1, A2 and A4, respectively. These characteristics are similar to those described in the literature for different verdigris variants [7–9].

The sample A1 shows very small particles and some of them are forming aggregates. They appear as pale blue bundles on the copper plate (Fig. 1a). Under the

microscope they appear as blue-green fibrous crystals (Fig. 2a) and examination by SEM(SE) shows that the crystals are very well formed (Fig. 3a) with dimensions around 20 $\mu$ m in length and 2,5 $\mu$ m in wide. These characteristics have been already described in some kind of basic verdigris.

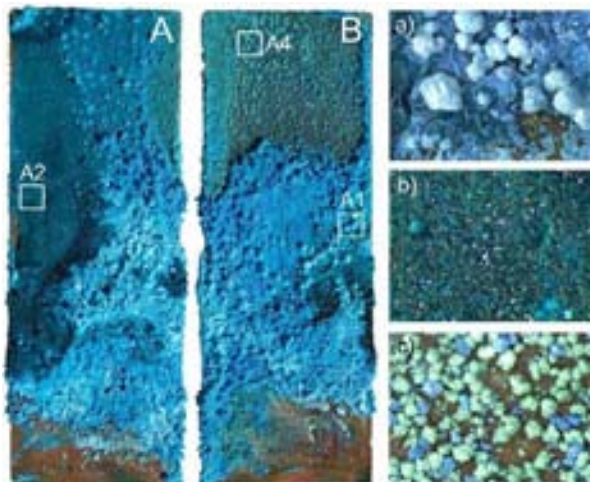


**FIGURE 1.** Corroded copper plate (both sides). Location and details of samples labelled as: a) A1; b) A2; c) A4.

The area of sample A2 shows a green-bluish colour (Fig. 1b). Under the microscope the particles present uneven morphology, irregular size and weak conchoidal fracture (Fig. 2b). However the image obtained by SEM(SE) (Fig. 3b) reveals the existence of prismatic

crystals pyramidal terminations with a rather wide size distribution (1–100 $\mu$ m). There are also abundant tabular particles. These characteristics are similar to those already described in the literature for copper(II) acetate hydrated  $\text{Cu}(\text{CH}_3\text{COO})_2 \cdot \text{H}_2\text{O}$  (neutral verdigris).

The sample A4 corresponds to one area with small globular shapes of pale-green colour (Fig. 1c). Under the plane-polarised microscope the particles appear prismatic and tabular, exhibiting weak birefringency. SEM(SE) images indicates several kinds of particles (Fig. 2c) with both prismatic (similar to the A2 sample) and acicular (as sample A1) geometries. In this same sample (A4), there are also a third group of particles which appears forming clumps of hexagonal plates. This morphology has been related to basic verdigris in the literature.

As described above, samples A1, A2 and A4 fall within the greenish range but they present obvious chromatic differences, so colorimetric measurements were performed in order to quantify these variations. The results are listed in Table 1. These results, together with the corresponding plot in the CIE  $a^*b^*$  diagram, and the reflectance spectra of the samples confirm the observed differences to the naked eye (Fig. 4).

**TABLE 1.** Colorimetric measurements.

Sample	L*	a*	b*	C*	$h_{ab}$
A1	68.56	-23.59	-22.74	32.77	223.95
A2	62.05	-40.96	-13.47	43.12	198.20
A4	77.05	-22.40	-0.84	22.42	182.14

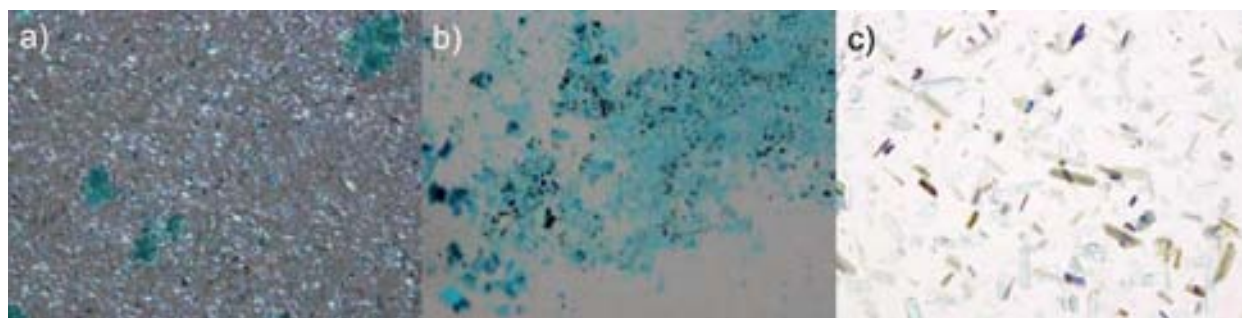


**FIGURE 2.** LM images: a) A1 TPL/100X; b) A2 TPL/ 100X; c) A4 PPL/200X.

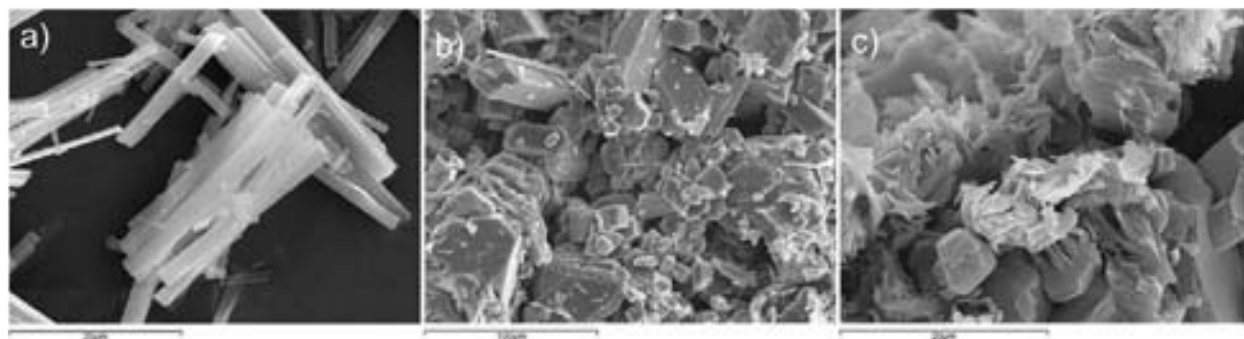


**FIGURE 3.** SEM(SE) images: a) A1 (bar 20 $\mu$ m); b) A2 (bar 100 $\mu$ m) and c) A4 (bar 20 $\mu$ m).

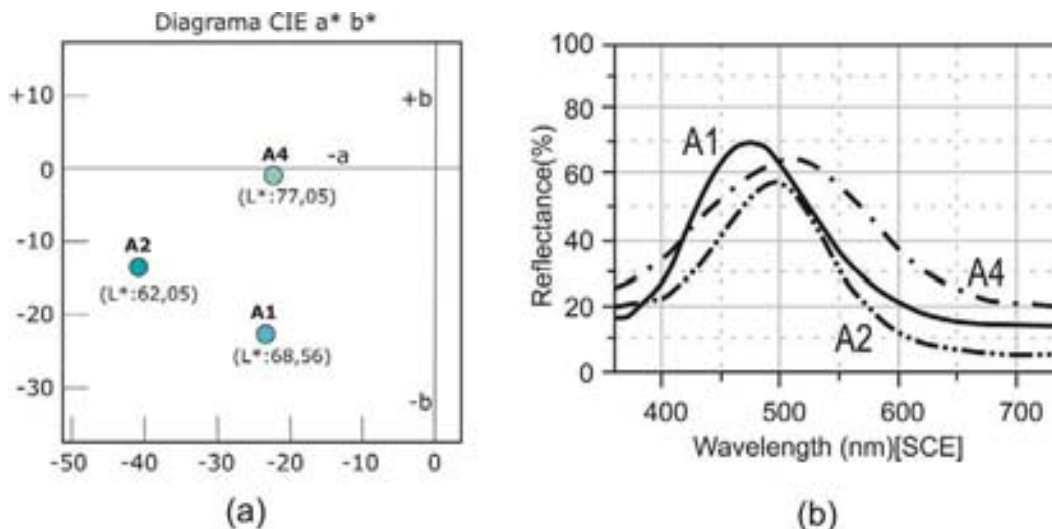


FIGURE 4. a) Representation in the CIE a\*b\* diagram, of samples analyzed. b) Reflectance spectra.

The chroma ( $C^*$ ) and hue ( $h_{ab}$ ) values show that all the samples are within the greenish range but present significant differences. Because of a value of  $h_{ab} = 180^\circ$  defines a green hue and  $h_{ab} = 270^\circ$  a blue hue, it can be deduced that the sample A4 has a green colour ( $h_{ab} = 182.14$ ) while samples A1 ( $h_{ab} = 223.95$ ) and A2 ( $h_{ab} = 198.20$ ) shows a greenish-blue colour, specially in the former case. These characteristics are confirmed by the corresponding reflectance spectra (Fig. 4b).

In order to establish a relationship between the described properties (colour and morphology) and chemical composition of these samples, they have been analyzed by micro-Raman and ATR-FTIR spectroscopies. All the spectra were recorded at room temperature. Raman and FTIR spectra provide complementary (weak FTIR absorptions are usually strong in Raman and vice versa) information [10].

According to the reaction conditions, the colour and morphological characteristics described above, it is assumed that all the samples analyzed are copper(II) acetates but with different degrees of hydration and/or basicity, so they can be generally regarded as organo-copper complexes. In order to confirm this hypothesis, bands corresponding to acetate groups ( $\text{CH}_3\text{-COO}$ ), hydroxyl ( $\text{-OH}$ ) and water of hydration have been identified. Figure 5 shows the Raman and ATR-FTIR spectra obtained from the three samples (A1, A2 y A4); they clearly show distinctive spectral features.

The Raman spectrum of sample A2 presents bands corresponding to the acetate group:  $\nu\text{CH}_3$  ( $2941_{(m)}$ ,  $2985_{(w)}$  and  $3023_{(w)}$   $\text{cm}^{-1}$ );  $\nu\text{COO}$  ( $1534_{(vw)}$  and  $1439_{(m)}$   $\text{cm}^{-1}$ );  $\delta\text{CH}_3$  ( $1416_{(m-sh)}$  and  $1358_{(w)}$   $\text{cm}^{-1}$ );  $\nu\text{C-C}$  ( $948_{(s)}$  and  $939_{(m-sh)}$   $\text{cm}^{-1}$ );  $\delta\text{OCO}$  ( $702_{(s)}$  and  $686_{(m-sh)}$   $\text{cm}^{-1}$ ). We have also identified some very weak bands at 3266, 3376 and 3466  $\text{cm}^{-1}$ , which correspond to hydration water. Moreover, the spectrum shows a clear correspondence to

the reference spectrum of the commercial compound copper(II) acetate monohydrate [ $\text{Cu}(\text{CH}_3\text{COO})_2\cdot\text{H}_2\text{O}$ ] (Fig. 5a) supplied by Aldrich (ref. 341746) and its micro-Raman spectrum has also been obtained in our laboratory.

In order to confirm the presence of hydration water molecules, sample A2 was analyzed by ATR-FTIR spectroscopy. The spectrum obtained shows three characteristic bands at  $3454_{(m)}$ ,  $3364_{(m)}$  and  $3267_{(m)}$   $\text{cm}^{-1}$ , which are due to the O-H stretching vibration from the water molecule associated with the acetate group. Additional characteristics features are those from acetate group:  $\nu_{as}$  and  $\nu_s$   $\text{-CH}_3$  ( $2990_{(w)}$  and  $2942_{(w)}$   $\text{cm}^{-1}$ ),  $\nu_{as}$  and  $\nu_s$  (COO) ( $1594_{(vs)}$  and  $1417_{(vs)}$   $\text{cm}^{-1}$ ),  $\delta_{as}$  and  $\delta_s$  in plane  $\text{-CH}_3$  ( $1435_{(s)}$  and  $1354_{(m)}$   $\text{cm}^{-1}$ ),  $\nu_{tr}$   $\text{-CH}_3$  ( $1049_{(m)}$  and  $1033_{(m)}$   $\text{cm}^{-1}$ ). There are also interesting bands at:  $686_{(vs)}$  and  $626_{(s)}$   $\text{cm}^{-1}$ , which can be assigned to  $\delta(\text{OCO})$  and  $\pi(\text{COO})$  modes, respectively. Moreover, this spectrum coincides with the reference spectrum of the compound purchased to Aldrich (Fig. 5b), so the spectrum can be unambiguously ascribed to the monohydrated copper(II) acetate [ $\text{Cu}(\text{CH}_3\text{COO})_2\cdot\text{H}_2\text{O}$ ] [11].

The interpretation of the vibrational spectra of samples A1 and A4 is more complex though. In both samples, some bands corresponding to the hydroxyl groups and hydration water have been identified. So they are very likely hydrated copper(II) hydroxyacetate. [ $x\text{Cu}(\text{CH}_3\text{COO})_2\cdot y\text{Cu}(\text{OH})_2\cdot z\text{H}_2\text{O}$ ] derivatives, but differing on the ratio of [ $\text{Cu}(\text{CH}_3\text{COO})_2$ ] and [ $\text{Cu}(\text{OH})_2$ ] subunits and on the hydration degree.

The Raman spectrum of the A1 sample shows good agreement with that provided by Bell *et al.*, who attributed their results to  $\text{Cu}_2(\text{CH}_3\text{COO})_2\cdot(\text{OH})_2$  (labelled as Verdigris no.2 in their paper) (Fig. 5a) [12]. However, our and their results differ from those reported by Chaplin *et al.* for the same compound [13]. In both spectra there

are bands assigned to hydroxyl groups [ ${}^{\text{H}}\text{OH}_{\text{hydroxy}}$  (ca.  $3476_{(\text{m})}$  and ca.  $3570_{(\text{m})} \text{ cm}^{-1}$ )]. On a previous study of this compound, San Andrés *et al.* [14] described very weak bands in the region of hydroxyl groups associated to hydration molecules [ ${}^{\text{H}}\text{OH}_{\text{water}}$  (ca.  $3400_{(\text{vw})}$   $\text{cm}^{-1}$  and ca.  $3200_{(\text{vw})} \text{ cm}^{-1}$ )]. In the ATR-FTIR spectrum these bands have also been identified, so these results allowed us to conclude that the A1 sample is a hydrated copper(II) hydroxyacetate [ $x\text{Cu}(\text{CH}_3\text{COO})_2 \cdot y\text{Cu}(\text{OH})_2 \cdot z\text{H}_2\text{O}$ ].

With regard to compound labelled as A4, it should be noted that its Raman and ATR-FTIR spectra show characteristic bands of the acetate group, but also present features in the region corresponding to the OH groups of both hydroxy group and water molecules (Fig. 5a and 5b). Our Raman spectrum is quite similar to those reported by Chaplin *et al.* for their sample A with, according these authors, composition [ $2\text{Cu}(\text{CH}_3\text{COO})_2 \cdot \text{Cu}(\text{OH})_2 \cdot 5\text{H}_2\text{O}$ ] [13].

In order to complement the results obtained by Raman and FTIR spectroscopies, samples A1, A2 and A4 were analyzed by XRD (Fig. 6). The results for sample A2 confirm that the composition is [ $\text{Cu}(\text{CH}_3\text{COO})_2 \cdot \text{H}_2\text{O}$ ], its diffractogram having a clear correspondence with the identified patterns JCPDS 00-010-0756 and 00-027-0145, which correspond to hydrated copper(II) acetate and

mineral hoganite, respectively, and both of them respond to the formula [ $\text{Cu}(\text{CH}_3\text{COO})_2 \cdot \text{H}_2\text{O}$ ].

The XRD data obtained for sample A4 have a clear correspondence with results of Pereira *et al.*, in relation to the hydrated copper(II) trihydroxyacetate [ $\text{Cu}_2(\text{OH})_3(\text{CH}_3\text{COO}) \cdot \text{H}_2\text{O}$ ], which is equivalent to  $\text{Cu}(\text{CH}_3\text{COO})_2 \cdot 3\text{Cu}(\text{OH})_2 \cdot 2\text{H}_2\text{O}$  [15]. It should be noted that the most intense diffraction lines in our diffractogram are coincident with the identified pattern JCPDS 00-050-0407, which stands for [ $\text{Cu}(\text{CH}_3\text{COO})_2 \cdot 3\text{Cu}(\text{OH})_2 \cdot 2\text{H}_2\text{O}$ ]. Therefore, we can conclude that sample A4 corresponds to a hydrated copper(II) hydroxyacetate identified as  $\text{Cu}(\text{CH}_3\text{COO})_2 \cdot 3\text{Cu}(\text{OH})_2 \cdot 2\text{H}_2\text{O}$ .

Finally, the diffractogram of the sample A1 has been compared to those published for the different basic verdigris varieties [1, 8]. No correlation was found to any of them; moreover, there are no coincident JCPDS identification patterns. Thus, although their Raman and FTIR spectra suggest that this is a hydrated copper(II) hydroxyacetate, the lack of reference XRD patterns did not allow us to determine the ratio [ $\text{Cu}(\text{CH}_3\text{COO})_2$ ] to [ $\text{Cu}(\text{OH})_2$ ] and degree of hydration.

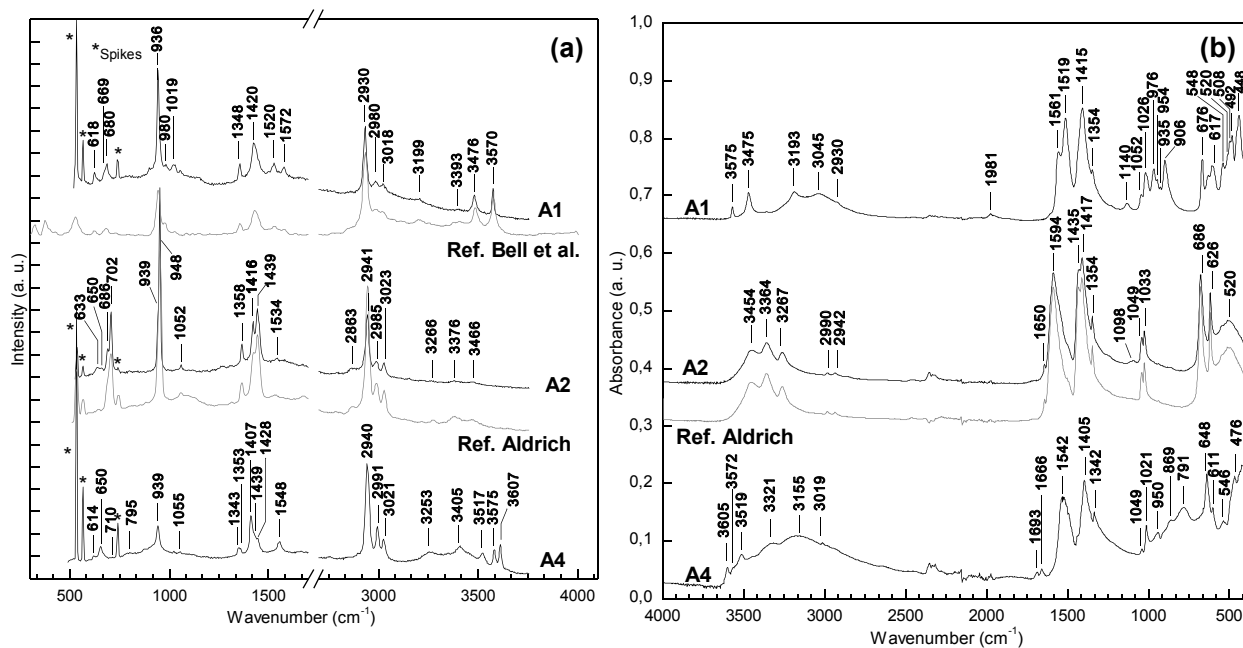


**FIGURE 5.** a) Raman spectra of samples A1 and reference verdigris no. 2 (Bell *et al.*); A2 and reference hydrated copper(II) acetate (Aldrich); A4. b) ATR-FTIR spectra of samples A1; A2 and hydrated copper(II) acetate (Aldrich); A4.

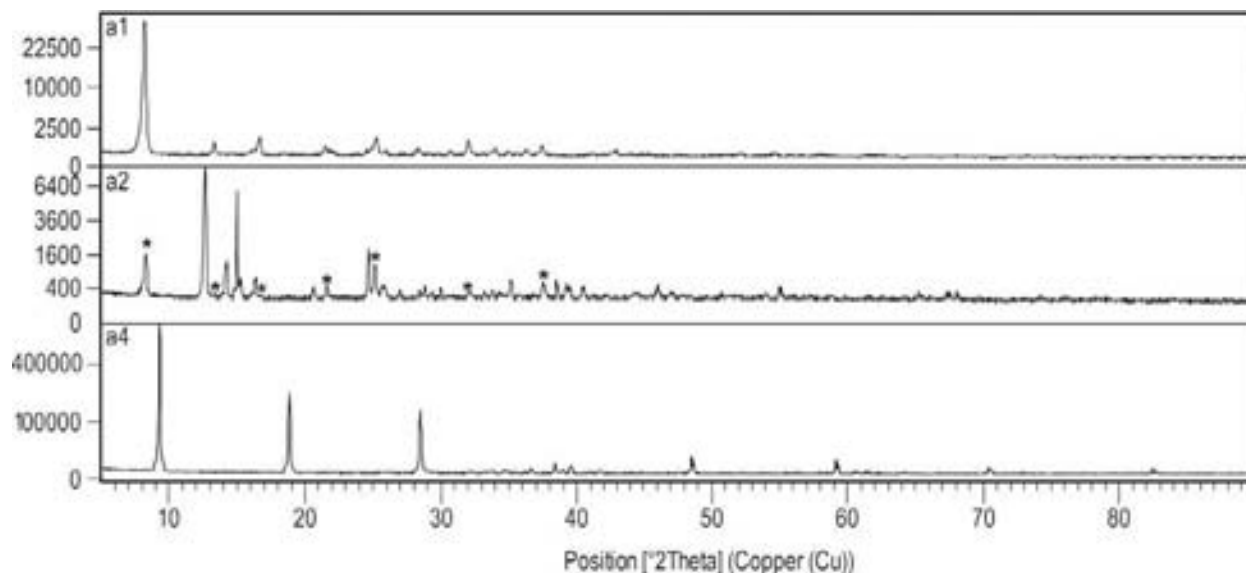


FIGURE 6. XRD results: samples A1, A2 and A4. Asterisks correspond to traces of sample A1.

## CONCLUSIONS

The long exposure of copper to acetic acid vapours from vinegar (six months) leads to a complex mixture of different copper(II) acetate compounds that differ in their degree of hydration and basicity. These compositional differences are reflected in their Raman and ATR-FTIR spectra and in their structure, as revealed by XRD patterns. They have been identified three kind of verdigris varieties: neutral verdigris  $[\text{Cu}(\text{CH}_3\text{COO})_2 \cdot \text{H}_2\text{O}]$ , and two types of basic verdigris, one corresponding to the composition  $[\text{Cu}(\text{CH}_3\text{COO})_2 \cdot 3\text{Cu}(\text{OH})_2 \cdot 2\text{H}_2\text{O}]$  and the other to  $[\text{xCu}(\text{CH}_3\text{COO})_2 \cdot \text{yCu}(\text{OH})_2 \cdot \text{zH}_2\text{O}]$ . In this latter case the exact composition could not be fully determined. Finally, it should be noted that both the ratio  $\text{Cu}(\text{CH}_3\text{COO})_2$  to  $\text{Cu}(\text{OH})_2$  and the hydration content influence the morphology and colour of the pigment.

## ACKNOWLEDGMENTS

This work was funded by the Spanish Ministry of Science and Innovation under Project HUM2005-04618/ARTE. The authors are also grateful to CAI of X-Ray Diffraction and Electronic Microscopy from the Universidad Complutense de Madrid. The authors belongs to Research Group 930420 (UCM)

## REFERENCES

1. D.A. Scott, *Copper and bronze in art. Corrosion, Colorants, Conservation*. The Getty Conservation Institute, Los Angeles, 2002.
2. N. Eastaugh, V. Walsh, T. Chaplin, R. Siddall, *Pigment Compendium. A Dictionary of Historical Pigments*, Elsevier Butterworth-Heinemann, Oxford, 2004. pp. 385-386.
3. J. M. de la Roja, M. San Andrés, N. Sancho, S. Santos, *Color Res. Appl.* **32** (2007) 414–423.
4. M. Jiménez, M. San Andrés, J.M. de la Roja, *GeCuadernos* **1** (2009) (in press).
5. M. San Andrés, N. Sancho, J.M. de la Roja, *An. Quim.* **105** (4) (2009) (in press)
6. M. Clarke, *The Art of all Colours*, Archetype London, 2001: 133.
7. H. Kühn, “Verdigris and copper Resinate” in *Artists’ Pigments. A Handbook of their History and Characteristics*, Vol. 2, A. Roy ed., Oxford University Press, Oxford, 1993. pp. 131–147.
8. D.A. Scott, Y. Taniguchi, E. Koseto *Rev. Conserv.* **2** (2001) 73-91.
9. N. Eastaugh, V. Walsh, T. Chaplin, R. Siddall, *Pigment Compendium. Optical Microscopy of Historical Pigments*, Elsevier Butterworth-Heinemann, Oxford, 2004. pp. 78-86.
10. G. Socrates, *Infrared and Raman Characteristic Group Frequencies. Tables and Chartes*, John Wiley & Sons, West Sussex 2001.
11. A. Musumeci, R.L. Frost, *Spectrochim. Acta, Part A*, **67** (2007) 48-57
12. M. Bell, R.J.H. Clark, P. J. Gibbs, *Spectrochim. Acta, Part A*. **53** (1997) 2159-2179
13. T.D. Chaplin, R.J.H. Clark, D.A. Scott, *J. Raman Spectrosc.* **37** (2006) 223-229
14. M. San Andrés, J.M. de la Roja, V.G. Baonza, N. Sancho, Contributions to the 5<sup>th</sup> International Congress on the Application of Raman spectroscopy in Art and Archeology (RAA), Bilbao, 2009. pp. 99-100
15. D.C. Pereira, D.L.A. Faria, V.R.L. Constantino, *J. Braz. Chem. Soc.* **17** (2006) 1651 – 1657.

## **Chemical Changes in Pictorial Models: Characterization by FT-IR Spectroscopy**

Verónica Urbina<sup>1</sup>, Trinitat Pradell<sup>1</sup>, Nativitat Salvadó<sup>2</sup>, Salvador Buti<sup>2</sup>  
and José Luis Ruvalcaba<sup>3</sup>

<sup>1</sup> *Department de Física i Enginyeria Nuclear, Universitat Politècnica de Catalunya, Campus Baix Llobregat, ESAB, Av. Canal Olímpic, s/n, 08860, Castelldefels, Barcelona, SPAIN. e-mail: verónica.urбина @upc.edu*

<sup>2</sup> *Departament d' Enginyeria Química, EUPVG, Universitat Politècnica de Catalunya, Av. Victor Balaguer, s/n, 08800, Vilanova i la Geltrú, Barcelona, SPAIN.*

<sup>3</sup> *Instituto de Física, Universidad Nacional Autónoma de México, Circuito de la Investigación Científica s/n, Ciudad Universitaria, C.P. 04510, México, D.F, MEXICO.*

**Abstract.** In order to understand the interaction between copper containing pigments and the organic binders in paintings, as well as reaction/alteration products, a series of pictorial models have been prepared and naturally aged. For this research, Fourier transform infrared spectroscopy (FT-IR) is used as the analytical technique, while it is useful in detecting functional groups, so it allows the identification of significant changes in the cured mechanism of the system prepared. For simulating the oil painting system, the methodology was based in thin-films so previously synthesized copper green pigments – identified as copper acetates, copper hydroxichlorides and mixtures of acetates and hydroxichlorides – have been mixed with the binding media (drying oils). These mixtures were layered on glass supports. By means of FT-IR measurements the oxidation is evident while a decrease in the hydrocarbon stretching and bending frequencies is observed (bands at 3000-2800 cm<sup>-1</sup>). Another change in the models is the appearance of a shoulder in the region between 1500 to 1600 cm<sup>-1</sup>, which turns into a peak during the decay process.

**Keywords:** Aging, Oil paint, Copper based pigments, Binding media, Pictorial model.

### **INTRODUCTION**

The study of the reaction/alteration products resulting from the interaction between metals containing pigments and the organic binders in paintings such as egg yolk and drying oils, has a high interest in order to understand the colour alteration.

The present work is focused in the browning of copper based pigments shown by art works corresponding to the fifteenth and sixteenth centuries, the period of transition between Gothic and

Renaissance in Catalunya. Some evidences on the formation of reaction products when copper containing pigments are mixed with organic binders have been obtained [1].

In order to understand this problem, a series of pictorial models simulating oil paintings have been prepared and naturally aged. The binder media studied will be one of the most used in this period: drying oils. The copper salts and copper compounds typically used as pigments during the Middle Age and in the Renaissance were obtained by technical processes used by artists and craftsmen at that time [2].

## MATERIALS AND METHODS

The methodology for the pictorial models was based in thin-films. Previously synthesized copper green pigments identified by SEM-EDS, X-ray power diffraction, FT-IR and Raman spectroscopy as  $\text{Cu}(\text{CH}_3\text{COO})_2 \cdot \text{H}_2\text{O}$  copper (II) acetate hydrate and mixtures of copper (II) acetate hydrate and copper hydroxichlorides  $\text{Cu}_2(\text{OH})\text{Cl}_3$  [2] were used as pigments for preparing the films. These copper pigments were prepared according to old recipes through the exposure of copper bars to the vapours of vinegar and the addition of different reagents for every recipe. For reproducing the recipe VS1 and VS5, the reagents added were sodium chloride (NaCl) and honey, for recipe 80 sodium chloride (NaCl) and for recipe 221D only the exposure to the vapours of vinegar [2]. Then oil films containing 50%(w/v) pigment were prepared and applied on thin sheet of glass or microslides ( figure5 and table 1).

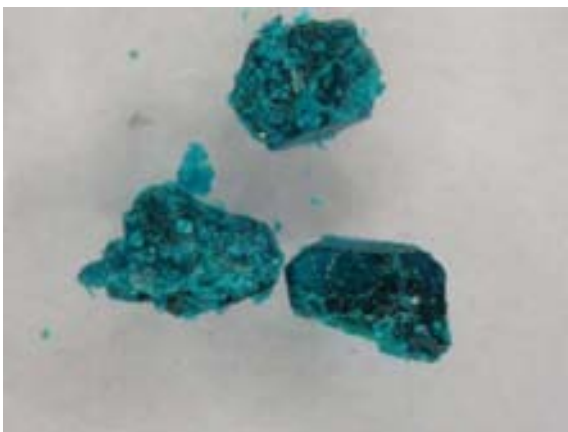


**FIGURE 1.** Pigment from recipe VS1.

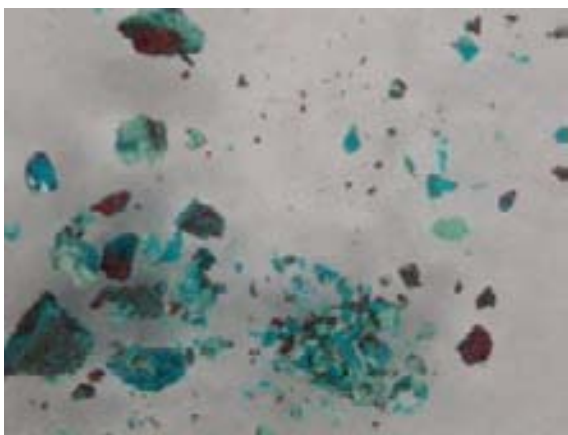


**FIGURE 2.** Pigment from recipe VS5.



**FIGURE 3.** Pigment from recipe 221D.



**FIGURE 4.** Pigment from recipe 80.

In all models the drying oil was cold pressed linseed oil (Zecchi). As a reference pigment was employed copper (II) acetate hydrate reagent (Probus) and a model was prepared containing no pigment (labelled as L). The models were stored in the dark at room temperature for 12 months and the sampling was carried out in the outer surface of the pictorial model. For identification of models see table 1.



**FIGURE 5.** Pictorial models.

## FT-IR Measurements

A FT-IR spectrometer Nicolet Nexus 670 was employed. Spectra in the 400 to 4000  $\text{cm}^{-1}$  range were obtained by 64 scans with a resolution of 4  $\text{cm}^{-1}$ , the samples were ground and prepared in potassium bromide (KBr) pellets, the measurement mode was transmission. Models spectra were recorded in fresh (f) and aging (a) state.

## RESULTS AND DISCUSSION

The IR spectra collected of the aged models A (figure 8), C (figure 9) and S (figure 7), show similar behavior, while they include the same pigment, copper (II) acetate hydrate. Specific IR peaks were monitored in all samples during the process under study. It includes changes in the *cis*-CH, CH<sub>2</sub> and C=O stretching band absorptions [3]. These changes can be summarized as follows:

The assigned bands [4] to the pigment, copper (II) acetate hydrate at 3477, 3376, 3271 (coordinated water molecules), 1604 (unsymmetrical stretching vibration), 1053, 1033 ( $-\text{CH}_3$  vibrations) and 692 (bending mode for  $-\text{COO}$ ) have a sharp decrease.

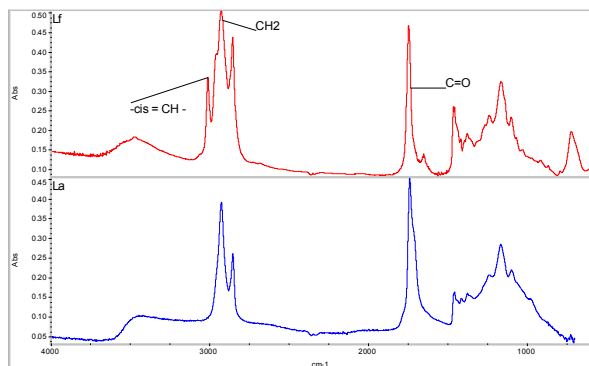


FIGURE 6. FT-IR spectra for model L.

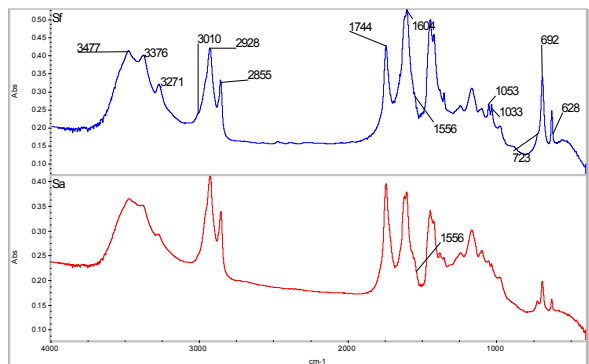


FIGURE 7. FT-IR spectra for model S.

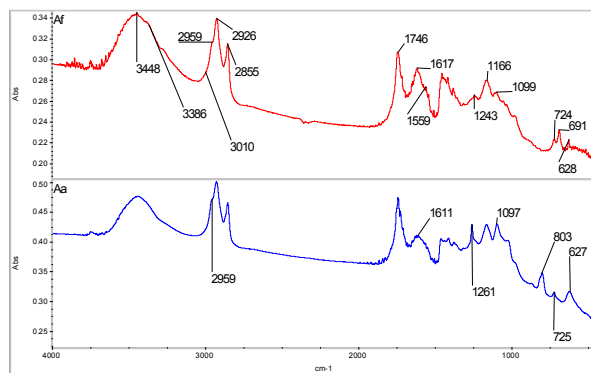


FIGURE 8. FT-IR spectra for model A.

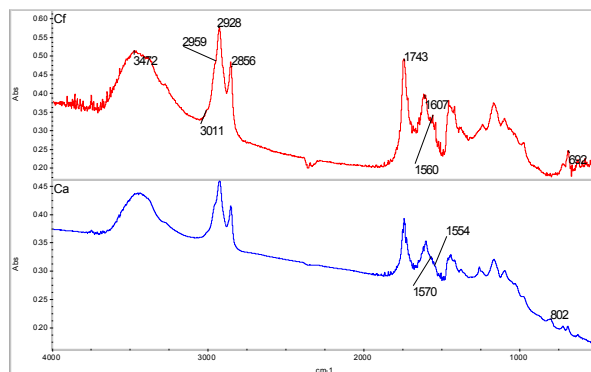


FIGURE 9. FT-IR spectra for model C.

According with the literature [3] the aging of linseed oil presents transformation of all-*cis* polyunsaturated chains to *cis* ( $-\text{cis}=\text{CH}-$ ), loss of hydrogens attached in the saturated chains (CH<sub>2</sub>) and increase of carbonyls (C=O) and it was confirmed in the model L or figure 2 (only oil). However in figure 4 and 5 the *cis*-CH stretching at 3010  $\text{cm}^{-1}$  decreases abruptly but it remains like a nearly negligible shoulder. There are other two changes, a gradual decrease of the CH<sub>2</sub> antisymmetric stretching at 2855, 2928 and 2959  $\text{cm}^{-1}$  and a broadened of the carbonyl band at 1743  $\text{cm}^{-1}$ . Though, in the model S, which is the standard model, there is a slight increase in both, CH<sub>2</sub> and C=O bands. But, the change in the shape and the intensity in the 1500-1600  $\text{cm}^{-1}$  range is notable, while in the fresh spectra the absorption at 1556  $\text{cm}^{-1}$  is a negligible shoulder, in the aged model it is recognizable. For model C there is a variation about this absorption, from 1554 to 1570  $\text{cm}^{-1}$  and for model A this change is not clear.

The pigment used for the models B (figure 10) and D (figure 11), was a mixture of acetate and hydroxichlorides.

In the aged state the spectra show that at high wavenumber region, the assigned bands[2] to the copper hydroxichlorides in structure like atacamite and paratacamite remain ( figure 6, 3443 and 3361  $\text{cm}^{-1}$ ,

figure 7, 3440 and 3356  $\text{cm}^{-1}$ ) however in the 1000-400  $\text{cm}^{-1}$  range the bands are insignificant.

Changes in the cis-CH, CH<sub>2</sub> and C=O stretching bands absorptions show the same tendency as model A and C. The difference with the model A and C is in the range 1500-1600  $\text{cm}^{-1}$ . The shoulders, which are shown by model B at 1555  $\text{cm}^{-1}$  and model D at 1558  $\text{cm}^{-1}$  are negligible.

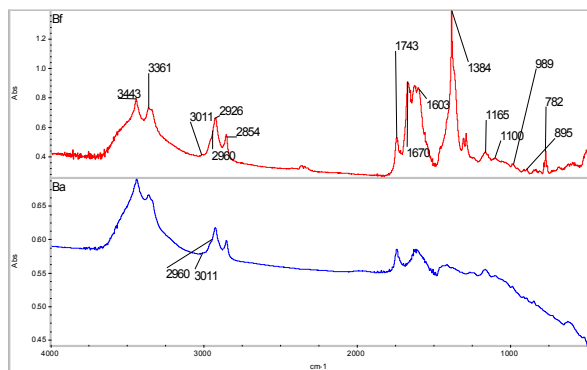


FIGURE 10. FT-IR spectra for model B

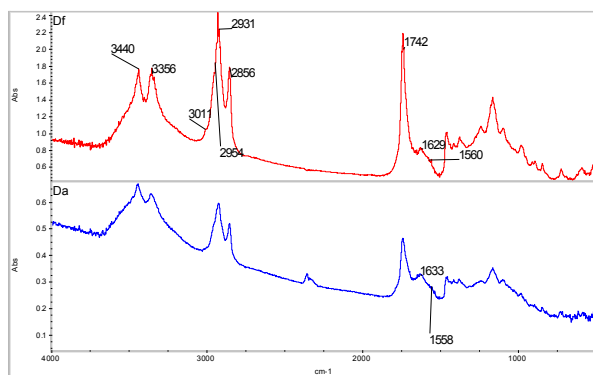


FIGURE 11. FT-IR spectra for model D

## CONCLUSIONS

Through FT-IR spectroscopy was possible the identification of significant changes in pictorial models under natural curing.

Differentiation in reactivity between used pigments was detected, while copper (II) acetate hydrate shows the highest reactivity. For our study it is of great importance since old masters used a wide variety of copper salts as pigments while their manufacturing methods were countless.

Absorbances of the cis-CH bonds, at 3010  $\text{cm}^{-1}$ , do not disappear completely then the presence of copper pigments inhibits in some ways the conversion of cis unsaturation to trans C=C bonds and the gradual decrease of the CH<sub>2</sub> bands represents a lower weight loss in the form of hydrogens, so producing a lower amount of cross-linking.

Widening and asymmetric form in the carbonyl band at 1743  $\text{cm}^{-1}$ , which is originally due to the C=O stretching of the carbonyl ester groups, possibly involves the presence of others various carboxylic compounds, produced by the degradation reactions.

All samples containing pigment are characterized for a changeable set of shoulders in the 1500-1600  $\text{cm}^{-1}$  range: between 1554 to 1558, 1572 to 1575 and at 1566  $\text{cm}^{-1}$ . Only in the standard model S, the absorption at 1556  $\text{cm}^{-1}$  reveals clearly the formation of a new band. Then aging periods under natural conditions must be older than 12 months for the correct assignment of the absorptions in this range 1500-1600  $\text{cm}^{-1}$ .

TABLE 1. Models simulating pictorial layers.

Materials layered on glass support	Symbol	Previous pigment identification by FT-IR
Cold pressed linseed oil	L	x
Cold pressed linseed oil + Copper (II) acetate hydrate reagent	S	Copper (II) acetate hydrate
Cold pressed linseed oil + Recipe VS1	A	Copper (II) acetate hydrate
Cold pressed linseed oil + Recipe VS5	B	Copper (II) acetate hydrate Atacamite Paratacamite
Cold pressed linseed oil + Recipe 221D	C	Copper (II) acetate hydrate
Cold pressed linseed oil + Recipe 80	D	Atacamite Paratacamite Copper (II) acetate hydrate

## ACKNOWLEDGMENTS

To CONACyT-Mexico by funding Veronica Urbina research. Authors thank to IF-UNAM and Dr. J. Ocotlán Flores from CCADET-UNAM for experimental facilities.

This research has been partially supported by PAPIIT-UNAM grant IN403210.

## REFERENCES

1. N. Salvadó, S. Butí, M.J. Tobin, E. Pantos, J.N. Prag, T. Pradell, *Analytical Chemistry*, **77** (2005) 3444 -3451.
2. V. Urbina, unpublished data (personal communication, May, 2009).
3. R.J. Meilunas, J.G. Bentsen, A. Steinberg, *Studies in conservation* **35** (1990) 33-51.
4. A. Roy A., H. Kühn, "Verdigris and Copper Resinate", *Artists' Pigments, A Handbook of their History and Characteristics*, Vol. 2, Oxford University Press, New York, 1993

## **The Mobility of Imitation: An Analysis of 18<sup>th</sup> Century Chinese Style Furniture with IR-UV Imaging, Portable XRF and SEM**

S. Zetina<sup>1</sup>, E. Arroyo<sup>1</sup>, T. Falcón<sup>1</sup>, E. Hernández<sup>1</sup>, J.L. Ruvalcaba<sup>2</sup>, M. E. Espinosa<sup>3</sup>, V. Aguilar<sup>2</sup>, D. Ramírez<sup>2</sup>, V. Santos<sup>1</sup> and F. Riquelme<sup>4</sup>.

<sup>1</sup> *Instituto de Investigaciones Estéticas, Universidad Nacional Autónoma de México, MEXICO.  
e-mail. sandra.zetina@gmail.com*

<sup>2</sup> *Instituto de Física, Universidad Nacional Autónoma de México, MEXICO.*

<sup>3</sup> *Instituto Nacional de Investigaciones Nucleares, MEXICO.*

<sup>4</sup> *Instituto de Geología, Universidad Nacional Autónoma de México, MEXICO.*

**Abstract.** Regular trade between Europe and Asia created a taste for the Oriental during 17th and 18th centuries. Silk fabrics, tapestries, lacquered furniture and other goods were imported, but at the same time, local craftsmen imitated Asian decorative techniques, and Asian cabinetmakers developed a special production for exportation. In New Spain - Colonial Mexico - the Acapulco harbor served as the direct entry for Asian goods. Two pieces, a cabinet and a folding screen, both with Chinese motifs painted in bright red along with metal applications from the Franz Mayer Museum were studied. The material study provides a particular insight into the production of furniture, and considers the imitation of Asian lacquers with Western materials. An integral analytical approach, including imaging techniques such as IR reflectography, UV-VIS imaging, radiographs, as well as non-destructive characterization by XRF, and selective sampling was done. Cross sections of the micro samples permitted the study of the layering decorative technique; microstructure analysis was performed with SEM.

**Keywords:** Polychrome furniture, IR reflectography, UV-VIS imaging, radiographs, PLM, XRF, SEM.

### **INTRODUCTION**

Technical studies reveal critical information for establishing the provenance of an artifact, but when additional data regarding the provenance is absolutely absent the interpretation of the technology is central; mainly if the object, like in the present case, is a cross-cultural product.

In the present study a folding screen and a cabinet from the Museum Franz Mayer's collection with similar chinoiserie scenes and colors were studied in order to bring more information about their provenance. Both objects share common traits: a glossy finish, a bright red background, metal

applications, and a limited palette. In both cases, the Chinese motifs were finely delineated with black color. Regarding the iconographic features art historian Gustavo Curiel has inscribed them into the last part of eighteenth century, and proposed New Spain or Manila as their possible place of origin [1]. The aim of this study is to define the facture of both objects, and to look for a technical explanation that contributes to support Art History's attributions.

Chinoiserie is a term related to the imitation of objects manufactured in Asia, something that happened throughout the Western world when encountered with artifacts from Oriental traditional techniques (silks, lacquered boxes and furniture,

porcelain), and that can be called a worldwide phenomenon. New Spain received an important influence of the Asian cultures because a direct trade route through Manila and Acapulco, in the Pacific Ocean was established since 1565 [2]. The export of goods from China by the Manila Galleons, had to cross New Spain's wide territory to reach the Atlantic, and from there carry on to Seville. This encounter created a taste for the Asian, and New Spanish craftsmen and artists began to create objects in an "Oriental fashion". Some copied their Chinese equivalents, for example, ceramic designs imitated porcelain; but others, like the folding screens, were new in their function and were rapidly adopted by New Spain's society. The concept was reutilized but transformed in materials, techniques, sizes, or topics. Folding screens became and almost indispensable good in New Spanish houses during 17th and 18th centuries [3]. Inexpensive and unpainted versions were also available: most of the houses had a folding screen to divide spaces. Different sizes of folding screens served different purposes: some were designed to conceal the bed, others used for the *estrados*, reception chambers in raised platforms [4]. This screens were usually made with a wooden structure that held together a series of stretchers with canvases of linen cloth, in most cases, different from the Japanese or Chinese ones, which were absolutely made of wood, or else, with stretchers with silk screens or several layers of mounted paper. The painting technique also differs considerably: Asians used resins obtained from the resin tree *Rhus verniciflora* and the wax tree *Rhus succedanea*, known as *urushi* in Japan or *chi* or *chiam* in China. There are at least five lacquer techniques used throughout Asia; painting with lacquer, inlaid lacquer, carved lacquer, surface relief work and the use of metallic leaf and powders [5]. Around the seventeenth century, several European recipe books collected information about Asian lacquering techniques and also techniques to imitate the effects of these objects. In the Hispanic tradition, the Genaro Cantelli and the Francisco de Orellana books of secrets and recipes compiled and translated information from French, Italian and possibly English books [6].

There are very few publications regarding the study of the techniques involved in the construction of chinoiserie furniture in New Spain. In comparison, the Asian lacquering techniques have been fully analyzed, and also some studies from examples pertaining to France, England and Brazil, have been performed. The approach of this study is to give more information about these particular objects: to compare the manufacturing technique of both furnishings, and to contrast this results with the technical studies of chinoiserie from other parts of the world, as well as to the existing books of secrets written in Spanish.

From the reading of the 18th century Western recipe books, one can think that the features of the

Chinese lacquers that Westerners were most keen on are the golden effects, the smooth surfaces, and their saturated colors; since many recipes are directed to attain this goal. In this study we will focus mainly on the technique used to obtain the red color of the surface, and the golden effects. We will leave aside the complex modifications of the cabinet, and the painting technique on the whole.

## ANALYTICAL STUDIES

A general observation of the physical characteristics of the furniture under visible light and other radiations allowed determining the homogeneity of sections. UV lighting was used to detect interventions, and the response of some pigments and varnishes. IR reflectography proved useful to see some preparatory drawings, and gave information about the composition of the pigments, due to their opaque or transparent response to infrared radiation. X-ray images were taken to define the general structure of the wooden pieces; it helped notice posterior aggregates or interventions, and gave information on the technique and composition of the pictorial layers.

XRF informed on the chemical elements of the materials, and it was performed in situ (Mo X-ray tube, 45 kV, 0.2 mA) with portable equipment [7].

Cross-sections of the micro samples were analyzed by polarized light microscopy (PLM) at the Laboratorio de Diagnóstico de Obras de Arte, IIE, UNAM. Samples' microstructure and composition was analyzed with scanning electron microscopy (SEM 5900 LV fitted with an EDX microprobe Oxford with a Si-Li detector) at Instituto Nacional de Investigaciones Nucleares. Experimental conditions were 20 kV, 70mA, low vacuum mode, low vacuum pressure 20 Pa inside the microscope chamber. Organic materials (colorants, adhesives, mediums and varnishes) were not identified. The textiles were identified by their structure in transverse sections, and transmitted light at the LDOA, IIE-UNAM.

## THE OBJECTS

### Chinoiserie Folding Screen

The folding screen (Figure 1) is composed of twelve canvas mounted on wooden stretchers (the dimensions of each frame are 230 x 45 cm, the total length extended is 540 cm). This kind of structure is coincident with other folding screens from New Spain dedicated to conceal the bed, as the one called Courtship and Leisure on the Terrace of a Country Home, ca. 1750-60.



**FIGURE 1.** Folding screen, Franz Mayer Museum, Mexico City.

Even if the topic is quite different, the structure is also conformed of arches at the top, and a rectangular frame at the bottom, with foot and *chinoiserie* depictions [4]. The scene represents a walled village: the houses are depicted as traditional pagodas and people are dressed in an oriental fashion. The village is surrounded by a landscape composed of lakes and mountains. The scale indicates a representation on simultaneous planes: at the extremes of the folding screen, and the lower part of the different sheets the objects are bigger to convey their closeness to the viewer. The uppermost figures represented in a tiny scale, are the farthest planes of the composition. The architecture follows its own rules of perspective.

The canvas was identified as flax by PLM (polarized light microscopy): the linen is thin, simple woven. The back of the screen is also decorated with monochrome designs in blue over white. It looks like tempera because of the matte finish. The painting is divided at the middle by the cross bars of the stretcher: on the upper part are mountains and oxen on different landscapes; the lower parts are painted with flower bundles.

### **Chinoiserie armoire**

This wardrobe (Figure 2) reutilizes four old panels with chinoiserie decoration; the structure of the furniture is modern, as the drawers and shelves in the interior reveal. The decorated panels were painted on a canvas, glued to a wooden support, which was cut by an electric saw, and later attached to the modern structure. The texture of the linen cloth is visible with ranking light. The back of the armoire reutilizes antique planks without decoration. X-ray images show

that the original panels had some damages and also a conservation treatment.

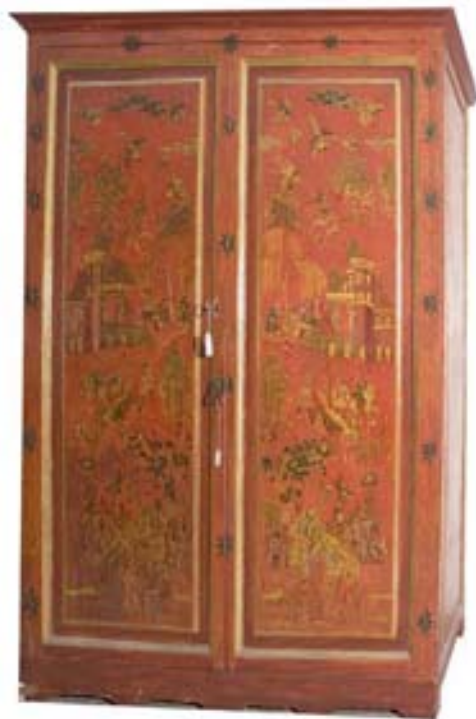


**FIGURE 2.** Armoire, Franz Mayer Museum.

The designs of the front panels are identical, a hunting scene, painted in mirror. As in the folding screen, the lower depictions are bigger in scale, to represent closeness, and there is a division in three horizontal registers: an aquatic in the lower part,

earthly in the middle, and celestial in the upper part. In the first plane, herons rest in a lake surrounded by rocks with flowers, the second develops the hunting scene, and in the sky a group of birds fly around clouds, painted in the oriental manner. The lateral panels are also divided in three: in the lower register there is a dragon, the middle portrays a large vase full of flowers, with butterflies and birds surrounding them. The upper register consists of undulated clouds with birds, similar to the front panels.

### Grounds

The folding screen has a painting technique similar to that of traditional eighteenth century oil on canvas. The linen was prepared with a porous white ground, composed of calcium carbonate of organic origin. The morphology of these particles has a quadrangular shape, and microscopic tunnels. The particles were interpreted as fragments of calcareous filamentous algae: EDX analysis shows a high percentage of Ca and a low percentage of Mg that may be related to the surrounding bedrock, possibly a magnesian limestone (Figure 3). These structures are only viewable with SEM at 1000X magnifications or higher.

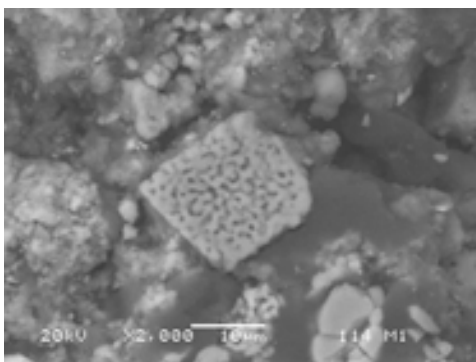


**FIGURE 3.** Calcareous filamentous algae, preparatory layer, folding screen (M1): EDX: 42% C, 31% O, 2.2% Mg, 22.3% Ca, less than 1% Si, P, S, K.

The armoire has at least two different kinds of white ground: the front panels' plaster is made of diatoms exoskeletons seen with SEM at 3000X (Figure 4). The composition of these particles is mainly Si, but the diatoms are mixed with other acicular particles of gypsum (Ca and S in SEM), that were either original to the bedrock or added. The lateral panels of the armoire present a double layer: one made of diatoms and gypsum, and on top of it, another one of calcareous filamentous algae, identical to those found on the folding screen ground. This white ground composed of algae relates both objects, although, as it will be explained later, are not identical in the pictorial stratigraphy, bronzing and gilding techniques.

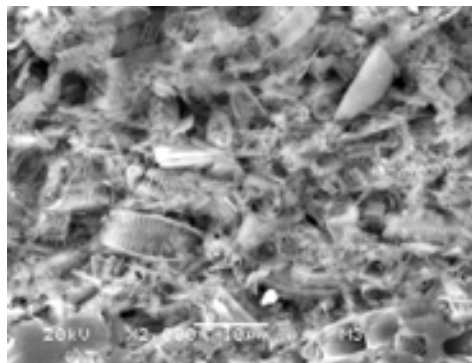


**FIGURE 4.** Diatoms and gypsum particles, preparatory layer, cabinet (M3): C 43%, O 27%, Ca 12%, S 9%, Si 8%. The punctual test on the diatoms raised Si content to 18%.

### Red layering

The cabinet and the screen have a layering process that use different red pigments. The application sequence places the less expensive or precious pigment in the first strata, and the most expensive in the last. The final appearance is obtained by the succession of red colors that constitute the background. On the folding screen a red iron oxide (a natural clay) was applied after the white ground. This coating was covered by a layer of red lead (minium), and lastly by another one of extremely thin vermilion. The armoire only has the layers of red lead after the ground and then the vermilion one. On some samples, also a red glaze (of organic nature, possibly a red lake) was applied on top of the vermilion.

### Gilding and bronzing techniques

The folding screen has diverse golden effects, acquired through the use of different materials: gold shell (Au identified by XRF) to highlight sections of clothing on people, animals, flowers and architectural details (figure 5). Other areas were completely covered with brass flakes and brass leaf that were colored with glazes of yellow, green or brown tonality to modify the metallic surface.

Figure 6 shows the stratigraphic sequence of a gilded tree branch, and its composition in EDX: over the red finish a green glaze made of massicot and Prussian blue with a lot of medium (C, O, Fe and Pb) was covered by a very thick layer of organic mordant (C, O, Ca, Fe) that adheres brass flakes; possibly Dutch metal, brass with high Cu content, low percentage of Zn (approximately 10%). The brass was colored with a green glaze made with a few particles of verdigris or copper resinate, and massicot (Cu, Pb) in a lot of medium. These metal applications have a dark (almost black) response to ultraviolet light, whereas the areas painted with gold powder respond

with an intense yellow. There are two kinds of gold decorations, one uses gold leaf, and the other gold shell (powdered gold). It is possibly an oil base gilding, yet further analysis are to be done. All the motifs were delineated with black lines.

In the cabinet most of the gilding is composed of gold leaf (Figure 7). The gilding was placed over a thin red colored layer rich in medium that in SEM-EDX has Pb and Ca (Figure 8). We did not analyze the organic content but the application technique points to an oil based gilding technique. A dark glaze was placed over the gold leaf, which contains Si and Ca, it is possibly a colored varnish with lakes. The trees and some delicate brushwork also contain some percentage of silver in the gold powder.

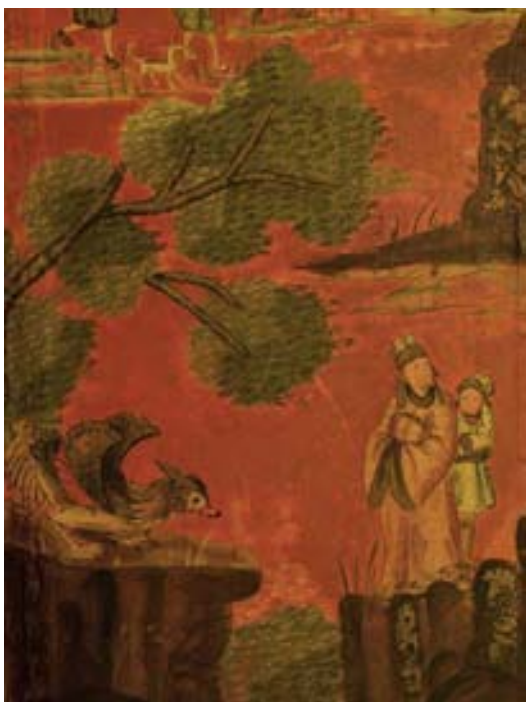


**FIGURE 5.** Folding screen, panel 4, visible light, IR reflectography and UV images. Gilded areas are yellow under UV, and brass with glazes looks dark.

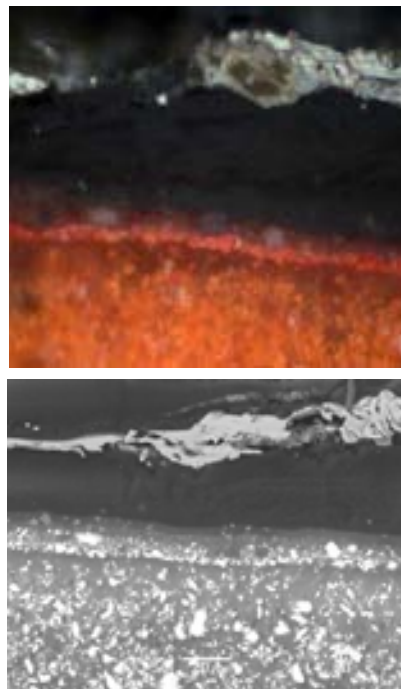


**FIGURE 6.** Sample 1, folding screen's stratigraphy, from bottom to top: minium, vermilion, red glaze, green glaze, mordant, brass flake, green glaze.



**FIGURE 7.** Cabinet, right door panel, visible, UV and IR images. Gold leaf over the clothes, and gold powder applied with brush seems yellow under UV. Pink and blue colors, transparent to IR, and with K, are possibly lakes or dyes.

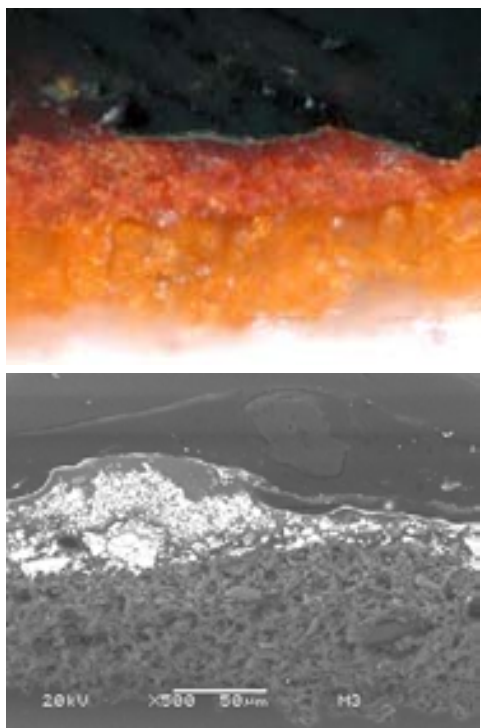


**FIGURE 8.** Sample 3, armoire's stratigraphy, from bottom to top: minium, vermilion, red glaze or mordant, gold leaf, green glaze, modern varnish.

### XRF Measurements

Due to the fact that the objects were sampled in very few areas to determine the general stratigraphy of the paintings, XRF served as the basic guideline to determine the pigments' composition. All the measurements in the cabinet detected Pb and Hg in high intensity; Ca, Cu and Fe occurred in varying concentrations; changes in these elements depend on the analyzed color (Figure 9). The regular content of Pb and Hg, is a result of the lead red and vermilion ground layers that cover the whole surface, as well as Ca, that comes from the calcium sulfate ground. A strong signal of Ni was found in the low intensity region of the XRF points of analysis; this may be due to the fact that the object was varnished in the 20<sup>th</sup> century. The signal of Fe increased in ochre, red and brown colors, indicating the use of earth pigments. A low intensity indicator of Mn appeared on the dark brown colors, due to pyrolusite (manganese dioxide) present in brown ochre. Prussian blue may be present in some dark blues and greens due to the raise of the Fe signal. Additionally greens contain As, that may indicate the use of orpiment, although it was not found in yellow colors. Some cherry red colors, that have a transparent response in IR reflectography, raised K and Ca intensities, possibly indicating red lakes. Some

brass powders (Cu, Zn) are related to later overpainted areas where Cr, Ba are present.

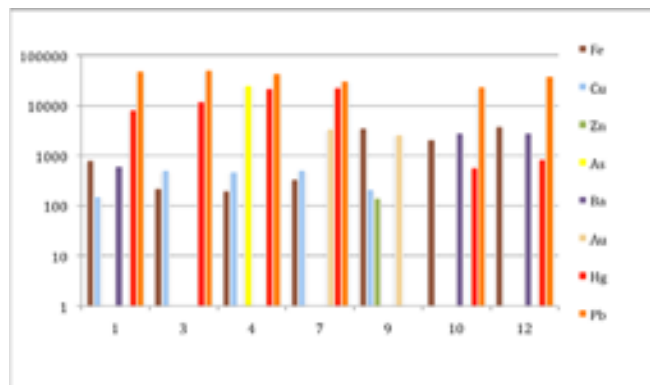


**FIGURE 9.** XRF areas of analysis on lateral panel of the armoire, the Ba contents indicate areas of repair (1, 10 & 12). Under IR lighting the green leaves are transparent.

In general, the overpainted areas have Ba and Cr in medium to low intensities. Ba was also identified with SEM-EDX in the red overpaint as barite, a common paint extender. On the other hand, the areas with more recent retouches in the yellow and green colors have Cr, due to the use of yellow and green chrome pigments.

The folding screen has Pb, Hg Fe, S, Cu and Ca in almost all the sampled areas, due to the preparation layers and the background: minium, vermilion, red iron oxide and calcium carbonate. The Cu signal is present in almost all the measurements, and raises in areas with copper resinate. The presence of Ni (in 26% of the areas studied) has to be analyzed with more profundity, at the time being we believe it has to do with a restoration varnish, and it links this object, or its treatment with that of the cabinet. Yellow and green colors have orpiment (As), this element was also found on some regions with brass. Contents of Ba were detected in overpainted areas. The application techniques of the golden details reduce to two in the folding screen: brass leaf and flakes, detected by an increase in the Cu and Zn signals; and gold (possibly in powder) on details. On the other hand, blues from the back of the folding screen have a high content of K pointing to the use of an organic pigment, probably indigo, yet a low intensity signal of this element is reported on almost all the samples.

## DISCUSSION

This study gives prove of the differences and similarities present in the manufacture of both objects. The white ground made of calcium carbonate algae is present in the folding screen. The cabinet, on the other hand has a ground made of diatom and gypsum, but the lateral panels present a second stratigraphy with calcium carbonate filamentous algae. This relates both furniture, and at the same time points towards the use of different panels for the construction of the cabinet. White ground composed of relates both objects, although, they are not identical in the pictorial stratigraphy, bronzing and gilding techniques. The calcium carbonate filamentous algae have never been reported in other objects from the New Spain viceroyalty, yet not many folding screens from 18<sup>th</sup> century have been studied. A deeper research on the possible provenance of this kind of material may bring more clues about the origin of both objects.

The painting's support for the folding screen is made of linen cloth, on the cabinet we find linen on the lateral panels, but were not able to see this material on the front ones, even with the aid of X-ray radiographies. Again, the lateral panels of the cabinet share material characteristics similar to that of the folding screen.

The red layering process is similar to what Genaro Cantelli and Francisco de Orellana books of recipes recommend to obtain a color red, as "excellent as coral". After the gesso or ground, they advise to put a coat of lead red with glue, after it, a coat of cochineal lake, and then, cover it with ultrafine carmine, which is a lake obtained from Brazil wood [6]. Somehow, the method is to apply several red coats, following the idea of Chinese lacquers built in layers, but using materials that were common to their painting tradition. In the folding screen, the first coat of red iron oxide has enough tinting strength to cover completely the white ground, an also it may also help to prepare the surface as a priming, filling in the unevenness. Then, the minium layer gives a more vibrant color, although too orange, but promotes an effective use of vermilion, a more expensive pigment. Also in the cabinet, a similar logic was followed, but the red color started with a coat of lead red, then the thin vermilion coat, and possibly a red lake finish. The selection of pigments implicates a difference in the value of the furniture. The cabinet not only has a more expensive selection of pigments, it also only uses gold for the gilding; whereas the folding screen combines the use of gold with bronzing.

Craftsmen at faraway places such as France and Brazil followed similar strategies to obtain brilliant red surfaces that imitate the oriental lacquers. The study of an altarpiece with *chinoiserie* decorations at Catas Altas, Minas Gerais, Brazil, reports a similar sequence: a gypsum ground (gesso sottile and gesso grosso), a

layer of red iron oxides with graphite content (bole), a layer of red lead and vermilion, a mordant layer, copper resinate layer with metallic microleaves of brass (Cu with low amounts of Zn) covered with a coat of varnish. In other sample with similar stratigraphy, instead of bronzing the study reports the use of oil-size gilding placed over a mordant, delineated with black afterwards, and covered with a varnish; exactly the same procedure as in the furniture here studied [8]. On another study of the bronzing technique of sculptures in a 17<sup>th</sup> century French *chinoiserie* cabinet, the figures were coated with a chalked-base ground bound with a cow or horsehide glue medium. Next, it was applied a layer of red earth pigment, followed by a thin layer of vermilion, both bound with similar glue. Egg white or glair was used as a sealer over the red ground, after it, was applied a thin layer of pigmented oil mordant (vermilion, white lead and a heavily heat-boiled drying oil), and also, the bronzing powder was nearly pure copper [9] as found in the folding screen samples of the present study.

The most interesting feature of the manufacture technique of these objects is that they intend to produce the striking surfaces of the red lacquers with gilded areas, using strategies to produce transparencies and contrast with Western materials.

## ACKNOWLEDGMENTS

We wish to thank Gustavo Curiel, from IIE-UNAM who promoted this research; Héctor Rivero Borrell, Director of the Museum Franz Mayer, Ricardo Pérez Álvarez, Director of Conservation and Collections at Museum Franz Mayer, and Teresa Calero, for their support to carry out this research. This research has been partially supported by CONACyT Mexico grant MOVIL U49834-R.

## REFERENCES

1. G. Curiel, "Perception of the Other and the Language of 'Chinese Mimicry' in the Decorative Arts of New Spain" in *Asia & Spanish America, Trans-Pacific Artistic & Cultural Exchange, 1500-1850*, Denver: Denver Art Museum, 2009, pp. 25-30. Gustavo Curiel asked for this study, he also found possible connections with contemporary prints in treatises on chinoiserie.
2. D.F. Lach, E.J. Van Kley, *Asia in the Making of Europe*, Vol. 3, Chicago: University of Chicago Press, 1998, p. 37.
3. D. Pierce, "At the Crossroads: Cultural Confluence and Daily Life in New Spanish Painting, 1550-1700" in *Painting a New World. Mexican Art and Life 1521-1821*, Denver: Denver Art Museum, 2004, p.30.
4. G. Curiel, "Courtship and Leisure on the Terrace of a Country Home" in *Painting a New World, in Painting a New World, Mexican Art and Life 1521-1821*, Denver: Denver Art Museum, 2004, p. 226-229.

*LASMAC & IMRC 2009 – Selected Papers*

5. M. Webb, *Lacquer: Technology and Conservation*, UK: Butterworth, 2000, p. 3-4, 38.
6. G. Cantelli, *Tratado de Barnizes y Charoles*. Valencia: Joseph Estevez Dois, 1735, and F. V. Orellana, *Tratado de Barnices, y Charoles*. Calatrava: Joseph García, 1775.
7. J.L. Ruvalcaba, D. Ramírez, V. Aguilar, F. Picazo, *X-ray Spectrometry* **39** (2010) 338-345.
8. L.A.C. Souza and C. Avila "Chinese Motifs in the Baroque Art of Minas Gerais, Brazil" in *Painted wood: History and Conservation*, Williamsburg Virginia, November, 1995, Los Angeles: The Getty Conservation Institute, 1995, p.212.
9. A. Heginbotham, "Hercules and Hyppolita Reinterpreted: A Technical Study of Two Sculptures on a Remarkable Cabinet by André-Charles Boulle" in *Verband der Restauratoren VDR Beiträge*, Bonn, 2007, num. 1- 2, p. 33 -44.

## The Sky of Salamanca. An Example of Experimental Methodology Applied to a Singular Work of Art

M.A. García<sup>1</sup>, M. Gómez<sup>1</sup>, D. Juanes<sup>2</sup> and C. Vega<sup>1</sup>

<sup>1</sup> *Institute of Cultural Heritage of Spain, Madrid, SPAIN. e-mail: djuanes@ivcr.es*

<sup>2</sup> *Valencian Institute of Conservation and Restoration of Cultural Heritage, Valencia, SPAIN*

**Abstract.** The Sky of Salamanca is the unique Renaissance mural painting attributed to Fernando Gallego, about 1480. It has a special interest in his splendid pagan iconography related to Astronomy. In the middle of the s. XX paintings had been detached by "strappo" to remove from the vault of the old library to the hall of the Museum of the University of Salamanca. A detailed study on the new site shows that the appearance of the paint differ from the historical moment of its execution, while much of the pictorial layers, that reflects the making process of the artist, remains in the original location. The professionals of the Institute of Cultural Heritage of Spain, in collaboration with an expert from the Valencian Institute of Conservation and Restoration of Cultural Heritage developed an ambitious study to provide evidence for the remnants of Gallego and differentiate them from subsequent restorations. This would facilitate any intervention, as well as to provide a new view of the author for historians of the art. This contribution shows the previous studies methodology supporter by both institutions and the wide variety of analytical techniques employed, improving the results and minimizing the damage. First, photographs were made with infrared CCD and UV fluorescence, providing damages and losses and additions materials mapping. Then, a scanning X-ray fluorescence without sampling was made to identify materials and their surface distribution. Based on the results the planned extraction of microsamples was planned to complement the study. Their analysis has provided the identification and exact location of the materials used by the painter and the damage due to subsequent interventions.

**Keywords:** Renaissance mural painting, infrared CCD photography, UV fluorescence photography, X-ray fluorescence, microsampling analysis.

### INTRODUCTION

The Sky of Salamanca is the unique Renaissance wall painting attributed to Fernando Gallego, about 1480-1490 [1]. These paintings decorated the ceiling of the ancient library of the University of Salamanca, and has a special interest in his splendid pagan iconography related to Astronomy. It's a new theme in the Spanish wall painting and represents the sky with the constellations interpreted by cultural renaissance Spanish mentality of second half of the XV century.

In 1506 the paintings were severely damaged when the floor of the library was removed to install a new altarpiece in the chapel below. The wall paintings were restored in early sixteenth-century too. Several figures of whole were repainted with oil painting on original temple painting and many stars from the sky background were removed. This affected negatively the original composition of the wall painting.

Around 1760, two thirds of the sky of Salamanca collapsed, leaving in place only the section we know today, at the end of the chapel. Between 1761 and 1767, a new vault was constructed below the original

and the remains of the sky of Salamanca were abandoned and forgotten [2].

In 1950 the mural was taken down by "strappo" process and moved to its current location, at the Museum of the University [3]. The way how strappo process was made, it caused that a lot of paints in the original location, in addition to the preparatory drawings, decorated and gilded moldings, etc. In addition, in the process of moving the paint was repainted (figure 1-2).



**FIGURE 1.** Cloak of the Sun God at the current location



**FIGURE 2.** Remnants of the cloak of the Sun God at the original location.

New consolidants were added (wax) that are causing important conservation problems (flaking, loss of paint...). However, only in the museum of the University we can get the overall impression of wall painting. So, in this situation with the problems presented by the wall painting and the great importance for the history has this work of art, the professionals of the Institute of Cultural Heritage of Spain (IPCE), in collaboration with the Valencian Institute of Conservation and Restoration of Cultural

Heritage (IVC+R) developed an ambitious study to provide evidence for the remnants of Gallego and differentiate them from subsequent restorations. This would facilitate any intervention, as well as to provide a new view of the author for historians of the art.

## METHODOLOGY OF STUDY

This contribution shows the previous studies methodology supporter by both institutions and the wide variety of analytical techniques employed, improving the results and minimizing the damage. The analysis were made in both locations following a logical sequence in which the results of a technique were the basis for the study to the next, taking into account that the techniques used are subject to the work of art and to the aim of the analysis. First, non-destructive techniques without sampling are used, starting with global studies and punctual analysis. The infrared and UV fluorescence CCD photographs gave us damages and losses and additions materials mapping. A scanning X-ray fluorescence without sampling was made to identify materials and their surface distribution.

Based on those results, extraction of microsamples was planned to complement the study. Their analysis has provided the identification and exact location of the materials used by the painter and the damage due to subsequent interventions. This step is based on all previous results, making the microsampling an optimized process that minimizes its number and the damage to the object.

The experience shows that the analytical studies, with or without sampling, provide desired results and other unexpected, and their combination enhances this possibility can greatly enrich the studies [4]. This combined analytical methodology can also generate new questions and doubts which were not raised at first and may have great importance in preserving the object.

## RESULTS

### Infrared and UV fluorescence CCD Photography

#### *Present Location at the Museum University*

In the analysis by infrared and ultraviolet photography, we used two digital cameras with CCD, which reaches 1.1 micron spectral range, (NIKON D-80 and Nikon D-100): one for the visible and the infrared. A platform was used that allows a complete

scanning of all the paintings. In total 196 images were taken.

Then, UV photography study was made. This technique has allowed us to detect the original paint from the current location, fillers and coatings materials used during the restorations, and repaint and colour retouching (figure 3).



**FIGURE 3.** UV CCD photography of the centaury at the present location.

### EDXRF Analysis

An X-ray fluorescence study was made based on the results of the visible, infrared and ultraviolet photograph analysis. An extensive scanning of the two locations was made. In total 254 areas (5 cm diameter) was studied, 67 correspond to the remains of the wall painting of the original location (figure 4) and 187 correspond to paint of the University Museum.



**FIGURE 4.** The X-ray fluorescence device during the analysis process of wall paintings in their original location.

We compared the remains of paint at the original location over the chapel of the University with the paintings at the University Museum after it's moved.

### *Original Location on the Chapel*

The data analysis allowed us to identify the original pigments and the pigments used in restoration of the 16th century. Thus, white is lead white. We detected two blue pigments: azurite and an organic pigment or ultramarine blue (the X-ray fluorescence technique can not differentiate between these pigments), the red is vermilion; the orange colour was obtained through red lead or an organic dye. We found two green pigments, a green copper and other organic dye. We also identified two brown pigments, earths and organic dye. And finally, the painter used an organic black and gold for gilding.

### *Present Location at the Museum University*

Then X-ray fluorescence analysis was made on the paintings in the present location. In choosing the points of analysis was very useful photographic documentation of both locations, allowing us to distinguish which parts of the mural painting came from the original location and were retouching areas.

The results of the analysis EDXF of the wall paintings in the present location provides us three different kinds of areas:

*-Original:* Painting areas that were in the original location.

*-Overpaint or isolated retouching:* rest of original paintings that were punctual or partial retouched.

*-Colour retouching:* areas where the original has been lost, and where a new paint layer similar with the original areas around them, was applied.

An example is the white colour areas analyzed. The white areas generate three different X-ray fluorescence spectra. The original zones are characterized by the presence of lead, the isolated overpainting areas is characterized by the presence of calcium, zinc and lead. Finally, the colour retouching areas has calcite and zinc only (figure 5).

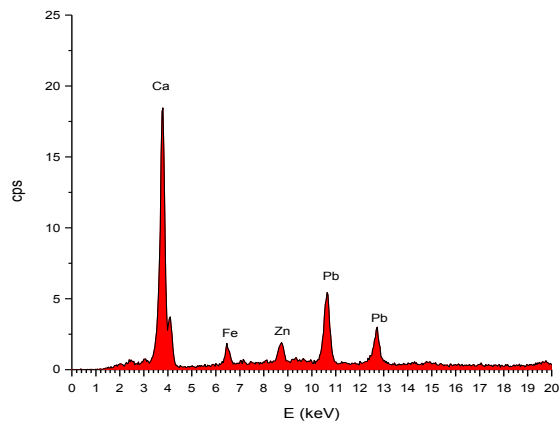


**FIGURE 5.** EDXRF spectra from a white retouching area.

A way to jointly judge the results and differentiate between different types of areas is to represent fluorescence peak net area of various elements normalized to 100 for each white zone analyzed (figure 6). In the case of white colour, the lead white is the remains of the wall painting were in the original location. The chromatic reintegration areas are characterized by white zinc and / or lithopone. Finally, the overpaints are characterized by the presence of white lead and zinc white.

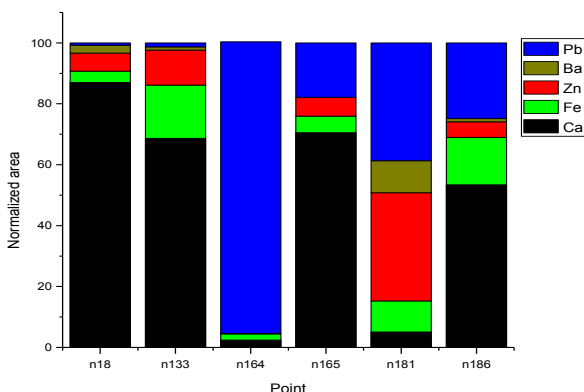


FIGURE 6. The fluorescence peak net area of various elements normalized to 100 for each white zone analyzed

Another example is the blue areas. Some blues is characterized by the presence of copper and lead, other areas by the presence of calcium, iron, barium, zinc, and finally we have spectra with the presence of zinc and lead.

In the same way, we have been identified the original areas by the presence of lead white and azurite, colour retouching by zinc white and / or lithopone and an organic blue pigment and finally, the overpaints areas are characterized by cobalt blue, titanium white and lead white (figure 7).

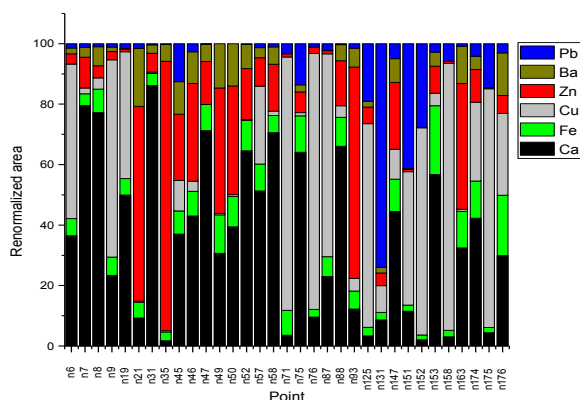


FIGURE 7. The fluorescence peak net area of various elements normalized to 100 for each blue zone analyzed

The results of the X-ray fluorescence analysis of paintings at the present location allowed us to identify the different pigments used in the retouching process

after the strappo process. So, the lithopone and possibly calcite was used as filler in big lost of paintings, the zinc white and titanium white were used like white pigment, and the yellow pigment is organic pigment. We have identified two blue pigments, an organic pigment or ultramarine blue and cobalt blue. As regards the red pigments used in restoration, have identified three along the vault: red earth and probably lithopone or cadmium red. The orange was made with cadmium red or red lithopone and the green is an organic dye. The browns were obtained with brown earths and an organic dye and the black is black organic. Finally, the gilded was made with gold, false gold and an organic pigment.

### Microsamplig Analysis

Finally, an analysis of microsamples taken from both locations was made. The microsampling was very limited and planned. It was based on the results obtained with the non-destructive techniques [5].

First we used microscopic analytical methods such as optical microscopy and scanning electron microscopy. Optical microscopy was used to study cross sections, stain tests and study of thin films. The scanning electron microscopy was used for identification of elements and produce maps of distribution of elements. Then we have also been used instrumental techniques such as FTIR and GC-MS for the analysis of binding media.

### Original Location on the Chapel

The study began with the microsamples taken from the original location. The objectives of this analysis in the original location were the study the Renaissance painting technique, the detection of eighteenth century repainting and overpaints which may correspond to older restorations, to determine the materials added at the current location and to distinguish them from the original location, and to establish the most suitable environmental conditions for its conservation.

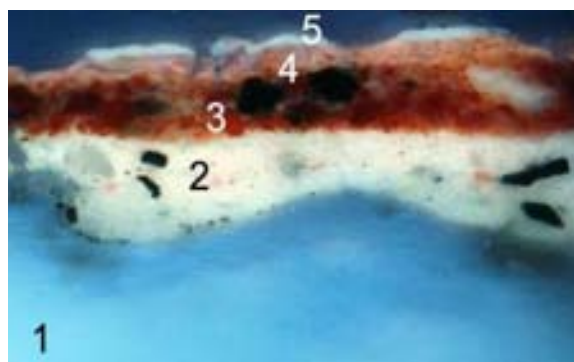


FIGURE 8. Cross section from deep red from Mercury's hat, obtained by optical microscopy with Wood's lamp

Several samples were taken of different areas and colours. This has enabled us to know the original materials used in painting, and later added materials (Table 1). On the other hand, has allowed us to detect potential problems of conservation of the original paintings. The figure 8 is a cross section of a red sample from the mercury's hat obtained with Wood's lamp. The cross section shows the gypsum plaster layer (1); a light grey pink layer made with red lake, lead white and black carbon (2); a deep red obtained with vermilion small amount of carbon black (3); a glaze layer made with red lake (4), and rest if glue from the strappo process (5). These glue residues on the surface of the wall painting may cause conservation problems because the dirt is fixed on layer, obscuring the painting. In addition, the glue is hygroscopic, which may create other conservations problems.

#### *Present Location at the Museum University*

The study paints at the present location was also very limited and planned. The microsampling was based on the results from the non-destructive techniques. In this case the aim of the study was not only related with the original and added materials, but for other very important related with the optimal environmental conditions. So, the objectives of this study were:

- To identify the materials and the sequence of layers; to distinguish the repainting of the layers from the original location.
- To study the alterations produced by the strappo process.
- To answer the questions created with the visible, infrared, UV and EDXRF analysis.
- To identify problems that the presence of certain materials may cause with the variation of environmental conditions.
- To advise on those material aspects that can influence the restoration process.

The first result is the identification of materials in paints, differentiating between the original materials and additives in the moved process (table 2).

The cross section of several microsamples that was at the original location shows a similar sequence of layer. The figure 9 is an example of a blue-greenish sky. In the cross section we can see a layer of gypsum mortar, a layer of carbon black, remnants of original blue layer obtained by lead white and azurite. Then there is a whitish layer of lead white, red lead, gypsum and calcium carbonate, and finally, a layer of light blue with Prussian blue on alum and lead white. In this sample, it is important that the layers 5 and 6 are organic coatings added after the strappo process.

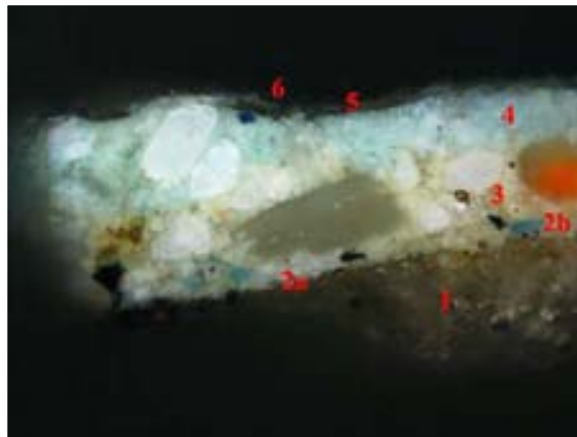


**FIGURE 9.** Cross section blue-greenish of sky, obtained by optical microscopy with incandescent lamp

Other samples show the use of fillers and coatings, like de beeswax and paraffin, and also have identified the causes of different alterations in the wall paint as loss in the plaster and the original paint layer, disintegration, flaking and stair-shaped layers.

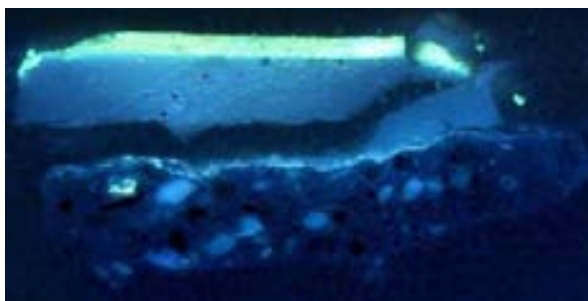


**FIGURE 10.** Cross section from yellow star, obtained by optical microscopy with Wood's lamp

The figure 10 shows an example of several conservation problems that the mural painting at the present locations has. It is a microsample from a yellow star at the blue background sky. First, there is filler made with calcium carbonate, gypsum, earths and industrial pigments bound with paraffin, and then there is a coating layer of beeswax and finally a yellow overpaint.

The animal glue used in the strappo process and was not subsequently removed causes paint flakes. It has also been observed separation between the paint layers is due to the low adhesive strength of beeswax. The wax also causes the surface stains on the entire surface of the painting, probably due to animal droppings or dirt adhering to the wax.

**TABLE 1.** The materials identified in the analysis of microsamples from the original location

<b>Original material</b>	
Mortar	White plaster: gypsum adulterated with small quantities of calcium carbonate and earths
	White plaster: pure gypsum
	Binder: animal glue
Painting layer	White: lead white
	Yellow: lead-tin yellow and earths
	Blue: azurite
	Orange: red lead
	Green: verdigris
	Brown: earths
	Blank: carbon black
Binders: linen oil and egg	
<b>Added material</b>	
Ground	There is not mortar or intermediate plaster
Painting layer	Lead white, Prussian blue and Paris green
Coatings	Animal glue from strappo process

**TABLE 2.** The materials identified in the analysis of microsamples from the current location

<b>Original material and old restorations</b>	
	White plaster: gypsum
	Binder: animal glue
Painting layer	White: lead white
	Yellow: lead-tin yellow and earths
	Blue: azurite, Prussian blue
	Red: vermilion and red earths
	Orange: minium and earths
	Green: verdigris
	Brown: earths
	Blank: carbon black
Binders: linen oil and egg	
<b>Added material in the strappo process</b>	
Ground	Calcium carbonate
Painting layer	White: barium white, zinc white, lithopone and titanium white
	Yellow: organic pigment and cadmium yellow
	Blue: artificial ultramarine blue and cobalt blue
	Red: cadmium red
	Green: organic pigment
	Violet: cobalt violet
	Brown: earths
Binders: dry oil, probably nut oil	
Coatings	Animal glue from the strappo process
	Beeswax

## ACKNOWLEDGMENTS

We explicitly acknowledge the contribution of Leandro de la Vega, restorer from the IPCE, Araceli Gabaldón and Tomas Antelo, from the physical studies department of IPCE, and finally Pedro Pablo Perez and Angela Arteaga, from laboratory of materials of IPCE.

## REFERENCES

1. M. P. Silva, Maroto, *Fernando Gallego*, Caja Duero, 2004.
2. L. E. Rodríguez-San Pedro Bezares, *Historia de la Universidad de Salamanca, V. II, Estructuras y flujos*, Ediciones Universidad, Salamanca, 2004.
3. J. Gudiol, *Goya* **13** (1956) 8-13.
4. M Gómez, M., Navarro, J.V., Martín de Hijas, C., del Egado, M. Algueró, M., González, E., Arteaga, A., Juanes, D., “Revisión y actualización de los análisis de policromía de la Dama de Baza. Comparación con la Dama de Elche” en *Bienes Culturales. Ciencias aplicadas al patrimonio*, numero 8, Ministerio de Cultura, Madrid, 2008, pp. 211-221.
5. M. Gómez, M. San Andrés, “Metodología de análisis físico-químicos en obras policromadas de gran formato”, en *La Ciencia y el Arte II*, M.A. Egido, D. Juanes, Instituto del Patrimonio Cultural de España, Madrid, 2010, 93-112.

## **Material Investigation in the Course of the Restoration of a Series of Colonial Paintings**

F. Eisner-Sagüés<sup>1</sup> and C. Ossa-Izquierdo<sup>2</sup>

<sup>1</sup> *Centro Nacional de Conservación y Restauración, Laboratorio de Análisis,  
Tabaré 654, Recoleta, CP 8420262, Santiago de Chile. CHILE. e-mail: feisner@cncr.cl*

<sup>2</sup> *Centro Nacional de Conservación y Restauración, Laboratorio de Pintura,  
Tabaré 654, Recoleta, CP 8420262, Santiago de Chile. CHILE*

**Abstract.** The restoration of the *Serie grande de Santa Teresa del Monasterio de San José del Carmen* in Santiago de Chile, a series seventeen paintings brought from Cuzco, Peru, around 1690, was a remarkable occasion to conduct an investigation with the objective of reconstructing the material history of the paintings, to understand deterioration and to assist intervention processes. Our interdisciplinary approach was that of a group conducted by conservators and assisted by conservation scientists, historians and photographers. All studies were made during the intervention, and considering that we were studying a serial painting, a workshop creation. Several non-destructive and micro-destructive techniques were used to answer material questions: radiography, infrared reflectography fluorescence photography, microchemistry tests, optical and electronic microscopy, x-ray diffraction and gas chromatography. The resultant corpus of material information is large and diverse, giving us a good picture of the general layer structure and composition of woods, fabrics, grounds, pigments and binders used by the artists' technique, and chronological changes of the series. In most cases results are coherent with historic and scientific references for colonial Peruvian art. However some exceptions and non solved questions are discussed.

**Keywords:** Cusco, Colonial Painting, SEM-EDS, cross-section.

### **INTRODUCTION**

The “*Serie Grande de Santa Teresa*”, representing the most important episodes in the life of Santa Teresa de Avila, is part of the rich patrimony owned by the Monasterio del Carmen de San José in Santiago de Chile. It's a series of seventeen paintings of large format (200X250 cm), on cotton fabric, from the late XVIIth. century, belonging to the Escuela Cusqueña. Currently, thirteen of these paintings are in the Monastery, while four are in private collections.

We ignore the path followed by the paintings to get to Santiago, because no commitment was found in archives, and the series is not mentioned on colonial sources and neither is signed. We have not explicit confirmation that the series was painted in Cusco,

nevertheless, all the aesthetic, historic and material investigation allow us to say that belongs to the Escuela Cusqueña.

The paintings are based on another series conserved in Santa Teresa Convent in Cusco [1], which was painted by the famous colonial artist José Espinoza de los Monteros, who used the Flemish engravings by Collaert and Gallé, as iconographic source. Both series are very similar, nevertheless the one in Chile is anonymous.

The objectives of restoration were to recover the mechanical-material stability of the paintings and the aesthetic and iconographic aspects, to learn about history and technology of colonial painting, and to understand the creation period and their original religious function.



**FIGURE 1.** Part of the restoration and investigation team on the workshop.

The restoration took 20 months, with 16 graduate and more than 20 non-graduate professionals, working together: conservators, chemists, photographers, historians and biologists. During August and September of 2009 all the paintings were shown to the public at a big exhibition at the National Fine Arts Museum. The exhibition also shows other paintings belonging to the Order, and didactic videos and animations showing conservation processes and analysis results. This was of main importance to understand the restoration of paintings that have not been out of the convent in 300 years.

Also during this after-project year, will be published a book that resume all the research done about the paintings [2]. Four chapters are included. One about the Flemish engravings on which the paintings are based. One about the Carmelo Order and another about Santa Teresa's spiritual life. And, of course, the chapter about the restoration and the materials and historical investigation, which in fact open the book.

Both the exhibition and the book are enormous achievements for us and for the development of conservation in Chile.

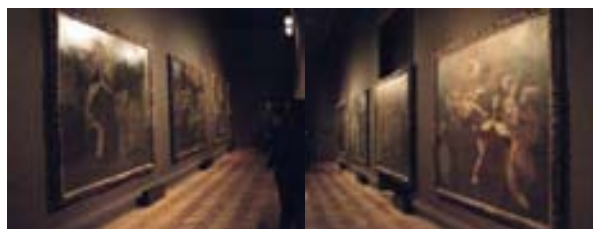


**FIGURE 2.** The exhibition of the restored paintings at the Fine Arts Museum in Santiago.

## METHODOLOGY

Our interdisciplinary approach was that of a group conducted by conservators and assisted by conservation scientists, historians and photographers.

All studies were made during the intervention, and considering that we were studying a workshop creation.

Science had as objective to identify the materials of the paintings and to complement the historic investigation; that is, to provide those pieces that history cannot. In consequence we had to understand the layer structure of the picture films with their varnishes and lacquers, to help to set cleaning levels, and to assist the comprehension of decay processes seeking realistic solutions with the most adequate materials.

The analysis techniques used were cross section observation, spot tests, morphologic and histological analysis, and instrumental techniques as electronic microscopy (SEM-EDS) and gas chromatography (GC-MS). All this was supported and contrasted with visual non-destructive techniques such as macro photography, UV fluorescence, IR reflectography and radiographies.

Conservation discipline allowed us to put together scientific studies with aesthetics and history, to understand the values that these paintings transmit from each area of knowledge.

## RESULTS

### The Woods

Stretcher's wood was identified as Cupresaceae family, Thuja genre. One case was *Thuja plicata* Donn. ex. Commonly known as "Western Red Cedar", Giant Cedar or Tree of life. Also *Thuja occidentalis* L. was found, known as "Northern White-Cedar", and also Tree of life. Both identified species are originally from North America.

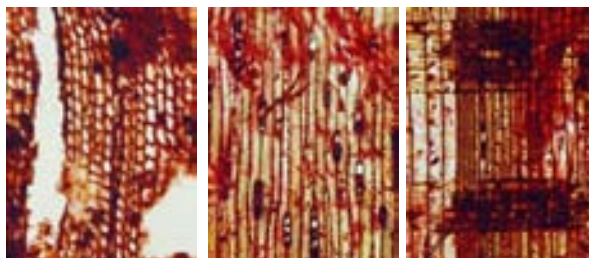


**FIGURE 3.** Stretchers made on Cedar from North America. Transversal, Tangential, and Radial view under the microscope. 10X, polarized transmitting light.



**FIGURE 4.** Frames made on Patagua, an endemic Chilean Tree. Transversal, Tangential, and Radial view under the microscope. 10X, polarized transmitting light.

Frames are made of *Crinodendron patagua*, *Elaeocarpaceas* family, an endemic Chilean tree, which tell us that frameworks were done in Chile and not in Cusco, as it was possible to think. They have on relief phytomorphic ornamentations, gold leaf, and are red painted as usual in Spanish baroque frameworks [3].

### Grounds and preparation

Most of the canvases had a first translucent amber layer with little ground, applied to improve the adherence of the ground preparation to the fabric. This layer has between 10 a 40  $\mu\text{m}$ .

Over this first layer we found a rough preparation, with heights from 50 to 400  $\mu\text{m}$ . Under the microscope the preparation is brown with plenty of black inclusions. In some cases we could find ligneous fragments, and red and translucent particles.



**FIGURE 5.** Cross-section showing gray preparation with black inclusions, and two ochre layers. 10X, polarized light.

Observation of thin sections allowed us to get deeper in grounds composition and to cross information with SEM-EDAX analysis. Were identified hydrobiotites (ferric mica), quartz y feldspars. Probably the preparation appearance does not correspond to the original, since according to archives information [4]; the paintings were “refreshed” by the nuns cleaning first with mixtures of turpentine and alcohol at 50%, and latter refreshing with linseed oil. Application of these products would have changed the color of preparation and altered its composition, making more confuse the original binding media characterization.

The binding analysis by GC for the preparation revealed presence of linseed oil, but in a low total fat of 3%. One hypothesis is that could corresponds to later interventions, as those mentioned by the nuns.

One painting called *Apparition in Segovia*, had a gray preparation. A theory that would explain the difference is that gray could be the original color for all preparations, and that refreshing mixtures had darkened them until the current brown-reddish tonality. In despite of the color, cross sections are similar in heights and grounds.

By SEM-EDAX, silica, aluminosilicates, iron oxides, lead, phosphorus and arsenic traces were found. Phosphorous is exclusively found in black inclusions, and allowed us to conclude that bone black was used.

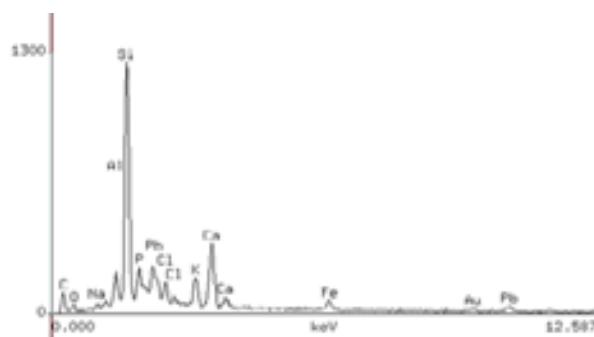


**FIGURE 6.** Spectrum of a black inclusion on SEM-EDS. Note the presence of phosphorous indicating Bone Black. Metallization: Au-Pd.

### Red lines

Some paintings presented a special preparatory drawing in fast and accurate red brushstrokes, sometimes non-coincident with the final image. This phenomenon, mentioned by Carrillo y Gariel [5] for mural paintings in Mexico, was clearly present in four paintings.



**FIGURE 7.** Detail of the red lines around the face of Santa Teresa.

The lines were so evident that we wondered if it was a preparatory drawing or some kind of re-marking of figures, as they look so superficial.

Cross sections helped to affirm that actually they are preparatory drawings, under-laying other colors; however it seems that the thick brushing produced the material losses over the lines. It was observed that the thicker the line, the more the layer losses.



**FIGURE 8.** Cross sections of two red lines on the same painting, showing the relationship between the thick of the red line and the losses of over painted layers. 10X, polarized light. SEM-EDAX showed differences between red paints in lines and those in final reds. The lines are composed mostly by pure hematite, while other reds have hematite, lead red and vermilion.

### The yellow “dots”

An intriguing phenomenon is something we called yellow dots, kind of dispersion of yellow particles randomly distributed, of variable dimensions, between 0.1 to 2 mm.



**FIGURE 9.** Detail of yellow dots over a green layer.

These dots are mainly associated with green and blue layers, and in general terms were observed on dresses and mantles, and in one case were found on the sky.

As demonstrated by SEM-EDEX, the yellow material is Orpiment or Arsenic trisulfide ( $A_2S_3$ ).

Among the thirteen paintings, orpiment only was found used as yellow layer, what means, used to be seen as yellow just in one case, *The ecstasies in front Avilas's Bishop*, on decorations of Bishop's mantle.

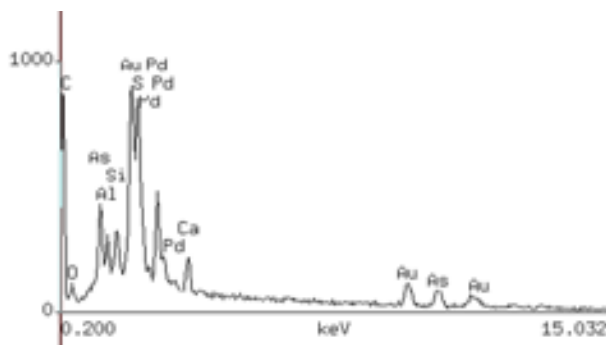


**FIGURE 10.** Spectra of orpiment grain on SEM-EDS. Presence of arsenic and sulfur. Metallization: Au-Pd.

Yellows are not common in this Series, and only are clearly appreciated on the *Coronation of Santa Teresa*, where the pigment is a yellow earth mixture.

Yellow dots are hard to understand. We should imagine that, on the freshly finished paintings, this chaotic pointillism was as evident as we see it today.

Our hypothesis is about a technological problem. Under the microscope we measured an orpiment bar of 500  $\mu\text{m}$ , which suggests a grinding subject. Orpiment has a monoclinic crystal structure that difficult size reduction to a few microns, as is adequate for pigments, especially when horizontal grinding is applied. Big fragments of orpiment wouldn't have mixed homogeneously, forming dots. Obviously the problem doesn't end there. We need to understand the relation between orpiment and green or blue layers. Since Carrillo y Gariel, green paintings are mixtures of blue (indigo) and yellow ochre [5] it seems that green preparation from yellow and blue was of common use, even starting from different minerals. Siracusano informs a very similar case to our green for the Marcos Zapata's *Salomon*, where green is a mixture of indigo and orpiment [6].



**FIGURE 11.** Cross sections of green layer with yellow grains included of disperse size. 10X, polarized light.

This explains the use of orpiment, but how do we explain yellow dots over blue cloths? It is evident that if pigments reach the needed grinding, blue and yellow will give green, otherwise will remain the same. However, how do we understand paintings where pointillism is so evident? We don't have the final answer, but we believe that the big format, thought to be watched from several meters, and the speed of creation, made dots overlooked.

## Organic materials

Two samples of pigments binding media were analyzed by GC-MS. One of them, a white from *The death of Santa Teresa*, through cluster analysis [7], revealed to be egg the binding medium, with no drying oils present, and with some collagen, what we assume as belonging to the preparation.

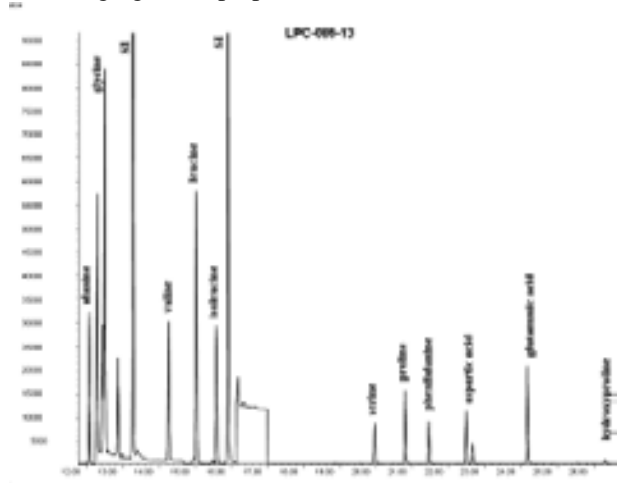


**FIGURE 12.** GC-MS chromatogram of sample composed by egg and some collagen.

The second sample, from “The ecstasy in front Avilas’s Bishop”, resulted to be only oil binder, probably linseed oil, meaning hence, this Series was painted in a transition period, in which both techniques, oil and temple, were used. In despite we analyzed only two samples, we think that is a relevant finding, however need further studies.

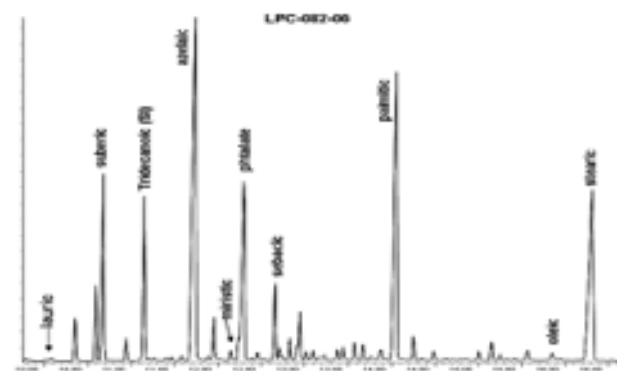


**FIGURE 13.** GC-MS chromatogram of sample composed by drying oil.

Also one sample of varnish was studied by GC-MS. The sample was relieved from a varnish accumulation on *Carmelo’s Reform*, which allowed us to obtain a “pure” fragment cleaned from other layers.



**FIGURE 14.** Drop of analyzed varnish.

The chromatographic peaks were mostly lipidic, with some triterpenic peaks. Here it is interesting how both, Carrillo y Gariel and Pacheco, mentions he use and preparation of oil varnishes, suggesting Sandaraca resin or Jupiner’s gum [5,8].

Some paintings showed us their organic colored glazes, what we usually found over colored layers which were applied to modify colors. Curiously in some cases we found only the glaze, and in others the glaze covered by an oxidized varnish. In microscopic level, it’s not always easy to differentiate between glaze and varnish. However, based on this and other facts, as for instance one painting not varnished and others without varnish under the frames, we believe that the paintings were varnished in an undetermined time after the creation, and probably partially cleaned even in recent times.



**FIGURE 15.** Cross sections of reddish-brown mantle with red glaze and over all varnish. 40X, polarized light.

## CONCLUSIONS

During the colonial period technique wasn’t at all only one in the entire continent. Other important artistic centers as Quito, México and Brazil had their own peculiarities. However all agree on the gradual adaptation to local materials, by the hand of incorporation to workshops, in an ever more decisive way, of Indian artists. That’s why colonial technique is still in a situation in which we know an important amount of materials and procedures, but we still found singularities, so different from those studied for

European painting, that many times we just overlook them as non-understandable, without finding if those singularities are the exception or the rule.

Usage of local materials, especially organic, speed of execution, and improvisation given the lack of materials signed on European handbooks, produced a technical framework still today on the way of being understood.

We learned to understand these series of paintings, leaving aside the rigid and static concept of Series, to adopt one more flexible where conducting threads as thematic, materiality, technology, pallet and iconography guides us to consider a group of paintings as a series.

The resultant corpus of material information is large and diverse, giving us a good picture of the general layer structure and composition of woods, fabrics, grounds, pigments and binders used by the artists' technique, and chronological changes of the serial. In most cases results are coherent with historic and scientific references for colonial Peruvian art. However some exceptions and unanswered questions are still on discussion.

This project was a great chance and a big challenge for us. We proposed to restore the material to bring back the historic, aesthetic and spiritual message. These canvases had never left the convent, and to keep them for two years, allowed us to carry on this investigation and learn more about colonial painting.

The extended time of research simultaneously to restoration, allowed us to guide sampling and analysis, encouraging new aesthetic and historic questions.

We believe that all this is give us a good starting point for further investigation on colonial art.

## ACKNOWLEDGMENTS

This research has been supported by the Centro Nacional de Conservación y Restauración, BBVA

Bank, National Law for Cultural Donations and Cooperación de amigos del Patrimonio Cultural de Chile.

Participation on LASMAC 2009 it's been possible thanks to the support of the Artistic and Cultural National Funds of Chile, (FONDART).

The authors acknowledge to Dr. Perla Colombini, University of Pisa, for GC-MS binders analysis; to Dr. Marta Maier, University of Buenos Aires, for GC-MS varnish analysis; to Dr. Mónica Rallo, Universidad de Chile, for woods identification; to Dr. Gladys Olivares, Universidad de Santiago de Chile, for SEM-EDS cross-sections analysis; and to Dr. Eugenia Fonseca, Sernageomín, for thin sections interpretation.

## REFERENCES

1. L. Mebold K., *Catálogo de pintura colonial en Chile. Obras en monasterios y conventos de religiosas de antigua fundación*. Ediciones Universidad Católica de Chile, Santiago, 1987.
2. Catalogue *Visiones develadas*, Centro Nacional de Conservación y Restauración, Santiago de Chile, 2009.
3. J.Turner, *The Dictionary of Art*. Oxford University press, New York, 1996, vol. 11.
4. A. Benavente, C. Jiménez, *Investigación sobre la instancia material de una obra pictórica a través de métodos de análisis científicos y su aplicación en la Serie Grande de Santa Teresa*. Facultad de Artes, Pontificia Universidad Católica de Chile, Santiago, 1989.
5. A. Carrillo y Gariel, *Técnica de la pintura de Nueva España*; Universidad Nacional Autónoma de México, Mexico, 1946.
6. G. Siracusano, *El poder de los colores: de lo material a lo simbólico en las prácticas culturales andinas. Siglos XVI – XVIII.*, Fondo de Cultura Económica, Buenos Aires, 2005.
7. A. Andreotti, I. Bonaduce, M. Colombini, G. Gautier, F. Modugno, E. Ribechini, *Anal. Chem.* **78** (2006) 4490-4500.
8. F. Pacheco, 1564-1644. *Arte de la Pintura*, LEDA, Barcelona, 1968.

## **Images Analysis Coupled With PIXE Technique for Picture Characterization**

E. Kajiya<sup>1</sup>, M. A. Rizzutto<sup>2</sup>, V. Pagliaro<sup>2</sup>, S.I. Finazzo<sup>2</sup> and P. R. Pascholati<sup>2</sup>

<sup>1</sup>*Mattos & Kajiya Ltda, Conservação e Restauro, São Paulo, SP, BRAZIL.*

<sup>2</sup>*Instituto de Física, Universidade de São Paulo, Cidade Universitária, São Paulo, SP, BRAZIL.  
e-mail: rizzutto@if.usp.br, elizabethkajiya@uol.com.br*

**Abstract.** Image capturing and analysis can be used to examine and document objects of artistic and historic values. The image inspection analysis with fluorescence of ultraviolet radiation (UV), visible light, near-infrared reflectography (NIR) and tangential light play an important role in assessing the conservation status of the paintings, to test authenticity, and detect changes in the underlying drawings made by the artist. All these image processes are non-destructive optical techniques in which the image is obtained from a digital camera with a CCD sensor. The UV and NIR images were obtained with appropriate filters coupled to the lens to transform the ultraviolet and infrared radiation reflected by the object into a visible image. The camera used in this case can operate in the spectra range of 380-1000nm. Particularly the resulted IR image is a combination of observed phenomena of reflection, absorption and transmission of the surface layer, revealing the hidden features. The display of hidden drawings depends on two factors: contrast and transparency. The contrast is related to the material used in the design and reflectivity of the preparation bases. Transparency is related to the pictorial layer and depends on the composition of the pigments. When carbon is used for designing, the absorption of the IR is high and increases the difference in reflectivity of the preparation bases. In this case it is possible that the design is clearly visible even though the pictorial layer is opaque. The UV radiation permits to obtain superficial information of the pictorial surface layer while observing the dirt, fungi, tears, cracks in the polychrome and retouched areas, where it is difficult to distinguish between them and the original painting. The use of grazing light highlights all the roughness of the surface, deformation of the support and also reveals cracks and tears, but this image can reveal “the way of the artist’s painting”. This paper describes the image analysis of an oil painting on canvas, 40 x 76 cm, named “Landing and Combat” of the XIX century, belonging to the Pinacoteca do Estado de São Paulo collection (RM0139). To complete these investigation PIXE (Particle induced X-ray Emission) analysis was performed to give a better information of the elements present in the pigments.

**Keywords:** Imaging techniques, UV radiation fluorescence, Near-Infrared reflectography, Tangential light, PIXE.

### **INTRODUCTION**

In scientific studies of art and archaeological objects, in addition to the documentary and historical research, the chemical and physical non-destructive analyses are increasingly used in the characterization and investigations of these objects. In the field of

applied sciences the research on the cultural heritage are very extensive and the objects are diverse. Interdisciplinary studies are increasingly applied in this area, resulting in accurate diagnoses of the type of materials used by the artist, period or school, as well as their techniques applied in the creation of objects, underlying drawings and also the restoration interventions. Knowing the composition of materials

and technology used in the manufacture of cultural heritage objects, it is possible to develop means and methods to better conservation of the work [1].

The scientific methods are sometimes classified in destructive or non-destructive and examination of surfaces or points. The methods for surface analysis are based on processes of the electromagnetic radiation interaction with matter which include photographic techniques such as: tangential or grazing light, fluorescence visible with ultraviolet radiation (UV), visible light, reflectography infrared (NIR), radiography, etc. These methods visualize the work as a whole and can be used without extracting samples and are classified as non-destructive. The methods considered as spot analysis require, as a rule, the extraction of samples and has a wide range of instrumental methods of analysis, such as optical microscopy, the scanning electron microscopy, the X-ray diffractometry, chromatography (the thin layer chromatography and high-pressure liquid), mass spectrometry, infrared spectrophotometry, etc.

However to make spot checks, it is not always necessary to take samples [2] as in the elementary analysis with X-ray spectroscopy such as X-ray Fluorescence (XRF) or particle induced X-ray emission (PIXE) or gamma-ray emission (PIGE) that are non-destructive techniques. The last two methods use ion beams from nuclear accelerators. This work with non-destructive techniques, aimed the analysis of one easel painting belonging to the Pinacoteca do Estado de São Paulo collection (RM0139) as seen in figure 1. The diagnostic imaging was done by reflectography infrared (NIR), fluorescence visible with ultraviolet radiation (UV), light tangential or grazing and visible light. The elemental analysis was realized with atomic-nuclear technique PIXE, which gives information of the chemical elements present in the pigments used in the work.



**FIGURE 1.** Picture image with visible light of an easel painting, 40 x 76 cm, named “Landing and Combat” of unknown authorship of the XIX century, belonging to the Pinacoteca do Estado de São Paulo collection (RM0139). In details the IR image.

## ANALYTICAL METHODOLOGY

With the individual analysis of each technique and their characteristics it is possible to correlate all the information that lead to a better understanding of the object under study. In this analysis we used the following techniques:

### Visible light photography

Photograph in visible light allows recording the images of the painting and were obtained with a digital camera of 10.7 Mega Pixel with a CCD sensor. The illumination was performed with constant light, in this case, two halogen lamps 3200 °K, 1000 W each, approximately at 45 ° in the direction of the object.

### Infrared reflectography

The IR reflectography is a non-destructive optical technique in which the image is obtained from a digital camera with CCD sensor and IR filter connected to the lens. In the near-infrared spectrum, Cabral [2] divides the IR spectrum into three smaller bands differentiated by wavelength that had been called IR1 (between 750 ~ 950nm), IR2 (between 950 ~ 1150nm) and IR3 (between 1200 ~ 1550nm). These measurements of IR were used with constant light sources consisting of two beams of halogen 3200 °K with 1000 W each, focusing also on the object at 45 degrees. The digital camera used has high resolution and can operate between the UV spectrum, visible light and IR at a wavelength of 380nm to 1000nm. The images observed resulted from the conjunction of the phenomena of reflection, absorption and transmission of the surface layer revealing hidden peculiarities [3]. The display of drawings depends on two things: contrast and transparency. The contrast is related to the material used in the design and the underlying reflectivity with the base preparation. Transparency is related to the pictorial layer and depends on the composition of the pigments. When the environmental to drawn is carbon-based the absorption of IR is high and increases the difference of reflectivity in relation to the base preparation. In this case it is possible that the design is clearly visible even though the pictorial cover is opaque.

### Visible fluorescence image obtained with ultraviolet radiation

Image technique which is recorded by the fluorescence generated by UV radiation that focuses on the painting [4]. This incident radiation has the ability to excite the molecules of the material of certain and cause

electronic transitions and therefore the immediate issue of energy by radiation of wavelengths (fluorescence) distinct from that incident radiation. The process of phosphorescence can also occur in the process of excitation, but is much slower than the fluorescence and can last a few seconds or more [5].

The fluorescence and phosphorescence occur, especially in organic compounds and it is rare in inorganic compounds. Different materials can exhibit different colors and intensities of fluorescence which can provide information of the paint surface by detecting fungi, tears and cracks in polychrome and retouched areas, where it is difficult to distinguish between them and the original painting. These differences are recorded by UV rays when the finishing touches were applied long after the painting elaboration, especially when a cover of varnish was applied. If the varnishes covering the work are very old and thick a green fluorescence produced, when projected on the UV rays, is sufficient to reduce or prevent the observation. Pigments excited by ultraviolet radiation give rise to fluorescence of different colors according to the combination (yellow, orange, violet, lilac, pink, white, blue and green). The pigments that contain sulfide, strontium and barium and zinc also produce the same phosphorescence of iridium, cadmium and uranium [2]. In the UV measurements were used four beams of UV light, Granilight of 40 W each and a filter coupled to the lens in a dark environment.

### Light Grazing

Bring out all the roughness of the surface, deformation of the support, relieve (cracks in the raised or buried pictorial layer), cracks, fungi, tears which can also reveal the way of painting of the artist. However, it is necessary to pay particular attention to lighting to highlight these changes. With the lighting positioned tangentially to the surface of the picture or changing the position of the light source - the angle of the projected beam - it is possible to obtain precise

reference to the conservation status of the work. In this analysis we used the equipment Komlux Kompact 150 with fiber optic.

### Particle Induced X-ray Emission (PIXE)

The PIXE method is distinguished by its high sensitivity and specificity and is a physical method for quantitative analysis of multi-element and is a non-destructive technique [6]. This method consists of irradiating the sample to be analyzed with an ion beam such as  $H^+$  (protons), to induce the X-ray emission features. The detection is done with a specific X-ray radiation detector and the method allows the detection and quantification of elements with  $Z > 10$ , being more sensitive in the range  $20 < Z < 40$  and  $Z > 70$ , where it can reach the detection limit of the order of ppm ( $10^{-6}$   $\mu\text{g/g}$ ). This method of analysis is suitable for examining paintings because of the low background level produced by the organic compounds present on the screen, chassis, binders, varnishes, etc.

Also the chemical elements present in different pigments can be easily identified which is an important information for identification of age or authorship of the painting, if this information is provide in the literature [7]. The PIXE measurements were performed at the Laboratory of Material Analysis with ionic beams at the Institute of Physics, University of São Paulo (LAMFI - [www.if.usp.br/lamfi/](http://www.if.usp.br/lamfi/)) that has an electrostatic accelerator that provides beams of protons and helium of energy up to 3 MeV.

### RESULTS

The main features that can be observed with the IR measures are the drawings that reveal the underlying hidden peculiarities of the artist's creative process. By reflectography IR and comparing it with visible light image of the final painting (figure 2) it was possible determine the creation process and changes made by the artist in this work.

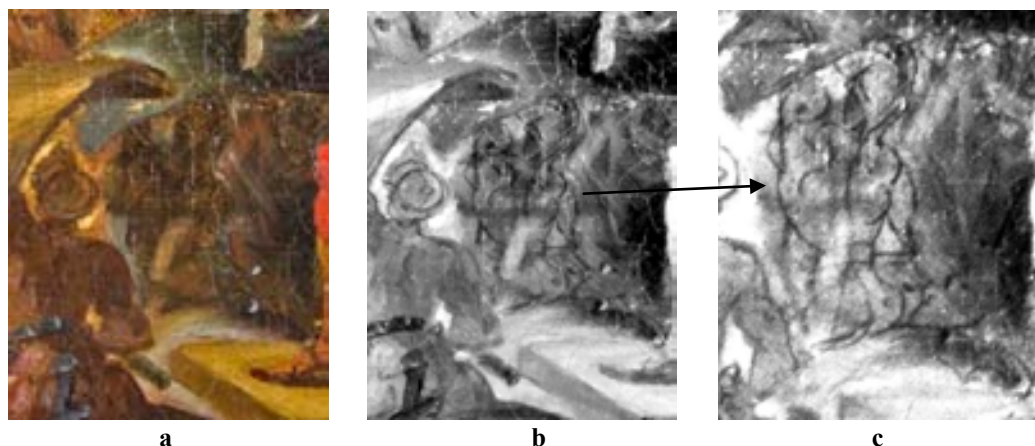


**FIGURE 2.** Detail of the photograph (a) with visible light (b) with IR1 (c) with IR2.

In figure 2b, using the reflectography of IR1, we detail the preparation of the drawing revealing, for example, the soldier in the background that shows traces of the overlay design. Figure 2c, with the technique IR2, shows the same detail as in the previous figure and there are more noticeable details of the design and underlying changes in the creative process, in comparison with the final painting drawn by the artist.

In the technique of ultraviolet radiation was possible observe mainly the regions of touches and cracks in polychrome. The image of figure 3 shows different colored tones as greenish-yellow, pink, blue, etc., which corresponds to different chemical elements present in the pigments. Moreover, it was possible see clearly the areas of restoration carried out since this are on leave in relation to the original pigment.



FIGURE 3. Photograph of with UV.

The analysis with tangential light (figure 4a and 4b) allowed observe the roughness and irregularities, undulations, fungi, cracks and craquelure in the polychrome. Also it was possible see some trace style of the painter, pictorial reintegration (restoration) and helped to determine deformations in general and the conservation status of the object.



FIGURE 4. Photograph with visible tangential light (a) details of the presence of fungi (b) detail of craquelure in several directions.

PIXE measurements were taken in the arrangement of the external beam at LAMFI where is possible analyze different materials of various shapes

and sizes [8]. The figure 5 shows in detail the experimental setup in PIXE measurements of the painting, as well as in figure 6 we have the marks of the points chosen for PIXE analysis in the different pigments.



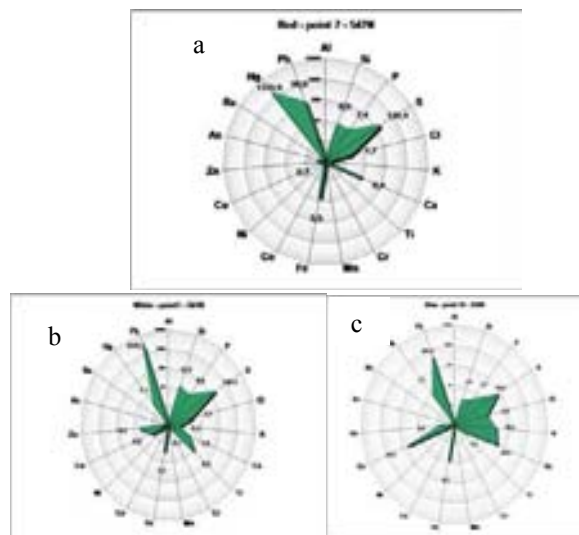
FIGURE 5. The oil in canvas picture being analyzed in the arrangement of the external beam PIXE.



FIGURE 6. Photography with visible light and the points marked to PIXE measurements.

The PIXE method has identified elements such as Fe, Cr, Zn, Ti, Pb, Hg, S, Cu, Si, Cl, K, Ca, Mn, Co, Ba, As, P, present in the chemical composition of various pigments used in this work. PIXE analysis at different points allows to measure characteristic elements in the pigments helping to characterize each color as can be seen in figure 7. In PIXE measurement of point 10 (blue color) we have elements as Pb, Hg, Fe and Cu. The high quantity of Cu in this point, in comparison with the other blue shades, suggest the pigment Azurite ( $2\text{CuCO}_3 \cdot \text{Cu}(\text{OH})_2$ ). The presence of this pigment helps to indicate the age of this picture, because this pigment has been used since the antiquity until the XIX century, confirming the expected date of this work of nineteenth century. In the point 7 (red color) we observe a large amount of mercury suggesting the pigment Vermilion ( $\text{Hg}_2\text{S}$ ) (figure7a). The element lead can be seen in various pigments measured thereby revealing the bright colors and even the spot

1 (white color in figure 6c) was produced with lead white,  $2\text{PbCO}_3 \cdot \text{Pb}(\text{OH})_2$ , used since antiquity.



**FIGURE 7.** Graphs stars representing the chemical elements present in different points measured with the PIXE technique (a) spot 7 (b) spot 1 (c) spot 10.

## CONCLUSIONS

The examination methods on surface with different wavelengths of light can be realized and helped to analyzed and characterized an easel painting of the nineteenth century. The photograph with visible light makes possible record the images of the painting. Coupled with the tangential image light it provide information about the deformations presents in support, the cracked, cracks, fungi, etc., resulting in a precise diagnosis of the status conservation of the work and also the characteristic of the medium used by the artist.

Images with ultraviolet radiation allowed observe the phenomena of fluorescence of the pigments, and differentiating interventions of restoration and the original painting. The studies carried out with the method of infrared reflectography, through the phenomena of reflection, absorption and transmission of the surface layer, revealed peculiarities hidden view of the underlying designs and alterations made by the artist. The physics method multi-elementary, non-destructive PIXE helps to identify and quantify the chemical elements present in the different pigments used by the artist. It was possible to identify the presence of chemical elements in the pigments such as Fe, Cr, Zn, Ti, Pb,

Hg, S, Cu, Si, Cl, K, Ca, Mn, Co, Ba, As, P with different relative intensities for the various colors of the paint. The red pigment is probably the Vermilion due to the presence of Hg and S. PIXE has detected Cu as another characteristic element present in the blue shades that can be characterized as Azurite helping to confirm the expected date of the work which is the nineteenth century. The Pb was also detected by PIXE in various pigments suggesting that the different shades and even the white pigment were obtained with white lead. In short words we can say that the addition of various imaging techniques coupled with PIXE technique allowed a detailed analysis of this oil in canvas picture by providing detailed information about the painting techniques used by the artist, the current state of conservation work and the chemical elements present in the pigments.

## ACKNOWLEDGMENTS

This research has been supported by FAPESP. Authors thank Pinacoteca do Estado de São Paulo and the Conservation and Restoration team.

## REFERENCES

1. D.I Tellechea, "Pintura en restauro". Instituto Domingo Tellechea, São Paulo, 1998, v.2.
2. J.M. P. Cabral, "Exame científico de pinturas de cavalete" *Fundação Calouste Gulbenkian*, 1995. <<http://zircon.dcsa.fct.unl.pt/dspace/handle/123456789/214>>.
3. M. Gargano, N. Ludwing, G. Poldi, *Infrared Physics and Technology*, **49** (3) (2007) 249-253.
4. A. E. Obrutsky, D. Acosta, "Infrared reflectography, and NDT technique for images diagnosis". *III Pan-American Conference for nondestructive testing. 2003*. <http://www.aaende.org.ar/sitio/biblioteca/material/T-066.pdf>.
5. L. A. Carcelen, A.G. Mozo, "Uso de la Luz: Ultravioleta para el Estúdio del Estado de Conservación de La Pintura de Caballete". in: *II Congreso del GEIIC. Investigación en Conservación y Restauración*. 2005.
6. S. A. E. Johansson, J. L. Campbell, *PIXE: A Novel Technique for Elemental Analysis*, John Wiley and Sons, New York, 1988.
7. M.A. Rizzutto, "A física nuclear nas artes e na arqueologia". *Ciência Hoje* **44** n. 262, (2009) 29-33.
8. M. A. Rizzutto, et al., *Nucl. Instr. and Meth. in Phys. Res. B* **240** (2005) 549-553.

# **Infrared Reflection Spectrometry Analysis as a Non-Destructive Method of Characterizing Minerals and Stone Materials in Geoarchaeological and Archaeometric Applications**

M. Ostrooumov

*Departamento de Geología y Mineralogía, Instituto de Investigaciones Metalúrgicas, Universidad Michoacana de San Nicolás de Hidalgo, MEXICO. e-mail: ostroum@umich.mx*

**Abstract.** The purpose of this paper is to show the benefits and applications of using mid and far infrared reflection spectrometry (IRS) in the analysis of archaeological materials. Infrared spectral databases do not yet exist for rocks and principal minerals. In support of IRS techniques, a catalogue and new spectral database have been created with over 500 infrared reflection spectra in mid and far ranges from more than 250 different archaeological minerals and stone materials. The reflection spectrum serves as a “fingerprint” of all these materials. This new, nondestructive method is useful for spectrometric identification and crystal chemical characterization of many rocks and minerals commonly found in archaeological contexts. Three brief examples of IRS analysis of archaeological materials are presented as test cases. It is suggested that IRS could and should become a routine approach in geoarchaeology and archaeometry for identification and provenance studies.

**Keywords:** infrared reflection spectrometry, geoarchaeological and archaeometric application, minerals and stone materials

## **INTRODUCTION**

The purpose of this paper is to show the benefits and applications of using mid and far infrared reflection spectrometry (IRS) in the analysis of archaeological materials. IRS is a non-destructive technique which can provide diagnostic and crystal chemical information on the mineralogical phases of stone artifacts, artworks, and building materials. Since non-destructive methods are preferred in geoarchaeological and archaeometric identification, the IRS method, which utilizes non-contact light beams, is considered to be an appropriate method for this aim. IRS is also useful as an alternative to the more traditional methods of X-ray analysis such as XRD, SEM/EDS and EPMA.

It is well known that a variety of minerals can occur in stone samples from archaeological contexts. Minerals are also found as pigments and fillers in paint films, in soil molded into earthen artifacts and mud brick, as corrosion products on metal surfaces, in stone fabrications such as sculpture and architectural monuments, in cements, in building stones, and in ceramics. In recent years several papers have been published dealing with IRS analysis of various rocks and minerals, but most of these studies were performed on powdered material [1, 2].

To my knowledge, only a few studies have been devoted to the study of principal minerals and gemological materials using in situ non-destructive IRS experiments [3-8], and literature dealing with IRS studies of minerals and stone materials found in archaeological objects is even more uncommon.

The current study was undertaken to compensate for the absence of published literature referent to the IRS of mineral and stone artifacts. IRS is a non-destructive method, and thus potentially a very important tool for archaeometrists and geoarchaeologists. Existing infrared spectral databases for minerals are comprised of data collected from powdered dispersions [9,10]. IRS presents many comparative advantages in comparison to infrared absorption spectrometry of minerals [6-8], and thus there is a need for a new reference database of infrared reflection spectra of mineral and stone materials. An IRS database such as presented here will facilitate spectral searching and characterization of minerals and stone materials found in archaeological contexts.

## ANALYTICAL APPROACH

The infrared reflection spectra were obtained with equipment available for the spectrometric groups installed at: 1. Mineralogical Laboratory (Saint Petersburg Mining Institute, Russia), 2. Mineralogical and Gemological Laboratory (Mainz University, Germany), 3. Crystal Physics Laboratory (Institute of Materials, Nantes University, France), 4. Mineralogical Laboratory (Metallurgical Institute, University of Michoacan, Mexico). Various spectrometric equipment used in this study include the Spectrometer IRS-29 (Russia), Spectrometer UR-20 (Germany), Spectrometer Perkin-Elmer 1760 FTIR (Germany), Spectrometer Bruker IFS-28 (France), Spectrometer Nicolet 20SXC-FTIR (France), and Spectrometer Bruker Tensor 27 (Mexico). For verification purposes, the same spectra were tested in various laboratories and with different spectrometric equipment.

## SAMPLES

The creation of an infrared reflection spectra catalog dictates the need for obtaining spectra on samples with the greatest possible purity. For that reason, more than 250 mineral species and stone materials of sufficient dimension were selected to be oriented and carved. These samples were of the greatest purity and were identified by traditional mineralogical methods (XRD, EPMA, XRF). Most samples were acquired, often as single crystals, from the Saint Petersburg Mining Museum. Other samples were obtained from the Ostrooumov collection in Russia and Mexico or from private individuals.

IRS spectra were also collected on polished sections and non-uniform surfaces of various igneous, sedimentary and metamorphic rocks. The comparison among the spectra on polished and unpolished sections has shown that no elaborate rock sample preparation is required.

Each "standard" mineral or stone material sample was typically examined with electron microprobe and X-ray diffraction to assure sample purity and to establish the chemical and mineralogical compositions. Microprobe analyses were performed with the Electron Probe Micro Analyzer CAMECA SX 100 at the Saint Petersburg Geological Institute (Russia). All samples were characterized by X-ray diffraction using a Siemens D-5000 X-ray diffractometer with Cu K $\alpha$  radiation.

Recent IRS instrumental improvements have been made at various levels, such as the introduction of high throughput microscope optics (micro-FTIR technique), fiber-coupled spectrometers and sensitive IR detectors. Moreover, when using the mobile infrared equipment, it is possible to analyze the artifacts in-situ and non-destructively, overcoming the need of destructive sampling or transportation of the artifact to the laboratory. Thanks to recent instrumental developments, the spectrometers are now compact in size, easy to operate in scientific laboratories, and the reproducibility of all IRS spectra is excellent.

## RESULTS

### Geoarchaeological and archaeometric applications

As an example of how IRS can be used in conservation efforts, the method was used to analyze pyroclastic volcanic rocks (ignimbrites) used in building construction in the historical downtown area of the city of Morelia in southern Mexico, focusing on the ex-convents of San Francisco and San Agustin

The original pyroclastic rock (ignimbrite) from the quarry consists largely of the phenocrysts of potassic feldspars, plagioclases, polymorphs of silica (quartz, cristobalite, tridymite), biotite and the fragments of volcanic glass with different degrees of devitrification (Figure 1).

Under conditions of urban weathering, pyroclastic stone materials from the ex-convents San Agustin and San Francisco were characterized mainly by secondary alteration materials of low scale mainly in the form of altered crusts containing an exotic mineralogical association (neo-formations): gypsum, calcite, clay minerals and amorphous calcium phosphates (Figure 1b).

The formation mechanism of the recent mineral phases and other products in the alteration process of historical monuments and buildings can be different for compounds of different compositions. For example, in this particular case, the genesis of sulfates is explained by the reaction between plagioclase of acid-medium composition (oligoclase-andesine) and

sulfuric acid that provokes the formation of calcium sulfate, hydrated with complementary anions.

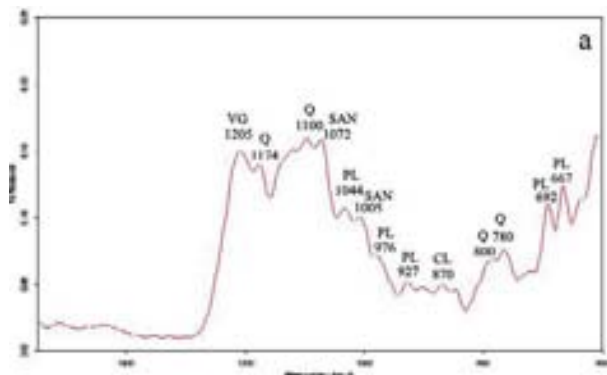


**FIGURE 1 a.** IRS of unweathered ignimbrite material from the quarry:Q, quartz,PL, plagioclase,SAN, sanidine,VG, volcanic glass.

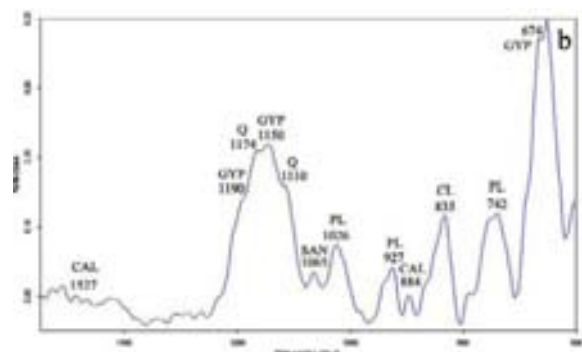


**FIGURE 1 b.** IRS of unweathered ignimbrite material from the quarry:GYP,gypsum,CAL,calcite,CL, clay.

Another application of IRS was conducted in the Saint Petersburg State Hermitage Museum (Russia) where the collection of the stamp-stones used by Russian aristocracy in the XVIII and XIX centuries are housed. Mineralogical characterizing of archaeological pieces has two basic objectives: a) determine the mineral composition and b) identify the raw material source. Both aspects are essential to develop a better understanding about trade and exchange of high-priced items in the past. The mineralogical characterization of the stamp-stones was carried out with the IRS because of its non-destructive character and efficiency in mineral studies. To determine the usefulness of this technique for archaeometric identification, infrared reflection spectra were obtained with reflection accessory and fiber optic instrumentation. Both techniques yielded the same results.

One of the analyzed stamp-stones (Figure 2) contains an aristocratic emblem and is part of the Russian Tsar Romanov Family collections, dating to the middle 19<sup>th</sup> century: great prince K. Romanov).

The infrared reflection spectra were obtained in two directions in order to take into account the effect of orientation of the mineral crystal which provides significantly stronger directional differences among infrared reflection spectra in the x-, and y-directions. Spectrometric results indicate that this sample is Beryl ( $\text{Be}_3\text{Al}_2\text{Si}_6\text{O}_{18}$ ) (aquamarine variety).

Another question addressed was where was the raw material source for this specimen? In the 19<sup>th</sup> centuries only two types of pegmatites were known in Russia: rare-element pegmatites (type LCT-lithium, cesium, and tantalum from Ilmen in the Ural.



**FIGURE 2.** Stamp-stone with the Russian aristocratic emblem (Hermitage museum, Saint Petersburg, Russia).

Mountains) and miarolic pegmatites with typical minor elements such as beryllium, yttrium, REE (Rare Earth Elements), and fluorine (Transbaikalie, southern-eastern Siberia). The crystals of Li-beryl from Ural pegmatites are characterized by infrared reflection spectra with three typical reflection bands (Figure 3) at 1180, 1140 and 1060  $\text{cm}^{-1}$  [4]. In contrast, these bands have not been observed in the infraredreflection spectra of aquamarine crystals from miarolic pegmatite deposits which have been found in Transbaikalie region. Thus, all spectrometric features show that in this case the studied aquamarine crystal was extracted from the Transbaikalie pegmatite region [6]. This Russian region was geologically investigated in the early 19<sup>th</sup> century and the first extraordinary mineral crystals recovered from the area were donated to gemstone Tsar collections.

A third application of IRS analysis is the study of mineralogical features in ancient pottery. The nondestructive IRS method is equally effective for characterizing ceramic matrix and temper composition as well as determining firing temperature of these sintering materials. Eighteen archeologically well controlled plainware pottery fragments were analyzed for the first time by the systematic IRS measurements. Eight fragments are from the site of Cuanalan, a

formative village that predates the beginnings of Teotihuacán. The other ten fragments of pottery analyzed in this study are from the Kaminaljuyú area in Guatemala. Representative FTIR reflection spectra of the ceramic matrix of Cuanalan pottery (Figure 4a) was indicative of noncalcareous ceramic materials showing strong SiO vibration of meta-clay.

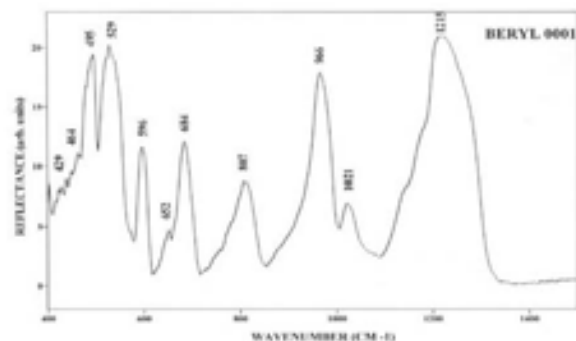


**FIGURE 3.** Infrared reflection spectra of beryl (aquamarine variety, Transbaikalie region, Russia). Note the absence of the bands at 1180, 1140 and 1060  $\text{cm}^{-1}$  which have been observed in the beryl IRS spectra from rare-element pegmatites (type LCT-lithium, cesium, tantalum from Ilmen in the Ural Mountains).

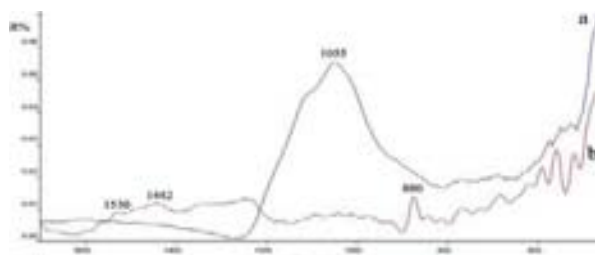


**FIGURE 4.** Representative FTIR reflection spectra in the range 1700-400  $\text{cm}^{-1}$  of the ceramic matrix of pottery excavated at (a) Cuanalan, a Formative village, (Mexico), and (b) Kaminaljuyú area, Guatemala.

In the FTIR reflection spectra of the pottery fragments, the main Si-O stretching band appeared in the range 1047-1055  $\text{cm}^{-1}$ . According to the thermo-FTIR spectroscopy analysis, these locations in IR spectra were close to those observed by [11] after firing the soil raw materials between 800 and 900°C. The locations at 463-467  $\text{cm}^{-1}$  of the Si-O, Al-O deformation also confirm the same temperature of the firing. In this case, IRS demonstrates an ability to reconstruct firing temperatures in pottery manufacture.

The Mayan ceramics from Guatemala have a different mineralogy and chemistry. The IRS spectrum indicates a weakly calcareous ceramic matrix with weak  $\text{CO}_3$  vibration of microcrystalline calcite (Figure 4b). The main  $\text{CO}_3$  reflection bands (at 1530, 1442 and 880  $\text{cm}^{-1}$ ) were obtained in the heterogeneous samples by using an infrared microscope capable of

distinguishing small mineral inclusions and eliminating the characteristic bands of the silicate matrix in the range 1047-1055  $\text{cm}^{-1}$ . These results demonstrate that the firing and cementation of ceramics from this area was obtained by low temperature sintering.

## CONCLUSIONS

In support of IRS techniques, the first systematic catalog and a new spectral database with automatic search software have been created with over 500 infrared reflection spectra in mid and far ranges from more than 250 different minerals and stone materials [6]. The IRS reference catalog now allows the technique to be used by geoarchaeologists and archaeometrists for comparison of the infrared reflection “fingerprint” of an unknown mineral or stone object with the fingerprints of a series of “standard” minerals and stone artifacts. Three case studies presented above demonstrate the application of IRS spectrometry in the field of non-destructive mineralogical analysis of artifactual and architectural materials [3-8]. This analytical technique is increasingly being employed in nondestructive crystal chemical analyses. Moreover, with the development of an IRS mobile instrument, it is possible to conduct nondestructive tests of large objects that cannot be transported to the laboratory.

IRS has the potential as a primary investigative tool in archaeometric and geoarchaeological research as it has advantages over other methods. For example, unlike Raman spectrometry theirs does not utilize a laser beam that can cause damage to the studied material. Moreover, archaeological objects need no preparation with IRS; an isolated, rough material can be analyzed without preparation. This includes a cut stone, a stone mounted in a jewel, or any cultural object that contain minerals and rock stones. Other applications of IRS in geoarchaeological and archaeometric research are likely to be developed in the future.

## REFERENCES

1. P. McMillan, A. Hofmeister, “Infrared and Raman spectroscopy” in *Spectroscopic Methods in Mineralogy and Geology*, F.C. Hawthorne ed., Reviews in Mineralogy **18**, Washington, 1988, pp. 99-160.
2. J. Salisbury, L. Walter, N. Vergo, M. Dana, *Infrared spectra of minerals*. The Johns Hopkins University Press, Baltimore, 1992.
3. M. Ostrooumov, *Nature* **3** (1982) 45-53 (in Russian).
4. M. Ostrooumov, *Proceedings of the USSR Mineralogical Society* **4** (1987) 486-497.
5. M. Ostrooumov, B. Lasnier, S. Lefrant, *Analysis* **23** (1995) 39-44.

6. M. Ostrooumov, E. Fritsch, B. Lasnier, S. Lefrant, “Infrared reflection spectrometry of minerals and gemstones” in *Applied Mineralogy: Developments in Science and Technology*, M. Pecchio ed., 2004. pp. 595-598
7. M. Ostrooumov, “Infrared reflection spectrometry of minerals and gemological materials” WEB page 2006. <http://www.mineralog.net>
8. M. Ostrooumov, *Espectrometría Infrarroja de Reflexión en Mineralogía Avanzada, Geomología y Arqueometría*, Monografías del Instituto de Geofísica 12, Universidad Nacional Autónoma de México, Mexico, 2007.
9. A. Marfunin, *Advanced Mineralogy*, Springer Verlag, New York, 1995.
10. A. Hofmeister, “Infrared microspectroscopy in earth science” in *Practical guide to infrared microspectroscopy*, H.J. Humecki ed., Marcel Dekker, Inc. New York-Basel-Hong Kong, 1995. pp.377-415.
11. S. Shoval, P. Beck, *Journal of Thermal Analysis and Calorimetry* **82** (2005) 609-616.

## **Preliminary Analysis on Micro-Indentation Hardness of Prehistoric Lithic Raw Materials**

**Kaoru Yonekura**

*Department of Philosophy, History and Cultural Studies, Tokyo Metropolitan University, JAPAN.  
e-mail: yonekura@center.tmu.ac.jp*

**Abstract.** In order to conduct a comprehensive study of the various material-related issues of the early stages of human history, it is essential to carry out detailed studies on the intrinsic material properties of prehistoric stone implements to derive a functional knowledge of the relationships between material properties and manufacturing processes including heat treatment and the performance of completed tools, which may be evaluated in terms of edge capability and tool durability. Further, the approach used by prehistoric toolmakers to recognize and select material also can be explored through analyses of the characteristics of such materials. In this preliminary study, to measure one of the primary attributes of stone materials that could have affected the various stages in the life cycle of stone tools, the Vickers microindentation hardness test was performed on several lithic raw materials commonly used for prehistoric flaked tools, such as flint, obsidian, chert, andesite, dacite, shale, and chalcedony. Despite the differences in the types of rocks in terms of texture, composition, and structures, a specific hardness of 500–1200 HV was observed in these prehistoric lithic materials, which is almost equal to that of modern metallic materials used for present-day cutting implements. The result implies that close analyses of inherent material properties of prehistoric tools have the potential to provide useful and practical information on the materials used in the prehistoric ages.

**Keywords:** Prehistoric Lithic Raw Materials, Mechanical Properties, Vickers Microindentation Hardness

### **INTRODUCTION**

Lithic raw materials used in prehistoric ages contain considerable information on the selection and utilization of materials in early stages of human history. For instance, it is probable that the various properties of lithic raw materials, particularly mechanical properties, could have influenced the manufacturing processes of tools, such as flaking processes, rejuvenation and reuse of tools, and alteration by heating. They could also have affected the general performance of completed tools, such as their edge capability and tool durability. Therefore, the selection of materials by prehistoric toolmakers could

have been influenced by the inherent material characteristics, especially their mechanical attributes. Furthermore, as the mechanical properties of rock materials have been known to affect the abrasion of rocks [1], detailed information on material peculiarity is required for use-wear analysis of stone implements. Thus, precise and quantitative analyses of properties of prehistoric lithic raw materials can provide helpful information on various material-related issues of prehistoric ages.

In this regard, the first pioneering article pointing out the need for a quantitative and objective analysis of the material properties of flaked stone tools was published in 1944 [2]. Following this, some related works on flaking properties [3, 4] and mathematical

approaches to fracture mechanics [5-11] as well as detailed studies on quantitative and semi-quantitative assessment of lithic materials [12, 13] were carried out. Among them, Domanski et al. effectively dealt with the mechanical properties of lithic materials through heat treatment analyses [14, 15]. However, the structural evaluation and quantitative assessment of lithic raw materials in the field of archaeology have not been fully established to date [15, 16].

On the basis of this background, to measure one of the mechanical properties which could have influenced on manufacturing stages and functional aspects of tools, the quantitative hardness test was tentatively applied to several lithic raw materials commonly used in prehistoric ages. The present work aims to provide fundamental and practical data on the hardness of lithic raw materials in order to supplement the analyses on material exploitation in prehistoric ages and the use-wear studies of primary stone tools.

## TEST SETTINGS

### Vickers Microindentation Hardness Test

Vickers microindentation hardness test was employed for the quantitative measurement of rock hardness. In this method, a pointed square-based pyramidal diamond indenter with  $136^\circ$  face angles was forced into the surface of materials under a predetermined load (Fig. 1). After the load was removed, the surface-projected diagonals of the resulting impression were measured with a microscope, and the material hardness was computed using the following formula:

$$HV = k \frac{F}{S} = 0.102 \frac{2F \sin \frac{\theta}{2}}{d^2} = 0.189 \frac{F}{d^2} \quad (1)$$

where  $k$  = constant (approximately 0.102),  
 $F$  = load, in N,  
 $S$  = surface area of indentation, in  $\text{mm}^2$ ,  
 $d$  = average length of the two diagonals of the indentation, in mm,  
 $\theta$  = face angle of the indenter ( $136^\circ$ ).

The hardness was measured with a Vickers hardness testing device (Akashi, MVK-H2) under room-ambient conditions by applying a load of 1.96 N for a loading time of 15 s. Prior to the test, the samples were fixed in resin to prevent their movement during the test. Subsequently, the surface of the specimen was polished in several steps with waterproof abrasive papers, alumina suspension, and diamond slurry. Afterwards, the sample surfaces were coated with a 200- $\mu\text{m}$  gold layer by vapor deposition to obtain sharp

images of the indentations for measurement. The hardness test was performed 50 times for each sample to prevent variations in hardness due to mineral distributions, micropores, and inclusions in the rock samples.

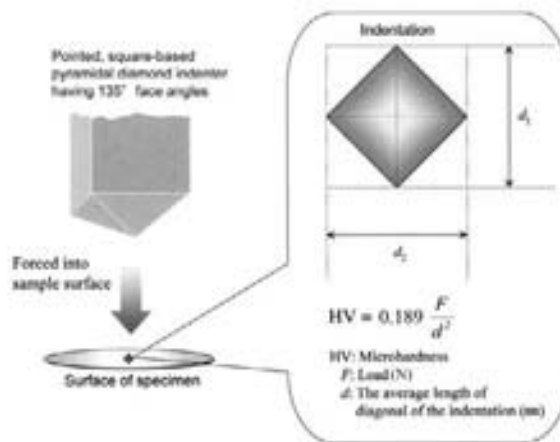


FIGURE 1. Schematic view of the Vickers hardness test setup.

### Raw Materials

Seven different types of rock samples—flint, obsidian, chert, andesite, dacite, shale, and chalcedony—were prepared for the hardness test.

Among the rock samples, flint, chert, shale, and chalcedony are occasionally classified as similar kinds of rocks, particularly as sedimentary rocks composed primarily of microcrystalline quartz [17]. In fact, according to the preliminary X-ray diffraction (XRD) analysis, these four types of rock samples exhibited the identical diffraction patterns of quartz without significant peaks of other minerals. Besides, although chalcedony is petrologically defined as a fine-grained fibrous variety of quartz and silicon dioxide, preliminary observation using transmission electron microscope (TEM) indicated that the granular state rather than the fibrous form of quartz constitutes the analyzed chalcedony samples.

In this work, seven chert samples were prepared in total, among which five were from the Kanto area in Japan and two were collected from Nevada, USA. Five flint samples were from France, and eight shale samples and six chalcedony samples were collected in the northeast region of Japan.

In addition to those types of rocks, obsidian, andesite, and dacite were also selected for the hardness test. Obsidian is recognized as one of the materials most frequently used in prehistoric ages worldwide. This type of rock is generally defined as a volcanic glass comprising rhyolite and dacite, and it may

sometimes also contain embryonic crystal growths (crystallites) and phenocrysts. Eight obsidian samples were obtained from Hokkaido in Japan.

As andesite samples, five native “sanukite,” which is generally defined as an aphanitic bronzite andesite occurring in the Setouchi volcanic province in Japan and contains an acicular phenocryst of orthopyroxene [18], were prepared.

As dacite, 16 trachy-dacite samples were collected from British Columbia in Canada. Dacite is generally considered as an aphanitic rock of volcanic origin that is composed chiefly of sodic plagioclase and free silica with subordinate dark-colored minerals. Preliminary XRD analysis indicated that plagioclase content is predominant in the dacite samples analyzed in this study.

Rock specimens that had characteristics and surface morphologies similar to those of actual flaked stone tools found in archaeological sites were provided for each type of rock.

## RESULTS

Figure 2 indicates the average values of the hardness in each sample. Despite the differences in rock types, all the rock materials frequently used in prehistoric ages exhibited microhardness values of more than 500 HV.

Specifically, obsidian, andesite, dacite, and chalcedony had similar hardness values of around 700 HV. Although there are diversities in the texture, composition, and structures in each type of rock (obsidian has hyaline texture; andesite and dacite have porphyritic texture with microscopic crystals; chalcedony analyzed here is characterized as microcrystalline rocks containing minute quartz grains), significant differences were not observed in their hardness results. In addition, chert and a part of the flint samples showed higher hardness than other types of rocks, which is more than approximately 900 HV. On the other hand, some shale samples showed

relatively lower hardness of less than 600 HV. The hardness values of shale, chert, and flint vary widely, whereas those of obsidian, andesite, and dacite exhibit less variation.

Although the hardness of native rocks naturally distributed in riverbeds or outcrops ordinarily varies widely (rocks with hardness less than 500 HV being more common), lithic raw materials frequently used for stone tools tend to have more than a certain level of hardness. This result implies that materials with certain hardness might have been preferably used for prehistoric implements because of their functional aspects.

Hardness values of modern metallic materials used for present-day cutting implements might provide some knowledge on the background of this material preference in prehistoric ages. The hardness values of some modern-day steel knives—standard martensitic stainless steel (SUS-440A and SUS-440C), which is widely used for kitchen knives—are generally reported to be more than 620 HV and 640–680 HV, respectively. Another stainless steel used for knives, AUS-8, also possesses a hardness of around 620–680 HV. As the hardness of the analyzed prehistoric lithic raw materials was more than 500 HV, and those of many samples were more than 700 HV, these materials had characteristics comparable or even superior to modern-day cutting tools in terms of hardness. This implies that the lithic raw materials could have sufficient cutting ability from a view point of hardness.

**TABLE 1.** Vickers microhardness values of some modern metal materials and lithic raw materials.

Materials of modern knives	Vickers hardness
SUS-440A	620 HV
SUS-440C	640–680 HV
AUS-8	620–680 HV
Lithic raw materials of prehistoric stone tools	500–1200HV

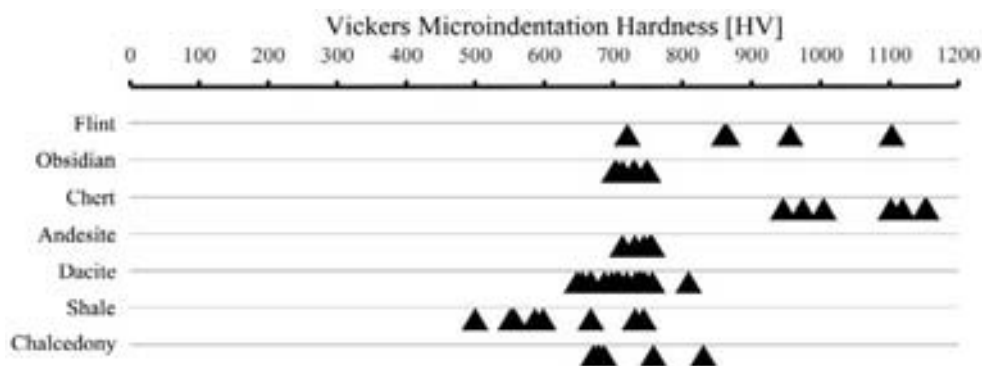


**FIGURE 2.** Results of Vickers microindentation hardness test for each sample.

Needless to say, many rock properties other than hardness, and geological factors including circumstances of rock occurrence and accessibility to resources, must have considerably influenced the prehistoric material exploitation. Hence, material selection in prehistoric ages was presumably carried out taking into account these various contributory factors relevant to material exploitation and utilization.

The preliminary results obtained here imply that the objective data of material properties of stone implements has a potential to provide comprehensive knowledge on the selection and utilization of materials by human beings in the prehistoric times.

### ACKNOWLEDGMENTS

This work was partially supported by a Grant-in-Aid for Scientific Research from the Japanese Ministry of Education, Culture, Sports, Science and Technology.

I am deeply indebted to Professor Suzuki and Professor Komodori of Keio University for their generous assistance and support.

### REFERENCES

1. S.T. Greiser, P.D. Sheets, "Raw Materials as a Functional Variable in Use-wear Studies" in *Lithic Use-*

*Wear Analysis*, New York: Academic Press, 1979, pp. 289-296.

2. M.E. Goodman, *Am. Antiq.* **9** (1944) 415-433.
3. J.S. Rinehart, *Int. J. Fract. Mech.* **2** (1966) 534-551.
4. J.B. Sollberger, *Lithic Technol.* **15** (1986) 101-105
5. J.G. Fonseca, J.D. Eshelby, C. Atkinson, *Int. J. Fract. Mech.* **7** (1971) 421-433.
6. J.D. Speth, *Am. Antiq.* **37** (1972) 34-60.
7. J.D. Speth, *Tebiwa.* **17** (1974) 7-36.
8. B.A. Bilby, *J. Mater. Sci.* **15** (1980) 535-556.
9. B. Cotterell, J. Kamminga, P. Dickson, *Int. J. Fract.* **29** (1985) 205-221.
10. B. Cotterell, J. Kamminga, *J. Archaeol. Sci.* **13** (1986) 451-461.
11. B. Cotterell, J. Kamminga, *Am. Antiq.* **52** (1987) 675-708.
12. E. Callahan, *Archaeol, East. North Am.* **7** (1979) 1-180.
13. R. Bradley, P. Meredith, J. Smith, M. Edmonds, *Archaeometry.* **34** (1992) 223-233.
14. M. Domanski, J.A. Webb, *J. Archaeol. Sci.* **19** (1992) 601-614.
15. M. Domanski, J.A. Webb, J. Boland, *Archaeometry.* **36** (1994) 177-208.
16. J.D. Clark, *Man and Environment.* **4** (1980) 44-55.
17. B.E. Luedtke, *An Archaeologist's Guide to Chert and Flint*, Archaeological Research Tools 7, Los Angeles, Institute of Archaeology, University of California, Los Angeles, 1992.
18. Y. Katsui, H. Sato, "Sanukite" in *Cyclopedia of Earth Science* (in Japanese), The association for the geological collaboration in Japan (AGCJ) (ed.), 2002, p. 493..

## **Non-Destructive Characterization of Green Stone Pieces from La Joya Site, Veracruz, Mexico**

J. L. Ruvalcaba Sil<sup>1</sup>, A. Daneels<sup>2</sup>, M. Vaggi<sup>1,3</sup> and M. Aguilar Franco<sup>1</sup>

<sup>1</sup> *Instituto de Física, Universidad Nacional Autónoma de México, MEXICO. e-mail: sil@fisica.unam.mx*

<sup>2</sup> *Instituto de Investigaciones Antropológicas, Universidad Nacional Autónoma de México, MEXICO*

<sup>3</sup> *University College London, U.K.*

**Abstract.** The studied objects are from the East platform of La Joya, a Classic site of first order in the junction of the rivers Jamapa and Cotaxtla, in the center of Veracruz, Mexico. The platform is considered a palace with administrative, ceremonial and habitation areas with six epochs of construction from medium Classic period (300-700 A.D.) to Late Classic period (700-1000 A.D.). A first set of pieces was discovered on the floor of a spaciousness elite habitation with evidences of Teotihuacan contacts (green obsidian, candlesticks), dated by <sup>14</sup>C around (300-400 A.D.). The second set of items is a part of ornaments of a main people buried in a big pottery vase and related to rich offerings. This corresponds to the end of the third epoch of construction (c.a 600 A.D.) when the habitation unit became the base of a pyramid. The third set of objects corresponds to filling material of the fourth epoch that covers and seals the previous one and it is dated to late Classic period. Findings of green stone are scarce in the central area of Veracruz. Thus, these items with a well established and dated archaeological context provide outstanding information about the elites in society of the Classic period in the Gulf area or Mexico. For this reason, the green stone objects were non-destructive analyzed using Raman and Mid-FTIR spectroscopies in order to identify the mineral composition while PIXE and Ionoluminescence were applied to contribute to the mineral identification and to determine the probable provenance of the items. Some artifacts were analyzed using X-ray diffraction (XRD). Few objects were identified as jadeite from known beds in the Motagua river basin in Guatemala. In this work, the used methodology, technical examination, and the main results are presented.

**Keywords:** Green stone, jadeite, PIXE, Ionoluminescence, XRD, FTIR, La Joya, Veracruz, Classic period, Mesoamerica.

### **INTRODUCTION**

Green stone was one of the most appreciated materials since the early times for the peoples of Mesoamerican areas. Various green minerals were used to produce objects as ornaments and ritual items for elite groups [1]. Jadeite (NaAlSi<sub>2</sub>O<sub>6</sub>), serpentines such as antigorite (Mg,Fe<sup>2+</sup>)<sub>3</sub>Si<sub>2</sub>O<sub>5</sub>(OH)<sub>4</sub> and lizardite Mg<sub>3</sub>Si<sub>2</sub>O<sub>5</sub>(OH)<sub>4</sub> and green quartz are among the most used materials for these purposes. Nevertheless, jadeite

was the material most appreciated and the most difficult to obtain since the sources are in the distant Motagua river area in Guatemala [2-4]. The availability of this material and the knowledge of manufacturing such a hard material were certainly very important and specialized workshops were settled and developed in the Maya area, like in the case of Cancuen site [4-5].

Certainly, exchange routes were established to trade the jadeite materials and the manufactured items

from the Maya areas, but other green minerals were exploited and manufactured locally. Mesoamerican peoples were able to distinguish the quality of the materials based on their hardness and color properties and jadeite was preferred and used for the social and political elites and the most important offerings.

## ARCHAEOLOGICAL CONTEXT

La Joya, a Classic site of first order in the junction of the rivers Jamapa and Cotaxtla, in the center of Veracruz, Mexico [6]. It was the main settlement of a coastal state where cotton was intensively cultivated between 350 to 550 A.D. Probably this production allowed contacts and exchanges with other areas [7], including the main culture of central Mesoamerica, Teotihuacan.

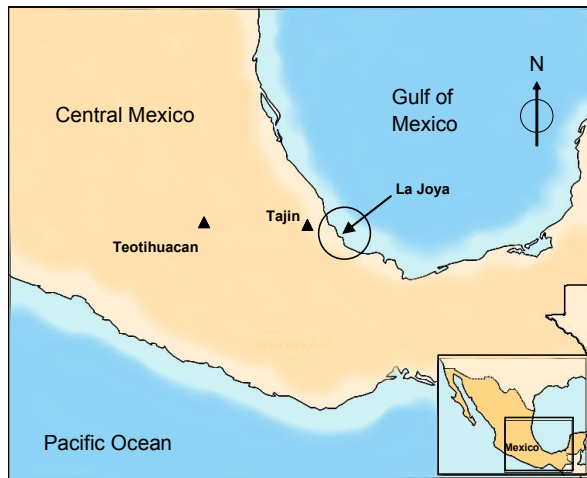


**FIGURE 1.** Geographical area of La Joya Site, Veracruz, Mexico.

The main platform of the site (Figure 2) is considered a palace with administrative, ceremonial and habitation areas with six epochs of construction from medium Classic period (300-700 A.D.) to Late Classic period (700-1000 A.D.) [8].

The fourteen green stone objects discovered, mainly ornaments and beads, are shown in Figure 3. A first set of pieces was discovered on the floor of a spacious elite habitation with evidences of Teotihuacan contacts (green obsidian, candlesticks), dated by <sup>14</sup>C around (300-400 A.D.) – stage IIIA - structure 3. The second set of items is a part of ornaments of a main people buried in a big pottery vase and related to rich offerings –stage IIIB. This corresponds to the end of the third epoch of construction (c.a 600 A.D.) when the habitation unit became the base of a pyramid. The third set of objects corresponds to filling material of the fourth epoch that covers and seals the previous one and it is dated to late Classic period –stage IV-. The findings of green stone

are scarce in the central area of Veracruz. Thus, these items with a well excavated and dated archaeological context provide outstanding information about the elites in the societies of the Classic period in the Gulf area of Mexico.

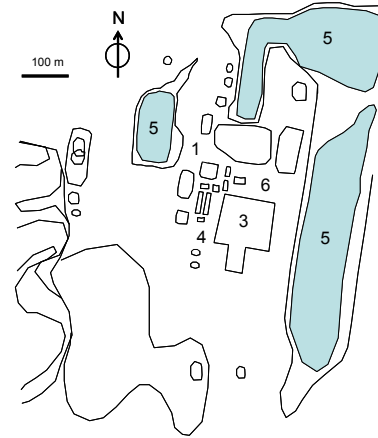


**FIGURE 2.** Main platform structures of La Joya site. 1. Pyramide 2. North Platform 3. East platform 4. Ball game court. 5 Cisterns. 6. Main square



**FIGURE 3.** Sets of pieces discovered in east structure 3. a) floor pieces of stage IIIA. b) Burial artifacts of stage IIIB. c) IV stage.

## ANALYTICAL APPROACH

Due to the importance of the finding, a non destructive analysis was necessary to determine the mineral composition and the elemental contents. Depending on its size and shape, some artifacts were analyzed by X-ray diffraction (XRD) on flat areas without sampling and powdering. A special sample holder for this purpose was used in a Bruker AXS diffractometer model D8 Advanced with a Linx eye detector. Since the working plane in the diffractometer may vary a little due to the position of the piece in the sample holder, corrections are made directly in the acquisition software.

Since it was possible to analyze only few artifacts by XRD, and in order to complete the mineral identification of the set of the pieces, the analytical methodology involved as well the use of Raman and Mid-FTIR spectroscopies using the portable equipments of our MOVIL project [9]. Colorimetric measurements were carried out as well by a probe and optical fibers connected to an Ocean Optics USB2000 spectrometer and a halogen light source on the light, medium and dark green areas of the artifacts. These data are reported in [8].

The FTIR measurements in the Mid-IR region were carried out by a fiber optic Remspec spectrometer. The analyzed area has a 3 mm diameter. The resolution of the system is  $10\text{ cm}^{-1}$  in and the range covers  $900$  to  $1500\text{ cm}^{-1}$ .

On the other hand, the Raman measurements were done by a Raman Inspector spectrometer using a 785 nm laser of 120 mW. The resolution is  $8\text{ cm}^{-1}$  in the range of  $200$  to  $2000\text{ cm}^{-1}$ .

PIXE and Ionoluminescence were applied to contribute to the mineral identification and to determine the elemental concentrations for probable provenance of the items. The experimental setup is described in [10]. An external proton beam of 3 MeV was used to irradiate an area of 1.5 mm diameter on the artifact surface. Characteristic X-rays and induced luminescence by the proton beam were simultaneously detected by two X-ray detectors (light and heavier trace elements) and an Ocean Optics USB2000 spectrometer connected to an optic fiber. For elemental analysis a set of standard reference materials from NIST (SRM2704, SRM2711) and three jadeite mineral reference samples from Motagua were irradiated under the same conditions. Then AXIL code and the PIXEINT program were used for quantitative analysis.

In order to improve the Ionoluminescence emission detection a second round of measurements were carried out using two fiber optics connected to Ocean Optics USB 2000 spectrometers to cover a light wavelength range from 200 to 1000 nm with higher efficiency in the ultraviolet and near infrared regions.

Figure 4 shows the experimental device and the irradiation of one of the ear ornaments.



**FIGURE 4.** External beam setup using two optic spectrometers for a 200 -1000 nm wavelength range. The typical green light emission from jadeite was observed in the ear ornament.

## RESULTS AND DISCUSSION

### X-ray diffraction (XRD)

Despite XRD is an ideal technique for mineral identification, it was only possible to analyze directly only four pieces. Figure 5 shows XRD spectra obtained for these artifacts. There is little interference in the identification of the minerals due to crystal preferential orientation. The comparison of the pattern reflections with the database with the JCPDF indicates that the pieces 2, 3, 9 and 12, correspond to antigorite, amazonite, jadeite and diopside, respectively.

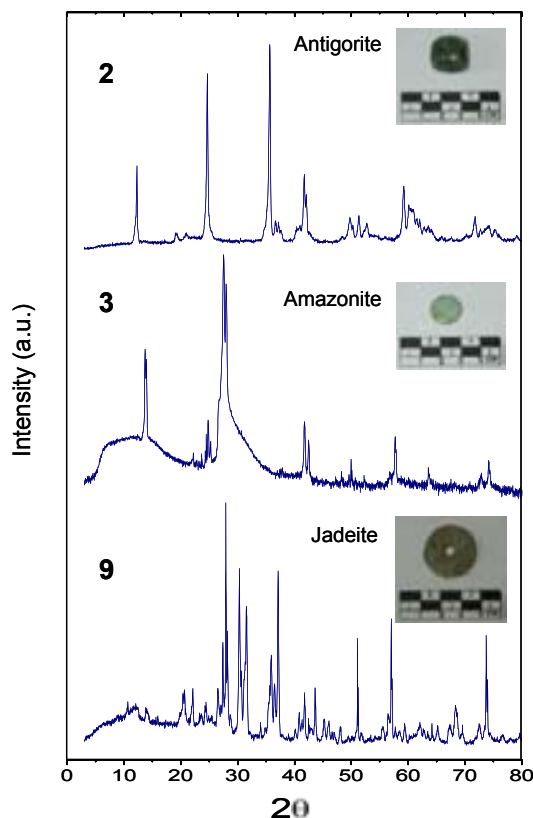


FIGURE 5. XRD patterns and the mineral identification for pieces 2, 3 and 9.

### Raman measurements

Raman is considered a very suitable method for mineral identification in specific regions, in particular of jadeite [11]. Nevertheless in our case, it was very difficult to obtain appropriate spectra due to the high fluorescence background with the red laser (785 nm) and the very polished surface of the artifacts. These difficulties have been observed for other artifacts from other collections. In some cases, such as the piece 9, 45° beam incidence allowed to observe on the background low intensity signals at 380, 700 and 1038 cm<sup>-1</sup>, related to jadeite (Figure 6).

### Mid-FTIR analysis

In contrast to Raman spectroscopy, FTIR technique was very adequate for the characterization of the minerals composition. The identification can be achieved by comparison of the pieces spectra with spectra of reference materials of known minerals and data bases [12]. Two groups of pieces may be differentiated, a first one with a main phase of jadeite and a secondary phase of albite –the mineral precursor of jadeite-, and second group of other green minerals. In figure 7 and 8, it is shown some representative spectra of these two groups of the green stone artifacts.

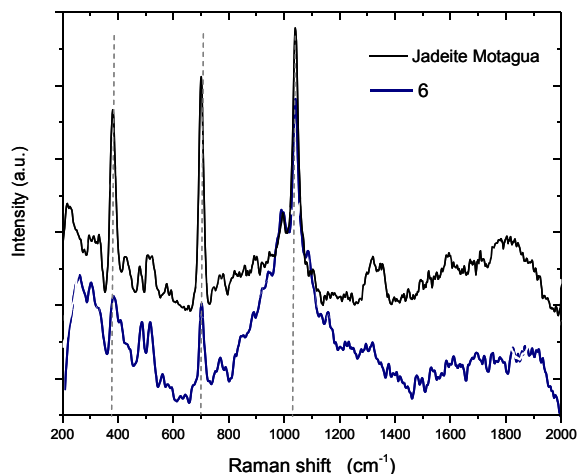


FIGURE 6. Raman spectra of piece 6 and the reference of jadeite from Motagua region.

In the non-jadeite group several pieces have similar spectra to the serpentine mineral sample with different contributions of albite and other minerals. There is a good agreement with the identification by XRD, like in the case of the amazonite bead (piece 3). The complete identification is shown in Table 1.

TABLE 1. Mineral Identification of the pieces from XRD and FTIR results.

Piece	Stage	Description	Identification	
1		III A	Spherical bead	Jadeite
2		III A	Tubular bead	Diopside
3		III A	Circular pendant	Amazonite
4		III A	Tubular bead	Serpentine
5		III A	Asymmetric bead	Jadeite
6		III B	Asymmetric bead	Jadeite+albite
7	a	III B	Plate- ear ornament	Jadeite+albite
7	b	III B	Ear ornament	Jadeite+albite
8	a	III B	Plate- ear ornament	Jadeite+albite
8	b	III B	Ear ornament	Jadeite+albite
9		III B	Circular pendant	Jadeite+albite
10		IV	Ear ornament	Serpentine
11		IV	Convex piece	Serpentine
12		IV	Convex piece	Antigorite
13		IV	Circular pendant	Jadeite
14		IV	Irregular fragment	Jadeite

### Ionoluminescence

It has been shown that the luminescence induced by the proton beam gives rise to specific spectra for minerals and impurities in the materials [13]. Jadeite ionoluminescence presents a green intensity emission at 540 nm due to Mn<sup>2+</sup> impurities (Figure 9).

On the other hand albite presents at 350 nm, the typical emission of aluminosilicates in the ultraviolet region. For some pieces it is possible to observe the emission of jadeite, or both, jadeite and albite, as a function of the composition of the object. In some cases, other emission, due to still non-identified mineral phases, may appear in the spectra. This is the case of the emission at 690 nm.

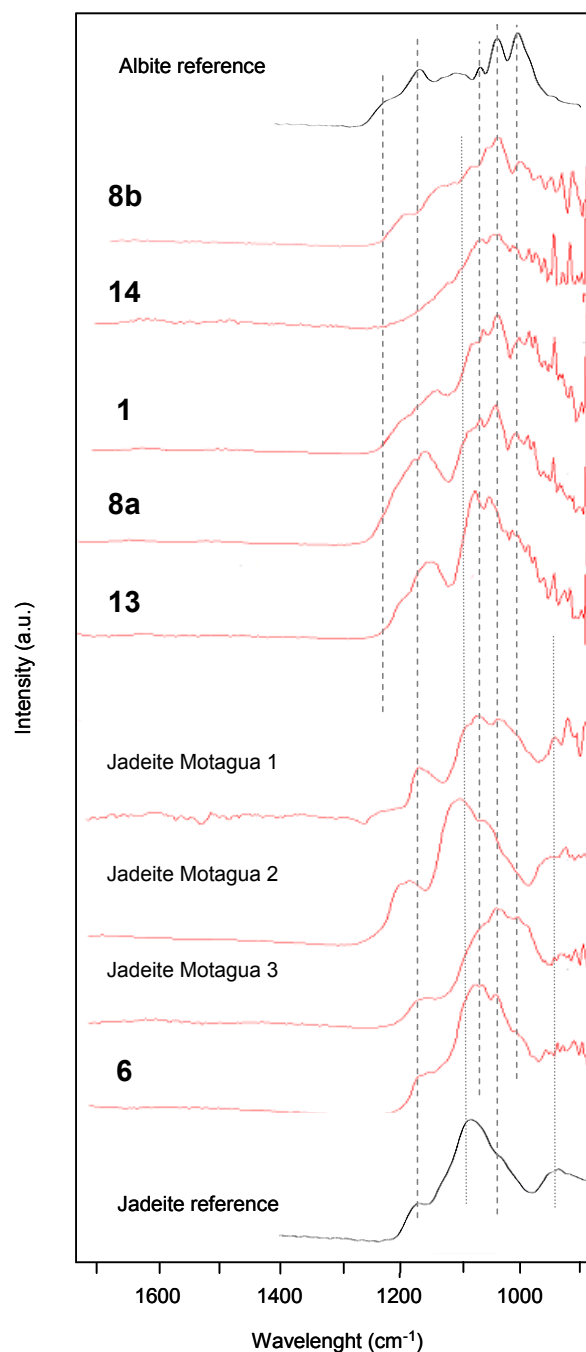


**FIGURE 7.** FTIR spectra of pieces 1, 6, 8, 13 and 14 and their comparison with material references of jadeite and data base spectra.

The ionoluminescence results agree with the identification provided by XRD and FTIR when there is light emission. This is the case, of jadeite, jadeite-albite and amazonite pieces. For amazonite there is a specific spectrum composed by intense emissions at 290 and 690 nm and a broad emission between 350 and 630 nm. This combined emission gives rise to an intense violet colour at the proton beam spot.

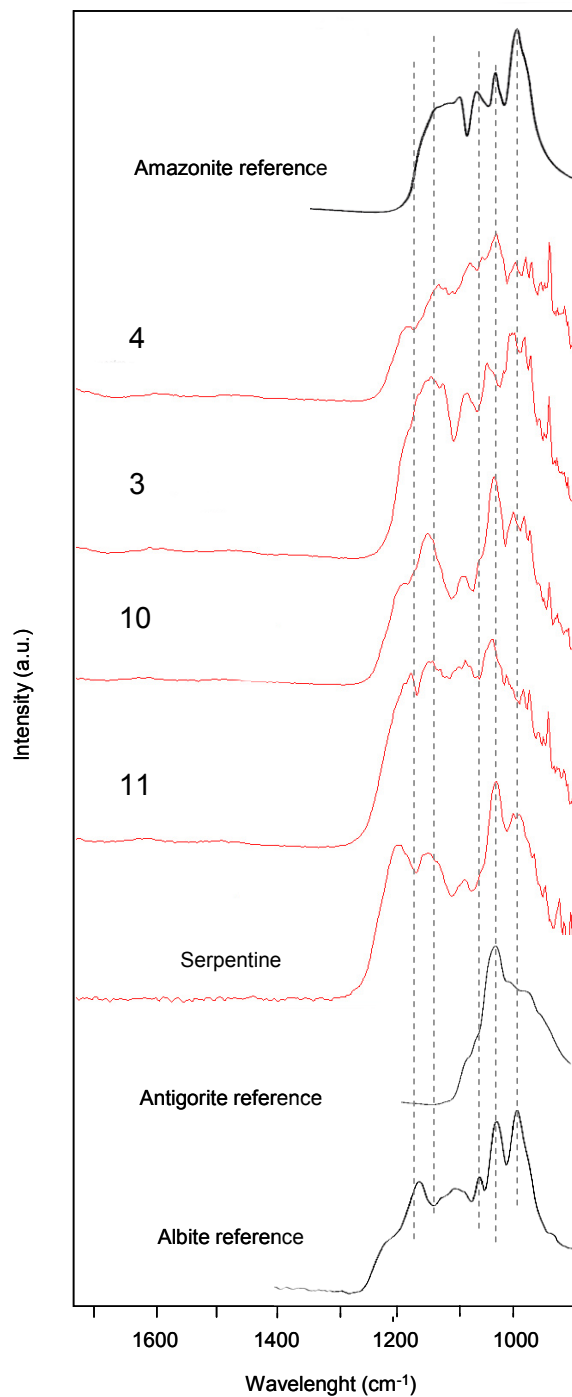


**FIGURE 8.** FTIR spectra of pieces 3, 4, 10 and 11 and its comparison with material references and data base spectra.

In the case of other green stone minerals, such as serpentines, there was not observed any luminescence, probably because of the quenching effect of Fe. Finally, the fine peaks observed in the UV region are due to He ionization by the proton beam, He flux is set in the Si-PIN X-rays detector of the external beam to improve light elements detection.

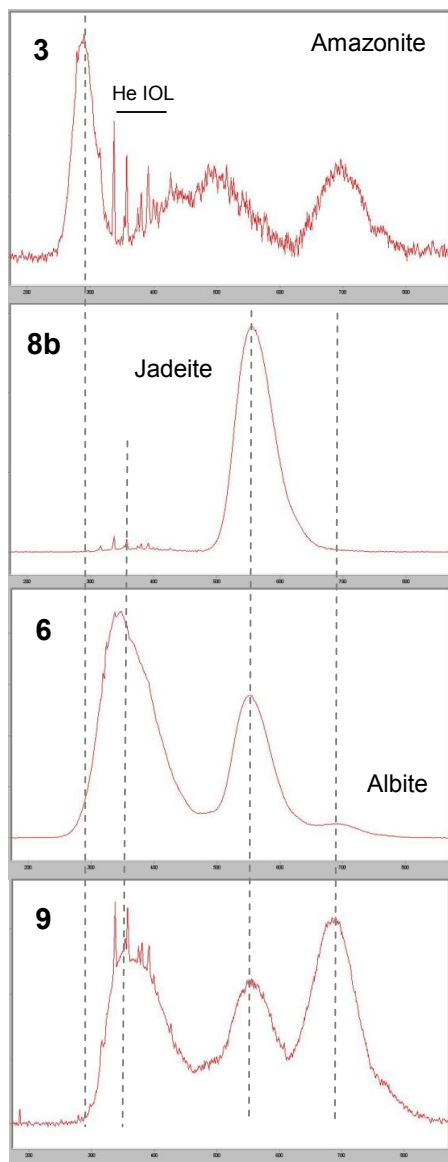


**FIGURE 9.** Ionoluminescence spectra of pieces 3, 6, 8b and 9 using the spectrometer with higher efficiency in the UV region.

### PIXE results

The elemental concentrations for the artifacts are shown in Table 2. For the provenance study, principal components analysis was carried out using the logarithm of the elemental contents (in % weight) and a normalized varimax rotation. This statistical analysis was done only for pieces previously identified as jadeites. Motagua samples as well as reported data in previous studies [10] are used for comparative analysis. In figure 9, the graph of factor 1 vs factor 2 is shown.

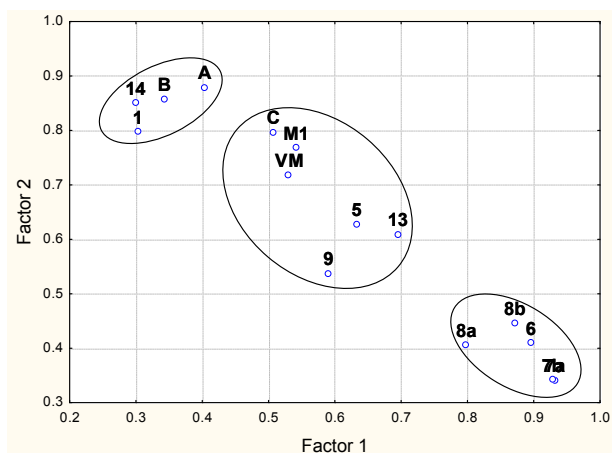


**FIGURE 10.** Graph of factor 2 vs factor 1 from principal component analysis for jadeite pieces. M1 and VM correspond to jadeite from Motagua. A,B,C are jadeites from a Teotihuacan offering.

In the figure 10, there are three groups of composition, i.e. three sources [10]. Some artifacts (9, 5, 13) fit the Motagua samples composition (VM and M1) while pieces 1 and 14 are related to two of the Teotihuacan pieces from a different source. All the ear ornament pieces of the burial are from another source, different of the previous ones. It is interesting that the best objects of the set, the ear ornaments from the burial are all in the same cluster; perhaps they were produced in the same workshop and were traded together.

Our results agree with other studies of jadeite sourcing, since additional beds different from Motagua have been observed in analytical studies on Cancuen jadeite workshops [5].

Concerning the other pieces made of other green minerals, further studies and field work must be still carried out in order to explore beds and to determine probable sources. It has been suggested that serpentine sources of artifacts of Veracruz area may be in Oaxaca region of Cuicatlán, about 200 km distant while the Motagua jadeite sources area at least 900 km away.

On the other hand, in the case of amazonite, the sources are reported for the Postclassic period in the South-West of USA, in Colorado and Chihuahua in North Mexico [9].

### CONCLUSIONS

The problem of identification and sourcing of green stone materials in Mesoamerica may be quite complex due to the variability of the minerals, their natural heterogeneity and the mobility of the pieces due to long distance exchange routes.

TABLE 2. Elemental concentration determined by PIXE analysis. Uncertainties of about  $\pm 10\%$  of the reported measurement

Piece	Mg %	Al %	Si %	P %	S $\mu\text{g/g}$	Cl %	K %	Ca %	Ti %	Mn $\mu\text{g/g}$	Fe %	Ni $\mu\text{g/g}$	Cu $\mu\text{g/g}$	Zn $\mu\text{g/g}$	Ga $\mu\text{g/g}$	Rb $\mu\text{g/g}$	Sr $\mu\text{g/g}$	Zr $\mu\text{g/g}$
1	1.67	11.6	30.5	0.119	36	239	0.131	2.86	0.040	235	0.50	912	99	-	-	32	88	-
2	2.25	5.01	22.2	0.068	-	87	0.011	5.62	0.002	356	0.82	852	83	-	-	-	59	-
3	0.14	10.5	29.6	0.021	119	119	1.211	0.28	0.005	-	0.05	-	109	-	35	14521	-	-
4	1.39	10.6	28.4	0.095	97	171	0.025	2.78	0.010	215	0.56	492	149	10	14	5353	59	-
5	0.49	12.8	27.7	0.353	3196	484	0.077	1.64	0.045	227	0.68	439	246	40	-	30	121	-
6	0.48	15.2	34.6	0.127	90	285	0.040	0.59	0.056	139	0.52	437	184	-	9	-	-	-
7a	1.27	9.5	28.9	0.158	117	167	0.069	3.04	0.034	233	0.63	2020	122	10	-	-	-	-
7b	1.29	8.3	23.8	0.159	113	55	0.032	3.26	0.029	312	0.86	1984	142	25	-	-	-	-
8a	1.66	8.02	25.2	0.095	80	17	0.058	3.48	0.035	298	0.78	2354	120	15	-	24	-	-
8b	0.53	13.8	36.4	0.161	74	101	0.028	0.78	0.033	149	0.48	109	188	12	13	-	-	-
9	0.90	10.8	24.2	0.098	470	19	0.016	2.67	0.046	325	0.87	727	98	28	-	-	-	-
10	0.40	15.0	42.6	0.101	721	200	0.053	0.37	0.021	72	0.22	109	202	11	5	-	64	-
11	0.35	8.04	38.8	0.123	140	286	0.263	0.24	0.118	143	0.47	86	92	19	-	78	595	51
12	17.3	1.26	18.4	0.057	129	273	0.020	0.03	0.021	478	1.30	3098	128	32	-	-	61	-
13	0.32	10.3	26.6	0.065	72	346	1.270	0.36	0.055	90	0.34	27	136	11	13	4123	910	-
14	0.43	5.53	22.5	0.206	128	193	0.267	1.35	0.216	278	1.08	21	45	98	-	-	394	-

If consider that green stone artifacts are rare in the Central Veracruz area of Mesoamerica, it is necessary to use a methodology of analysis including various complementary techniques for a complete characterization of the mineral identification and elemental composition for provenance studies. Our results provide outstanding data about the set of green stone artifacts discovered in La Joya site.

## ACKNOWLEDGMENTS

This analytical research has been supported by CONACyT Mexico grant U49834-R and PAPIIT UNAM project IN403210. Authors thank K. López and J. Beristain for Pelletron accelerator operation., as well as J. Pineda and J.G. Morales for technical support. XRD measurements were carried out by M. Aguilar.

## REFERENCES

1. M.H. Turner, "Style in Lapidary Technology: Identifying the Teotihuacan Lapidary Industry" in *Art Ideology and the City of Teotihuacan*, J.C. Berlo ed., Dumbarton Oaks Research Library and Collection, Washington 1988. pp. 89-112.
2. R Seitz, G.E. Harlow, V.B. Sisson, T.A. Taube, *Antiquity* **75** (2001) 687-688.
3. W.F. Foshag, R. Leslie, *Am. Antiquity* **21** (1955) 81-83 (2004) 177-180.
4. K. Taube, Z. Hruby, L. Romero, *Jadeite Sources and Ancient Workshops: Archaeological Reconnaissance in the Upper Río El Tambor, Guatemala*, FAMSI reports 2004. <http://www.famsi.org/reports/03023/index.html>
5. B. Kovacevich, Brigitte, H. Neff, R. Bishop, "Laser Ablation ICP-MS Chemical Characterization from a Jade Workshop at Cancuen, Guatemala", in *Laser Ablation ICP-MS in Archaeological Research*, R.J. Speakman, H. Neff, University of New Mexico Press, 2005, 39-58.
6. A. Daneels, Monumental Earthen Architecture at La Joya, Veracruz, Mexico. Foundation for the Advancement of Mesoamerican Studies. Crystal River, 2008 ([www.famsi.org/reports/07021](http://www.famsi.org/reports/07021)).
7. B. Stark, L. Heller, M. Ohnorsorgen, *Latin American Antiquity* **9** (1), 1998, 7-36.
8. A. Daneels, J.L. Ruvalcaba Sil., Cuentas de piedra verde en una residencia Clásica del Centro de Veracruz, in *Estudios Recientes sobre Jade y Piedras Verdes*, W. Wiesheu, G. Guzy, eds. INAH, Mexico, in print.
9. J.L. Ruvalcaba Sil, L. Filloy, M. Vaggi, L.H. Tapia Gálvez, R. Sánchez Becerra, "Estudio no destructivo in situ de la Máscara de Malinaltepec" in *La Máscara de Malinaltepec*, S. Martínez del Campo coord., CONACULTA-INAH, México, 2010, 153-168.
10. J.L. Ruvalcaba Sil, L. Manzanilla, E.R. Melgar Tisoc, Ru. Lozano Santa Cruz, *X-ray Spectrometry* **37** (2008) 96-99.
11. D.C. Smith, "Mesoamerican Jade" in *Raman Spectroscopy in Archaeology and Art History*, H.G.M. Edwards, J.M. Chalmers, RSC Analytical Spectroscopy Monographs, London, 2005, p. 412-424
12. M. Ostrooumov, *Espectrometría Infrarroja de Reflexión en Mineralogía Avanzada, Geomología y Arqueometría*, Monografías del Instituto de Geofísica 12, Universidad Nacional Autónoma de México, Mexico, 2007.
13. H. Calvo del Castillo, J.L. Ruvalcaba, T. Calderón, *Anal. Bioanal. Chem.* **387** No. 3 (2007) 869-878.

## **Chemical Characterization of Mortar from San Roque Church (San Francisco de Campeche, México)**

J. Reyes<sup>1</sup>, Y. Espinosa-Morales<sup>1</sup>, P. Maldonado<sup>1</sup>, G. Ancona<sup>2</sup>, P. Bartolo-Pérez<sup>3</sup> and J.A. Azamar-Barrios<sup>3</sup>

<sup>1</sup> *Centro de Investigación en Corrosión, Universidad Autónoma de Campeche, MEXICO.  
e-mail: javreyes@uacam.mx*

<sup>2</sup> *Facultad de Ciencias Químico Biológicas, Universidad Autónoma de Campeche, MEXICO.*

<sup>3</sup> *Centro de Investigación y de Estudios Avanzados del IPN, Unidad Mérida, MEXICO.*

**Abstract.** This study was carried out in order to characterize chemical composition of mortars from the facade and west wall of San Roque Church, a colonial building built at the end of XVII century in San Francisco de Campeche City. FTIR Spectroscopy and SEM/EDX techniques were employed in order identified mineral phase and elemental composition of degradation products formed as a consequence of the interaction of the building materials with the environment. FTIR results indicated that mortars were made with a mixture of calcareous materials and sand. Calcium carbonate and silicates were the major compounds. Other compounds such as gypsum and calcium oxalates were present, which are characteristic neo-formation compounds related with to the sulfur dioxide reaction and biodegradation activity, respectively. Mortar elemental composition obtained by SEM/EDX confirmed that C, O and Ca are the main components. Also earth minerals and external elements deposited on mortar surface thought atmospheric process were identified.

**Keywords:** mortar, colonial buildings, SEM/EDX, FTIR, San Francisco de Campeche

### **INTRODUCTION**

San Roque Church is a colonial building included into the historic, military and architectural complex built during Seventeenth to Nineteenth Centuries in San Francisco de Campeche City, the most important port for trade of goods from Yucatán Peninsula (México) to Europe during the Colony. In 1999, this historic complex was included into UNESCO Cultural Heritage List.

The Church was built at the ending of the XVII century over calcareous stone substrate. Foundations, column, ceiling and walls were base masonry constructed within local calcareous materials from the region including limestone blocks, sand, slake lime and carbonate clay marls known as sascab in Yucatan

Peninsula. These materials were also used to manufacture mortars employed for joints and coating films. Actually some areas of the building show the rest of hydraulic mortars made with modern cement product of recent reparations.

The building is located in the corner of 59 x 12 streets closer to the main square of the City (Figure 1 and 2). Because of their location, during the day, those streets have of continue vehicle flow.

The main and west façade of the building are then exposed to vehicle emissions without so far enough studies about the role of these emissions in deterioration of the buildings has been carried out. On the other hand, the interaction with the predominant tropical climate of the City induce several mortar degradation pathologies affecting the mortars in

the buildings including blistering, cracking, decohesion, erosion and the presence of numerous microorganisms colonies (see Figure 3).



**FIGURE 1.** San Roque Church, San Francisco de Campeche, Mexico.

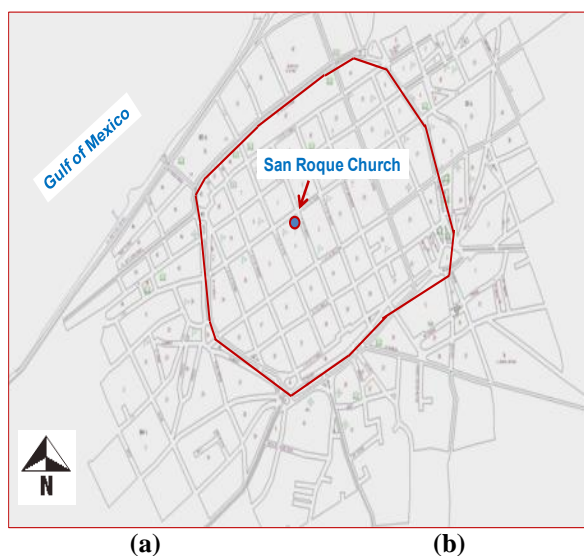


**FIGURE 2.** (a) San Roque Church. (b). Location of the Church at the historic center of San Francisco de Campeche City.

This study was carried out in order to characterize chemical components of mortars from the walls of San Roque Church aimed in the determination of mineral

compounds related with the interaction of building materials with the environment.

## MATERIALS AND METHODS

### Sampling

Six representative mortar surface layers from San Roque Church were retired at different sites from the lower and upper outside walls of the building by using small chisels, hammer and scrapers. Three samples from the main façade bordering 12<sup>th</sup> street (North face) and three samples from the lateral façade bordering 59<sup>th</sup> street (West façade). All the samples were kept in hermetic bags and stored under dried conditions until the analysis was performed.

### FTIR spectroscopy analysis

5 mg of each sample was grinded and mixed with 195 mg KBr by using an agatha mortar. After that, the mixture was deposited in an HATR support and analyzed in a Thermo Nicolet Nexus 670 FTIR spectrophotometer. The analysis was conducted in a medium infrared region ( $400\text{-}4000\text{ cm}^{-1}$ ) within a spectral resolution of  $0.09\text{ cm}^{-1}$  and  $32\text{ scans min}^{-1}$ .

### SEM/EDS analysis

Fragments about  $1\text{ cm}^2$  of each sample were examined without previous preparation in a scanning electron microscopy (Philips XL30 ESEM) coupled with X-ray dispersive analysis system. The analysis was performed at 20 kV, working distance of 10 mm and tilt angle of  $0^\circ$ . An X-ray SUTW-Sapphire detector was used.

## RESULTS

### SEM/EDS analysis

SEM analysis on mortar fragments revealed an irregular surface with the presence of diffuse porous along the samples. The matrix appears to be of compact structure with high porosity that favors the development of longitudinal micro fractures across the

mortar and small holes probably interconnected by porous systems and cracks (Figure 3a).

Diverse biological structures can be observed inside the microcracks. Bio-films cover surface areas of mortar or have penetrated across the mineral matrix (3b). Several authors indicated that fungus and lichens produce supported structures named hyfaes which grown inside the mortar matrix and induce intergranular decohesion and cracking [1,2,3].



**FIGURE 3.** Several aspects of degradation phenomena in San Roque Church.

Higher magnification (at 500 and 1000X) indicates the growth of crystals with dendritical, rhomboidal, fibroses and ovoid forms related with calcium carbonate (Figure 4).

On the other hand, cubic crystal corresponding to sodium chloride were also observed on the surface of sample 5 (Figure 5), collected on the lower part of the main facade of the church.

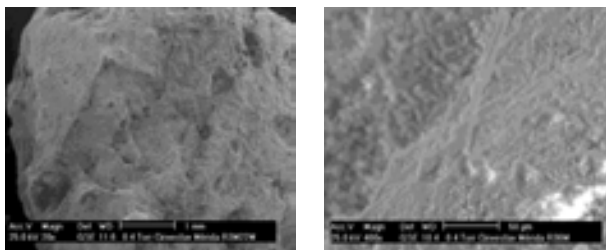


**FIGURE 4.** (a) General aspect of mortar micro-structure (left) (b) Microbial biofilm over mortar surface, at the center a longitudinal hyfae structure (right).

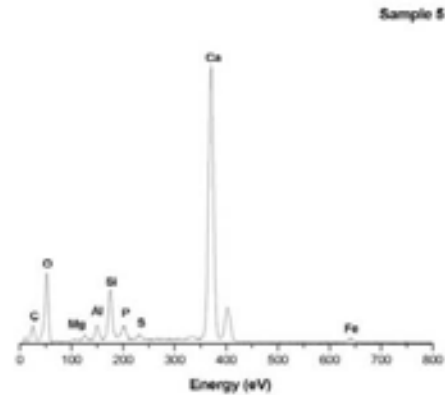
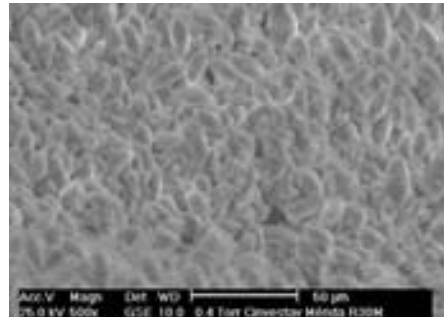


**FIGURE 5.** Ovoidal- shape structures characteristic of calcium carbonate crystals present in mortar sample and their corresponding EDS spectrum.

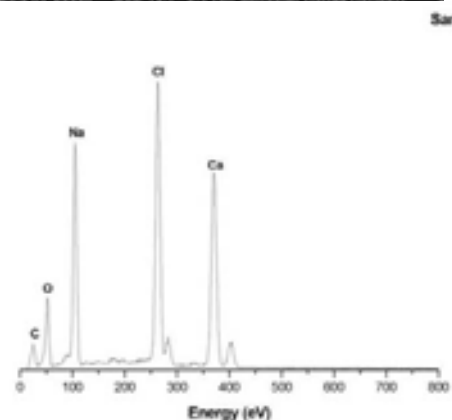
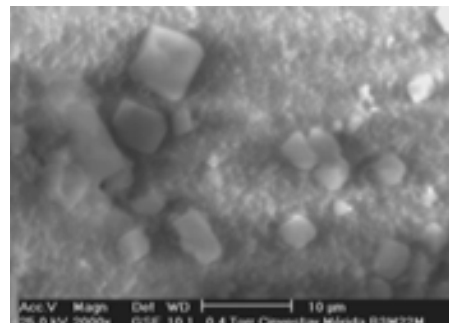


**FIGURE 6.** Cubic sodium chloride crystals deposited over mortar samples and their corresponding EDS spectrum.

Al, Si, Fe and Mg and K are crustal element normally present in stone materials used for building construction, including modern cements. Other sources of these elements are soil and dust particles. Si is always present in sand used during limestone mortar preparation. Also Si and Al form part of clays compounds like kaolinite [6]. The last one was identified during FTIR analysis as will be discussed later.

Atmospheric pollution is the main source of S in urban environments. S is produced during fossil fuel combustion in vehicle exhaust and power plants. It is constituent of sulfur dioxide (SO<sub>2</sub>), a very reactive gas that induces gypsum formation during their interaction with calcareous materials [4, 7]. S also can be incorporated to the mortar surface directly from sulfate atmospheric airborne particles.

The presence of Cl and Na shows the noticeable presence of marine aerosols and their source. Other elements like K and Mg can also have a marine origin. All they are external elements deposited on mortar surface across atmospheric process [5].

### FTIR analysis

Mineral composition was investigated by FTIR spectroscopy in order to determinate mortar alteration products (Table 2). The results indicate that mortars were made with a mixture of calcareous materials and sand. Figure 6 shows a characteristically FTIR spectrum obtained during the analysis of mortar samples.

Typical stretching C-O (1459 cm<sup>-1</sup>) and bond C-O (875 cm<sup>-1</sup>) signals indicated that calcium carbonate (CaCO<sub>3</sub>), was the major mineral phase observed in the samples. Other calcium carbonate signals were observed at 712, 1795 and 2523 cm<sup>-1</sup>.

Mineral phases of silicon compounds present in the samples manifested medium and weak signals. Si-O-Si asymmetric stretching vibration at 1169 cm<sup>-1</sup> and symmetric stretching vibration at 776 cm<sup>-1</sup> indicated the presence of quartz mineral phase (SiO<sub>4</sub>). Si-O-Si at 1032, Si-Al-Si at 470 and 1016 and outer hydroxyl anion signals at 3680 cm<sup>-1</sup> were assigned to the aluminosilicate kaolinite ([Al<sub>2</sub>(Si<sub>2</sub>O<sub>3</sub>)OH<sub>4</sub>]).

Quartz is a typical compound of marine sand used traditionally in the preparation of original mortars and posterior reparation operations carried out in the walls of San Roque Church along the time.

Kaolinite is mineral clay present in sascab as have been reported by Torres [8], in a study to characterize the performance of traditional mortars under natural and artificial weathering. This material is traditional carbonate clay marl used since Mayan period for the construction of masonry structures in the Yucatán Peninsula. Quartz and kaolinite either can be derived from wind bone surface particle deposition processes as have been suggested by Maravelaki\_Kalaitzaki in studies realized in historic areas of Athens [7].

**TABLE 2.** Main compounds identified by FTIR in mortar samples from San Roque Church.

Mineral phase	Sample code					
	1	2	3	4	5	6
Calcium carbonate (C)	+	+	+	+	+	+
Quartz (Q)	+	+	+	+	+	+
Kaolinite (K)	+	+	+	+	+	+
Gypsum (G)	+	+	+	+	+	+
Aliphatics (A)	+	+	+	+	+	+
Nitrates (N)	+	+	-	-	-	-
Esters (E)	+	+	+	+	+	+
Hematite	+	-	-	-	+	-

**TABLE 1.** Elemental composition of mortar samples from San Roque Church and their origin. (+) Present, (-) not present.

Elements	Sample code						Origin
	1	2	3	4	5	6	
C	+	+	+	+	+	+	Calcareous materials, neominerals and organic matter
Ca	+	+	+	+	+	+	
O	+	+	+	+	+	+	Minerals compounds, neominerals and organic matter
K	-	-	-	+	+	+	
Al	+	+	+	+	+	+	Clay minerals and marine aerosols
Si	+	+	+	+	+	+	
S	+	-	+	-	+	-	Crustal elements
Mg	+	-	+	+	+	+	
Fe	+	-	+	+	+	+	Sand and crustal element
Na	+	+	-	-	+	-	
P	-	-	-	-	+	-	Atmospheric pollution, soil particles and neominerals
Cl	+	+	-	+	-	-	
							Biologic (bird drops)
							Marine aerosols and clay minerals
							Crustal elements, marine aerosols
							Crustal elements
							Marine aerosols and clay minerals
							Biologic (bird drops)
							Marine aerosols, saline water

Iron oxides also were present in the samples with a weak signal, overlapped by  $470\text{ cm}^{-1}$  peak signal corresponding to kaolinite. Their characteristic band absorption could be assigned at  $517\text{ cm}^{-1}$  to hematite ( $\text{Fe}_2\text{O}_3$ ). Iron oxides have been reported as constituent of ochre and red pigments [6,9]. It is important to note that San Roque Church, as occurred with other colonial building in San Francisco de Campeche City, usually was covered with paint.

Other compounds like gypsum ( $\text{CaSO}_4 \cdot 2\text{H}_2\text{O}$ ) were present. The medium vibrations frequency signal of sulphate at  $1078$ ,  $1633$  and  $622\text{ cm}^{-1}$  are indicative of gypsum presence. Gypsum is characteristically neo-formation compound produced during chemical weathering of stone related materials buildings [7, 10, 11].

Gypsum is consequence of sulfur dioxide ( $\text{SO}_2$ ) reaction with calcareous materials and is a typical component of weathering crust in urban environments. It also can be naturally in small quantities in calcareous materials used in building constructions. On this way, because of the low pollution levels in San Francisco de Campeche City [12], the natural origin of gypsum cannot be discarded.

Around  $1385\text{ cm}^{-1}$ , it was observed a clear signal corresponding to the double degenerated antisymmetric N-O stretching mode of nitrate groups ( $\text{NO}_3^-$ ). The origin of this compound in monuments is variable and can be appointed to  $\text{NO}_x$  reaction with calcium carbonate, biological activities or absorption of nitrates from the soil [1,13].

A medium signals observed at  $2875$  and  $2895\text{ cm}^{-1}$  corresponding to -CH- aliphatic chains and an estearic weak signal ( $\text{C}=\text{O}$ ) at  $1728\text{ cm}^{-1}$  could be assigned.

The presence of esters and aliphatic compounds in mortar samples is consequence of numerous microorganisms which grown above and inside of mortar structure. Most of them can be related with calcium oxalate production and could have an active role in mortars chemical and mechanical degradation mechanisms [1, 5, 13].

## CONCLUSIONS

In this paper, a chemical and mineralogical characterization of mortars from San Roque Church, an historical building from the colonial city of San Francisco de Campeche, was realized by using SEM/EDX and FTIR techniques.

SEM/EDX analysis indicate that microstructure of the mortars seems to be affected by weathering agents including microorganisms that origin mechanical stress and induce the loss of mechanical properties.

Elemental composition reveals the existence of crustal elements, derived from calcareous materials and aggregates employed during mortar manufacturing.

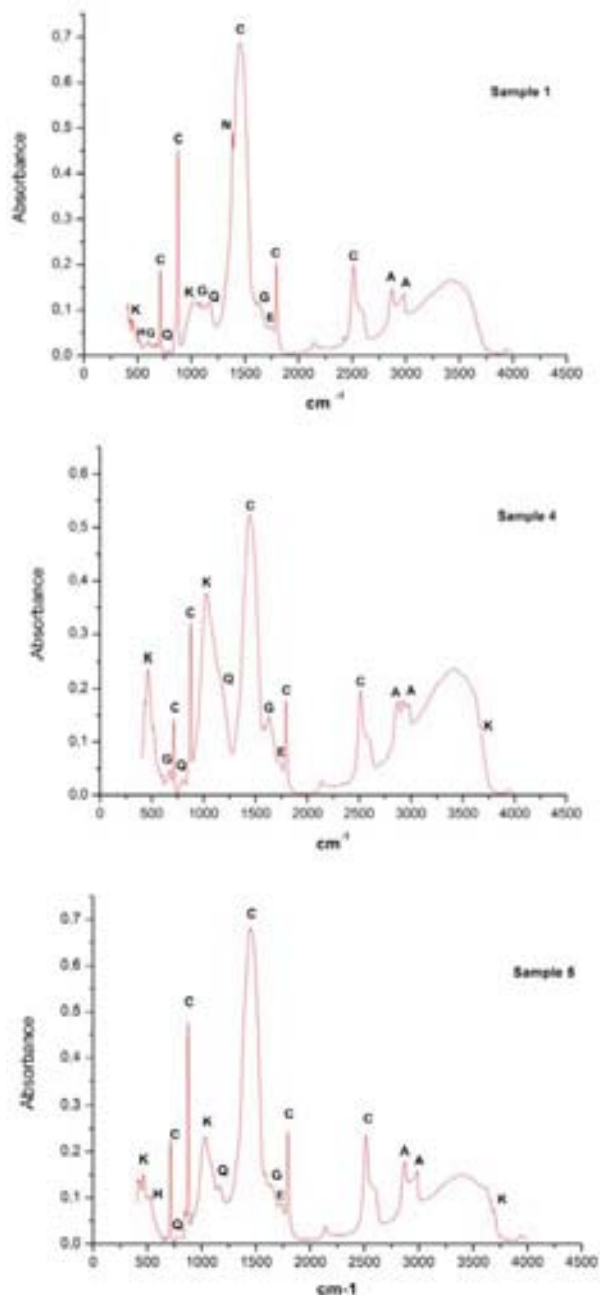


**FIGURE 7.** Characteristically FTIR spectra obtained during the analysis of mortar samples. A, aliphatics; C, calcite; E, esters; G, Gypsum; H, hematite; K, kaolinite; N, nitrates; Q, quartz.

Other external elements like Cl, Na and S also present in the samples indicate the interaction of mortar with environmental agents. The last one was confirmed by FTIR analysis. Mineral phases like calcium carbonate, quartz and kaolinite identified by this technique are considered natural components of calcareous stone, quartz and sascab.

Gypsum was the unique neomineral phase identified in mortar samples. Moreover, because the low levels of sulfur dioxide in San Francisco de Campeche City, the origin of gypsum is not clear. On the other hand, the presence of aliphatic compounds and an estearic group are indicative of biological activity.

Finally, it is important to note that other analytical techniques must be employed in order to obtain more complete information about degradation phenomena of historic buildings in San Francisco de Campeche City.

### ACKNOWLEDGMENTS

This research was supported by FOMIX CAMP-2005-C01 and CONACYT 59998 projects. Authors thanks to Centro INAH-Campeche, México and Campeche State Government General Office for Historical Sites and Monuments for their authorization and help during the sampling.

### REFERENCES

1. G. Gómez-Alarcón, B. Cilleros, M. Flores, J. Lorenzo, *Sci. Tot. Environ.* **167** (1995) 231-239.
2. M. Monte, *Journal of Cultural Heritage* **4** (2003) 255-258.
3. J. Arocena, T. Siddique, T. Thing, S. Kapur, *Catena*. **70** (2007) 356-365.
4. C. Cardell, F. Delalieux, K. Roumpopoulos, A. Moropoulou, F. F. Auger, R. Van Grieken, *Constr. Built Mat.* **17** (2003) 165-179.
5. J. Reyes, G. Gutierrez, G. Centeno, D. Aguilar, P. Bartolo, P. Quintana, J. A. Azamar, T. Pérez, *Chemical characterization of crust formed in mortars of historical buildings in San Francisco de Campeche City, México*, Proceedings 1<sup>th</sup> Historical Mortar Conference. Lisbon, Portugal, 2008.
6. Casadio, Ch. Colombo, A. Sansonetti, L. Toniolo, M. P. Colombini, *Journal of Cultural Heritage* **6** (2005) 79-88.
7. P. Maravelaki-Kalaitzaki, *Anal. Chim. Acta.* **532** (2005) 187-198.
8. F. Torres, *Efecto de la lluvia en el deterioro del patrimonio histórico del estado de Campeche*. Master Thesis. Facultad de Ingeniería. Universidad Autónoma de Campeche, México, 2009.
9. P. Maravelaki-Kalaitzaki, N. Kallithrakas-Kontos. *Anal. Chim. Acta.* **497** (2003) 209-225.
10. N. A. Duran, M. D. Robador, C. C. Jimènez de Haro, V. Ramirez-Valle. *J. Therm. Anal. Calorim.* **92** (2008) 353-359.
11. P. Maravelaki-Kalaitzaki, D. Anglos, V. Kilikoglou, V. Zafiropoulos, *Spectrochimica Acta B.* **56** (2001) 887-903.
12. F. Corvo J. Reyes, C. Valdes, F. Villaseñor, O. Cuesta, D. Aguilar, P. Quintana. *Water, Air, Soil Pollut.* **205** (2010) 359-375.
13. C. Genester, C. Pons. *Journal of Cultural Heritage* **4** (2003) 291-298.

## **Warrior's Belt from the Middle Volga Burial Ground X A.D. - Technology and Origin**

I. Saprykina<sup>1</sup>, O. Zelentsova<sup>1</sup> and R. Mitoyan<sup>2</sup>

<sup>(a)</sup> *Institute of Archaeology Russian Academy of Sciences, RUSSIA. e-mail: dolmen200@mail.ru*

<sup>(b)</sup> *Geological Faculty, Moscow State University, RUSSIA.*

**Abstract.** A belt from ancient Mordovian burial ground VIII-XI a.d. of the Middle Volga-river region (Central Russia) has a good safety and complete and has analogies from Hungary where it is connected with the period of «Conquest the homeland», and from the North Region of Russia where it is connected with presence of warrior's group. Burial with the belt from Krjukovsko-Kuznovsky cemetery differs from the majority researched in it by a ceremony of cremation. The belt was found in the 1930th and the author of excavations supposed that the belt was silvered. Our investigation shows that silver was added to standard alloy composition, which was traditional for jeweler's manufacture in this region. Presence of silver in alloy and gold amalgams on face of belt details shows high social and hierarchical level of client and, possibly, it must be connected with movement of ancient Hungarians to Magna Hungaria through the Middle Volga region.

**Keywords:** Ancient Mordovian burial ground of the Middle Volga Region, Hungarian type belt, manufacturing techniques, XRF-analysis.

### **INTRODUCTION**

Krjukovsko- Kuzhnovsky burial ground belongs to group of the Finno-Ugric funeral monuments located in a basin of the middle reaches of the Tsna river - the right bank of Volga. This monument was opened and researched in the 30th years of XX century P.P. Ivanov – founder of Morshansky Regional museum [1]. In total he excavated 586 burials which are dated within the limits of VIII-XI centuries and related to a stage of early history of the Finno-Ugric Mordovian population of the Middle Volga Region.

Special feature of pre-Christian funeral culture of ancient Mordovian population is a presence of wide variety of metal ornaments and details of clothes both in female and male burials. One of the widespread elements of a man's suit was «belt with plaques», actually consisted of leather belt decorated by metal plaques; belt have a tip on other end of it. A belt set could be simple and consist of a strip decorated by

plaques and tip, or complex - with vertical pendant small straps which were decorated with plaques and ended by a tip.

Belt sets were an accessory of a man's suit in Krjukovsko - Kuzhnovsky burial ground. In burial the belt, as a rule, settled down around hipbones and in most cases was clasped. In other words it was a doubtless element of a suit. Knives in sheaths, needle-holder with needles, awls were hanged to the belt. Leather or clothes small bags with wick tubules, steels and flint, were attached to it.

As a rule, there are one or several arms supplies: sword, dagger, spear, battle axe, arrows, etc. in a complex with such belt. Other special feature of such burials was a presence of metal ornaments in a suit: finds of bracelets, rings, ear-rings, sometimes - pendants.

Many researchers mentioned that the belt with plaques in a suit had a special nature connected with certain sign function – it was an insignia of authorities. A significant amount of such burials dates

from the X century - period of extension of influence of Khazar Kaganate on the territory of the Middle Volga Region.

The burial 505 of Krjukovsko - Kuzhnovsky cemetery dated from the X century is interesting for that matter. It stands out both a ceremony of a burial place - cremation, and structure of grave goods. Besides traditional subjects - temporal ring, sulgam, wick tubule there were spear, scraps of a small bag, wooden scoop with silver facings in a pine grave. Finds of a bit, girth buckle and bells testify that buried man was a horseman.

Unique for this territory belt with plaques had a special place in the burial. It was rolled into a spiral and was situated in the central part of burial, on calcinated bones. From P.P. Ivanov's diary: "... The belt is entirely covered with right-angled, cogged platques, bronze - cast, silvered and gilded inside of pattern, with clasp in one end and a tip coming down in the form of handing ornament in another (Figure 1). Plaques, clasp and tip equally are ornamented in the form of two crosses with the end expanded below. A tip is narrow with two plaques, heart-shaped form with a cut" [1].



**FIGURE 1.** Rectangular plaque (face) with gilding surface.

The belt set consists from clasp, tip and 48 plaques (Figure 2). The clasp is with a triangular frame in sizes 2x3. Its short ear is situated on a core in the basis of rectangular plate with semicircular ledges in a back part. A tip of the belt (6.5x2.8 cm) is with rectangular - rounded lower edge and three semicircular dredging on the top edge. There are two kinds of plaques in total. Vertically on the belt there were rectangular plaques (3.7x3 cm - 23 objects) with two three-petal ledges on the top edge and small spear-rectangular cut on the lower edge. Other, horizontal plaques of square proportions (3x3 - 25 objects) had three semicircular ledges on one vertical side and three same dredging - on opposite one. Horizontal plaques fastened on the belt one inside to other. All details of the belt are

ornamented with clubs-shaped figures covered by yellow metal.

Plaques and clasp were fixed on the leather belt by pins. Leather end of the belt was inserted into a tip, and the back side was closed by a thin plate. Actually leather belt had also complex cut: leather belt in thickness 2-2.5 and width about 3 cm formed its basis. It was covered with a leather of more thin workmanship in thickness up to 1 mm. Edges of the second were incurved and attached to a thick belt with prong of plaques. Besides the middle part of the belt was laid behind for greater durability by one thinner strap in width 1-1.2 sm. So plaques were not simply attached to the leather belt, but also fastened all its components.

115 cm of the leather belt were kept in a collection. The length of the belt reconstructed on plaques, tip and clasp comprises 170-172 cm. In a diary of excavation P. P. Ivanov showed that the end of the belt with a tip "coming down in the form of handing ornament". So-called Hungarian belts of epoch of «conquest the Magna Hungaria» with one end of which freely hanged down, passed through a holder or thrown through a belt are widely known in literature [2-3]. In a collection from burial 505 there is a belt holder in which a long end of a belt was passed through and hanged down.



**FIGURE 2.** Tip (face) and clasp (back) from belt.

Not incidentally nearest known analogy to this belt set is a belt found in Hungarian burial ground Karancslajto in 1939 [4-6]. The Hungarian burial as judged by a set of things is man's. Grave pit is focused

on a line of the north-south that is atypical for the Hungarian burial grounds. The burial from Northern Hungary, as well as Krjukovsko – Kuzhnovsky burial dated from the Xth century [5-6]. Judging by publications, the belt from Karancslajto is practically a full analogy of Krjukovsko – Kuzhnovsky burial, differing from the second in a little bit greater length of plaques and a little other composition of ornament from clubs-shaped figures.

The second analogy to the belt from the Middle Volga Region is from northern areas of Ancient Russia - from burial ground Minino 2 on Kubenskoye lake [7]. Here five plaques were found, came from cremations in a derived condition. Researchers combine these plaques into a unified set [8]. Finds are presented with two vertical and two horizontal plaques strongly deformed under influence of fire. Mininsky belt differs from above described by smaller size of plaques, horizontal plaques have not cut at the bottom, clubs-shaped figures are made in other art manner.

Presence of practically identical belt sets on so distant monuments is enough unique fact. Here one can talk about existence of specific warrior's culture. Its expression was, with other marks, belt sets developed under influence of Hungarian "fashion". This fact was marked in the archeological literature [9-10]. At the same time full identity of the researched belt set to the belt from Hungarian burial ground Karancslajto, and also presence in ancient Mordovian burial grounds on the right bank of Volga of enough noticeable amount of belts of "the Hungarian type" allow to raise the question that these artifacts are traffic markers of movement of ancient Hungarians from Middle Volga to "Magna Hungaria".

The main focus of our work was to study the technology and chemical composition of belt details from burial 505 at Krjukovsko-Kuzhnovsky cemetery.

## METHODOLOGY

All researches were done in local museum; so, main focus in studying of belt set is researching a chemical composition of metal and technology of its manufacturing using the portable equipment. Metallographic research on this phase of investigation was not done.

XRF was used to analyze the chemical composition of the metal (12 fragments of the belt have been analyzed). The analysis was done in the spectral laboratory of the Geological Faculty of the MSU with a portable XRF analyzer: laptop with special software, multichannel analyzer, sensor with radioisotope source ( $Am^{241}$  and  $Cd^{109}$  isotopes) (developed by R.A. Mitoyan, S.A. Koloskov, N.V. Yeniosova, T.G. Saracheva). The measurement procedure is standardized, measurement accuracy is set for each individual element; the measurement

procedure is standardized, the methods of the experiment are given in the study [11]. The resulting data is presented in the table 1.

The reconstruction producing technologies of objects were examined with help of binocular microscope Motic BA-300 with magnification ranging from  $4\times(0.10)$ ,  $10\times(0.25)$ . Photofixing was carried out using digital camera Moticam 2300 (compulsory increase  $0.5\times$ ).

## RESULTS AND DISCUSSION

Reconstruction of technology of belt sets details manufacturing are presented by a significant spectrum of researches [9, 12-14]. In the context of these researches other belt sets from Krjukovsko-Kuzhnovsky cemetery were also examined.

All researched details of the belt set from burial 505 - 1 clasp, 1 tip of a belt, 48 plaques of square and rectangular forms - are made by casting in composite forms.

Constructive elements of plaques - negatives of edging, sides with width of 0.7 mm, cuts in the sizes  $10\times 0.4$  mm, ornament (from the front side is negative, from the back one is positive), are casting too. Measurements of keyword parameters of constructive elements of plaques (both square and rectangular forms) showed their coincidence, the calculating error is not more than 5-7%. Plaques thickness are 0.7-1.09 mm.

The negative of the casting form was received on a print of matrix (use of a complete product as a matrix is not also excluded). The matrix (complete product) of two forms was used for getting of square and rectangular forms of plaques, differing both by constructive elements and ornamental line. The print used for negative shaping of a rectangular form of the plaque is more complicated. Here it is necessary to keep a relief of a cut in the top part of the plaque having borders with width of 0.7 mm. Prints were made on both wings of casting form, possibly, on one-stage operation. However they were not deep, the relief only was outlined. Discrepancy of ornament corner boards clearly show it: sharp corners of front side against smooth contours on the back one, presence of ornament defects on the complete product which were arisen because of prints in casting forms (absence of the top petals, displacement of border lines).

In total 3 types of matrixes (complete products) were used in the analyzed samples. There was one defect for 50% of sample – lack of relief right flower on the reverse side of rectangular plaques.

Details (plaques and tip) were improved after casting. Sides were sawn round, sides of cut were formed, the surface was polished, and defects of casting (gas porosity, cavern) were removed. On some

plaques defects of casting were significant - full filing of ornamental details of plaques is fixed here.



**FIGURE 3.** Example of defects – lack of relief right flower on the reverse side.

Emphasis of after-casting processing was concentrated on improving of ornamental relief by means of a cutter or engraving burin. The significant filing was made on sites for gilding.

Defects which had arisen in results of work by a cutter such as ruptures of metal on sites of a bend, deep, fixed visually lines of a cut etc. were fixed on these sites.

Survey of these sites has shown that cutting of metal was made by a deep method - not less than 0.5 mm was removed.

Thickness of a plate in a ground part of the ornament on a product made often less than 0.2 mm. The gold from back side of product "was dropped out" on the back side of a product, in a contour of the ornament, because plate was strongly thin.

Belt clasp from this belt set was cast using of composite casting form. Shield of clasp was cast with

using of a form which had analogy with a form used for casting plaques of the square form. It was connected with a form used for casting of clasp's frame (the frame has standard form). Runouts are fixed on that place where shield crossed the frame. Presence of casting hole for a core under ear shows that a core was used as the basic fastening element for connection of two casting forms.

Shield of belt clasp was processed by the same method of plaques processing. The framework was carefully filed away, ground and polished. Ear of a clasp also was cast by a method of casting with sledge pin. Its making was exposed to forging and bending process for shaping of the necessary form.

The back side of plaques and clasps shield of belt is supplied by sprigs made from casting wire of round section. Their diameter is about 0.2-0.3 mm, height - no more than 1 mm. Sprigs have traces of cut; they are soldered to a turn of plaques, tip and clasp with tin in the form of balls in diameter no more than 0.3 mm was used as solder.

Last stage of work at details of belt sets was application of gold gilding. Gilding was made by a method of amalgam. The analysis of a chemical composition of metal fixed presence of Au tying together Hg. Application of amalgam was made using either a special rake, or a brush. Specially prepared sites of the ornament on preheated object were exposed to amalgamation (temperature of heating should not exceed 350-420<sup>0</sup> C; [15]).

In some cases it was possible to restore sequence of application of amalgam on a surface of plaques. First of all edged borders were gilded and then the front site of plaque. If the front site of plaque wasn't exposed to any additional processing (presence of gilding splashes outside of its patterning indicate it) after gilding any more, edged borders could be filed in addition on a stage of belt making - for more compact fitting of plaques to each other.

**TABLE 1.** XRF dates for the investigated samples (data of analysis are given in atomic %).

Samples	Cu	Sn	Pb	Zn	Ag	As	Fe	Au	Hg
374	53.33	-	3.83	5.34	33.08	-	4.41	-	-
374a	28.61	-	-	6.07	21.32	-	0.23	26.96	4.08
375	54.49	-	1.68	6.77	33.01	-	0.76	0.3	-
376	24.3	-	-	3.38	15.97	-	0.25	51.81	4.3
376a	75.6	-	2.62	5.01	15.14	0.09	1.55	-	-
377	58.85	9.72	1.42	6.24	21.52	0.09	2.15	-	-
378	70.18	0.35	-	2.24	24.0	0.31	2.93	-	-
379	50.07	-	5.39	3.69	27.64	0.27	12.93	-	-
380	61.67	0.51	3.56	5.14	25.42	0.02	3.69	-	-
381	60.28	0.54	1.6	4.9	31.84	0.08	0.77	-	-
382	52.92	0.57	-	3.85	24.99	-	0.74	15.24	1.69
383	62.51	0.55	1.69	6.8	26.89	0.06	1.51	-	-
384	61.08	0.52	1.8	6.03	29.71	-	0.68	0.18	-
385	55.63	0.59	1.39	4.53	35.02	-	0.96	1.32	0.57



**FIGURE 4.** Gold splash from amalgamation zone.

Archeologist researched burial 505 in the 1930<sup>th</sup> described that the belt "was cast from bronze and silvered ...." The XRF-analysis showed that the researched belt was really made not from precious metal, but from a brass (CuZnPb) with concentration of zinc within the limits of 2.24-6.8 % and lead within the limits of 1.39-5.39 %. Silver was added into this basis with concentration 15.14-36.01%, accompanying of traces of arsenic (tab.1). Thus, details of the belt from burial 505 were not silvered.

Most likely, the choice of brass with concentration of zinc up to 6.8 % as a basis does not belong to the conscious choice in this case - using of brass was wide-spread at Volga-river region during the IX-XII a.d. Brass is a basic type of alloy for jewelers in some areas of Volga Bulgaria [13].

Thus, silver was brought into standard type of alloy and probably its presence in alloy show a social (hierarchical) level of the order. So concentrations of silver of the analyzed belt set are comparable to the data received by researching of belt sets from a burial grounds of early Hungarians [16].

Distinctive feature of researching samples is a presence of Fe in average concentration up to 4.41 % in alloy (tab. 1). From our point of view, Fe is a background impurity, possibly, got in alloy from polymetallic pyretic ores and at present setting out on a surface because of corrosion processes. Its absence in tests from outside is evidence that restorers paid a lot of attention to appearance of a product that was quite explainable, considering unique character of this belt for territory of the Volga-river region.

## ACKNOWLEDGMENTS

This research was produced with support of RFFI grant 08-06-00299a.

## REFERENCES

1. *Materials in Mordovian History VIII-XI a.d.* Morshansk. 1952 p.160 (in Russian).
2. V. Murashova. "Reconstruction of Old Russian composite belt's character X-XI a.d. (by materials from warrior's group barrows)" in: *Paper of Historical State Museum.* **93** (1997). Moscow, 72-90 (in Russian).
3. J.R. Dienes. *Honfoglalo magyarok sirjai Nagyköröson.* in AE. **86** (1960).Budapest. p.185.
4. *The Ancient Hungarians: Exhibition Catalogue.* Budapest. 1996, 389-399, fig.1.
5. I.R. Dienes, Fol. Arch. **16** (1964) 79-112.
6. I.R. Dienes *A karancslapújtói honfoglalás kori öv és mordvinföldi hasonmása* [The Conquest period belt from Karancslapújtó and Mordvinian parallels]. ArchErt. Budapest, 1964, pp.18-40.
7. *The Archaeology of Rural Areas of Northern Rus 900-1300 AD.* Medieval settlements in the Kubenskoye lake region. Vol. 1. Nauka, Moscow, 2007, 274-275, fig.248, 1-3 (in Russian).
8. *The Archaeology of Rural Areas of Northern Rus 900-1300 AD.* Medieval settlements in the Kubenskoye lake region. Vol. 2, Nauka, Moscow, 2008, 93-96, fig.82 (in Russian).
9. V. Murashova. *Old Russian composite belt ornaments (X-XIII a.d.).* Nauka, Moscow, 2000, p.91 (in Russian).
10. S. Rjabtseva, R. Rabinovich. *Revista archeologica. Seria nova.* **III**, nr.1-2. (2007) 195-225 (in Russian).
11. N. Eniosova, R. Mitoyan, T. Saracheva. Methods for the study of nonferrous chemical compounds. in: *Nonferrous and precious metal alloys in Eastern Europe in the Middle Ages.* Nauka, Moscow, 2008, 114-120. (in Russian).
12. N. Eniosova, V. Murashova, *Journal of Archaeological Science* **26** (1999)1093-1100.
13. I. Zajtseva. Non-ferrous alloys in North-Eastern Rus and Volga-Bulgaria: comparative historical analyze. In: *Paper of II All-Russian Archaeological congress in Suzdal.* II (2008). Nauka, Moscow, 332-333 (in Russian).
14. S. Stanilov. *Die Metallkunst des Bulgarenkhanats an der Dunau (7.-9. JH.).* Versuch einer Empirischen untersuchung. Sofia. 2006.
15. J. Barrio, J. Chamon, M. Ferretti, M. Arroyo, A.I. Pardo. "Metallographic study of gold amalgams and gilding technology of Medieval Islamic gilded objects from the Iberian peninsula" in: *Archaeometallurgy in Europe 2007. Aquileia. Italy. Selected papers.* Milan. 2009, 402-409.
16. S. Valiulina, R. Hramchenkova, "The chemical composition of the article of non-ferrous metals of the Bolshe-Tigansky burial ground" in: *Ancient craftsmen in Urals.* Materials of All-Russian Scientific conference. Izevsk. 2001. pp.266-270 (in Russian).

## **Microstructural Study of Gilded Copper Artifacts from the Chichén-Itzá Cenote**

J. Arenas Alatorre<sup>1</sup>, J. Contreras<sup>2</sup> and J.L. Ruvalcaba Sil<sup>1</sup>

<sup>1</sup> *Instituto de Física, Universidad Nacional Autónoma de México, MEXICO. e-mail: jarenas@fisica.unam.mx*

<sup>2</sup> *Esc. Nal. de Restauración, Conservación y Museografía, Inst. Nal. de Antropología e Historia, MEXICO.*

**Abstract.** The studied artifacts samples comes from the sacred Cenote at Chichén-Itzá, one of the major Mayan archaeological zones. These artifacts are soles of sandals and other pieces of the costumes dressed by the ones sacrificed in this. Some artifacts showed a gilded heterogeneous surface; polished and rough, in different colors: Copper, golden and black. This alteration was due not only to the long burial period in the water, but to an inadequate method of extraction that included the use of a dragger, and an acid and mechanical "cleaning" method done in the 1960's. Previously, XRF was used at the conservation laboratory to determine the metal compositions and homogeneity of the gilding of all the artifacts. From this analysis, few artifacts were selected to carry out a more fine analysis by Particle Induce X-rays Emission (PIXE) and Rutherford Backscattering (RBS) in order to measure the gilding thickness, the elemental depth profile of Au, Ag and Cu and to identify the gilding procedures. From the results, it was determined that the metallic support is mainly copper while the plating is a rich Au-Ag alloy. In this work, microscopic studies were performed to refine the gilding thickness measurements, its homogeneity and the technology used. Some fragments isolated before the conservation processes were kept for its analysis with Scanning Electron Microscope with an electron microprobe (SEM-EDS) and Transmission Electron Microscopy (TEM). These measurements confirmed that a procedure of electrochemical deposition gilding was used. Since this technology was not developed in the Mesoamerican area, we conclude that these pieces were obtained by commercial exchange with Central and South America. The methodology applied was suitable for the full characterization of the materials and the manufacturing of the artifacts.

**Keywords:** Gilding, Maya, TEM, LV-SEM, EDX.

### **INTRODUCTION**

In ancient Mesoamerican cultures, gold was used for ornamental purposes as a symbol of wealth and social position. The physical properties of the metal enable it to be easily hammered into thin sheets and this led to the application of gold to the surface of base metal objects in order to improve their appearance and enhance their apparent value. Gilding technology

developed from the simple wrapping of gold foil around an object to the sticking of gold leaf to the surface in a number of different ways [1-2]. In fact, it is accepted that metallurgy developed in Mesoamerica from exchange and contacts with South America.

Chichén-Itzá was one of the major Maya sites in the North of Yucatan peninsula from 600 to 1300 A.D., but its main apogee was reached from 948 to 1150 A.D. [3]. The first reference about the objects in

the Cenote comes from the XVI century (Figure 1), of Diego de Landa, a bishop of Yucatan, who mentions that beyond just throwing men alive as a sacrifice to the gods to Cenote also threw stones and gold [4,5].



**FIGURE 1.** The Sacred Cenote of Chichén-Itzá has about 60 m of diameter, 22 m depth from the border to the water surface and a maximum depth of 13.5 m [5].

For that reason, many people were interested in extracting objects from the Cenote, the first try was done by the French Desiré Charnay in 1882, using Toselli automatic sounding machines, as it did not worked, he finally desisted. Afterwards, Edward Thompson used two techniques: From 1904 to 1907 a dredge was employed, that caused enormous damage to the objects, and from 1909 to 1911 using diving techniques. In 1959 during the 58th Congress of American Anthropologists, the Peabody Museum gave back a number of, apparently, gold pieces to the Mexican State. The Mexican exploration began until the decade of 60's under the direction of archaeologist Roman Pina Chan, among the artifacts extracted were found soles of sandals and other pieces of the costumes of the people dresses slaughtered in the Cenote, its constituent material is rich in copper artifact assemblage was composed of nine artifacts among them, axes, sole sandals, a stamped sheet, earrings and a disk. Representative images of these objects are shown in the Figure 2.

Because of the characteristics and style of the gilded objects, and analyzing the commercial exchanges of Chichen Itza, the archaeologists propose that were obtained by means of commerce with Costa Rica and Panama areas [3-4].

The metallic samples studied in this paper come from the sacred Cenote at Chichén-Itzá and form part of the Yucatan's Museum of Anthropology collection, showed heterogeneous surface; polished and rough, in different colors: copper, golden and black and were sent to the conservation laboratory in order to eliminate corrosion products and stabilize its materials.

It is evident that the alteration was due not only to the long burial period, but to an aggressive extraction method, and a very inadequate "cleaning" that presumably included the use of sulphuric acid, due to the lack of calcareous patina expected from a rich calcium environments such as the cenote's waters and soil, the presence of sulphides and an evident chemical attack indicated by metal dissolution. Even of these incorrect treatments, the pieces conserve a large amount of gild which points to a gilding technique that allowed a strong binding to the artifact alloy.



**FIGURE 2.** Some metal artifacts found in sacred Cenote at Chichen-Itzá showed a gilded heterogeneous surface; polished and rough, in different colors: copper, golden and black.

## MESOAMERICAN GILDING TECHNIQUES

The term gilding covers a number of decorative techniques for applying fine gold leaf or powder to solid surfaces such as wood, stone, or metal to give a thin coating of gold. Methods of gilding include hand application and glueing, chemical gilding, surface gold enrichment and electroplating, the last also called gold plating [2, 6].

In Center and South America the work of metals reached a notable development, obtaining not only complex alloys like tumbagas, but also surface finishing and plating techniques [7].

Foil gilding is obtained by means of mechanical union of gold sheets; eventually the heat reinforced the bonding and caused some diffusion [2]. This gilding of 35-90  $\mu\text{m}$ , does not cover all the details of the substrate, and it is not the best option for thin sheets like the ones from the Sacred Cenote at Chichén-Itzá.

Fusion gilding requires frequently the application of molten gold or gold alloy to a supporting metal with a higher melting point, like copper or copper alloys [2]. This plating is thick also (up to 0.75 mm) and neither suitable for artifacts like the ones analyzed in this case.

Depletion gilding, probably the most outstanding of all gilding techniques of Central and South American [2], is done commonly from tumbaga, oxidizing the copper and silver at the surface and then cleaning its corrosion products and leaving on surface only a porous layer of gold. The process can be repeated and the gold enriched surface may range from 3 up to 35  $\mu\text{m}$  depending on the tumbaga composition.

On the other hand, electrochemical replacement plating implies the use of previously heated and acidic gold solutions [2]. As it has been proposed by Lechtman [8], the electrochemical reactions are due to the interactions between the ions of the metal to be plated and the gold in solution, the bonding need also heating. There is a solid state diffusion zone between the gold and the core metal, because of the heating necessary to the finish the process. The gilding layers obtained in this way are very thin, their mean thickness varies from 0.5 to 2  $\mu\text{m}$ , and they are relatively uniform, and there is no trace of flushing of the molten gold.

### PREVIOUS ANALYSIS

Previously, XRF was used at the conservation laboratory to determine the metal compositions and homogeneity of the gilding of all the artifacts. From this analysis, few artifacts were selected to carry out a more fine analysis by Particle Induce X-rays Emission (PIXE) and Rutherford Backscattering (RBS) at the laboratory in order to measure the gilding thickness, the elemental depth profile of Au, Ag and Cu and to identify the gilding procedures [9].

XRF measurements in situ were relevant to estimate major and trace elements. The XRF results indicate that the core metal of the artifacts is mainly copper with As traces. In some cases such as axes, they have Pb traces as well. This elemental profile fits the features of artifacts from west and central regions of Mesoamerica. On the other hand, the gilded objects present a non-uniform thickness but Au and Ag were detected in all the cases.

External beam PIXE-RBS was not useful for the analysis of the gilding on the selected artifacts that were transported to the accelerator because of the thin layer thickness. Instead, the elemental depth profile was measured in gilded and corroded areas of the sole sandals using a 3 MeV alpha beam in vacuum and a combined  $\alpha$ -IXE-RBS analysis [9]. The difference in the analyzed depth between protons and alpha particles is about a factor of 10. Table 1 shows the results of these measurements.

From the results, it was determined that the metallic support is mainly copper while the plating thickness ranges 0.4 to 0.6 mm and it was made from a rich Au-Ag alloy. Considering the thickness of the gilding and the diffusion observed at the interface

between the gilding layer and the copper support, we may consider that an electrochemical plating method was used [8-10].

In this work, microscopic studies were performed to refine the gilding measurements concerning its homogeneity and technology.

### SAMPLES

Some fragments isolated before the conservation processes were kept for its analysis. The pieces correspond to the analyzed soles of sandals and other pieces of the costumes. The optic microscope observations showed heterogeneous surface, polished and rough, in different colors: mainly black and gold (figure 3). This alteration was due to the long period of burial under the water and an inadequate method of extraction that involved the use of a dredger, and an acid used for "cleansing" in the 60s.

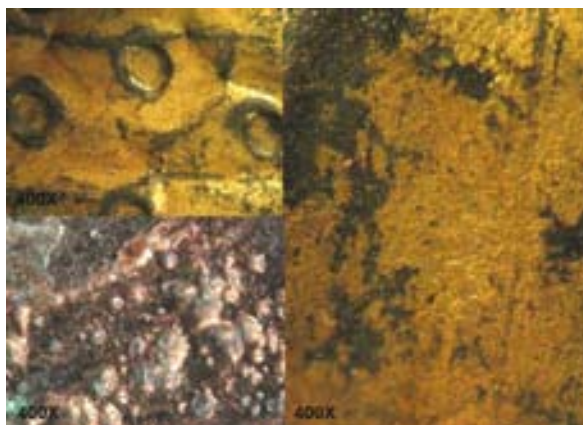


**FIGURE 3.** Micrographs obtained with light microscope to 400X, showing roughness and different colors, mainly golden and black, as a result of corrosion.

### SEM & TEM STUDIES

Samples were analyzed in a Low Vacuum Scanning Electron Microscope, equipped with microprobe for elemental chemical analysis by Energy Dispersive X-Ray Spectroscopy (EDS). For evaluate the homogeneity in superficial chemical composition, the metal artifacts were analyzed with backscattered electrons [11] and element mappings were performed.

On the other hand, small pieces of metal were prepared for crystallographic analysis by Transmission Electron Microscopy (TEM), using a JEM2010FEG TEM.

### SEM analysis

Scanning electron micrographs of the samples were obtained with backscattered electrons in order to study

their surface in more detail. SEM images from the gilded surface in two different regions at magnifications of 500X and 1000X, respectively, are presented in figure 4. In both images an inhomogeneous composition is observed. In figure 4a, the region 1 with high contrast is mainly composed by heavier elements - and EDS analysis showed high Au contents - while the regions 2 and 3 are much richer in Cu. EDS data of this sample are shown in the inset table in Figure 4. Also Ag, O and S were detected. All images obtained by SEM showed an irregular surface with high roughness, probably due to corrosion caused by the environment in which the artifact was kept.

Figure 5 shows an element mapping of the same area obtained from X-ray characteristics of Cu, Au, Ag and S. The whole core of the samples is mainly composed of Cu, while Au and Ag are observed together mainly in the areas corresponding to the gilding layer. Nevertheless, S is distributed uniformly over the sample but at low concentrations.

These results agree with the previous measurements by  $\alpha$ -IXE-RBS, but due to the low depth and spatial resolution of the electron microprobe in this kind of matrices ( $>1 \mu\text{m}$ ), the elemental data from EDS represents a mean elemental composition of the analyzed regions. For this reason the obtained elemental composition averages the layer and substrate information.

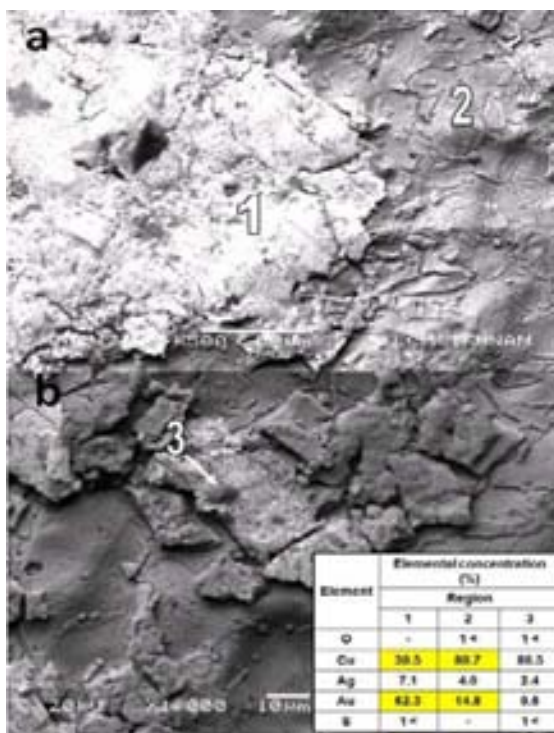


FIGURE 4. a) SEM images of the stamped sheet show an inhomogeneous composition, we can observe (a) areas with a high contrast in regions rich in Au (region1) and a Cu-rich zone of lower contrast (region 2 and 3).

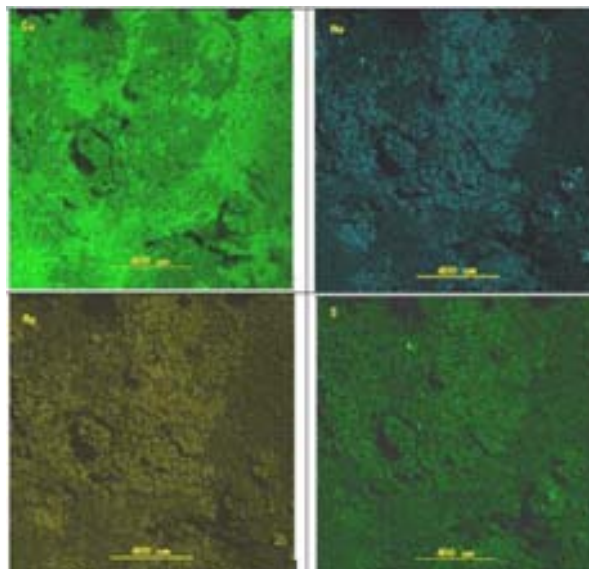


FIGURE 5. Element map of Cu, Au, Ag and S, obtained by characteristics X-rays.

### TEM analysis

High Resolution-TEM images (HRTEM) show the presence of Au and Ag oxide nanoparticles in the range 1-10 nm (Figure 6a). In HRTEM image of Cu oxide support, were measured mainly interplanar distances corresponding to CuO crystalline phase.

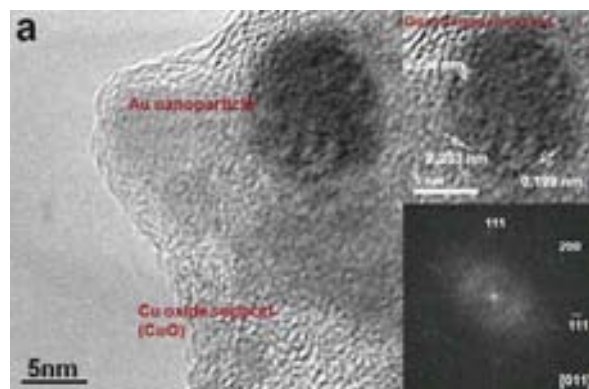


FIGURE 6. a) HRTEM image of Au nanoparticle of size 10 nm, embedded in CuO matrix, inset their respective Fast Fourier Transform (FFT).

On the other hand, in the figure 6b, is shown an image obtained by High Angle Annular Dark Field (HAADF) or Z-contrast technique. In them is observed semi circular areas with high contrast corresponding to zone with particles rich in Au and Ag.



**FIGURE 6.** b) HAADF image where it is observed semi-circular areas of middle size  $2\mu\text{m}$  corresponding to particles rich in Au and Ag.

In the figure 7, the HRTEM image of a nanoparticle of size 10 nm of AgO is shown. Note that the images obtained by HRTEM and HAADF shown semispherical nanoparticles of Au or Ag oxides, no bimetallic nanoparticles were identified. In contrast in core, only Cu was identified as CuO crystalline phase.

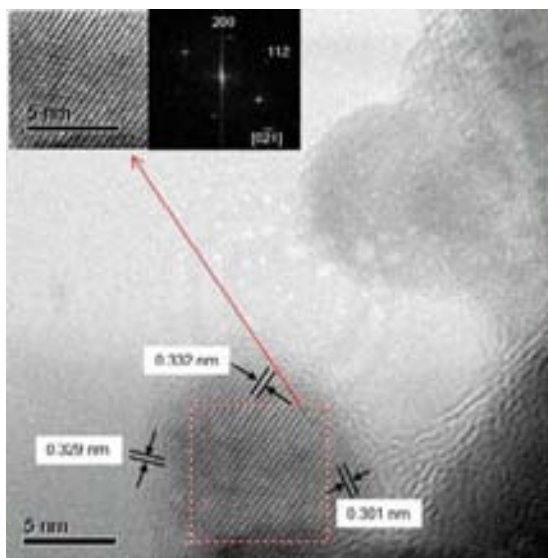


**FIGURE 7.** HRTEM image of AgO semispherical nanoparticle of size 10 nm, in Cu oxide support was identified.

## CONCLUSIONS

The metal samples analyzed from the sacred Cenote at Chichen- Itzá show that the main constituent

of the core is copper and the plating is rich in gold and silver. Moreover, HRTEM images show the presence of Au and Ag oxide nanoparticles in the range 1-10 nm. Bimetallic particles of Cu-Au, Ag-Au or Cu-Ag were not identified, as we may expect for depletion gilding or molten gold plating due to the formation of stable bimetallic phases. TEM techniques provide outstanding data for microstructure characterization.

The all set of measurements pointed out to an electrochemical replacement gilding technique, due to the uniform and thin gilding layer (0.3 to 0.55  $\mu\text{m}$ ), diffusion at the interface between the gilding and the copper sheet and the features of the microstructures.

Since this technology was not developed in the Yucatan region neither in other Mesoamerican areas, we conclude that these pieces were obtained by long distant exchange with Central and South America.

## ACKNOWLEDGMENTS

The authors would like to thanks to, J. Cañetas, R. Hernández and D. Quiterio for technical assistance, as well as CONACyT Mexico for financial support grants U49839-R and 82878 and PAPIIT UNAM fellowship IN403210.

## REFERENCES

1. W. A. Oddy M.A., *Endeavour* **15** (1991) 29-33.
2. B. Warwick, "Techniques of gilding and surface enrichment in pre Hispanic American metallurgy" in *Metal Plating and Patination*, Susan La Niece S. and P. Craddock (eds.), Butterworths-Heineman, London, 1993, 182-192.
3. R. García Moll, R. Cobos, *Chichén Itzá. Patrimonio de la Humanidad*, Azabache ed., Mexico, 2009.
4. C. Chase Coggins ed., *Artifacts from the Cenote of Sacrifice, Chichen Itza, Yucatan: Textiles, Basketry, Stone, Bone, Shell, Ceramics, Wood, Copal, Rubber, other Organic Materials, and Mammalian Remains*, Peabody Museum of Archaeology & Ethnology, Harvard University, Cambridge, 1992.
5. R. Cobos, *Arqueología Mexicana* vol. XIV, **83** (2007).
6. Sloan, Annie, *Decorative Gilding*, Collins & Brown, London 1996.
7. S. La Niece, N. Meeks, "Diversity of Goldsmithing traditions in the Americas and the Old World" in *Precolumbian Gold. Technology, Style and Iconography*, British Museum Press. 2000. 220-239.
8. H. Letchman, *J. Metals*, December (1979) 154-158.
9. J. Contreras, J.L. Ruvalcaba, J. Arenas Alatorre, Proceedings of the XI International Conference on PIXE and its Analytical Applications, Puebla Mex. 2007.
10. E.A.O Saettone, J.A.S. da Matta, W. Alva, J.F.O. Chubaci, M.C.A. Fantini, R.M.O. Galvao, P.Kiyohara, M.H. Tabacniks, *J. Phys. D: Applied Physics* **36** (2003) 842-848.
11. J. Arenas-Alatorre, Y. Silva-Velázquez, A. Alva Medina, M. Rivera, *Applied Physics A. Mat. Sci. and Proc.* **98** (2010) 617-62.

## **Study of Fragments of Archaeological Glass Objects by Portable Energy Dispersive X-Ray Fluorescence (PXRF)**

Carlos R. Appoloni<sup>1</sup>, Fábio L. Melquiades<sup>2</sup> and Fábio Lopes<sup>1</sup>

<sup>1</sup> *Departamento de Física, CCE, Universidade Estadual de Londrina, CEP 86051-990, Caixa Postal 6001, Londrina PR, BRAZIL. e-mail: appoloni@uel.br, bonn@uel.br*

<sup>2</sup> *Departamento de Física, Universidade Estadual Centro Oeste, CEP 85015-430, Caixa Postal 3010, Guarapuava, PR, BRAZIL.*

**Abstract.** This work presents the characterization of some archaeological glass objects fragments from the collection of the Archaeology and Ethnology Museum of the State University of São Paulo (MAE-USP), employing a portable Energy Dispersive X-ray Fluorescence (PXRF) system. The aim was to identify chemical elements present in the vitreous fragments composition and/or pigmentation. Four fragments were analyzed whose origins are attributed to Ancient Greece (codes 75/1.18a, 75/1.18d, 75/1.18e, 75/1.18h), one fragment of gold iridescent glass (code 73/9.62d) from Susa, Irã, Islamic period, and one sample of transparent contemporaneous glass. In each sample 3 to 5 points were measured, depending on its size and regions of interest. The measurement system, LFNA-PXRF03, is composed by: Si-PIN detector (5 mm<sup>2</sup>, 680 µm, 149 eV resolution for 5.9 keV) with 3 mm aperture Ag collimator, mini X-ray tube (4W, Tungsten target) and a support for the excitation-detection system and sample positioning with XYZ and rotation freedom degrees. The measurement live time was 500s. In the contemporaneous glass sample Si, K, Ca, Ti, Mn and Fe were identified. In all archaeological samples Si, S, K, Ca, Ti, Mn, Fe and Sr were present. Other elements like Cl, Cr, Co, Cu, Zn and Pb were also identified. Samples 75 (h, d, e), unlike the others, presented Co, Cu, Pb and Zn. Chromium presence was verified in 75a and 73d samples. Among the differences observed, two will be cited, as examples. For the modern glass, Fe/Ca ratio is 0.10, while for archaeological glasses it varied between 2.2 and 0.4. Fragment 75e has a blue color region which presents more Ca, Mn and Fe (217%, 135% & 68%, respectively) than the white background with black stripes, while this white region has 11.9 times more Ti than the blue one.

**Keywords:** glass, archaeological, chemical composition, PXRF.

### **INTRODUCTION**

Non-destructive analysis of art fragments using portable instruments has been increasing in last years. The advance in instrumentation, especially Peltier cooled detectors and low power X-ray tubes, allowed miniaturized equipments with performance similar to laboratory ones.

The main advantage in using non-destructive methodologies with portable system in art analysis is that “the laboratory goes to the museum” and the

sample does not need to be transported and even damaged.

Several works have been developed with glass samples and XRF in its different forms: conventional equipment [1-5], with synchrotron radiation [6-11] and with portable systems [12-17]. The main purpose of these works is archeological or forensic interest.

The objective of this work was to characterize some fragments of archaeological glass objects from the collection of the Archaeology and Ethnology Museum of the State University of São Paulo (MAE-

USP; <http://www.mae.usp.br>) employing a portable Energy Dispersive X-ray Fluorescence (PXRF) system. The aim was to identify chemical elements present in the vitreous fragments composition and/or its pigmentation.

## MATERIAL AND METHODS

### Samples

It were analyzed four fragments whose origin is attributed to Ancient Greece (museum collection codes 75/1.18a, 75/1.18d, 75/1.18e, 75/1.18h), one fragment of gold iridescent glass (code 73/9.62d) from Susa, Irã, Islamic period, and one sample of a transparent contemporaneous glass. The artifacts were not removed from the museum and were measured at its conservation laboratory.

As EDXRF is a non destructive technique, the samples were measured without any kind of preparation. In each sample, 3 to 5 points were measured, depending on its size and regions of study.

### Measurement system

The measurement system, LFNA-PXRF03, is composed by a Si-PIN detector (5 mm<sup>2</sup>, 680 µm, 149 eV resolution for 5.9 keV) with 3 mm aperture Ag collimator, a mini X-ray tube (4W, Tungsten target) and a special support for the excitation-detection system and sample positioning with XYZ translation and rotation freedom degrees (Fig. 1). The measurement conditions were 20 kV, 4 µA and 500 s live time.

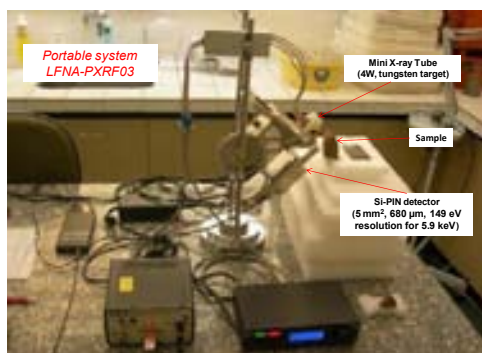


FIGURE 1. Portable EDXRF as employed during the measurements at MAE-USP.

## RESULTS

In the contemporaneous glass sample Si, K, Ca, Ti, Mn and Fe were identified. In all the archaeological

samples Si, S, K, Ca, Ti, Mn, Fe and Sr were present. Other elements like Cl, Cr, Co, Cu, Zn and Pb were also identified. Figure 2 presents the samples and their respective spectra.

Samples 75 (h, d, e), unlike the others, presented Co, Cu, Pb and Zn. Chromium presence was verified in 75a and 73d samples.

For the contemporaneous glass (actual), Fe/Ca ratio is 0.1, while for archaeological glasses varied between 9.8 and 0.4.

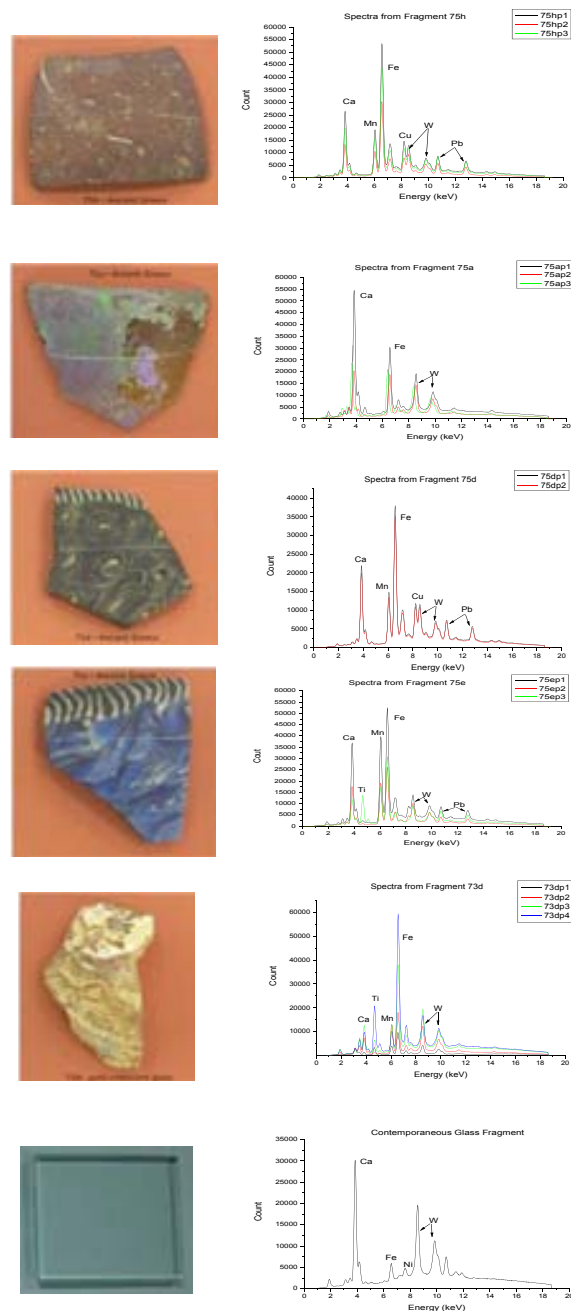


FIGURE 2. Samples and the spectra of each analyzed region.

### 2D Graphics Analysis

Bi-dimensional graphics of some elements ratios were plotted. Figure 3 present these results. 2D graphics separate clearly the samples in all cases: the contemporaneous glass from the others; samples 73d (iridescent glass from Irã) and 75a. Samples 75d, 75e and 75h appears mixed in a big group, although some discrimination could be inferred.

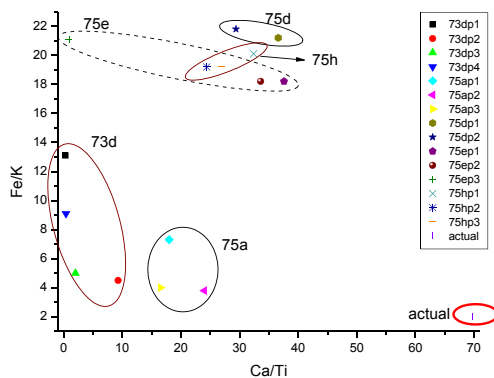
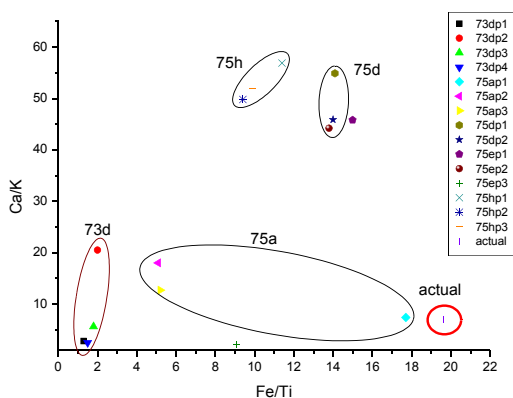
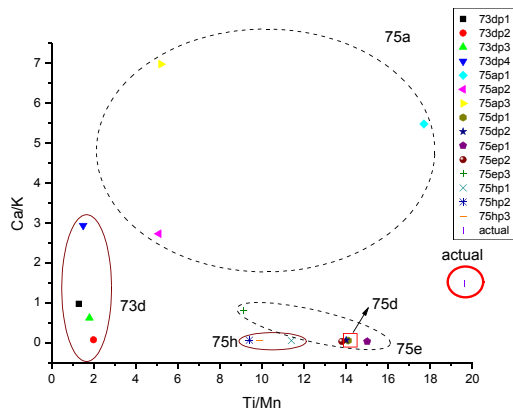


FIGURE 3. Bi-dimensional graphics for some elements intensity ratios. The graphics separate different samples.

### Cluster Analysis

Cluster analysis was performed by Ward Method using intensity ratios (Ca/K, Ca/Ti, Ca/Mn, Ti/K, Ti/Mn, Fe/K, Fe/Ca, Fe/Ti). The resulting dendrogram is presented at Figure 4.

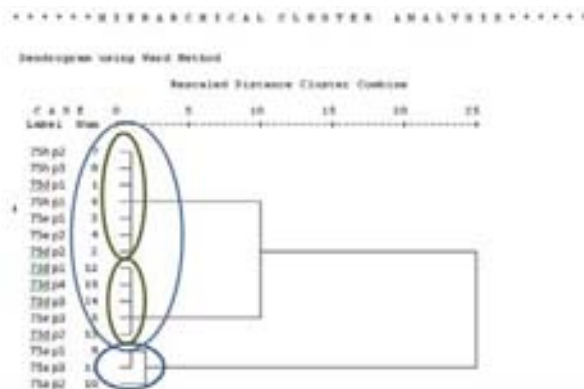


FIGURE 4. Dendrogram with data from the archaeological glass fragments using the intensity ratio for some elements.

The resulting dendrogram of the cluster analysis presents two major groups. Sample 75a is isolated from the rest of the group. In the upper subgroup, Irã fragment 73d is separated from the others. Samples 75d, 75e and 75h appear mixed. This result corroborates the bi-dimensional graphics results.

Fragment 75a presents relevant difference in Ca/Mn, Ti/Mn, Fe/Ca ratios compared with the others, suggesting singular composition.

Sample 73d differs from the others in Ca/K, Ca/Ti ratios.

### CONCLUSIONS

It was possible to identify different elements in the pigmentation of each sample. Besides the presence of some specific elements, also some element intensity ratios differentiate the fragments.

The PXRF system performance was excellent for glass characterization.

### ACKNOWLEDGMENTS

To the leaders of MAE-USP and to Silvia Cunha Lima for allow the measurements realization and to Conselho Nacional de Pesquisa e Desenvolvimento (CNPq).

## REFERENCES

1. R. Arletti, G. Vezzalini, S. Biaggio Simona, F. Maselli Scotti, *Archaeom.* **50** (2008) 606–626.
2. B. E. Naes, S. Umpierrez, S. Ryland, C. Barnett, J. R. Almirall, *Spectrochim. Acta B* **63** (2008) 1145–1150.
3. M. Milazzo, *Nucl. Instrum. Meth. Phys. Res. B* **213** (2004) 683–692M.
4. E. Hall, *J. Arch. Sci.* **25** (1998) 1239–1245.
5. P. Valério, A. Markowicz, P. Kregsamer, M. F. Araújo, A. Pires de Matos, E. Chinea-Cano, C. Carvalho, *X-Ray Spectrom.* **32** (2003) 396–401.
6. R. Arletti, G. Vezzalini, S. Quartieri, D. Ferrari, M. Merlini, M. Cotte, *Appl. Phys. A* **92** (2008) 127–135.
7. T. Nakanishi, Y. Nishiwaki, N. Miyamoto, O. Shimoda, S. Watanabe, S. Muratsu, M. Takatsu, Y. Terada, Y. Suzuki, M. Kasamatsu, S. Suzuki, *Foren. Sci. I.* **175** (2008) 227–234.
8. Y. Suzuki, M. Kasamatsu, S. Suzuki, T. Nakanishi, M. Takatsu, S. Muratsu, O. Shimoda, S. Watanabe, Y. Nishiwaki, N. Miyamoto, *Anal. Sci.* **21** (2005) 855–859.
9. Y. Nishiwaki, T. Nakanishi, Y. Terada, T. Ninomiya, I. Nakai, *X-Ray Spectrom.* **35** (2006) 195–199.
10. J.P. Veiga, M.O. Figueiredo, *X-Ray Spectrom.* **31** (2002) 300–304.
11. K. Janssens, G. Vittiglio, I. Deraedt, A. Aerts, B. Vekemans, L. Vincze, F. Wei, I. De Ryck, O. Schalm, F. Adams, A. Rindby, A. Knöchel, A. Simionovici, A. Snigirev, *X-Ray Spectrom.* **29** (2000) 73–91.
12. N. Kato, I. Nakai, Y. Shindo, *J. Arch. Sci.* **36** (2009) 1698–1707.
13. K. Tantrakarn, N. Kato, A. Hokura, I. Nakai, Y. Fujii, S. Gluscevic, *X-ray Spectrom.* **38** (2009) 121–127.
14. M.R. Iovino, L. Maniscalco, G. Pappalardo, L. Pappalardo, D. Puglisi, F. Rizzo, F.P. Romano, *Archaeometry* **50** (2008) 474–494.
15. T. Sawada, A. Hokura, S. Yamada, I. Nakai, Y. Shindo, *Bunseki Kagaku* **53** (2004) 153–160.
16. P. Moiola, C. Seccaroni, *X-Ray Spectrom.* **29** (2000) 48–52.
17. J. Kunicki-Goldfinger, J. Kierzek, *X-Ray Spectrom.* **29** (2000) 210–316.

# **Implementation of Techniques for the Study of Vitreous and Metallic Materials from the Archaeological Site “Guardia del Monte”, San Miguel del Monte, Buenos Aires Province**

L.P. Traversa<sup>1</sup>, M.I. Casadas<sup>2</sup>, M.E. Peltzer<sup>2</sup> and F.H. Iloro<sup>1</sup>

<sup>1</sup>*Laboratorio de Entrenamiento Multidisciplinario para la Investigación Tecnológica (LEMIT), La Plata, ARGENTINA.*

<sup>2</sup>*Instituto Cultural de la Provincia de Buenos Aires, ARGENTINA.  
e-mail: mariacasadas@yahoo.com.ar or mepeltzer@yahoo.com.ar*

**Abstract.** This report is part of a Historical and Archaeological Research Project in the site where the San Miguel del Monte fortress stood around 1845. This work presents the research achievements on glasse- like and metallic materials discovered during the archaeological excavations carried out between 2003 and 2006 by the Instituto Cultural de la Provincia de Buenos Aires. The technological studies done by the LEMIT showed different alterations and deteriorations of vitreous materials, moreover they were examined to determine a relative chronology, origins and uses to establish their typologies and archaeological representativity. Also, this paper shows the development of electrochemical techniques for metal cleaning from the same archeological site and the evaluation of their results.

**Keywords:** vitreous materials, metallic materials, San Miguel del Monte, Argentina, alterations, deteriorations.

## **INTRODUCTION**

During the archaeological excavations performed in the School N° 16 in San Miguel del Monte, Buenos Aires Province (Argentina), foundations and underground constructions where discovered, presumably belonging to the locker of the “Guardia del Monte” (Woodland Guard) and to the “Iglesia de la Divina Pastora” (Church of Divine Shepherdess). These sites operated on that place during the 19th and 20th centuries. The building corresponding to the “Iglesia de la Divina Pastora” was originally erected around 1745; probably was Juan Manuel de Rosas who ordered its reconstruction in 1829, and at the beginning of 20th century it was pulled down in order to build the nowadays existing School.

The aims of this work were based on the quantity and variability of the materials found during the excavations. Two series of analysis on the vitreous and

metallic materials classified until now, are presented: those commissioned by the “Instituto Cultural” and on the other side, those analysis made by LEMIT. The purpose of this assessment was to gather information about two fundamental points:

- Technological characterization, micro-hardness and metal dating.
- Chemical composition and alterations of vitreous material.

## **METALS**

The 473 metal pieces analyzed from the “Instituto Cultural” correspond to those materials found during the Test Drilling 2 and a percentage from rubble accumulation. The total data obtained are shown in Figure 1.

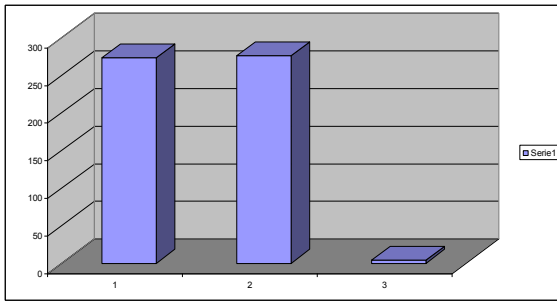


**FIGURE 1:** 1. Nails, 2. Various fragments, 3. Others.

### Technological characterization and temporal location

According to the technology used in the manufacture of metals, it is possible to distinguish three types of processes:

*Pre-puddling or Catalan forge:* primary iron was heated at 700 - 800 °C.

*Puddling:* During the 18th century, the iron melting was achieved with lower inclusions content. Silicates are present as bands in the metal deformation.

*Modern Iron:* It was developed during the second half of 19th century. Through overheating the settling of oxides was promoted. The product presents less inclusion content.

#### Studied samples: Technological Characterization

Metallographic studies were carried out through the microscopic observation of longitudinal and transverse cuts, polished and attacked with Nital. The pieces were subjected to a cleaning process employing cathodic technique.

*Piece Nr. 1:* Knife blade thickness 2.5 mm with corrosive process. (Figure 2), from rubble accumulation.



**FIGURE 2.** Piece Nr 1.

The microscopic observations made on cross-section and longitudinal section (Figure 3) shows the size, shape and two types of inclusions: oxides and silicates, which form continuous and parallel chains in the deformation direction. The chains are held after the attack with 2% Nital.

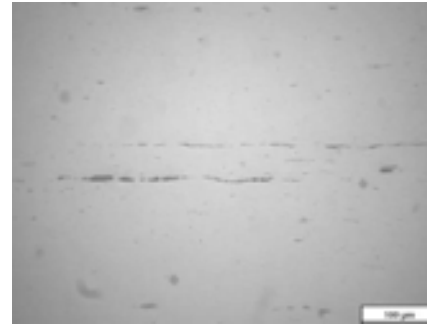


**FIGURE 3.** Longitudinal section (16 X). It is possible to observe shape, size and inclusions.

*Micro-hardness tests:* after applying 300 g load for 5 seconds, values of 150 Hv were obtained.

*Dating:* according to metallographic studies and micro-hardness values, it is possible to deduce that the sample would correspond to an old iron of 19th century.

*Piece No. 2:* Ornament possibly corresponding to an oil lamp from the Test Drilling 1, Level 23, before the cathodic cleaning (Figure 4).

*Applied technique:* cleaning by cathodic technique. It allowed to see a stripped piece with characteristic color of brass – a base copper alloy, with zinc as an alloy element – (Figure 5).



**FIGURE 4.** Piece no.2 **FIGURE 5.** After cleaning

The Figures 6 and 7 show the results of metallographic studies performed on Piece 1. In Figure 6 the section can be seen without attack, having a great amount of non-metallic inclusions, and the Figure 7 shows the same inclusions together with a dendritic structure of the material, characteristic of the

solidification process, revealed through a chemical attack with a reagent of alcohol and ferric chloride.

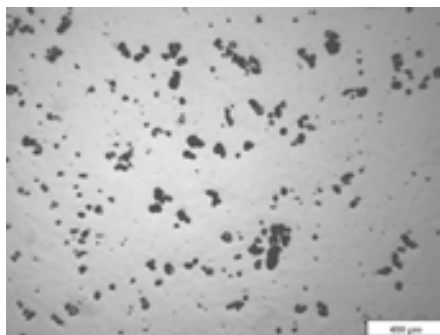


FIGURE 6. Metallography on Piece 1.

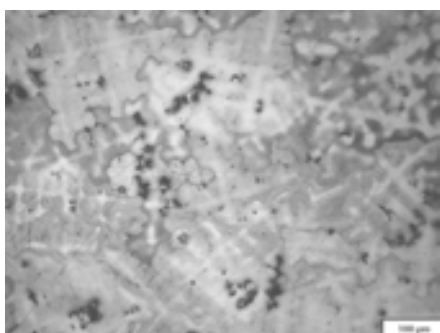


FIGURE 7. Metallography on Piece 1.

*Micro-hardness tests:* micro-hardness values were 170 Hv, with a load of 300 g during 5 seconds applying.

*Dating:* according to the results of micro-hardness and metallographic studies, this piece would be made in the early 20th century.

*Other metals found in the Site School No. 16:* correspond to different elements of iron (Figure 8) and various metallic elements (Figure 9) as a clock, a gun and coins.



FIGURE 8. Iron pieces.



FIGURE 8. Other pieces.

## GLASSES

The glass analysis commissioned by the Cultural Institute correspond to those materials found in the Test Drilling 2 and a percentage from “volquete”, for a total amount of 774 pieces, classified by color. The general findings are shown in Figure 10.

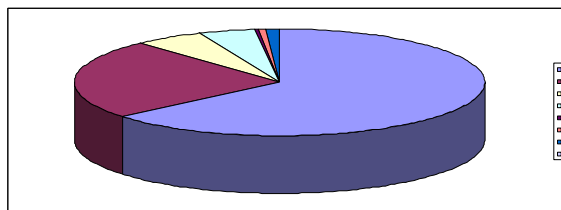


FIGURE 10. Total glasses classified by color.

Most of these glasses are transparent, followed in decreasing proportion by colors: green, blue, brown, iridescent, light blue, turquoise and black.

*Glass is an inorganic product of fusion which has been cooled to a rigid condition without crystallization.* Most of glasses are based on silicon oxide ( $\text{SiO}_2$ ) as a glass-forming substance.

## Deterioration of Glass

*Internal Causes:* These causes originate the "glass disease" according to the content of alkali ( $\text{Na}_2\text{O}$  and  $\text{K}_2\text{O}$ ), related to the calcium oxide ( $\text{CaO}$ ) content, since this compound can temper the effect of the presence of alkalis.

*External Causes:* They are related to the environmental moisture content and the aggressive characteristics of the medium. Extreme pH values, whether acidic or alkaline, are what determine the durability of the material (Figure 11).

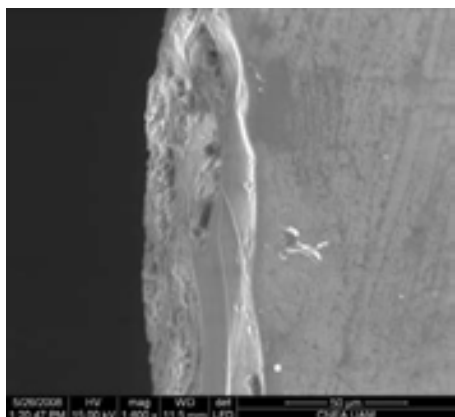


FIGURE 11. Glass cut with deterioration layer.

### Chemical Analysis

It was performed on six fragments of different objects, with variable colors and alteration degrees, and the results are given in Table 1. The samples studied in this work were: *Sample 1*: very altered as they tend to flake off the surface; *Sample 2*: not altered; *Sample 3*: somewhat altered; *Sample 4*: not altered; *Sample 5*: a high degree of deterioration (iridescent). *Sample 6*: with very significant alterations.

TABLE 1. Chemical analysis of samples

Element	Sample 1	Sample 2	Sample 3	Sample 4	Sample 5	Sample 6
Fe	0.14	2.43	1.17	2.10	0.64	1.68
Ca	7.70	14.28	9.84	18.10	7.84	12.76
Mg	0.46	2.68	1.76	4.13	2.40	2.13
Mn	0.38	0.56	0.28	0.41	0.10	0.07
Pb	1.42	0.00	0.00	0.00	0.00	0.00
Cu	0.00	0.00	0.00	0.00	0.00	0.00
Na	11.60	3.16	4.90	0.84	10.23	6.73
K	1.04	1.00	1.85	0.88	0.39	0.64

The behavior of glass in a moist environment with pH 3.3 depends on the sodium oxide – calcium oxide ratio. The higher degrees of alteration are observed in those samples with a high value of this ratio, greater than unity in the cases under study.



FIGURE 12. Altered glasses

## CONCLUSIONS

In this work it is shown how, the interdisciplinary work between historical archaeology and analysis by means of tests, laboratory methods and techniques (LEMIT), makes possible to evaluate metal and glass materials that have archaeological interest and, obtaining the results, to arrive at meaningful data for local and regional research.

### Metals

The metallographic studies carried out enabled to reach an approach to the dating of materials from the archaeological site under study.

### Glasses

The alteration is caused by the de-alkalized surface, where the alkaline compounds of the vitreous structure are solubilized in contact with high levels of humidity and / or water over long periods of time. This leads to devitrification, a natural process that occurs in siliceous materials, particularly in glasses with high content of sodium.

The alteration processes continue over time if the environmental factors that gave rise to them are kept constant (high relative humidity, water leaks from rain or condensation). The process is intensified if there is an acid attack caused by atmospheric pollution.

The surface layer of glass altering is a part of it and can act as a protective barrier, so it should not be eliminated by any chemical or mechanical mechanism.

## REFERENCES

1. M. I. Casadas and M. E. Peltzer, "Rescate Arqueológico en el Casco Urbano de la Ciudad de San Miguel del Monte" in *Problemáticas de la Arqueología Contemporánea, publicación del XV Congreso Nacional de Arqueología Argentina*, edited by Universidad Nacional de Río Cuarto, compiladores Antonio Austral y Marcela Tamagnini, Río Cuarto, Córdoba, 2004, pp. 223-227.
2. M. I. Casadas, M. E. Peltzer and N. Prieto, "Resultado de los Análisis Realizados sobre Materiales Constructivos Procedentes de las Excavaciones Arqueológicas en la Escuela N°: 16 de San Miguel del Monte, Provincia de Buenos Aires" in *Metodologías Científicas Aplicadas al Estudio de los Bienes Culturales, Actas del Primer Congreso de Arqueometría*, Edited by Humanidades y Artes, Rosario, 2005, pp. 167-176.
3. L. P. Traversa, J. L. Sarutti, O. Otero and N. H. Russo "Restauración Electroquímica y Restauración de Piezas de Hierro de Interés Arqueológico." Séptimo Encuentro

- de Historia Regional del Sur Santafesino y Norte Bonaerense, 2003.
4. L. P. Traversa, J. L. Sarutti, J. L. Vetere and L. Terminillo “Restauración y Estudio de Piezas de Hierro, Elaboradas entre los siglos XVII y XVIII”. Jornadas SAM 2000 - IV Coloquio Latinoamericano de Fractura y Fatiga, Bariloche, 2000.
  5. L. Traversa, R. Vetere, H. Russo. “Restauración electroquímica y caracterización de piezas arqueológicas”. Primer Congreso Nacional de Arqueología Histórica, Mendoza, 2000.
  6. R.H. Brill, H. A. Hood, *Nature* **189** (1961) 12-14.
  7. E. A. Marie “Apuntes para una historia del vidrio en la argentina”. *Jornada: "El vidrio en la arqueología y en la historia"*, Berazateguá, Marzo 1998.
  8. Z. Quatrin “Los objetos de vidrio en el contexto de la arqueología histórica de Quilmes”. Actas XII CNA, Tomo I, La Plata, 1997.
  9. L. P. Traversa, R. Perez., Z. Quatrin, S. Grimal, O. Otero “Estudios vinculados con la durabilidad de vidrios de interés arqueológico”. Actas del 1er. Congreso de Arqueología Histórica. Mendoza, 2000.
  10. N. Carmona, M. Garcia-Heras y M. A. Villegas. “Vidrios y grisallas del S. XV de la Cartuja de Miraflores (Burgos): características y estado de conservación”. Boletín de la Sociedad Española de Cerámica y Vidrio. 2005.
  11. A. F. Gomez, J. D. Czajkowski. “Confort en la conservacion de bienes historicos y culturales”. Actas del V Encontro de Conforto no Ambiente Construido, Fortaleza, 1999.
  12. L. P. Traversa, F. H. Iloro. “Alterabilidad de Vidrios de Interés Arqueológico y Patrimonial”. VII Jornadas de Tecnicas de Restauración y Conservación del Patrimonio. La Plata, 2008.

## **Blue Pigments in XVI-XVII Century Glazes: A Comparative Study between Portuguese Faiences and Chinese Porcelains**

M.O. Figueiredo<sup>1,2</sup>, T.P. Silva<sup>1,2</sup>, J.P. Veiga<sup>2</sup>, M.I. Prudêncio<sup>3</sup>, M.I. Dias<sup>3</sup>,  
M.A. Matos<sup>4</sup> and A.M. Pais<sup>4</sup>

<sup>1</sup> *Nat. Lab. Energy & Geol. (LNEG), Apt. 7586, 2721-866 Alfragide, PORTUGAL.  
e-mail: ondina.figueiredo@ineti.pt*

<sup>2</sup> *CENIMAT/ I3N, Fac. Sci. Technol., New Univ. Lisbon, 2829-516 Caparica, PORTUGAL.*

<sup>3</sup> *Nuclear & Technol. Institute (ITN), EN 10, 2686-953 Sacavém, PORTUGAL.*

<sup>4</sup> *Museu Nacional do Azulejo, R. Madre de Deus, 1900-312 Lisboa, PORTUGAL.*

**Abstract.** The trade of Chinese blue-and-white porcelains to Europe became intense along the XVII century following the maritime contact first established by the Portuguese navigators by the end of XVI century and nowadays European museums and traders face an increased need for ascertaining the authenticity of such art objects through non-destructive tests. With this purpose, a research project is being carried out on glazed faience and porcelain fragments collected during recent archaeological excavations by applying both laboratory techniques - X-ray fluorescence spectrometry and X-ray diffraction, instrumental neutron activation analysis - and X-ray absorption spectroscopy using synchrotron radiation at the European Synchrotron Radiation Facility in Grenoble/France. The blue chromophore role of cobalt in the glazes is discussed in relation to the speciation state and coordination environment of this element within the glassy silica-rich matrix. The results of both near-edge and extended fine structure analysis of Co 1s XAFS spectra are described and discussed, confirming the expected valence state (2+) of cobalt ions hosted as glass-forming components with an average coordination number close to four and a mean Co-O distance of about 2.0 Å. A confirmation of preliminary dating by Art Historians based on stylistic features is attained, taking into account the bulk chemistry of the glazes, particularly the presence or absence of lead and arsenic plus the relative contents of manganese, and iron versus cobalt.

**Keywords:** Blue glazes; cobalt speciation; ancient Chinese porcelains; contemporary Portuguese faiences.

### **INTRODUCTION**

Ancient blue glazes owe their color mainly to copper and cobalt, either employed separately or added together to the siliceous matrix to attain the desired tonality. Once the speciation states assumed by these two chromophore elements control the final coloring effect, X-ray absorption using synchrotron radiation (XAFS) is a particularly suitable spectroscopic

technique for interpreting the pigment performance. The analysis of both near-edge features (XANES) and extended fine structure (EXAFS) of X-ray absorption spectra has been successfully used to study not only chromophore ions but also modifier elements in other ancient glassy materials, namely tile glazes [e.g., 1-4].

The trade of Chinese blue-and-white porcelains to Europe became intense after the maritime contact first established by the Portuguese navigators by the end of

XVI century. European museums and traders have nowadays an increased need to ascertain the authenticity of such art objects through non-destructive assays. As a contribution to this subject, a XAFS study was carried out to characterize cobalt speciation plus coordination environment and tentatively confirm the Art-Historians' dating of a set of Chinese porcelain fragments supposedly manufactured in the XVI cent. A.D. (late Ming period, 1368-1644) and of glazed faïences with Chinese-type decorations recovered during recent archaeological excavations (Figure 1) conducted at the Monastery of Santa Clara-a-Velha in Coimbra, central Portugal [5], and in Lisbon Old-City.

The results of this study are described and discussed in conjunction with bulk chemical data obtained by a non-invasive X-ray fluorescence spectrometry qualitative assay.



FIGURE 1. Studied fragments of Chinese blue-and-white porcelains and contemporary Portuguese faïences.

## PROBLEMATIC

With the aim of accurately dating the ceramics, thermo-luminescence (TL) tests were conducted over the faïence fragments of Portuguese production collected at the already mentioned archaeological sites [6]. Regrettably, the reduced thickness of Chinese porcelain shards hindered the performance of TL tests. The problematic related to the studied archaeological shards is accordingly summarized in Table 1.

Ancient Chinese porcelains have been lately the object of many compositional studies applying X-ray and proton beam analytical techniques (namely, PIXE) to ascertain production periods and sites [e.g., 7-9]. It is known [10] that a shift from imported arsenic-rich Persian cobalt-based pigments towards native Chinese blue pigments - asbolane, a cobalt-containing manganese wad - has occurred during the early Ming Dynasty. This fact has rendered possible to outline a dating criterion based on the presence or absence of arsenic plus a combination of Mn/Co & Fe/Co ratios in the glaze.

The blue pigmentation properties of cobalt (2+) ions in tetrahedral coordination were established already forty years ago for Thenard's blue (ideally  $\text{CoAl}_2\text{O}_4$ , a spinel-type phase), and were recently reappraised for various cobalt pigments [11]. Beyond ascertaining the bulk chemistry of ancient blue glazes, another relevant purpose of the present work was then to confirm and validate the cause of coloring by studying cobalt speciation state in the glazes.

## EXPERIMENTAL

The non-destructive chemical study was performed using a Philips PW1400 wavelength-dispersive X-ray fluorescence spectrometer (XRF-WDS) equipped with a rhodium tube and a LiF200 analyzing crystal. A very small fragment taken from the larger pieces or the whole fragment in the case of smaller samples (nrs. 94, 95, 428, Figure 1) were irradiated and fixed-time counting was carried out over the  $K_\alpha$  diagnostic peaks of the relevant transition metals - Mn, Fe, Co, Cu. In view of the superposition of Pb  $L_\alpha$  line and As  $K_\alpha$ , the  $K_\beta$  peak of arsenic and the  $L_\gamma$  peak of lead were also measured to ascertain the presence of these elements.

TABLE 1. Dating problematic of studied archaeological shards.

Sample	Site and date of excavation	Dating problematic
94 and 95, Chinese porcelain fragments	Monastery of Santa Clara-a-Velha in Coimbra, central Portugal (<2003)	Very thin shards not suitable for thermo-luminescence dating
425, <i>id.</i>	Rua da Madalena in Lisbon (2007)	Chinese "Wanli" piece; 1573-1619 ?
426 and 428, <i>id.</i>	Calçada do Lavra in Lisbon (2004-5)	Also Chinese; 16 <sup>th</sup> century; 2 <sup>nd</sup> half ?
442, faïence of Portuguese manufacture	<i>Id.</i> (2007)	17 <sup>th</sup> cent., 1 <sup>st</sup> half ? Identical to faïence pieces were found in Hamburg, Germany
442, Portuguese faïence		<i>Id.</i> ; imitation of "Kraack" porcelain

**TABLE 2.** Chemical data obtained by X-ray fluorescence spectrometry in wavelength dispersion mode.

Sample reference	94	95	425	426	428	442	446
Element (2 $\theta$ )	Counts-per-second at the angular position						
Background (71.00)	360	314	123	112	190	182	188
<b>Mn <math>K_{\alpha}</math></b> (62.97)	<b>14 376</b>	<b>22 229</b>	<b>8 557</b>	<b>4 524</b>	<b>47 638</b>	409	378
<b>Fe <math>K_{\alpha}</math></b> (57.52)	<b>102 270</b>	<b>104 162</b>	<b>9 836</b>	<b>27 001</b>	<b>67 388</b>	6 501	17 024
<b>Co <math>K_{\alpha}</math></b> (52.80)	<b>5 522</b>	<b>3 649</b>	<b>1 841</b>	<b>1 414</b>	<b>11 073</b>	2 016	13 868
<b>Mn / Co ratio</b>	<b>2.6</b>	<b>6.1</b>	<b>4.6</b>	<b>3.2</b>	<b>4.3</b>	0.2	< 0.1
<b>Fe / Co ratio</b>	<b>18.5</b>	<b>28.5</b>	<b>5.3</b>	<b>19.1</b>	<b>6.1</b>	3.2	1.2
Cu $K_{\alpha}$ (45.03)	2 969	2 523	361	1 704	2 045	18 551	759
Co / Cu ratio	1.8	1.8	5.0	0.8	5.0	0.1	18.3
As $K_{\alpha}$ + Pb $L_{\alpha}$ (34.00)	2 163	2 188	296	959	1 531	<b>40 813</b>	<b>91 633</b>
As $K_{\beta}$ (30.45)	2 063	1 875	275	948	1 144	490	1 437
Pb $L_{\gamma}$ (24.07)	2 359	2 112	273	1 025	1 208	<b>3 388</b>	<b>6 655</b>
Background (21.50)	2 535	2 242	277	1 010	1 252	297	225

Spectra background was measured at the limits of the angular  $2\theta$  region of interest (21.50° and 71.00°); the registered counts (Table 2) roughly reflect the comparative size of irradiated samples.

Co 1s X-ray absorption spectra were collected using the instrumental set-up of beam line BM-29 at the European Synchrotron Radiation Facility (ESRF in Grenoble/France) by directly irradiating the glazed debris and detecting the fluorescence yield using a germanium detector. The energy was calibrated with a cobalt metal foil. Along with well crystallized cobalt silicate ( $\text{Co}_2\text{SiO}_4$ ), a commercial blue pigment based on  $\text{CoAl}_2\text{O}_4$  (which phase constitution was checked by X-ray diffraction) were both irradiated to model cobalt speciation and coordination environment in the glazes.

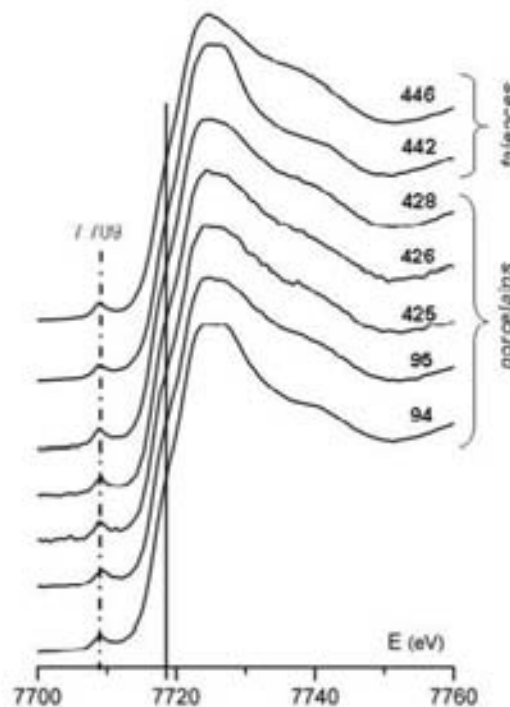
## RESULTS AND DISCUSSION

Chemical results obtained through the XRF-WDS non-invasive assay (Table 2) rule out the presence of arsenic in the glazes of porcelain shards; indeed, the count-rate values at Pb  $L_{\gamma}$ , As  $K_{\beta}$  and the energy-coincident  $L_{\alpha}$  and  $K_{\alpha}$  emission lines respectively from Pb and As are too close to for each porcelain sample; conversely, corresponding values for the two faience samples confirm the presence of significant contents of lead in the glaze, as expectable for a Portuguese XVII century manufacture.

Clearly distinct Mn/Co and Fe/Co ratios were obtained for thin (94-95-426) and thick (425-428) porcelain fragments, indicating that the first have a significantly higher iron content compared to manganese. Considering analytical results obtained for Ming porcelains by synchrotron X-ray fluorescence (SR-XRF) [9] and PIXE [8, 10], obtained ratios agree

with the advanced dating (late XVI to early XVII century, Table 1).

The Co  $K$ -edge X-ray absorption (XAFS) spectrum of the glaze (Figure 2) display the same general trend for all fragments: a relatively intense pre-edge feature centered at ~7709 eV, the edge at an energy (7718 eV) indicative of a divalent state of the cobalt ions and a subsequent poorly detailed EXAFS region (Figure 3).

**FIGURE 2.** Co  $K$ -edge XANES spectra collected from the blue glaze of studied archaeological fragments.

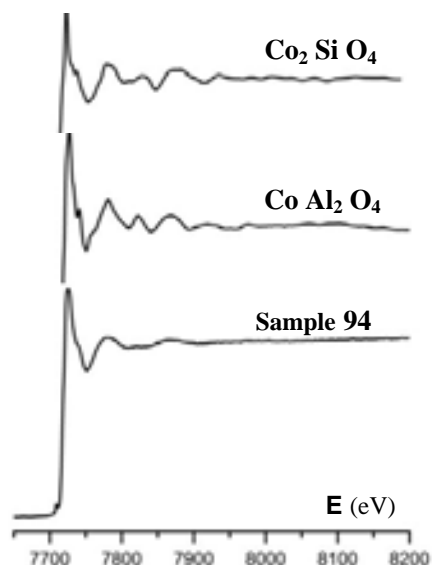


FIGURE 3. Comparison of Co *K*-edge XAFS spectra.

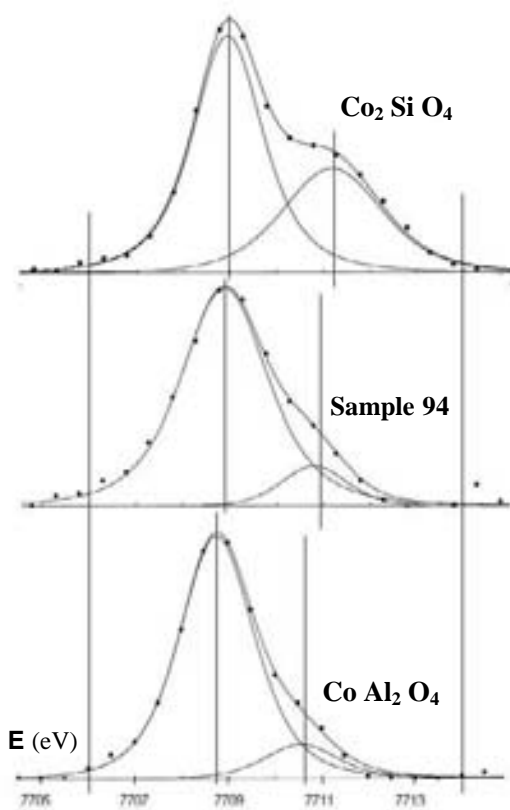


FIGURE 4. Comparison of resolved pre-edge details in Co 1s XANES spectra.

Co 1s XANES spectra of model oxides present dissimilarities in the near-edge layout as expected for  $\text{Co}^{2+}$  ions with distinct close oxygen coordination environments - tetrahedral and octahedral, respectively in the spinel  $\text{CoAl}_2\text{O}_4$  and in the silicate  $\text{Co}_2\text{SiO}_4$ .

The pre-edge spectral region was resolved with the Fityk program [12]. When comparing the contributing features obtained for the best-fit in model compounds with similarly resolved details of the XANES spectrum from a porcelain fragment (Figure 4), the prevailing tetrahedral environment around the  $3d^7$  transition metal ion  $\text{Co}^{2+}$  in the Chinese glaze becomes apparent.

The EXAFS spectral region was deconvoluted using the FEFF8 program based on a theoretical multiple scattering approach, along with the supporting IFEFFIT library [13-16]. Calculated pseudo-radial distribution functions (Figure 5) show a similar trend of Co-O distances in the spinel oxide and in the Chinese blue glaze; conversely, dissimilar tendencies are noticed for the silicate in which crystal structure the oxygen octahedra around  $\text{Co}^{2+}$  ions share edges, thus giving rise to close Co-Co distances.

Using the theoretical amplitudes and the phase parameters calculated with FEFF8, the experimental EXAFS spectra of the porcelains were fitted allowing the coordination number ( $N$ ), the atomic distances ( $R$ ) and the Debye-Waller factor ( $\sigma^2$ ) to vary freely. Fitting convergence could only be attained with  $\text{CoAl}_2\text{O}_4$  spectrum as illustrated by Figure 6. Resulting numerical values are  $4.4 \pm 0.6 \text{ \AA}$  for the coordination number and  $\sim 2.00 \text{ \AA}$  for the mean Co-O distances, with a Debye-Waller factor of  $0.010 \pm 0.002 \text{ \AA}^2$ . EXAFS data treatment then validates an average coordination environment close to tetrahedral for most cobalt ions within the glaze.

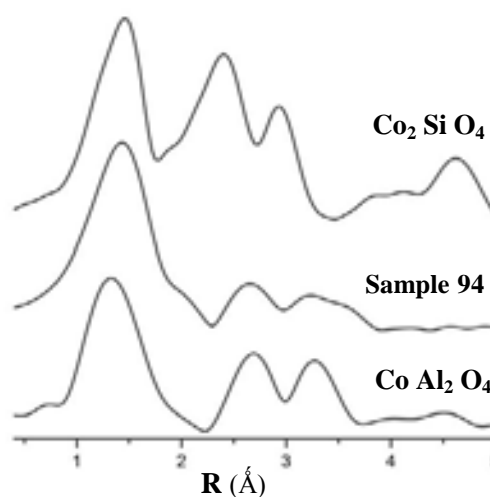


FIGURE 5. Pseudo-radial distribution functions extracted from experimental Co *K*-edge EXAFS spectra.

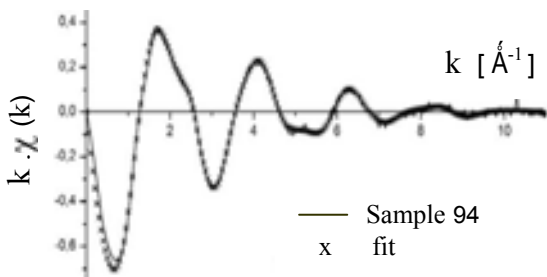


FIGURE 6. Best-fit of experimental data from a porcelain sample to the theoretically calculated spectrum of  $\text{Co Al}_2 \text{O}_4$ .

## CONCLUSIONS

Chemical data in general and particularly the absence of arsenic assigned through the present work conform to the dating advanced by Art-Historians through the examination of studied archaeological Chinese porcelain shards (Table 1). Actual results clearly demonstrate that lead – a fuser metal currently used in Portugal to manufacture ceramic glazes along the XVI-XVII century – was not employed to produce contemporary blue Chinese glazes for porcelains, thus providing a distinctive authenticity feature.

Concerning the Chinese porcelain fragments collected at the Monastery of Santa Clara-a-Velha, actual chemical data agree with recent results obtained in a larger study by energy dispersive X-ray micro-fluorescence carried out with a portable apparatus [17].

XAFS results confirm that cobalt plays the dual role of chromophore and network-former in the blue glaze of ancient Chinese porcelains, the tetrahedral  $\text{Co}^{2+}$  ions being responsible for a blue coloring [18]. Conversely, non-coloring pseudo-octahedral  $\text{Co}^{2+}$  ions occupy available coordination sites of the tetrahedral silica-rich glassy matrix.

Differences in the pre-edge features of XANES spectra from model oxides are explained by the local symmetry of  $\text{Co}^{2+}$  ions: regular tetrahedral coordination with site symmetry  $\bar{4} 3 m$  in  $\text{Co Al}_2 \text{O}_4$  (spinel-type oxide) and octahedral coordination with two site symmetries ( $\bar{1}$  and  $m$ ) in  $\text{Co}_2 \text{Si O}_4$  (olivine-type crystal structure). In fact, the absorption edge of  $1s$  XANES spectra from  $3d$  transition metals is due to electronic transitions from the  $1s$  core state to the  $4p$  conduction band, while pre-edge details arise from quadrupole transitions to  $3d$  empty states; when the inherent inversion symmetry is broken (as in tetrahedral  $\text{Co}^{2+}$ , a high spin  $3d^7$  ion with filled  $e_g$  and  $t_{2g}$  orbitals), local  $3d 4p$  wave-function mixing allows for dipole transitions to occur [19]. Considering the mean coordination number of  $\text{Co}^{2+}$  extracted from EXAFS spectra, these comments also account for the XANES

results obtained for the studied ancient blue glazes.

## ACKNOWLEDGMENTS

The financial support of the Portuguese Foundation for Science and Technology (FCT/MCTES) through the Project PTDC/HAH/69506/2006 is acknowledged, as well as the financial support of EU to perform the experiments at the ESRF through the action Access to Research Infra-structures.

## REFERENCES

1. S. Padovani, L. Borgia, B. Brunetti, A. Sgamellotti, A. Giuliani, F. D'Acapito, P. Mazzoldi, C. Sada and G. Battaglin, *Appl. Phys. A* **79** (2004) 229-233.
2. M.O. Figueiredo, J.P. Veiga, T.P. Silva, J.P. Mirão and S. Pascarelli, *Nuclear Instr. & Methods B* **238** (2005) 134-137.
3. M.O. Figueiredo, T.P. Silva and J.P. Veiga, *Appl. Phys. A* **83** (2006) 209-211.
4. J.P. Veiga and M.O. Figueiredo, *X-ray Spectrometry* **37** (2008) 458-461.
5. P.C. Santos, *Oriental Art* **49** (2003) 24-31.
6. M.I. Dias, M. O. Figueiredo, M. I. Prudêncio, C.I. Burbidge, T. Silva, J. P. Veiga, M. A. Matos and A. M. Pais, *37th Int. Symp. on Archaeometry (2008) Siena, Italy* (poster).
7. P.L. Leung and H. Luo, *X-ray Spectrometry* **29** (2000) 34-38.
8. H.S. Cheng, B. Zhang, H.N. Xia, J.C. Jiang and F.J. Yang, *Nuclear Instr. & Methods B* **190** (2002) 488-491.
9. R. Wen, C.S. Wang, Z.W. Mao, Y.Y. Huang and A.M. Pollard, *Archaeometry* **49** (2007) 101-115.
10. H.S. Cheng, B. Zhang, D. Zhu, F.J. Yang, X.M. Sun and M.S. Guo, *Nuclear Instr. & Methods B* **240** (2005) 527-531.
11. T. Mimani and S. Ghosh, *Current Science* **78** (2000) 892-896.
12. <http://www.unipress.waw.pl/fityk>
13. B. Ravel, *J. Synchr. Rad.* **8** (2001) 314-316.
14. M. Newville, *J. Synchr. Rad.* **8** (2001) 322-324.
15. A.L. Ankudinov and J. Rehr, *J. Synchr. Rad.* **10** (2003) 366-368.
16. B. Ravel and M. Newville, *J. Synchr. Rad.* **12** (2005) 537-541.
17. M. Larsson and J.P. Veiga, in *Proceedings Internat. Conf. Geoarch. and Archaeominer.* (2008, Publ. House St. Ivan Rilski, Sofia/Bulgaria) 134-138.
18. A.L. Fernandez and L. de Pablo, *Pigment and Resin Technology* **31** (2002) 350-356.
19. F. de Groot, G. Vankó and P. Glatzel, *J. Phys. Cond. Matt.* **21** (2009) 104207 (7pp).

## **Non-Destructive Analysis of Handwriting and Colored Drawings of the Printed Book *Divina Proportione* (1509)**

V. Aguilar Melo<sup>1</sup>, J.L. Ruvalcaba Sil<sup>1</sup> O. Escamilla Gonzalez<sup>2</sup>, L. Milan<sup>2</sup>,  
D. Ramírez Miranda<sup>1</sup> and Ma.C. León García<sup>3</sup>

<sup>1</sup> Instituto de Física, Universidad Nacional Autónoma de México, MEXICO. e-mail: sil@fisica.unam.mx  
<sup>2</sup> Biblioteca Ing. Antonio M. Anza, Facultad de Ingeniería, Universidad Nacional Autónoma de México, MEXICO.  
<sup>3</sup> Coordinación Nacional de Monumentos Históricos, INAH, MEXICO.

**Abstract.** The book *Divina Proportione* by Lucca Pacioli was printed in 1509 in Venice, Italy. This book has three parts and presents the fundamentals of the divine proportions (afterwards called in XIX century “golden rule”), an alphabet designed with this proportions, and the geometrical shapes from Leonardo’s drawings. This book became an outstanding treaty for architecture. The original printing preserved in the Biblioteca Antonio Anza of the Engineering Faculty of the Universidad Nacional Autónoma de México has several *ex-libris* and numerous handwritings, notes, and several colored drawings carried out by the owners of the book after its arrival to the colonial Mexico at the end of XVI century. The aim of this study is to identify the pigments of the drawings, inks of the colored drawings and to propose a grouping of the notes and handwritings from inks compositions, as well as to relate them to the various owners. For this purpose, a full non-destructive study by ultraviolet and infrared light imaging, portable X-ray Fluorescence (XRF) and Raman spectrometry was carried out. Imaging techniques were performed for a general examination. XRF was used for inks and pigments elemental analyses while Raman was applied for paper and pigments characterization. This is the first time that such amount of techniques was applied for the study of an ancient book. In this work, the used methodology, technical examination, and the main results of the composition comparison and the materials identification are presented.

**Keywords:** *Divina Proportione*, XRF, Raman, Ultraviolet Imaging, Infrared reflectography, ancient book.

### **INTRODUCTION**

The non-destructive study of ancient books and manuscripts provide outstanding information about the inks composition, the identification of pigments of decorations and the deterioration conditions of paper inks and colors without sampling [1-4].

In the last five years, the development of non-destructive and portable techniques made possible the study of the material analysis of unique books and manuscripts of the most important archives and libraries for a better understanding of these documents and conservation purposes. From the analysis of inks it was possible to determine different sequences and

moments of writing and decorations [5], the used of various printing papers, document additions, and the identification of pigments [6].

In Mexico, several documents and ancient books has been studied by our group, first using ion beam techniques at particle accelerators laboratories [7-8] and later by X-ray fluorescence portable devices [8-11]. Recently the set of portable equipments has been increased with Raman and Mid-FTIR spectrometers. These equipments are available for material analysis of the Mexican cultural heritage in the CONACyT MOVIL project fame [13-15]. The analysis performed to the *Divina Proportione* printed book was the first

non destructive in situ study of an ancient book using all these portable techniques [16].

## THE BOOK

The book *Divina Proportione* written by Lucca Pacioli was printed in 1509 in Venice, Italy, by the Paganini printer's family. This book has three parts and presents the fundamentals of the divine proportions (afterwards called in XIX century "golden rule"), an alphabet drawn with this proportions and the geometrical shapes from Leonardo's drawings. This book became an outstanding treaty for architecture. The original printing preserved in the Biblioteca Antonio Anza of the Engineering Faculty of the Universidad Nacional Autonoma de Mexico (UNAM) has several *ex-libris* and numerous handwritings, notes, and several colored drawings of walls and fortress carried out by the owners of the book after its arrival to the colonial Mexico at the end of XVI century. This is one of the oldest printing books in the UNAM faculty collections (Figure 1).

The historical research pointed out to several owners of the book. First, Melchor Pérez de Soto, Master of the Cathedral of Mexico, owned it before 1655. Afterwards, Jerónimo de Becerra, a Mexico Mint tester, kept it from 1644 to 1677. Later, the book was in possession of Juan de Peralta, a famous architect and professor of the University of Mexico from 1688 until 1769. After 1744, the book was used by other architects until the foundation of the Royal Seminary of Minery, when the document was in kept in its library from 1793 to 1799. Then, it belonged to the library of the School of Engineering in the period of 1834 to 1882. In 1910, when the School of Engineering of the National University (UNAM) was created, the book became part of its collection.

The aim of this study is to identify the pigments and inks of the colored drawings and to group the notes and handwritings from inks compositions, as well as to relate them to the various owners. In this work some of the most important results are presented in order to show the achievements of the applied methodology. Further results are provided in [16].

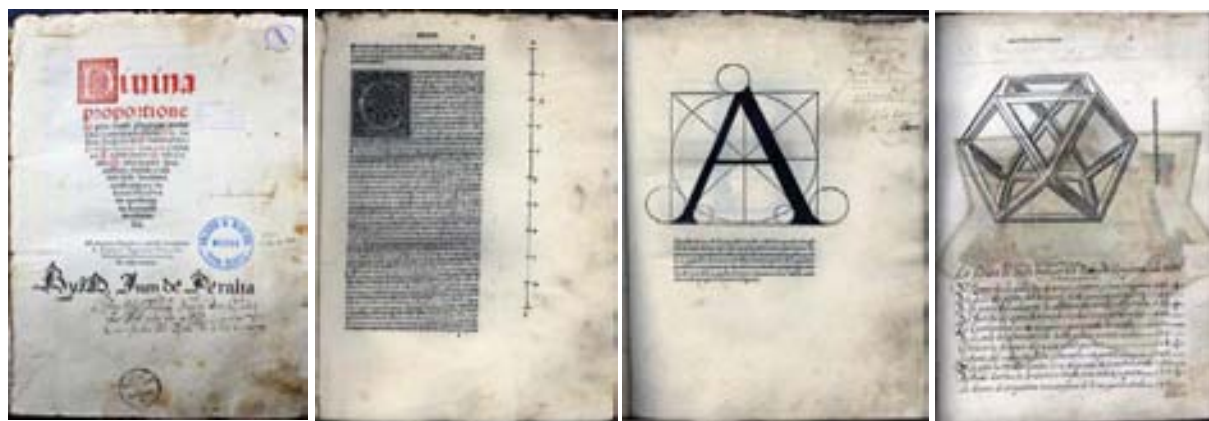


FIGURE 1. Cover and representative printed pages of the first, second and third parts of the *Divina Proportione* book.

## METHODOLOGY

The non-destructive study considered the use of ultraviolet and infrared imaging for a general examination of the document [3]. The comparison of the inks and pigments with reference materials provides a first identification.

The identification of the features of iron-gallic inks and pigments was carried out using a video camera Sony model in nightshot mode with an infrared filter (UV-VIS cut filter R72 from Edmund Optics) and indirect natural sun light as illumination in order to detect light from 700 to 1000 nm.

Ultraviolet imaging was performed using 8W handheld lamp illumination of 365 nm wavelength,

(UVGL-58 from UVP). The images were recorded by a Canon reflex digital camera without filter.

On the other hand, our SANDRA equipment [15] was used for X-ray fluorescence analysis to determine inks and pigments elemental contents. The spot on the document had 0.5 mm diameter and a Mo X-ray tube with 45 kV and 0.6 mA conditions was used. Each measurement lasted 180 s and more than 200 regions, including inks and colors, were analyzed.

Raman spectroscopy was applied for paper and pigments characterization by a Delta Nu Inspector spectrometer with a 785 nm laser of 120 mW. The resolution is  $8 \text{ cm}^{-1}$  in it ranges from 200 to  $2000 \text{ cm}^{-1}$ . About 100 measurements were carried out using the lower power output of the laser beam 20 mW to avoid any damage to the document paper and colors.

## RESULTS AND DISCUSSION

### UV and IR Imaging

The inks used in the *ex-libris*, drawings and handwritten notes indicates that they are in all the cases iron-gallic inks since they appeared very opaque under UV illumination and disappeared in IR images while the printing ink is always dark [3,13] as it can be expected for carbon base inks (figures 2). Concerning the colors, orange and red are very opaque under UV lighting [3,13]. The brown, blue, and green colors of the colored drawings present the typical behavior of organic materials: they look opaque under UV lighting and transparent or light gray using IR illumination [13]. Thus, the original ink drawing can be observed using IR lighting. Also, it is possible to observe some fluorescence when illuminating with UV the back side of the drawings of the fortresses and walls, probably due to a preparation layer and/or oil in the color (Figure 3).

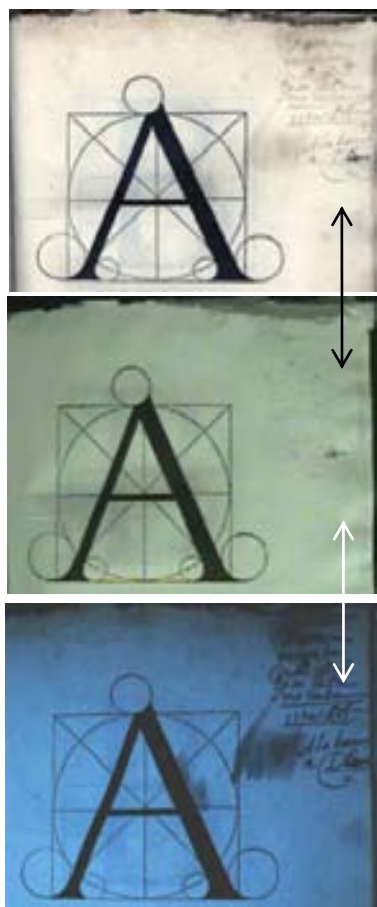


**FIGURE 2.** Visible light, IR and UV illumination images of handwritten and printing inks.



**FIGURE 3.** Visible light, IR and UV (front and back) images of one of the colored drawings of a fortress.

### X-ray fluorescence analysis

The measurements process by XRF is shown in figure 4 and a typical XRF ink spectrum is presented in Figure 5. It can be observed the presence of Cl, K, Ca, Mn, Fe, Cu and Pb.



**FIGURE 4.** XRF analysis of the book using the SANDRA equipment [15].

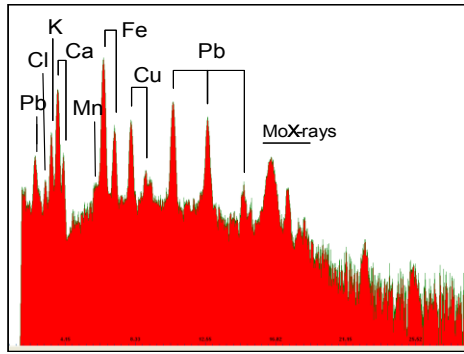


FIGURE 5. Typical XRF spectrum of the iron-gallic inks of the book.

A comparison between the inks analyzed in several regions of the *ex-libris* of Juan de Peralta (Figure 6) of the cover page of the book is presented in figure 7. Cu/Fe, Mn/Fe and Pb/Fe X-ray ratios are contrasted. Regions 6, 7, 8, 207 and 210 are very similar, but their elemental composition profile is different of 9, 209 and 217. Region 208 has a completely distinct composition. These results suggest that at least three inks are present and probably the *ex-libris* has been retouched in different times. Then, we may infer that this *ex-libris* composition cannot be used as reference ink to correlate the notes and drawings in the book to Peralta’s authorship.

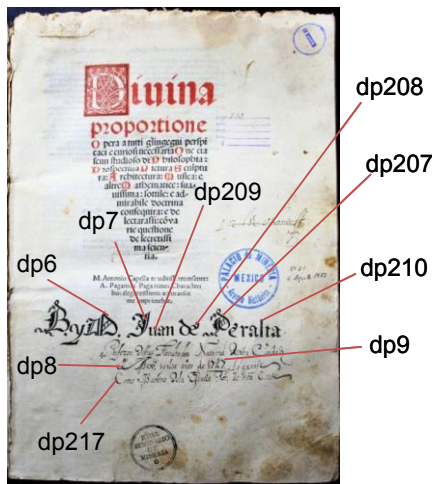


FIGURE 6. Analyzed regions on the Peralta’s *ex-libris* of the cover book.

On the other hand, in the case of the *ex-libris* of Jerónimo de Becerra, written beside the letter “A” in the first page of the alphabet in the second section of the book, the analyze regions are shown in figure 8. Figure 9 displays the metallic X-ray intensity ratios Cu/Fe, Zn/Fe, Mn/Fe and Pb/Fe. First it is clear that the inks are different of the Peralta’s *ex-libris*.

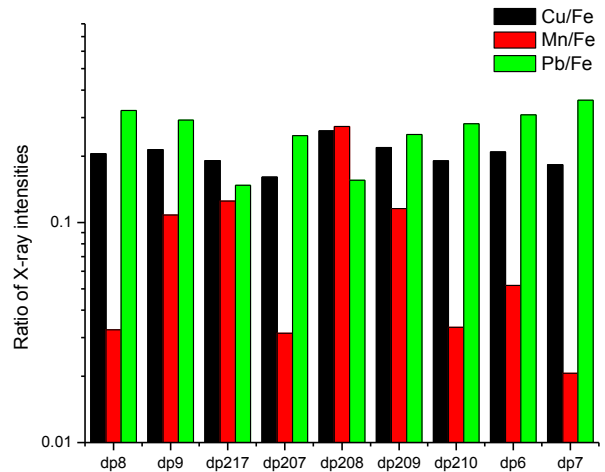


FIGURE 7. Metallic X-ray ratios for the inks of the Peralta’s *ex-libris* of the cover book –figure 5.

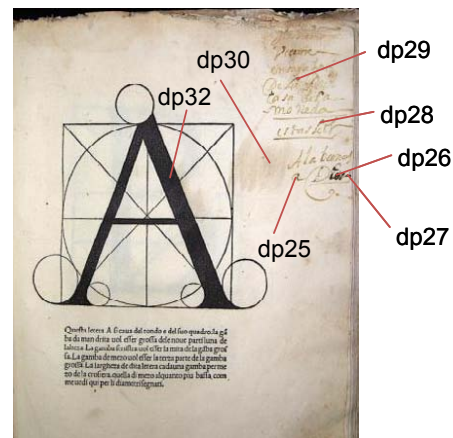


FIGURE 8. Analyzed regions on the Becerra’s *ex-libris*.

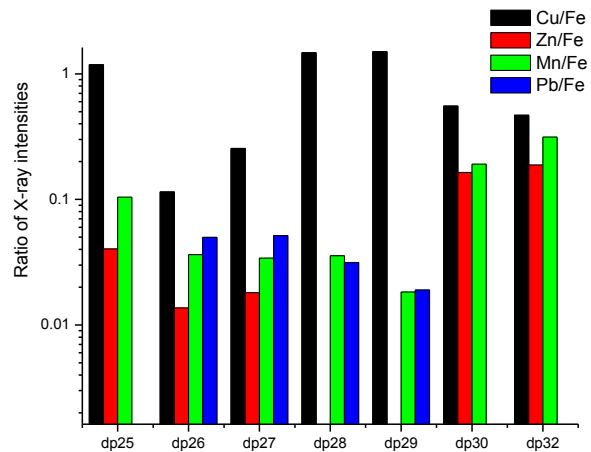


FIGURE 9. Metallic X-ray ratios for the inks of the Becerra’s *ex-libris* –figure 5.

The comparison of the ratios of *ex-libris* inks of regions 28 and 29, indicates as we may expected that the correction with a darker ink (zones 26 and 27) was done with a different ink. The ink stain of region 30 does not correspond to the handwriting inks but it is similar to the printing ink of letter “A”. At first sight, this may indicate that the stain was produced during the printing. In the corresponding UV image of figure 2, the inks stain if clearly visible in the same area of the page but also in the analyzed area of letter “A” however in the IR image, where the carbon base of the printing ink is quite visible, there is not trace of the stain. This indicates that the signals of the ink stain in the “A” printing area may give rise to confusion. The region 25 of ink is similar to the stain ink but with a higher Cu and Fe contents and in fact it has similar contents of these metals. We consider that the stain was lead by an iron gallic ink different from the *ex-libris* ones and there are three inks in the last sentence of the handwriting.

On the other hand, the orange color of the figures of walls and fortress of the third section of the book (e.g. see Figure 3 and 4) were also analyzed by XRF. Hg and Pb were detected and consequently vermilion and lead colors were identified as the main pigments. A comparison of the Pb/Hg, Fe/Hg, Cu/Hg and Ca/Hg X-ray intensity ratios provide a fingerprint of the color preparation and the episodes of coloring as well as the sequence of the coloring. In figure 10, these ratios are plotted for the regions of orange color of drawings on folios I, II, III, V, VI, VII, VIII, X, XI, XIII and XV.

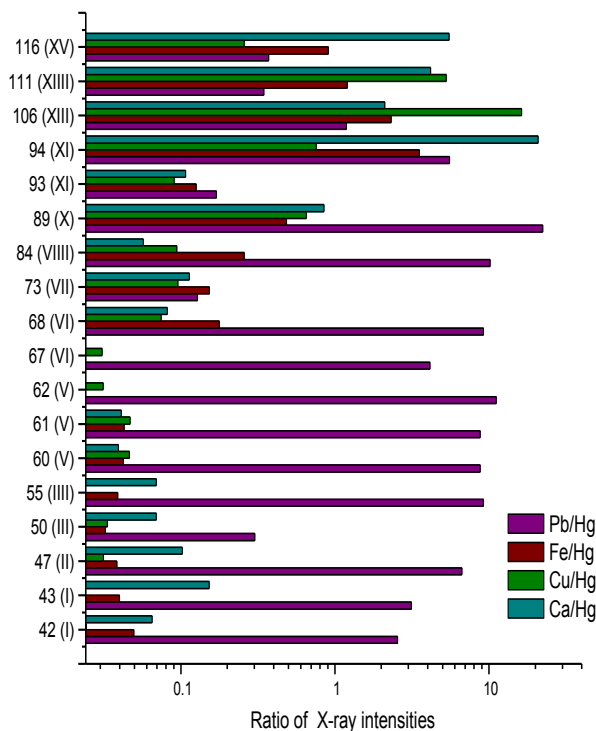


FIGURE 10. X-ray ratios for the orange color of drawings.

The comparison of the ratios indicates that the coloring of drawings of folio I (zones 42 & 43) is different of the next page (region 47). In folio III there are two preparations of the color (spots 50 & 55) that contrast to the previous pages ones. In folio V there are other two different preparations (spots 60 & 61 vs 62 & 67). So, at least two episodes may be observed in the folio III and V. From folio VI the orange color is very different and richer in Fe and Ca. The last colors have Fe and Ca X-ray intensity higher than the Hg one. An iron red and/or brown earth pigments replaced gradually the vermilion, and this result agrees with the less bright color observed in the drawings (compare those in figures 3 and 4). The composition of the orange-red color varies significantly from one page to other and we may expect individual episodes of coloring for each drawing; they are not consecutive. Thus, we consider that the coloring has only some regularity, and perhaps one author, only for the first five pages. From page VI there are probably several hands and periods of coloring.

### Raman measurements

Raman is considered a very suitable method for pigments identification in specific regions [3, 6]. The process of the analysis with our equipment is shown in Figure 11.

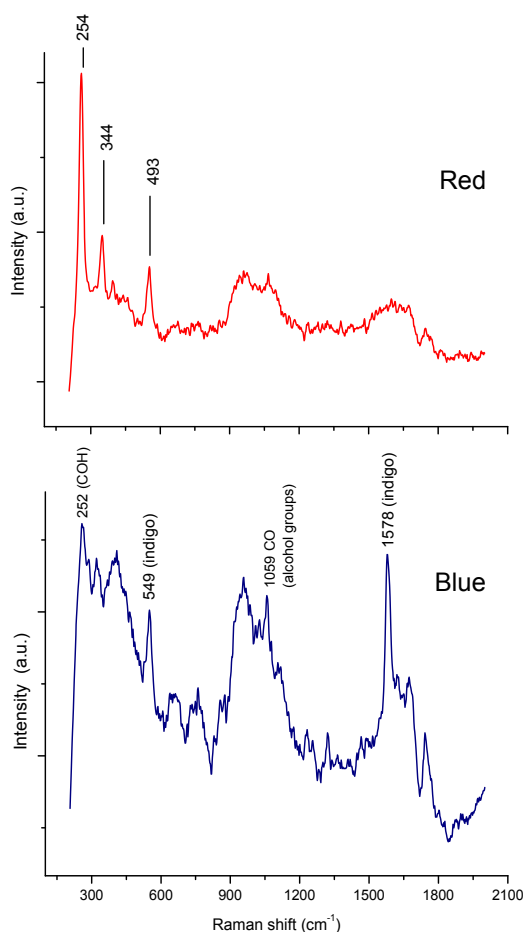


FIGURE 11. Raman analysis of the book using the Delta Nu Raman Inspector equipment.

The measurements were successful for inorganic pigment identification and for some blue colors. For instance, for the red and blue areas of figure 12, the spectra of figure 13 were respectively obtained. The comparison with the pigments databases of the literature [6, 17] allowed the identification. For the red color of the fortress wall, vermilion signals (254 and 344  $\text{cm}^{-1}$ ) are easily obtained but the red lead minium pigment signals are less evident (390 and 548  $\text{cm}^{-1}$ ). The bright red color is a mixture of these pigments. This result completely agrees with the XRF analysis results.



**FIGURE 12.** Some color regions analyzed by Raman technique.



**FIGURE 13.** Typical red and blue Raman spectra of colors shown in figure 10.

The paper signals give raise to the main background of the Raman spectra and it may difficult the identification, as we may observe for the blue color. The high intensity signals of Indigo at 548 and 1579  $\text{cm}^{-1}$  are barely detected. The XRF spectra of the

same blue regions did not provide diagnostic elements of inorganic pigments, and the observed IR imaging transparency pointed out to an organic blue color. The agreement between the techniques is very good. Nevertheless, it was not possible to obtain clear spectra for all the cases and colors.

Moreover, the Raman technique was very suitable for paper characterization. Figure 14 shows the comparison between the spectrum of a new paper and a typical spectrum of the *Divina Proportione* paper. In the new paper, the bands of cellulose detected were  $\tau(\text{COH})$ ,  $\delta(\text{CCC})$ ,  $\delta(\text{CCC})$ ,  $\delta(\text{COC})$ ,  $\nu(\text{COC})$ ,  $\rho(\text{CH}_2)$ ,  $\nu(\text{COC})$ ,  $\nu(\text{COC})$ ,  $\nu(\text{CC})$ ,  $\delta(\text{CH}_2)$  and  $\delta(\text{CH}_2)$  at 252, 380, 437, 520, 900, 999, 1097, 1122, 1153, 1338 and 1380  $\text{cm}^{-1}$ , respectively [6].

In the XVI century paper, the signal corresponding to the COC band (1097  $\text{cm}^{-1}$ ) reduces significantly, and the signals of  $\text{CH}_2$  at 999  $\text{cm}^{-1}$  increases. Also, in general it is observed a widening in the bands signals. This is result of the aging of the material and the degradation of the paper that produces the breaking of the cellulose bands. A comparison of these spectra with papers from XX to XVI century indicates that despite the deterioration observed, the paper of the book is in very good conditions.

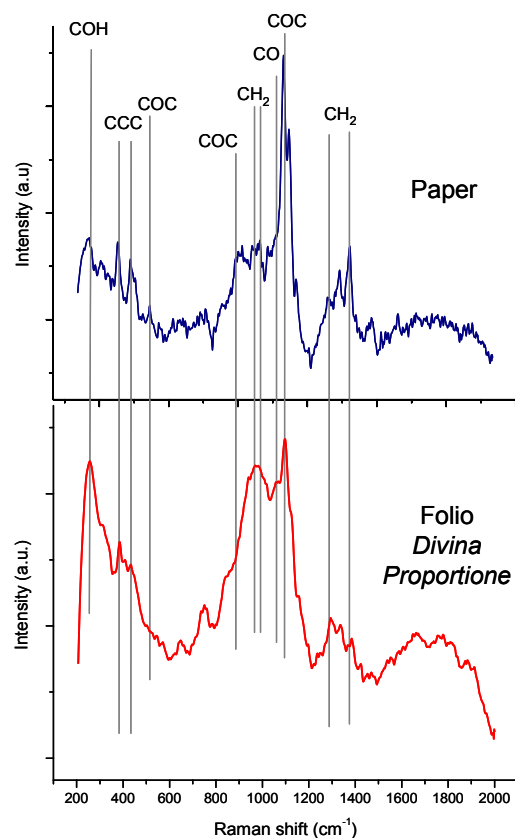


**FIGURE 14.** Typical paper Raman spectra for a new paper and the book's folio.

## CONCLUSIONS

The non-destructive methodology used in this work combine the use of imaging and spectroscopic techniques and it provides outstanding information about the inks, pigments and paper of the analyzed book and it can be used for the study of other documents.

The problem of identification of the owner's hands from the inks became more complex due to the presence of several inks in the *ex-libris*. Nevertheless, it has been possible to determine some correlations between the inks notes and the inks drawings in the third section of the book. For the colored drawings, some episodes of illumination have been observed from elemental ratios. For pigments identification and color combination, XRF is very suitable; despite in some cases the identification from diagnostic elements is not always feasible. Raman may provide a complementary identification if strong interferences are not observed.

Besides the composition of the materials, Raman spectra may be used for a deterioration diagnostics of the paper. Then, it is possible to propose preventive conservation and to follow the deterioration of the document.

Further analyses of the full data are in progress jointly with the conservators, historians and librarians for appropriate interpretation of the information.

## ACKNOWLEDGMENTS

This analytical research has been supported by CONACyT Mexico grant MOVIL U49834-R and PAPIIT UNAM ANDREAH project IN403210. Authors thanks to Dulce Maria Aguilar for imaging and photographic technical support. V. Aguilar received a fellowships from CONACyT grant 103918 and project PAPIIT UNAM IN403210.

## REFERENCES

1. Ciliberto E. y Spoto G. eds., *Modern Analytical Methods in Art and Archaeology*, Chemical Analysis, Series of Monographs on Analytical Chemistry and its Applications, Vol. 155, J.D. Winefordner Series Ed., John Wiley and Sons, N.Y., 2000.
2. Van Grieken R. & Janssens K. eds., *Cultural Heritage Conservation and Environmental Impact Assessment by Non-destructive Testing and Microanalysis*, A.A. Balkema Publishers, London, 2005.
3. H.G. M. Edwards, J.M. Chalmers, *Raman Spectroscopy in archaeology and art history*, The Royal Society of Chemistry, Cambridge, 2005.
4. C. Miliani, F. Rosi, B.G. Brunetti, A. Sgamellotti, *Acc. Chem. Res.* **43** (2010), 728–738
5. O. Hahn, W. Malzer, B. Kanngiesser, B. Beckhoff, *X-Ray Spectrometry*. **33** (2004) 234–239.
6. S. Bioletti, R. Leahy, J. Fields, B. Meehan, W. Blau, *Journal of Raman Spectroscopy* **40** (2009) 1043–1049.
7. J.L. Ruvalcaba, M. Monroy, “Estudio no destructivo de documentos y libros antiguos mediante haces de iones”, in *La Ciencia de Materiales y su Impacto en la Arqueología*, Academia Mexicana de Ciencia de Materiales A.C., D. Mendoza, L. Brito, J. Arenas coord., Ed. Lagares, México, 2004. 141-154.
8. J.L. Ruvalcaba Sil, S. Zetina, H. Calvo del Castillo, E. Arroyo, E. Hernández, M. Van der Meer, L. Sotelo, “The Grolier Codex: A Non Destructive Study of a Possible Maya Document using PIXE and RBS”, *Materials Issues in Art and Archaeology VIII*, Materials Research Society Vol. 1047, Boston, 2008, 299-306
9. J.L. Ruvalcaba y C. González Tirado, “Análisis in situ de documentos históricos mediante un sistema portátil de XRF” in *La Ciencia de Materiales y su Impacto en la Arqueología*. Vol II, Academia Mexicana de Ciencia de Materiales A.C., D. Mendoza, J. Arenas y V. Rodríguez coord., Ed. Lagares, México, 2005, 55-79.
10. L. Torner Morales, J.L. Ruvalcaba Sil, C. González Tirado, “FRX portátil y PIXE como Técnicas Complementarias para el Análisis de Libros Antiguos: Estudio de Guardas y Cantos Decorados” in *La Ciencia de Materiales y su Impacto en la Arqueología*, vol. III, Academia Mexicana de Ciencia de Materiales A.C., D. Mendoza, J. Arenas, V. Rodríguez y J.L. Ruvalcaba Sil coord., Ed. Lagares, México, 2006. p. 91-103.
11. J. Morales Ladrón de Guevara, L. Torner Morales, J.L. Ruvalcaba Sil, “Estudio y conservación de dos documentos del siglo XVI”, *Testimonios de la Fundación de la Ciudad de Puebla in Conservación de Bienes Culturales: Acciones y Reflexiones*. L. F. Guerrero Baca, coord., INAH, México 2009, 305-334.
12. Th. Velasco, O. Ibarra, J.L. Ruvalcaba-Sil, “Non Destructive Study of Ancient Choral Books from the Mexico City Cathedral by a Portable X-ray Fluorescence System” in *International Symposium on Archaeometry 2006 Proceedings*, J.F. Moreau, R. Auger, J. Chabot, A. Herzog, *Cahiers d'Archéologie*, du CELAT no. 25 Série Archéométrie no. 7, Université Laval, Quebec, 2009, 109-115.
13. S. Zetina, J.L. Ruvalcaba, T. Falcón, E. Hernández, C. González, E. Arroyo, *Painting Syncretism: a Non Destructive Analysis of the Badiano Codex*, 9th International Conference on NDT of Art, ART2008, Jerusalem, Israel.  
<http://www.ndt.net/search/docs.php3?MainSource=65>
14. J.L. Ruvalcaba Sil, L. Filloy, M. Vaggi, L.H. Tapia Gálvez, R. Sánchez Becerra, “Estudio no destructivo in situ de la Máscara de Malinaltepec”, in *La Máscara de Malinaltepec*, S. Martínez del Campo coord., CONACULTA-INAH, México, 2010. 153-168.
15. J.L. Ruvalcaba, D. Ramírez, V. Aguilar, F. Picazo, *X-ray Spectrometry* **39** (2010) 338-345
16. V. Aguilar Melo, *Análisis No destructivo para la Caracterización de Documentos Antiguos*, University dissertation work, Facultad de Ciencias, Universidad Nacional Autónoma de México, Mexico, 2011.
17. R.J.H. Clark, P.J. Gibbs, *Spectrochimica Acta A* **53**. (1997) 2159 -2179.

# **The Application of Portable X-Ray Fluorescence Spectrometer in Historical Photography: A Proposal of Experimental Configuration**

M. del Egado<sup>1</sup> and D. Juanes<sup>2</sup>

<sup>1</sup>*Instituto del Patrimonio Cultural de España.  
C/ Pintor el Greco, 4. 28040 Madrid. SPAIN. e-mail: marian.delegido@mcu.es*

<sup>2</sup>*Institut Valencià de Conservació i Restauració de Bens Culturals.  
C/ Pintor Genaro Lahuerta, 25, planta 3. 46010 Valencia. SPAIN.*

**Abstract.** X-ray fluorescence analysis (XRF) nowadays is a well-known non-invasive technique of investigation for cultural heritage objects analysis. It can be applied in a non vacuum environment, without any special preparation of the sample or without any sampling. During the last 30 years, many studies and results have been proposed for a large variety of materials and some experimental improvements have been developed. With these new advances, not only archaeological and art objects can be studied, but also other types of cultural objects could be benefited. In the case of historical photography, the photographs elemental composition is generally required by curators and conservators since the characterisation of materials and applied technique allow a better understanding of the physical properties and their interaction with the environment. This can be used to evaluate more adequate and efficient conservation- restoration strategies and to improve preventive conservation of their collection. Specific material and morphology used in photography gave us the motivation to carry out researches to improve experimental parameters and methodology of analysis in historical photographs with XRF. It has been showed the geometric configuration between X-ray tube, detector and the photographic plate under study influences the analysis efficiency. Therefore the results obtained with the diverse geometries can be used to optimize the XRF configuration. Such experiments have been carried out on glass photographic plates, from the start of the 20<sup>th</sup> century, and made of silver bromide without exposure. The conclusion is a proposal of experimental parameters and configuration for analytical photography with a portable XRF.

**Keywords:** portable XRF, photography analysis, configuration, non destructive analysis.

## **INTRODUCTION**

Photographic materials are a relevant part of our documentary cultural heritage. Its importance in the social life, its wide utilization as way of documentary information and their overlap with the applied chemical and physical sciences have turned it into a

very important part of our more recent cultural and historical heritage.

The importance of scientific support for the study and conservation of cultural property has long been recognized. Investigations concerning chemical composition remain one of the main concerns not only to improve the knowledge of the object and its context, but also to document the current state, to understand the deterioration processes and to be

advisable to proper conservation treatments.

Nevertheless, researches on conservation of historical photograph collections suffer a lack of data obtained by the analysis of the physical structure and the chemical composition, fairly common in other more traditional fields of cultural heritage.

X-ray fluorescence (XRF) is an elemental analytical technique, portable, non-destructive, fast, easily accessible and multi elemental. XRF has been widely applied to study cultural heritage on painting, metal, stone, enamel, glass etc. since 1960th [1-3], with successive improvements as the semiconductor detectors introduction [4] or thermoelectric cooled systems [5-6]. The importance of this technique has increased notably with the improvement on portability [7] and new exciting sources [8], electrons [9] or photons [10-13]. Therefore it is an analytic technique consolidated in the field of art and archaeology.

There are some studies carried out with this technique in the field of photographic materials. In the 1980's the first publications on XRF without taking samples applied to the historical photograph analysis appeared [14-15]. Little by little begins to be considered a very adequate technique in this area because, besides being carried out directly on the photographs, without taking samples and without contact with the surface, it offers surface analytic information in a band of dozen of microns, space in which the photographic emulsion appears. This technique has allowed to study with good results the palladium and platinum photographs indistinguishable only by their appearance [16-17], as to identify the elements used in the obtaining of a certain tonality [18]. One more example is the use of non-destructive techniques for the study of photographs on paper prints from the Album Durieu carried out by the Getty Conservation Institute [19].

The result of these analyses confirmed the potential of this non-destructive technique to identify the inorganic material and the photographic processes. Nevertheless, other researcher had identified important difficulties in the interpretation of the results because of the low concentrations of metallic elements and a high level of Bremsstrahlung [16].

The bibliography shows the applicability of XRF to several cultural beings with different geometrical dispositions without a clear distinction between the best of them. The aim of this work is to choose the most suitable configuration of a portable XRF spectrometer that provides with the qualitative inorganic elemental composition of historic photography with a non destructive but portable technique, to contribute to its study and its conservation.

## ANALYTICAL APPROACH

The physical principles of X-ray fluorescence are well known: electronic transitions can be induced in the inner-shells electrons of the object's constituent elements by electromagnetic radiation or charged particles of suitable energy. Outer-shell electrons fill the vacancies left and emit excess of energy as fluorescent x-rays whose energy and intensity are related to the type and abundance of the atoms concerned by the interaction. In practice, XRF can be used to rapidly identify elements with an atomic number greater than magnesium, due to the low fluorescence yield and the attenuation of X-rays by air and by the detector window for light elements. Because of the attenuation in the matter, only the X-rays emitted in the first layers under the surface can reach the detector.

The source provides the exciting radiation and is characterized in terms of energy and intensity, which both affect detection limits; though in principle radioisotopic sources can be used as well, aspects related to radiation hazard and system performance lead to prefer X-ray tubes. Low-power, air cooled miniaturized tubes are extremely attractive for their low-weight but the low voltage and current provide poor detection limits. But high-power tubes provide a wider excitation range and higher photon output, but they are heavy and complex. The detector allows measuring the energy and intensity of out coming fluorescence radiation; it is characterized by energy resolution and efficiency.

We selected an air-cooled x-ray tube with Pd target. The tube is driven by a 30 kV 1 mA high voltage power supply, providing a voltage range of 4 to 30 kV and 20  $\mu$ A and an acquisition time of 300 seconds (live time). The tube is equipped with a collimator producing an incident x-ray beam with a 5 mm in diameter at 1cm. of distance.

Within the family of solid state detectors, we chose an AMPTEK XR-100 CR thermoelectrically-cooled detector (Peltier effect), Si(Li) provided with good energy resolution of 162 eV FWHM for 5.9 keV X-rays (at 1000 counts per second). It has an active area of 7 mm<sup>2</sup> and a 8  $\mu$ m beryllium window.

Signals from the spectrometer are amplified and filtered and sent to the AMPTEK MCA 8000A, analog-to-digital converter, connected to a portable PC.

The geometry between primary beam, sample and detector are optimized in each specific case because we they can take arbitrary geometry according to each object. It includes a laser point and sensor movements for security reasons. It has been mounted in our laboratory selecting all the components and designing two different supports and positioning systems, both movable, that allows analysing objects in situ but with some specific characteristic in order

to work in a Museum, Archive, Laboratory or in a prehistoric cave or a scaffold. The object is placed at a distance of 1.5 cm. from both the X-ray generator and the detector.

### PHOTOGRAPHIC MATERIALS SELECTED

The photographic support selected for this study is glass and the technique, black and white silver bromide gelatine. From 1850 until 1950, glass has been the best considered support for the photographic images, both positive and negative, because of the great quality of the final image. For this reason, historical finds on glass have a large consideration by photograph curators, conservators and historians. Nevertheless, the scientific analyses carried out on glass photographs are not numerous.

We could count on the photographic funds of the Instituto del Patrimonio Cultural de España (IPCE) to achieve this goal. For this pilot study, we worked with a small photograph glasses collection not impressed proceeding from commercial factories (AGFA, Lumière and Fils, Jouglà), in most cases still sealed in its original boxes, and from the beginning of the 20th century. This study has been carried out with fragments of plates extracted for the first time of the boxes of the French firm "Lumière and Fils".

The glass plates had of thickness about 1 mm. and an emulsion layer of gelatine with silver bromide grains of thickness about 20  $\mu\text{m}$ . Some of the studied plates had an organic anti halation layer.

### RESULTS AND DISCUSSION

The geometry effects were examined in order to optimize the results. Specifically, the different possibilities of disposition between the spectrometer components and the photograph were examined.

We considered three geometrical possibilities, all of them with the photograph placed in vertical position on a special frame, designed taking into account stability, security and no interference with the analysis. In all cases, the photographs were analyzed with the same experimental parameters: 30 kV, 300s, 20  $\mu\text{A}$ , and at 1.5 cm. of distance.

- Configuration "A": The usual disposition for analyses of cultural beings, with X rays irradiates at  $90^\circ$  and the detector placed at  $45^\circ$ , both in relation to the photograph surface. The penetration depth of X-rays is better with this geometry, so it offers information about deep layers. This advantage is not so important for photograph materials, where the information is in some microns of the surface (Figure 1).
- Configuration "B": A second configuration with

the X-ray generator at  $45^\circ$  with respect to the surface of the photograph and  $45^\circ$  with the detector. Considering the solid angle subtended by X-rays, the irradiated area is bigger (Figure 2).

- Configuration "C": A third configuration with X-ray generator at  $90^\circ$  in relation to the detector, both at  $45^\circ$  to the photograph surface (Figure 3).

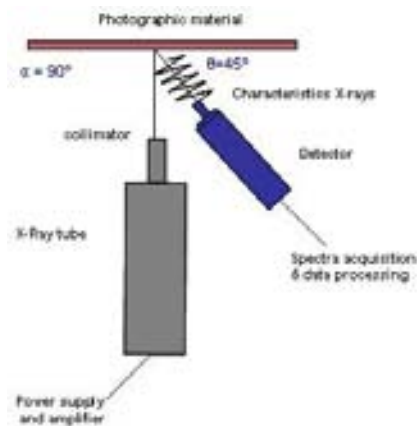


FIGURE 1. Configuration "A"

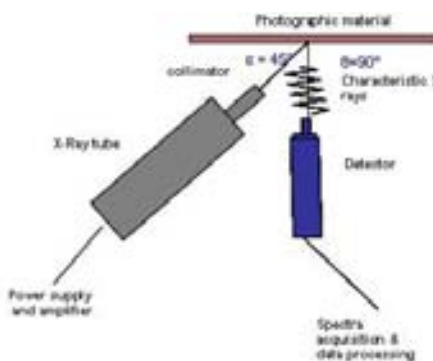


FIGURE 2. Configuration "B"

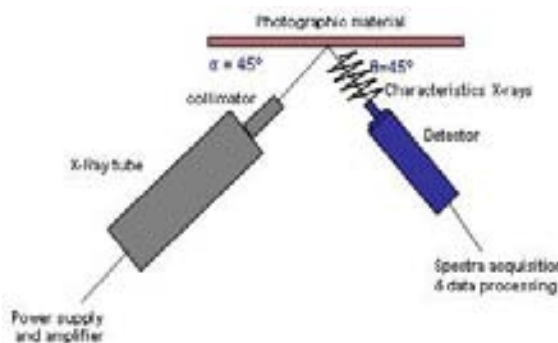


FIGURE 3. Configuration "C"

The spectra obtained with these three geometries, in both sides of glass photographs are represented in Figure 4.

As these results show, there are quite differences with every geometrical disposition. In order to evaluate the results, we consider every element and its net peak area with the standard deviation associated, in both sides of every photograph (Figures 5 and 6).

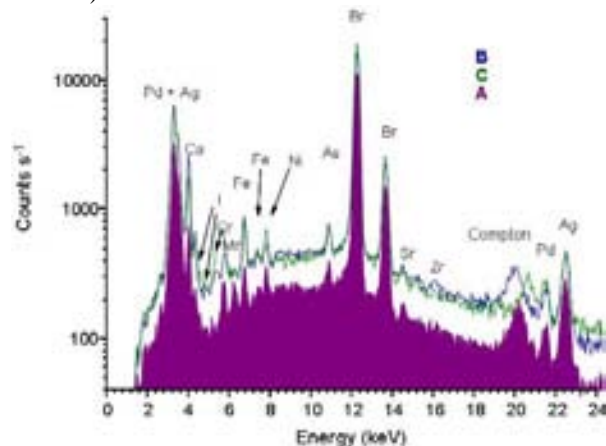


FIGURE 4. X-ray Fluorescence spectra obtained for emulsion in the three geometrical possibilities.

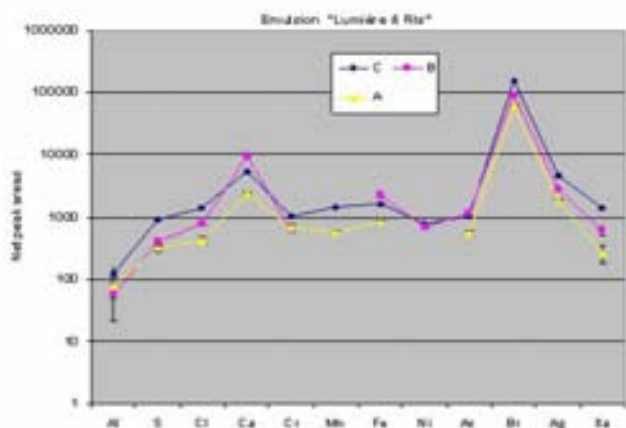


FIGURE 5. Net peak area obtained by the analyses on the emulsion side in each one of the three configurations.

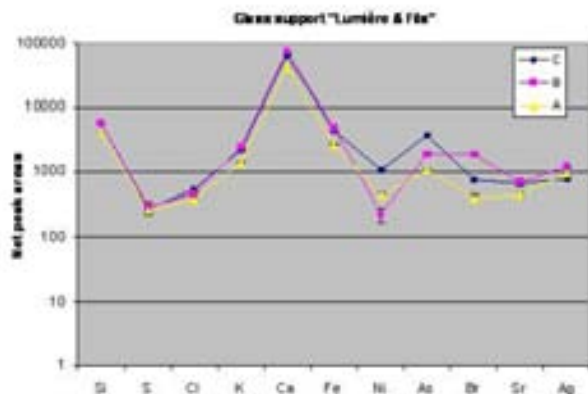


FIGURE 6. Net peak area obtained by the analyses on the glass side in each one of the three configurations.

The number of photons counted is bigger in the C configuration than others two studied possibilities. The standard deviation for each peak obtained is smaller in the C configuration too. This result accords with the Gaussian distribution presented in the spectra. With the A configuration, the spectrometer detects less photons, so the spectra are worse solved and the standard deviation is bigger than the other configuration.

Related to the B configuration, we can observe that the results approach to the C configuration, but there aren't so accurate.

In sum, the peak areas are greater and the standard deviations are lower in configuration "C" than "A" and "B", even if "B" is a nearly approximation.

The exceptions to this general behaviour appear only when the element detected doesn't belong to the layer where the beam comes in. For example, Cl is worse detected by the glass side with configuration "C" than configuration "B". In this situation, the standard deviation is 30%, so too high to consider Cl as a valuable result. The conclusion is that we have analysed the glass face of the photography, and the Cl owns to the emulsion face. The same explanation may be applied for the detection of Br and Ag by the glass side.

Considering the best detection on both sides, we can conclude that the elemental composition of the photographic materials is:

TABLE 1. Glass and emulsion composition obtained from EDXRF spectra.

	Si	S	Cl	K	Ca	Fe	As	Br	Ag	I
Emulsion		•	•		•	•	•	•	•	•
Glass	•			•	•	•	•			

The analyses with SEM-EDX made in some fragments of these photographic plates confirm this interpretation of the results.

In order to interpret these results, the theory of geometry effects was considered [20]. We have selected a source as a disk from the excited area of the photograph and a detector with a circular aperture, a distance  $d$  between detector and source. In all cases, the analyses were in air, the size and distances are the same, the only parameter we could change was the solid angle  $\Omega$  in the geometry. The solid angle subtended by the detector at the location of the source is the fraction of particles emitted by a point isotropic source and entering the detector.

The mathematical expression for  $\Omega$  is:

$$\Omega = \frac{\int_{A_s} \int_{A_d} \left( \frac{S_0 A_s d}{4\pi r^2} \right) A_d d \left( \hat{n} \cdot \frac{\mathbf{r}}{r} \right)}{S_0 A_s}$$

where:

$A_s$ : plane source of area

$S_0$ : particles isotropically emitted by s and  $m^2$

$d$ : distance between detector and source

$A_d$ : detector aperture

$\hat{n}$ : unit vector normal to the surface of the detector aperture

For our experimental configuration, we had a disk source and a detector with a circular aperture (Figure 7) and two different possibilities:

1. Source parallel to the detector

If  $R_d/d$  y  $R_s/d$  are less than 1,

$$\Omega = \frac{\omega^2}{4} \left[ 1 - \frac{3}{4} (\psi^2 + \omega^2) \right] \frac{15}{8} \left( \frac{\psi^4 + \omega^4}{3} + \psi^2 \omega^2 \right) - \frac{\omega^2}{4} \frac{35}{16} \left[ \frac{\psi^6 + \omega^6}{4} + \frac{3}{2} \psi^2 \omega^2 (\psi^2 + \omega^2) \right]$$

where  $\psi = R_s/d$ ,  $\omega = R_d/d$

In our spectrometer, we had as  $R_d$  of 1.2 mm,  $R_s$  of 2.5 mm, resulting 0.34% of particles detected.

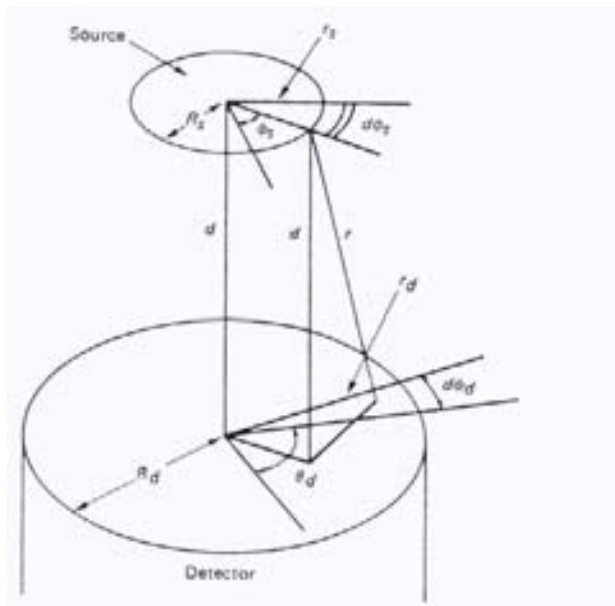


FIGURE 7. A disk source and a detector with a circular aperture [20].

2. Angle  $\theta$  between source and detector

If  $R_d/d$  y  $R_s/d$  are less than 1, and detector and source with an angle  $\theta$ , the solid angle is done by:

$$\Omega = \frac{\omega^2}{4} \left[ 1 - \frac{3}{4} (\psi^2 + \omega^2) \right] + \frac{\omega^2}{4} \frac{15}{8} \left[ \frac{\psi^4 + \omega^4}{3} + \psi^2 \omega^2 + \psi^2 \left( 1 + \frac{1}{4} \omega^2 + \frac{2}{3} \psi^2 \right) \text{sen}^2 \theta \right]$$

where  $\psi = R_s/d$ ,  $\omega = R_d/d$ ,  $\theta = 45^\circ$ , resulting 0.35% of particles detected.

Comparing these results, the augmentation of efficiency by geometrical reasons at  $45^\circ$  between source and detector is a 3%.

As the experimental results showed, the angle between photograph and detector is not the main responsible of the better results. In conclusion, the disposition at  $45^\circ$  between X-ray tube and photograph is the most important condition to obtain better spectra, and this condition is reinforced by an experimental disposition at  $45^\circ$  between detector and photograph, as shown in the Figure 3.

CONCLUSIONS

Different experimental configurations of a portable energy dispersive XRF spectrometer for the investigation of historical photograph have been discussed.

Concerning the characteristics of the selected spectrometer for daily analytical studies of old photographs, special attention was paid to easiness, low cost and portability.

The geometric disposition between x-ray tube, detector and photographic plate, has a direct influence in the effectiveness of the analyses.

It is possible to optimize the results with the choice of a specific geometrical disposition, with  $90^\circ$  between tube and detector and  $45^\circ$  with the plate. It is observed that, for a same material and type of photography, the total of accounts and the rate of count are reduced almost to the half in the "A" disposition, while the "C" and "B" are similar, being always a little greater the "C" one. Besides, in this disposition it is possible a greater approach of the detector to the plate of to 1 cm. of distance.

For all these reasons, it is concluded that the analyses by means of XRF that be carried out of historic photographic plates in glass support offers better results in disposition "C" and to 1 cm. of distance between detector and plate.

XRF offers a unique opportunity for the non-

destructive study of old photographs combining portability and possibilities of optimizing the equipment.

## REFERENCES

1. E.T. Hall, "Some Uses of Physics in Archaeology" in *Year Book of the Physical Society*, London, 1958.
2. E.T. Hall, *Archaeometry*, **3** (1960) 29-35
3. E.T. Hall, M.S. Banks, J.M. Stern, *Archaeometry*, **7** (1964) 84-89.
4. E.T. Hall, F. Schweizer; P.A. Toller, *Archaeometry* **15**, (1973) 53-78.
5. R. Cesareo, G.E. Gigante, P. Canegallo, A. Castellano, J.S. Iwanczyk, A. Dabrowski, *Nucl. Instr. and Meth.*, **A 380**, (1996) 440-445.
6. R. Cesareo, G.E. Gigante, A. Castellano, *Nucl. Instr. and Meth. A* **428**, (1999) 171-181.
7. A. Longoni, C. Fiorini, P. Leutenegger, S. Sciuti, G. Fonterotta, L. Strüder, P. Lechner, *Nucl. Instr. and Meth. A* **409** (1998) 407-409.
8. L. Giuntini, F. Lucarelli, P.A. Mandò, W. Hooper, P.H. Barrer, *Nucl. Instr. and Meth.* **B95**, (1995) 389-392.
9. C. Sistach, "El papel árabe en la Corona de Aragón". *II Congreso Nacional de Historia del Papel en España*. Cuenca. 1997.
10. G.W. Cariveau, M. Séller, *Nucl. Instr. and Meth.* **193** (1982) 297-301.
11. J.L. Ferrero, C. Roldán, C. Vergara, *Caesaraugusta*, **73**, (1997) 273-277.
12. C. Roldán García, J. Sánchez Real, J. Ferrero Calabuig, "Análisis de la composición elemental del papel de las actas municipales del Archivo Histórico de Tarragona. Estudio preliminar", *Actas del IV Congreso nacional de Historia del papel en España*. Córdoba, 28-30 de junio de 2001. pp. 35-41.
13. D. Juanes, "Diseño de sistemas EDXRF para el análisis de bienes del patrimonio histórico-artístico". Ph.D. Thesis, Universidad de Valencia, 2002.
14. J.L. Enyeart, A.B. Anderson, S.J. Perron, D.K. Rollins, Q. Fernando, *History of photography*, **7**, (1983) 99-113.
15. S. Rempel, "Qualitative Energy X-ray Fluorescence Examination of Historic Photographic Artifacts" *Photographic Materials Group Winter meeting of the American Institute for Conservation*, Charleston, S.C., 1986 (private communication).
16. C. McCabe, L.D. Glinsman, *Conservation Research*, (1996) 71-86. *Research Techniques in Photographic Conservation*, Denmark: The Royal Danish Academy of Fine Arts, 1995, pp.31-40.
17. A. Gottlieb, *Journal of the American Institute for Conservation* **34**, **1**, (1995) 11-32.
18. S. Penichon, *Journal of the American Institute for Conservation*, **38**, **2**, (1999) 124-143.
19. Getty Conservation Institute, "Conservation of photographic materials", *GCI Newsletter* **16.2**, (2001).
20. N. Tsoufanidis, *Measurement and detection of radiation*. Teyler & Francis, Washington D.C., 1995.

# **The Daguerreotype under High Magnification: An Ultra-High Resolution SEM Study of a 19<sup>th</sup> Century Daguerreotype's Surface Nanostructure**

Patrick Ravines<sup>1,4</sup>, Anne West<sup>2</sup>, John Minter<sup>3</sup> and Robledo O. Gutierrez Jr.<sup>3</sup>

<sup>1</sup>Ravines Art Conservation, 754 Hillside Avenue, Rochester, New York 14618, USA. e-mail: ravines55@gmail.com

<sup>2</sup>Eastman Kodak Company, (retired), 1999 Lake Avenue, Rochester, NY 14650-2104. USA.

<sup>3</sup>Corporate Engineering & Analytical Science, Eastman Kodak Co., USA..

<sup>4</sup>George Eastman House, 900 East Avenue, Rochester, New York 14607, USA.

**Abstract.** *The daguerreotype, the first viable imaging process developed by Louis-Jacques-Mande Daguerre, presented to the world in Paris in 1839, gave birth to photography and started the imaging revolution. The daguerreotype, unlike other silver-based black and white photographic processes, is a single and unique image that rests on the surface of a silvered copper plate. In this state the surface image particles are highly susceptible to mechanical and physical damage. The gilding step introduced by Armand Hippolyte Louis Fizeau in 1840, affixes image particles to the plate and enhances the image, became an integral part of the process and presumably coated the surface with a thin gold film. Despite this improvement, tarnishing has plagued daguerreotypes and been documented since the beginning and many cleaning methods developed to counter this. If the surface has been coated with gold, a noble metal, why then do daguerreotypes show tarnish colors ranging from light brown-yellows to browns to dark blue blacks? This is the area of our exploration and this work presents an electron microscopic study of a 19<sup>th</sup> century daguerreotype using a state of the art ultra-high resolution scanning electron microscope with magnifications ranging from 100,000 to 250,00x, to corroborate the metallurgical nature of the silver mercury amalgam image particles and demonstrate the nano-texture characteristics of the background surface. The daguerreotype investigated shows the nano-textured gold-capped silver nodules ranging in size in the tens of nanometers and smaller narrower nodule boundary regions. The ungilded nodule boundary regions expose silver metal to atmospheric contaminants thereby allowing tarnish to develop. The nano-texture features of the background surface provide information that potentially explains the occurrence of tarnish as corrosion in the inter-nodular regions on gilded daguerreotype surfaces.*

**Keywords:** daguerreotype, early photography, silver surface nodules, nano-structured surface, ultra-high resolution SEM.

## **INTRODUCTION**

The daguerreotype the earliest form of practical photography developed by Louis-Jacques-Mandé Daguerre (1787–1851) in Paris presented his invention

to the world in 1839. It rapidly spread to England and America, resulting in millions being produced during its heyday period between 1839 and 1860. This first imaging system realized the full potential of the photograph in its remarkable resolution and dynamic

range. Because each plate is a unique object that is labor intensive and technically difficult to make, its dominant period was short-lived as it was replaced by other less expensive photographic systems. Today the daguerreotype is increasingly treasured for its fine art and artefactual value as well as its documentary potential.

The daguerreotype is unique among photographic systems and presents a significant preservation challenge to museums, libraries and archives. The chemistry, physics and material science of the daguerreotype, the precise make-up of the ultra-fine structure of the image, and image-altering deterioration mechanisms have not been fully studied. Environmental conditions, contaminants and pollutants, and physical interaction can severely damage the delicate image structure. From their inception, various restorative chemical treatments have been applied to regenerate the daguerreotype image. However, there has been no comprehensive scientific evaluation of the effects of these treatments on the image structure. This study presents the use of modern ultra-high resolution electron microscopy imaging technologies to examine an historic example of the first imaging system - a daguerreotype from ca. 1850s.

Briefly, the photographic process presented in 1839 by Daguerre involved the following steps:

1. A silver plated or clad copper plate is polished to a mirror finish.
2. The plate is fumed with iodine vapors to produce a light-sensitive silver iodide layer.
3. The sensitized plate is exposed to an image in a camera.
4. The image is developed by exposing it to mercury vapors.
5. The remaining un-reacted silver iodide is removed with hypo (sodium thiosulphate).

At this point, the daguerreotype dark and shadow areas are bare polished and etched silver plate, and the grey areas and bright highlight areas are composed of silver-mercury amalgam image particles 'resting' on the surface directly proportional to the reduced silver of the latent image. This delicate surface arrangement of image particles could easily be physically disturbed. 'Gilding' was introduced by Armand Hippolyte Louis Fizeau (1819–1896) in 1840: the electrochemical deposition of gold on the silver surface from a gold-chloride-thiosulfate solution which is often locally heated. Gilding affixed the silver-mercury amalgam image particles to the surface, and made the highlights appear whiter and the shadow areas seem darker [1]. These two gilding features ensured its inclusion as the sixth essential step in the daguerreotype making process. The full nature of the image is the result of the complex interaction of surrounding illumination, surface optics (reflective properties) and surface geometry/topography [2]. The daguerreotype image results from minute image particles that are dispersed

over a polished silver plate. Their distribution is directly related to light exposure implying that white looking areas have higher concentrations of particles and dark areas have few to none [3]. Barger and White [4] have described the interaction of light with the daguerreotype surface.

Even after gilding daguerreotypes still tarnish with colors ranging from light brown-yellows to browns to dark blue blacks, and this has been observed and recorded since their inception. Tarnishing should not be occurring if the surface has been electrochemically coated with a thin film of gold, a noble metal. Earliest electron microscopy studies explained how light interacts with the daguerreotype surface to yield an image, image particle composition, estimates of gold film thickness, chemical composition of tarnish, and removal approaches [4,5]. The genesis and ubiquitous nature of tarnish development on the surface of daguerreotypes is not broached. This paper presents an electron microscopic study of a 19<sup>th</sup> century daguerreotype using a state of the art ultra-high resolution scanning electron microscope with magnifications ranging from 20,000 to 250,00x, to corroborate the metallurgical nature of the silver mercury amalgam image particles, and demonstrate the nano-texture characteristics of the background surface and that of the image particles.



**FIGURE 1.** Daguerreotype of an unidentified man from circa 1850s. Areas examined at high magnifications are the dark jacket lapel (Area 1) shown by the white arrow and the white shirt highlight area (Area 2) next to it.

## EXPERIMENTAL APPROACH & SAMPLE

The electron microscope used in this study was an FEI Sirion 400NC field-emission scanning electron microscope. The daguerreotype was imaged at 2 kV and 5 kV in "ultra-high resolution" (UHR) mode with the sample within 5 mm of the lens to enable the use of the "through-the-lens" detector using both secondary electrons and backscattered electrons.

During the heyday of daguerreotypes from 1839 to 1860, they were made available in standard sizes ranging from whole plates measuring 6.5 x 8.5 inches<sup>2</sup>/16.5 x 21.5 cm<sup>2</sup>, half plates of 4.25 x 5.5 inches<sup>2</sup>/11 x 14 cm<sup>2</sup>, quarter plates of 3.25 x 4.25 inches<sup>2</sup>/8 x 11 cm<sup>2</sup>, 6<sup>th</sup> plates 2.75 x 3.25 inches<sup>2</sup>/7 x 8 cm<sup>2</sup>, 9<sup>th</sup> plates of 2 x 2.5 inches<sup>2</sup>/5 x 6 cm<sup>2</sup> to the smallest 16<sup>th</sup> plates of 1.375 x 1.625 inches<sup>2</sup>/3.5 x 4 cm<sup>2</sup>. The daguerreotype used in this study is a small 9<sup>th</sup> plate of an unidentified man taken by an unidentified photographer circa 1850s from the collection of P. Ravines, Figure 1. The two areas examined are in the center of the 9<sup>th</sup> plate since it appears there is little to no tarnishing: Area 1, the left dark jacket lapel area indicated by the white arrow, and Area 2, the white shirt highlight area next to the jacket area.

## RESULTS & DISCUSSION

### Dark or Shadow Area of the Daguerreotype

The dark central areas of the jacket's left lapel chosen for examination have few to no image particles and allowed for the observation of the background without the potential interference of image particles. Additionally, the center areas avoided heavily tarnished areas, which appear more on the borders and edges of the daguerreotype plate since when stored in their cases or boxes, these areas are the first to come into contact with environmental factors. Images of the lapel area of the daguerreotype are shown in Figures 2, 3 and 4.

Figures 2 and 3 of the dark left lapel area show, as expected, that there are not many image particles present. As mentioned earlier, the daguerreotype image is a result of sub-micrometer and nanometer-sized image particles dispersed over a polished silver plate that scatter light, and their distribution is directly related to light exposure implying that white looking areas have higher concentrations of particles and dark areas have few to none. Their size at 20,000x magnification, Figure 2, allows for an overall view of the studied area. It shows about a dozen image particles, one large platelet-like particle in the left

center area and a sea of small whitish particles peppers the field of view. Not much more can be clearly observed or identified at this magnification. Increasing the magnification to 50,000x, Figure 3, shows more: three spheroidal and/or hexagonal-shaped image particles, the considerably smaller whitish particles, and the dark background area appears to have a fine texture not previously noticeable at 20,000x.

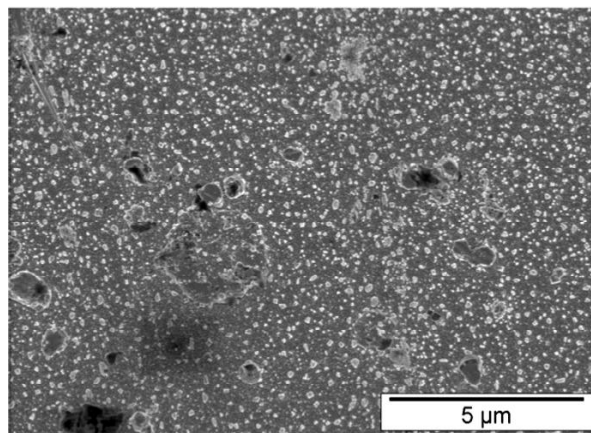


**FIGURE 2.** Electron micrograph of the dark left lapel area. Imaging conditions: Voltage 5 kV; Magnification 20,000x; SE; Working distance 5mm.

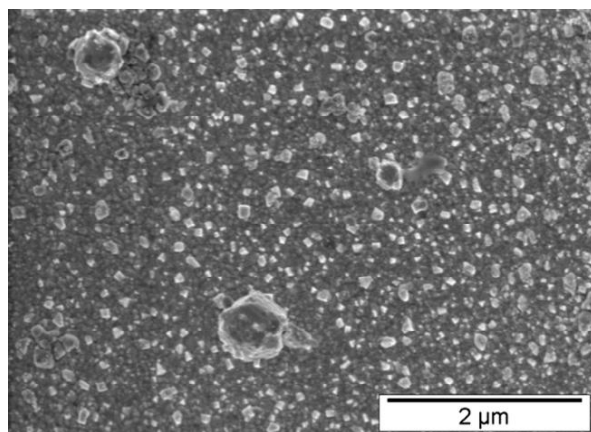


**FIGURE 3.** Electron micrograph of the dark left lapel area. Imaging conditions: Voltage 5 kV; Magnification 50,000x; SE; Working distance 5mm.

Figure 4 shows the left lapel background area imaged with both secondary and back scattered electrons at a magnification of 200,000x. Several notable daguerreotype nano-sized surface features are observed for the first time:

1. The lighter areas are likely to be raised areas of the surface silver nodules where gold was electrochemically deposited during the sixth and final gilding step;

2. The darker areas surrounding the lighter gold areas are boundary regions between silver nodules, which have an overall reticulated/network look, and expose silver metal to environmental conditions of relative humidity, air and gaseous pollutants; and
3. The small whitish angular particles may be classified as cubic crystallites emanating from the exposed silver nodule boundary regions and are likely to be silver corrosion or tarnish compounds such as silver chloride and silver oxide salts, both body centered cubic. It is surprising to observe at high magnifications such corrosion products in an area that to the naked eye does not appear to have been affected by tarnish. This implies that corrosion products are already developing and accumulating at the nano-scale level well before becoming observable to human vision.

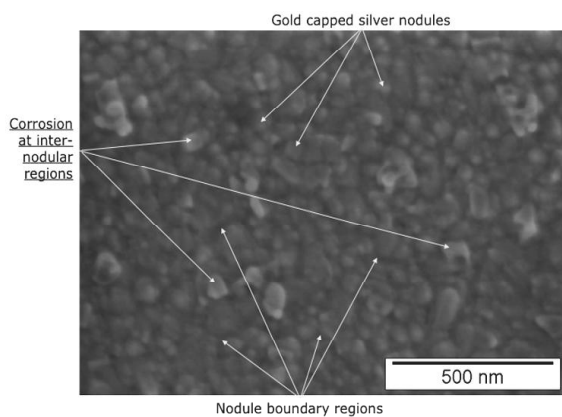


**FIGURE 4.** Electron micrograph of the dark left lapel area. Imaging conditions: Voltage 2 kV; Mag 200,000x; SE & BSE; Working distance 5mm.

This portion of the study used voltage settings of 5kV and a few of 2kV with magnifications up to 200,000x. These voltages are low in comparison to the early electron microscopy daguerreotype studies of Swan et al. [5] and Barger and co-workers in the 1980s, summarized in Barger and White [4], where voltages ranging from 20 to 40kV were used. Magnifications at the time were also low and did not exceed 10,000x due to instrumental limitations. Such high voltages and low magnifications provided combined surface and meso/sub surface data obfuscating the true nature of the surface. By using lower voltages there is a considerable decrease in the interaction volume of the impinging electron beam with the materials being investigated thereby yielding greater surface feature details, which are clearly observed in Figure 4.

## Shirt Highlight Area of the Daguerreotype

The unidentified man's white shirt is the brightest and whitest area on the daguerreotype and is also referred to as a highlight area. This highlight has been studied at several magnifications ranging from 20,000x and 100,000x to 250,000x, Figures 5, 6 and 7. As with the jacket area, the central location of the white shirt area was selected to avoid tarnished areas.

The bright white shirt highlight area imaged at a magnification of 20,000x, Figure 5, shows an area replete with geometrical shaped particles on the surface. At this magnification the hexagonal shape of the particles is readily noticeable. Our perception of the appearance of the daguerreotype white shirt is due to light being scattered by high concentration of these geometrically shaped image particles ranging in size from 200 nm to 800 nm [4].

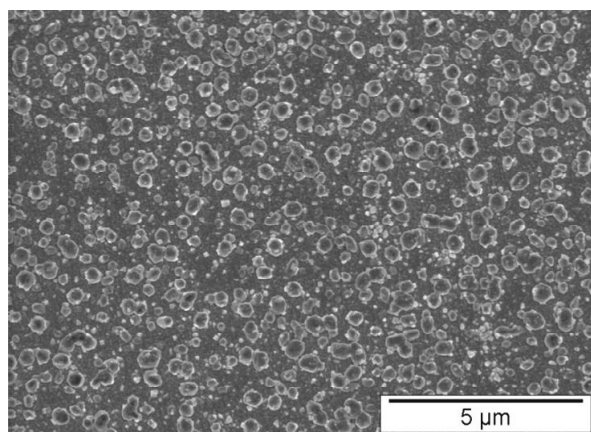


**FIGURE 5.** Electron micrograph of the white shirt highlight area. Imaging conditions: Voltage 5 kV; Mag 20,000x; SE; Working distance 5mm.

Figures 6 and 7 show the highlight areas imaged at magnifications of 100,000x and 250,000x. At these high magnification the hexagonal shapes of the image particles are clearly delineated and the particles also show they are composed of stacked layers. The hexagonal shape and stacking is an indication of the silver mercury amalgam type and crystal growth patterns. According to Barger and White [4], these are hexagonal close packed  $\epsilon$  (epsilon) amalgams with the chemical composition of  $\text{Ag}_{11}\text{Hg}_9$ .

As would have been expected, the background surface the image particles are on shows the same nano-textured surface features observed in the dark jacket lapel area. The background nano-textured surface features appear to be the same throughout the daguerreotype plate areas of white and dark. Both figures also show the cubic crystallites silver corrosion salts growing out from the inter-nodular boundary regions on the background surface. The top center area

of Figure 7 demonstrates with great clarity the cubic nature of the crystallites.

Interestingly, the 250,000x magnification of Figure 7 shows that the image particles themselves appear to have an even finer nano-textured surface than that of the background surface and, additionally, that these also have corrosion particles on them. There are globular and cubic corrosion particles on the image particle surfaces. The cubic corrosion particles are likely to be of similar chemical composition to the background area cubic crystallites. This is the first time globular corrosion particles have been observed. Since they are on silver mercury amalgam image particles they could well be mercury compounds. The globular particles are well demonstrated in the two adjoining hexagonal image particles in the left half of Figure 7, and a cubic crystallite resides on the top right image particle.

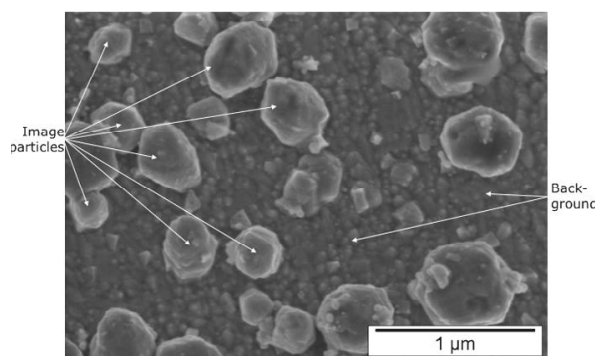


**FIGURE 6.** Electron micrograph of the white shirt highlight area. Imaging conditions: Voltage 5 kV; Mag 100,000x; SE; Working distance 5mm.

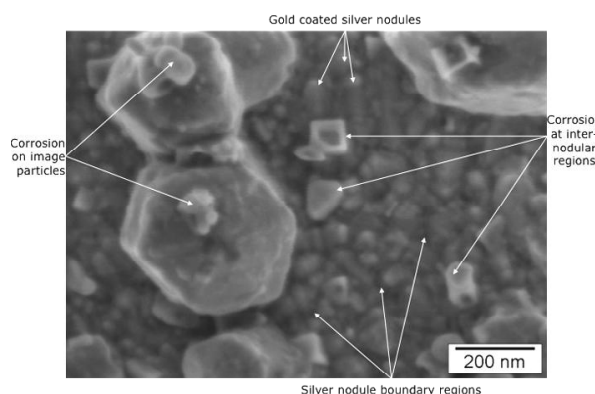


**FIGURE 7.** Electron micrograph of the white shirt highlight area. Imaging conditions: Voltage 2 kV; Mag 250,000x; SE & BSE; Working distance 5mm.

## CONCLUSIONS / SUMMARY

The use of a field emission SEM with low kilovoltage settings with high magnifications has allowed us to examine the nano-textured nature of the daguerreotype surface. Two types of nano-textures appear to exist: the background surface differs from that of the image particle surface. The background surface appears to be composed of silver nodules with their tops covered with gold, similar to snow capped mountains. The gold does not completely cover the silver nodules and the area between silver nodules or silver nodule boundary regions are exposed silver metal, akin to verdant valleys devoid of snow. The exposed silver metal at the nodule boundary regions is in contact with the local gaseous environment – air and pollutants - allowing for growth of inter-nodular cubic crystallite corrosion compounds. In this case, the likely body centered cubic corrosion candidates are  $\text{AgCl}$  &  $\text{Ag}_2\text{O}$ .

The nano-textured gilded background surface is the result of plate preparation. The first step is polishing the silver clad copper plate to a mirror finish followed by exposure with iodine and bromine gases to generate a thin film of silver iodide and silver bromide light sensitive salts. After plate exposure to light and mercury development, the remaining un-reacted silver halide salts are removed using ‘hypo’, a sodium thiosulfate solution, leaving an etched nano-textured background silver nodule surface. The final gilding step – electrochemical deposition of gold with a low concentration gold chloride thiosulfate solution – does not cover the entire silver surface. Gold appears to only coat and cover the tops of silver nodules.

The hexagonal image particles on the background surface appear to have a finer nano-textured surface as well as accompanying corrosion products. The finer nano-texture on the image particle is likely to be representative of the silver mercury  $\epsilon$  (epsilon) amalgam. The gold deposited on image particles during electrochemical gilding is also apparently not enough to completely coat and cover them. Areas gold has not coated expose silver mercury amalgam to air and gaseous components that interact with the environment to yield globular and cubic shaped silver and mercury corrosion products.

This renewed approach to the study of the daguerreotype surface is beginning to shed new light on many questions regarding the nature of the daguerreotype and its tarnishing reactions with its local environment. It has also corroborated Swan et al. [5] and Barger and White’s [4] description of the metallurgical nature of the partially gold-coated silver mercury amalgam image particles.

## ACKNOWLEDGMENTS

P. Ravines acknowledges Ralph Wiegandt, Project Conservator, Kay Whitmore Conservation Center, George Eastman House International Museum of Photography & Film, and Richard Hailstone, Associate Professor, Chester F. Carlson Center for Imaging Science, Rochester Institute of Technology.

## REFERENCES

1. A.H.L. Fizeau, Notes sur un moyen de fixer les images photographiques. *Comptes Rendus hebdomadaires des séances de l'academie des sciences*, 11 (1841) 237-238.
2. I. Motoyoshi, S. Nishida, L. Sharan, E.H. Adelson, *Nature*, 447 (2007) 206-209.
3. S. Barger, R. Messier, W. White, *Studies in Conservation* 29 (1984) 84-86.
4. S. Barger, W. White, *The daguerreotype: 19<sup>th</sup> century and modern science*. Smithsonian Institution Press & John Hopkins University Press, Washington, D.C., 1991, 117-134.
5. A. Swan, C.E. Fiori, K.J. Heinrich, Daguerreotypes: A study of the plates and the process. *Scanning Electron Microscopy* 1 (1979) 411-423.

## ***Nerita* Shell Objects in the Offerings of the Great Temple of Tenochtitlan**

A. Velázquez-Castro<sup>1</sup>, B. Zúñiga-Arellano<sup>2</sup> and Á. González-López<sup>2</sup>

<sup>1</sup> Museo del Templo Mayor, Instituto Nacional de Antropología e Historia, INAH. Seminario 8, Centro Histórico, México D.F. 06060, MEXICO. e-mail: adrianveca@yahoo.com

<sup>2</sup> Proyecto Templo Mayor, INAH, MEXICO.

**Abstract.** In the recent excavations of the Great Temple of Tenochtitlan a huge offering was found, which number is 126. Inside of this offering twelve *Nerita scabricosta* was found, which present traces of human work; this finding represent special interest as objects similar to these have not been previously found in Tenochtitlan or other Mesoamerican site. In the present paper the results of the technological analyses made to these objects are presented, which are made due work traces analyses using Scanning Electron Microscopy (SEM). A comparison with other shell objects made in similar species to *Nerita scabricosta* found previously in Tenochca offerings, as *Polinices lacteus* and *Neritina virginea*, is also presented in order to understand if this new findings correspond to the tenochca technological tradition of manufacturing shell objects.

**Keywords:** Tenochtitlan, Shell, *Nerita*, Offerings, Mesoamerica, SEM, Technology.

### **INTRODUCTION**

Pendants made from mollusks shell were very important ritual objects. Made of different species of snails, they were used by various deities, as we can see in paintings and sculptures of different times and regions; these objects have been found inside of burials as well as cache offerings.

1337 shell pendants and 162 fragments have been found until now in the excavations carried out in the sacred precinct of Tenochtitlan [1], the capital of the most powerful Mesoamerican empire of the period known as Late Postclassic (1325-1521). The families and genus used to make these pieces are Columbelloidea *Agaronia*, *Cassis*, *Conus*, *Marginella*, *Natica*, *Neritina*, *Oliva*, *Olivella* and *Polinices*. Nevertheless, in excavations made recently by Proyecto Templo Mayor seven singular shell pendants were found (Figure 1). They are made of *Nerita scabricosta*, a Panamic species that live in the Pacific

shore of the American Continent, from the Baja California Peninsula to the north of Peru. The shell of these snails is globose with rough-surfaced, strong spiral cords. In the case of the archaeological pieces the surface of the shells were abraded, maybe to even it, and polished as they present exceptional brilliance. Six pieces present irregular perforations made also by abrasion, in the ventral part of the shell, close to the umbilicus. One has a circular cutting in the same place. Other six shells of *Nerita scabricosta* were just abraded in their surfaces and polished, and no perforations were made on them.

These objects were found in offering number 126 which was buried at the front of the stairway of the 6<sup>th</sup> constructive stage of the Great Temple of Tenochtitlan, at the joint of the temples of the gods Tlaloc and Huitzilopochtli. This offering was placed approximately two meters below the sculpture of the goddess Tlaltecuhli, inside of the larger cist found until now in the sacred precinct of Tenochtitlan. The

*Nerita* shell pendants were found in the upper levels of the offering, close to its western wall, on bones of vertebrate animals and among other marine materials. In the presents paper the technology used to make the *Nerita scabricosta* shell pendants is analyzed; the results are compared with similar ornaments previously found in Tenochca offerings. On these basis the possible origins of the objects are discussed.

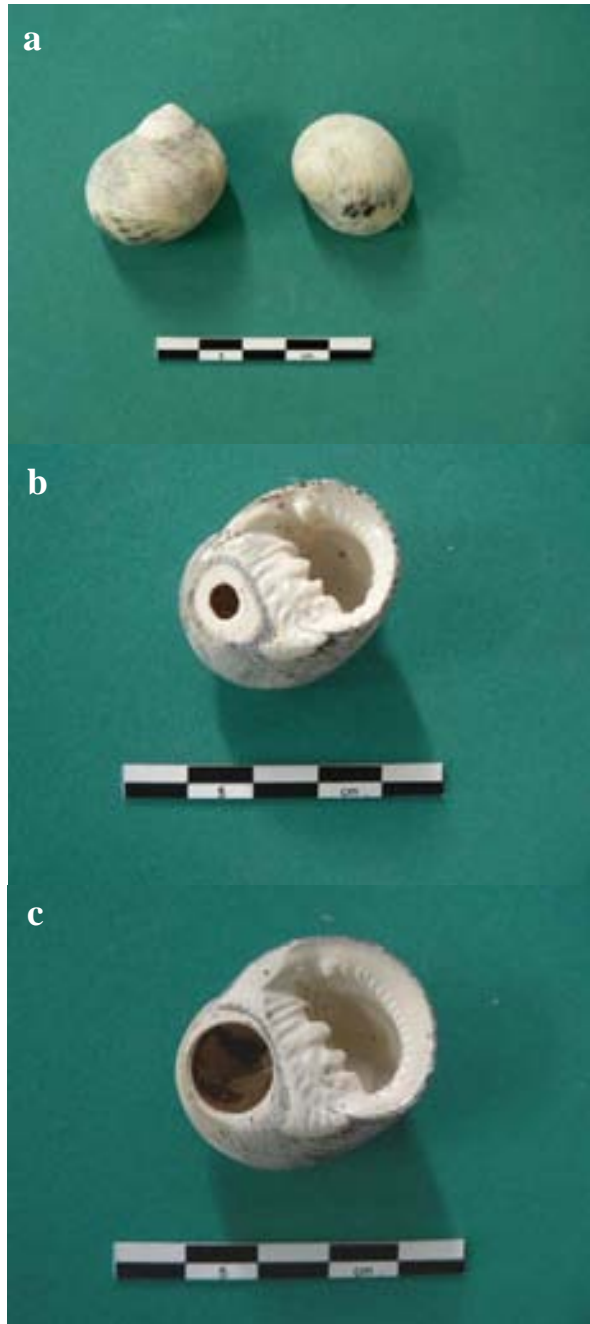


**FIGURE 1.** *Nerita* shell pendants a) view of surface polished, b) view of irregular perforation, c) view of circular cutting.

## MATERIALS AND METHODS

The biological identification of the shells were made using specialized bibliography [2-3]. The technological analyses were made in the project “Técnicas de manufactura de los objetos de concha del México prehispánico” [4]. In this Project the modification used to make shell objects are replicated experimentally using the techniques and tools supposed to be used in Pre-hispanic times. The way of testing the technological hypothesis is analyzing the traces led by experimental processes and comparing them with the archaeological ones. This is made by simple sight observation, stereoscopic microscopy at low amplifications (10X, 20X, 30X and 40X) and Scanning Electron Microscopy (SEM), being the latest one the best for this studies, as it is an ideal technique for the analyses of the surface characteristic of materials. To observe the technological traces by SEM, replicas of them are made in polymer resin softened with acetone, which are pressed against the part of the object to be analyzed. Then the samples are covered with gold ions which allow its observation in high vacuum mode. The samples are observed with the following conditions: high vacuum mode, 20 kV of power, a 42 beam aperture, secondary electrons signal (SEI) and a distance of 10 mm. Four amplifications of each sample are taken systematically at 100X, 300X, 600X and 1000X.

The *Nerita scabricosta* shell pendants were observed using stereoscopic microscopy at low amplifications. This allowed to select the better preserved exemplars to make replicas of its modifications. The images obtained by SEM were compared with the experimental data of the project as well as with images of other tenochca snail shell pendants, which also present the irregular perforations made by abrasion.

The other snail shell pendants were two *Polinices* from offering 83, IVb construction stage (1469-1481); two *Neritina* from offering 95, constructive stage IVb; four *Olivella* from offerings 6, 11, 13 and 57, the two first from constructive stage IVb and the latest ones from VII constructive stage (1502-1520).

## RESULTS

The low amplifications observations allowed observing fine straight lines on the surfaces of *Nerita scabricosta* objects, while these same traces were larger in the perforations; this confirmed the hypothesis that in addition to the abrasion of the surfaces of the shells in order to even them, a polished was applied. The concentric lines observed in the circular cutting of one piece indicate the use of a lithic tool.

SEM observations allowed getting the following results:

**Perforations**

Very fine lines 3 microns wide were observed which intercrosses each other to produce a textured surface. This is very similar to the traces produced by abrasion using sandstone tools (figures 2 and 3).

**Surfaces**

Fine lines 0.6 to 2.8 microns are observed which sometimes intercrosses producing a reticulated surface. These traces are identical to the ones produced by polishing using chert nodules (figures 4 and 5).

**Circular cutting**

At lager amplifications lines 3 to 4 microns wide are observed, which can run parallel to form wider traces or intercross with each other to produce a textured surface. These traces are similar to the ones produced by drilling with chert tools (figures 6 and 7).

In relation to the other snail shell pendants, all of them show traces of the use of sandstone tools to make their irregular perforations (figure 8).

**DISCUSSION**

It is surprising the use of sandstone the manufacture the *Nerita scabricosta* pendants, as the technological style for the manufacture of tenochca shell objects has been defined by the use of basalt stone tools to abrade, obsidian implements to cut and chert tools to drill [4]; very few pieces show polishing. This idea is supported by the great standardization and exclusiveness of the pieces many of which are just found in the offerings of the Great Temple of Tenochtitlan, being absent in the other buildings of the Sacred Precinct and in other sites of Mesoamerica. A different situation is found in *Oliva* shell pendants which relative heterogeneity can be explained by the existence of different productive groups; it has even been proposed that some of these objects got Tenochtitlan by tribute or long distance exchange.

It is interesting that the group of shell pendants analyzed in this work is completely different from what was known about the tenochca shell production, and that they form a unity through the time, from constructive stages IVb to VII. It can be inferred that the productive groups that made them were different from the ones that made *Pinctada mazatlanica* pieces, but the same through the time. It can be Hypothesized that they are foreign productions as sandstone, as far as is known, were not part of the technological traditions of Central Mexico [5].

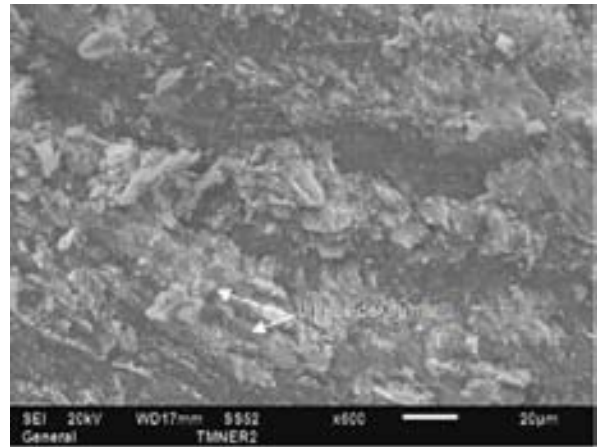


FIGURE 2. Perforation of archaeological *Nerita* shell pendant 126-563 (600X).

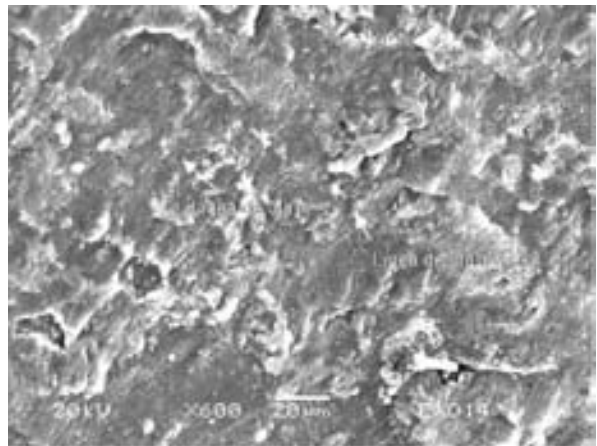


FIGURE 3. Experimental abrasion with sandstone in *Oliva* shell (600X).

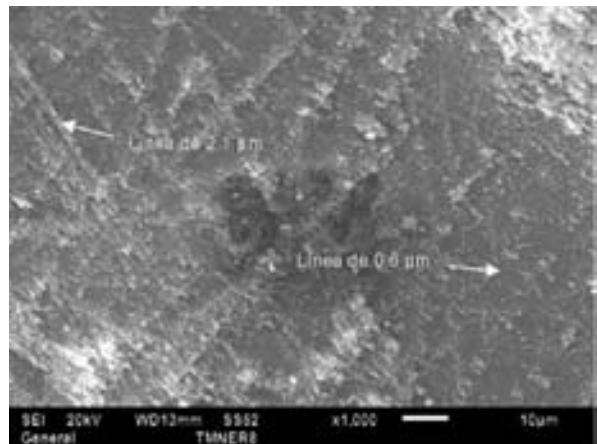
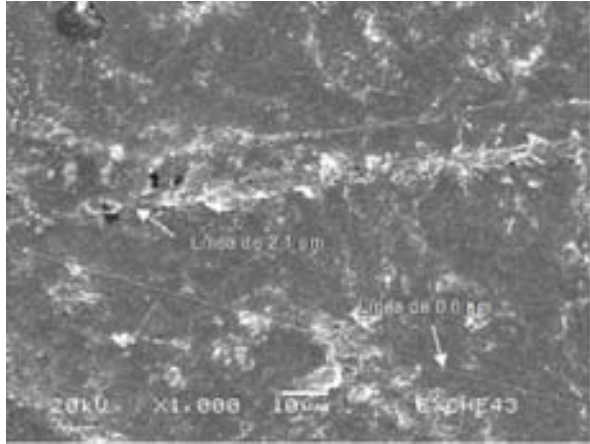
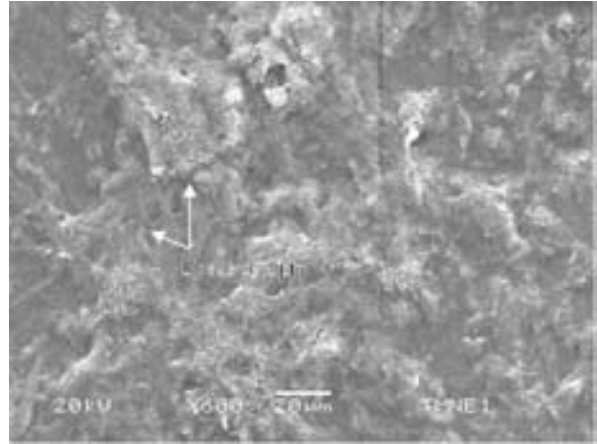


FIGURE 4. Surface of archaeological *Nerita* shell pendant 126-265 (1000X).



**FIGURE 5.** *Chama echinata* shell polished with chert nodules (1000X).



**FIGURE 8.** Work traces in the perforation of a *Neritina* shell pendant from offering 95, Great Temple of Tenochtitlan (600X).

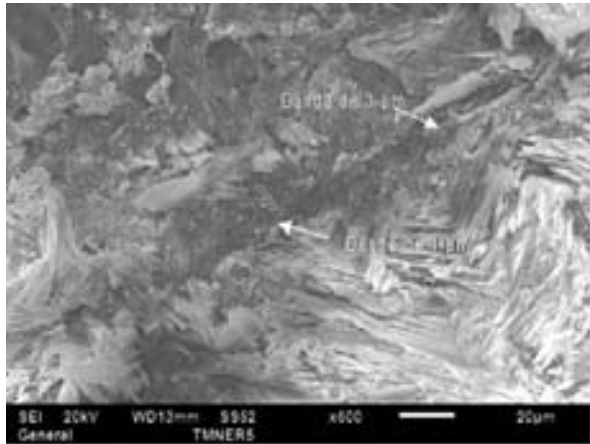


**FIGURE 6.** Work traces in the circular cutting of the archaeological *Nerita* shell pendant 126-476 (600X).

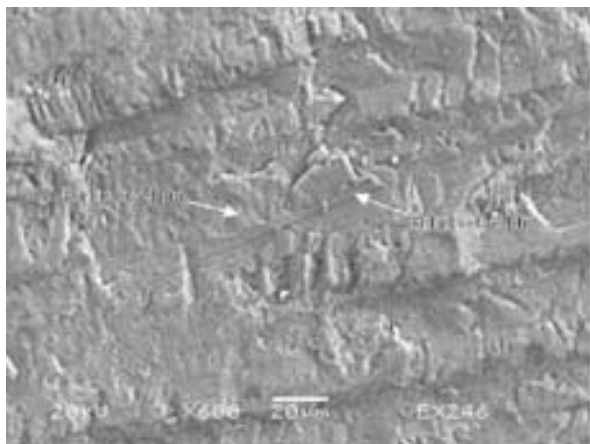


**FIGURE 7.** Work traces experimentally produced by drilling with chert perforator in *Polinices* shell (600X).

In this context it is interesting the finding of six *Olivella volutella* pendants in the Postclassic site of Tancama, Querétaro, which are identical to similar objects found in the offerings of the Great Temple of Tenochtitlan. Even more interesting is that through the technological analyzes of these piece it was known that sandstone was used to make them [6]. Several cultural traces of Tancama suggest a Huastec affiliation. It is worth remembering that the Huastec area was conquered by Moctezuma I to whom it is attributed the IV constructive stage. On this basis, could it be proposed that some of the shell objects that have appeared in the tenochca offerings were foreign productions, maybe from the Huastec area?

## ACKNOWLEDGMENTS

We want to thank Dr. Leonardo López Luján, Museo del Templo Mayor; Demetro Mendoza Anaya and Manuel Espinoza Pesqueira, Instituto Nacional de Investigaciones Nucleares; José Antonio Alva Medina, Instituto Nacional de Antropología e Historia; Valles de la Sierra Gorda Queretana Project, and Técnicas de Manufactura de los objetos de concha del México prehispánico Project.

## REFERENCES

1. A. Velázquez-Castro, *Tipología de los objetos de concha del Templo Mayor de Tenochtitlan*, INAH, México, 1999.
2. M. Keen, *Sea shells of Tropical West America*, Stanford University Press, Stanford, 1971.

3. T. Abbott, *American Seashells*, Van Nostrand Reinhold Company, New York, 1974.
4. A. Velázquez-Castro, *La producción especializada de los objetos de concha del Templo Mayor de Tenochtitlan*, INAH, México, 2007.
5. A. Velázquez-Castro, “Las tradiciones del trabajo de la concha en el Centro de México”, paper presented at 52 International Conference of Americanists, Sevilla, Spain, 2006.
6. D. Juárez, J. Quiróz, S. Romero, J. Bastida, G. Páez, A. Martínez, A. Velázquez, N. Valentín, B. Zúñiga, “Aproximación a un ritual funerario en Tancama: El entierro 1 del edificio 1”, paper presented at X Congreso Internacional Salud Enfermedad, de la Prehistoria al Siglo XXI, México, D.F, 2008.

## **Manufacture of *Spondylus princeps* Objects in Calica, Quintana Roo, Mexico**

E.A. Castillo Velasco and S.A. Páez Torres

*Dirección de Estudios Arqueológicos, Instituto Nacional de Antropología e Historia INAH,  
Lic. Primo de Verdad No. 3, Col. Centro, México D.F. C.P. 06010, MEXICO.  
e-mail: eacastillovelasco@gmail.com*

**Abstract.** Calica is an archaeological site located on the east coast of Quintana Roo in Cozumel. The Calica project found materials belonging to two different stages of occupation; the earliest one, during Late Formative and Early Classic periods, and the second in the late Postclassic period. Calica has an important collection of objects made with different seashell species. The ornamental objects of *Spondylus princeps* are the most representative ones with 435 artifacts. These are divided in beads, pendants, incrustations and pectorals. With the objective of knowing how and where the objects of *Spondylus princeps* were manufactured, the project "Materiales conchológicos del Complejo Calica, Quintana Roo" compares manufacture marks found on real pre-Hispanic objects with those produced on experimental pieces using an Scanning Electron Microscope (SEM). First we took using soft polymers on the artifacts surfaces, incisions and cuttings of the selected objects; then, we looked them through a SEM in four orders of magnitude (100X, 300X, 600X and 1000X). Finally, lines and bands on images are measured to recognize special marks of each tool and method. Analyses of the manufacture marks permit to recognize tools and methods used in order to identify if the production industry is whether local or foreign. In this project a representative corpus of artifacts was selected, including Formative, Classic and Postclassical objects to identify changes or continuity between chronological periods. The first results show that the marks observed in the objects correspond to limestone and flint for both stage periods.

**Keywords:** Seashell, *Spondylus princeps*, Calica, Manufacture, SEM.

### **INTRODUCTION**

Calica is a coastal site located in the municipality of Cozumel to the North area of the state of Quintana Roo, Mexico, at 8 km South of Playa del Carmen.

This site has a sequence of prolonged occupation began in the Middle Pre-Classic period between 400 or 300 BC. During the periods known as Superior Pre-Classic and Early Classic (150 BC and 300 AD) there was an increase in the population that was reflected in the architecture development; later there was an abandon in most of the ceremonial and residential groups. Later, there was again an increase in the

population in the Early Postclassic period (1000 - 1200 A.D.) having a new peak during the Late Postclassic period (1250-1450 AD). [1-2]

On the site, it was recovered a large collection of shell objects, utilitarian, votive and ornamental, related times of peak and apogee. The most abundant are the ornamental use, highlighting the objects made of *Spondylus princeps*, which are related to the contexts of the elite groups of Calica.

The research Project "Materiales conchológicos del complejo Calica. Un análisis morfofuncional", carried out analysis of the techniques of elaboration and equipment used, by studying the traces of manufacturing. One of the objectives is whether there

is continuity over time given the hiatus that occurs at the site during the Classic period. For this purpose, surface traces and perforations from objects made of *Spondylus princeps* corresponding to the two stages of occupation on the site were stamped on polymers. The marks were observed microscopically with scanning electron microscope (SEM) and compared with marks obtained experimentally in the workshop "Técnicas de manufactura de los objetos de concha del México prehispánico", directed by Dr. Adrián Velazquez Castro.



**FIGURE 1.** Structure from Superior Preclassic period of Calica, Quintana Roo.



**FIGURE 2.** "La Casa Azul", sanctuary built in the Late Postclassic period.

### MATERIALS AND METHODS

The objects in the collection were analyzed biological and typologically. From biological identification 67 marine species were recognized; 65 species belong to the Caribbean area and two of the Panamic area (*Pleuroploca princeps* and *Spondylus princeps*).

Typological analysis classified the objects according to their use in votive, utilitarian or ornamental. Ornamental objects represent the largest

percentage of the collection with 52 %, 309 pieces correspond to the first stage of occupation (Late Preclassic-Early Classic period) [3] and 154 artifacts are from Late Postclassic period [4].

The 39 % of ornamental objects were made of *Spondylus princeps* which gives them a special value as a foreign species that had to be transported from the Pacific coast; these objects are associated with ceremonial structures and elite housing of Calica. For these reasons, the objects made of *Spondylus princeps* can address different topics of research about the site.



**FIGURE 3.** Ornamental objects of *Spondylus princeps* of the Late Pre-Classic period.



**FIGURE 4.** Ornamental objects of *Spondylus princeps* of the Late Post-Classic.

The project developed by this investigation set out the technological study of shell objects and seeks to recognize the procedures and tools used in the manufacture of objects as well as to identify the presence of technological styles in the case of changes in the objects manufacture during Late Postclassic period.

To identify the procedures and equipment used, manufacturing marks analysis are performed, taking

into account that each process and each tool leaves specific marks. To observe the traces of manufacture polymers were stamped on surfaces and perforations of the objects made of *Spondylus princeps* corresponding to the two major periods of Calica occupation. Then, they were gold covered and analyzed by SEM with high-vacuum with a beam of 20 kV and using the secondary electron signals. Under these conditions, it was observed topology, roughness, porosity and particle size at 10 mm away from the polymer surface and at four different magnifications (100X, 300X, 600X and 1000X).

## RESULTS

The micrographs obtained showed the following results indicate specific tools and specific manufacturing processes without a temporal relation:

### Surfaces

In the surfaces were observed straight bands that are distributed in a hazardous manner and have different thicknesses from 6  $\mu\text{m}$ , 20  $\mu\text{m}$  and 60  $\mu\text{m}$ . This feature has been related to marks left for the wear with limestone [5-6]. Fine lines (0.6  $\mu\text{m}$  and 2.8  $\mu\text{m}$ ), were also observed on the traces of wear which smoothed observed, indicating flint nodule polishing. [7-8].

### Perforations

In the perforations were observed three different traits:

1. Rough and porous surfaces with bands from 1.3  $\mu\text{m}$  to 3.33  $\mu\text{m}$  intertwined that are grouped to form broader bands, the result of the perforation made with flakes of flint [9-10].

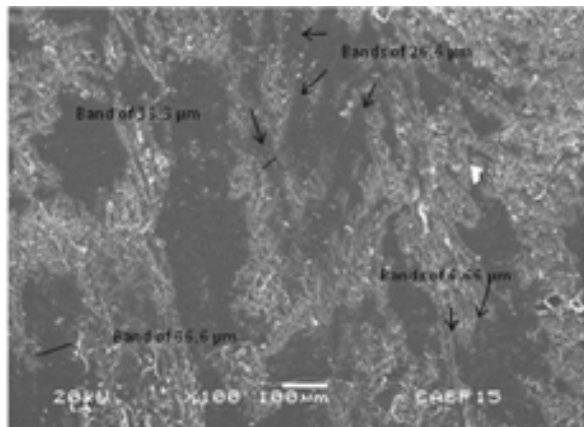


FIGURE 5. Traces of wear on the surface of an archaeological object of *Spondylus princeps*.

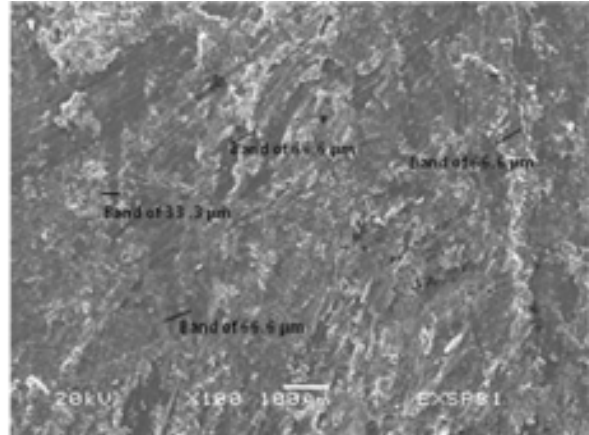


FIGURE 6. Traces of wear with limestone of an experimental object of *Spondylus princeps*.

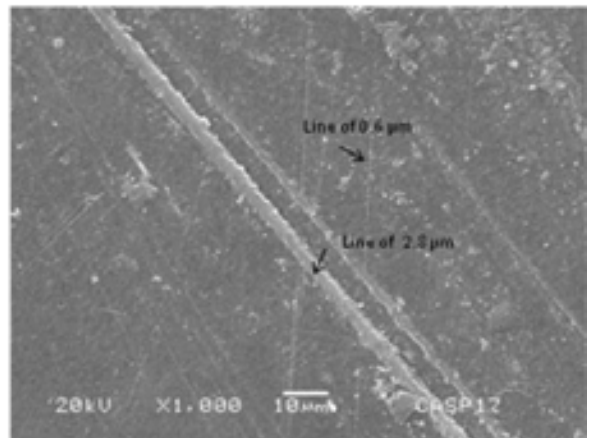


FIGURE 7. Traces of polish on the surface of an archaeological object of *Spondylus princeps*.

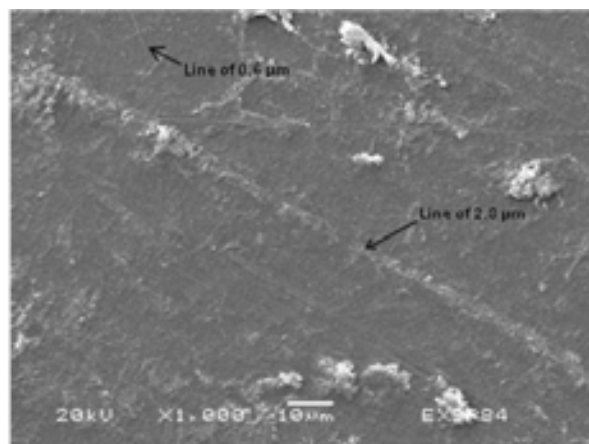
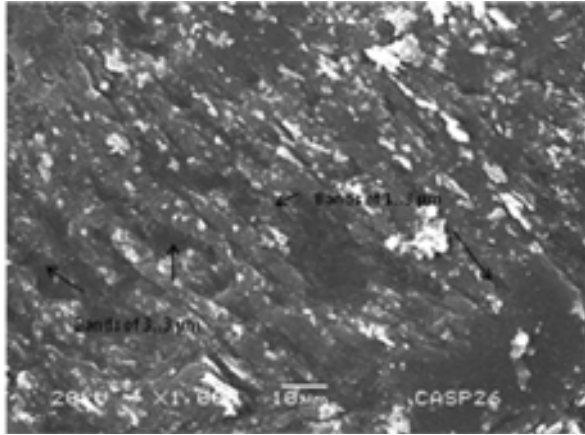
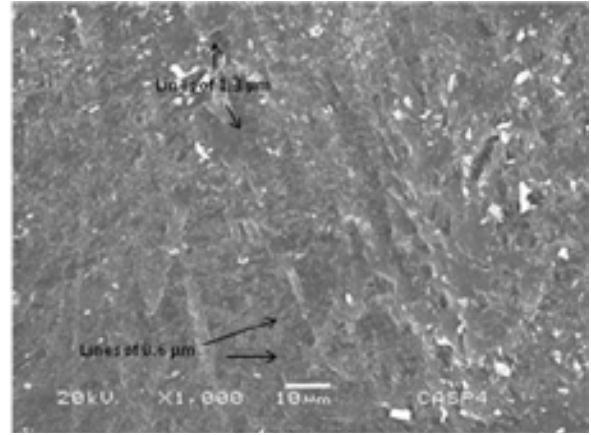


FIGURE 8. Traces of polished with flint nodule on the surface of an experimental object of *Spondylus princeps*.



**FIGURE 9.** Traces in perforation of an archaeological object of *Spondylus princeps*.



**FIGURE 11.** Marks of drilling in an archaeological object of *Spondylus princeps*.

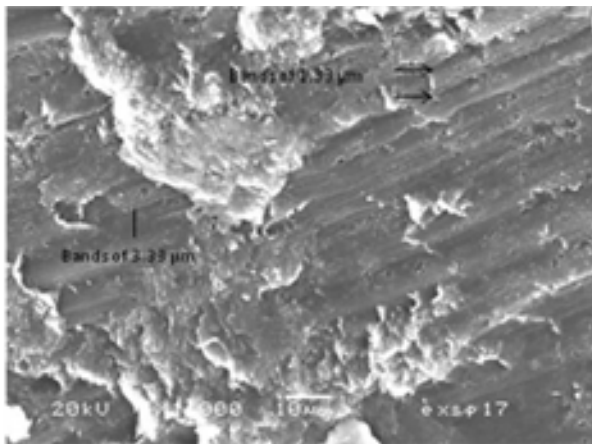


**FIGURE 10.** Perforation with drill of flint in an experimental object of *Spondylus princeps*.

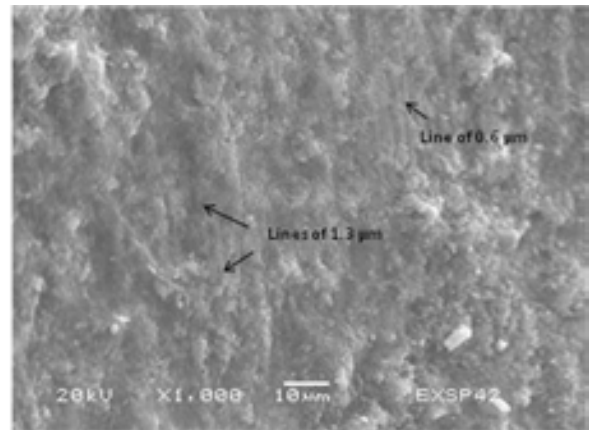


**FIGURE 12.** Perforation with flint powder in an experimental object of *Spondylus princeps*.

2. Very fine lines of 0.6  $\mu\text{m}$  and 1.3  $\mu\text{m}$  leaving a rough texture, softer than that observed in holes with flint flakes. This appearance suggests the use of powdered flint [11-12].

3. Homogeneous surface with lots of straight fine lines of 0.6  $\mu\text{m}$  resulting from the use of volcanic ash [13-14].

With this we can conclude that the ornamental objects of *Spondylus princeps* of Calica, of Superior Preclassic and Late Postclassic were made by limestone wear, giving them a finish with nodule of flint. The perforations were made through the use of flint flakes and abrasive like flint dust and volcanic ash

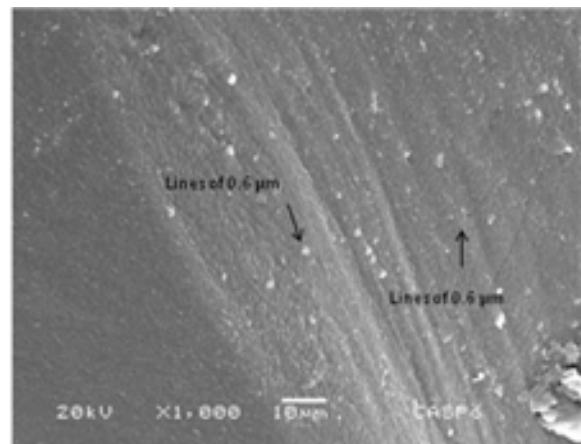


**FIGURE 13.** Perforation in an archaeological object of *Spondylus princeps*.

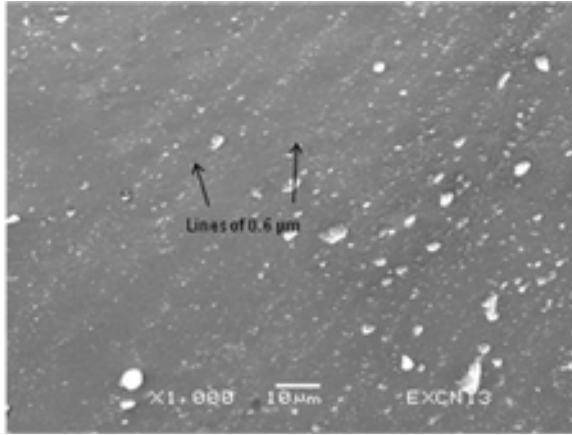


FIGURE 14. Perforation with volcanic ash in an experimental object of *Conus sp.*

## CONCLUSIONS

The presence of foreign material (*Spondylus princeps*) and the use of volcanic ash in the process, suggests the existence of direct or indirect relations with sites in other regions such as the Pacific coast.

The results show continuity in the manufacturing of *Spondylus princeps* objects reflecting the presence in the Late Postclassic period of the same group that inhabited the site during the Preclassic period. This explains that during the Classic is not observed at the site an abandonment total because there is archaeological evidence of sporadic visits of this group.

The partial abandon of Calica during the Classic period is explained by the growth of cities such as Coba that exercised a regional dominance favoring the reorganization of the population of peripheral sites to integrate to this new order.

In the Early Postclassic period, changes in social organization associated with the arrival of the Itza people in the region were observed. They dominated the East Coast until 1200 A.D. and when Chichen-Itza fell, the consolidation of politic, economy, population and architecture of the East Coast sites is favored; this defines the East Coast style.

As we mentioned above, this research opens the door to developing new hypotheses about the

importance of Calica and its role in the cultural dynamics of the Maya coastal region of Quintana Roo.

## ACKNOWLEDGEMENTS

This research could not be done without the support of Luis Alberto Martos López, who was Director of the Archaeological Project Calica and facilitated the materials as well as photographs of the project.

Authors thank Dr. Adrián Velázquez Castro for leading the project "Materiales conquiológicos del Complejo Calica. Un análisis morfofuncional" and providing the micrographs of the experiments obtained by the workshop "Técnicas de manufactura de los objetos de concha del México prehispánico".

Belem Zúñiga-Arellano and Norma Valentín Maldonado provided their assistance in identifying biological materials and species.

José Antonio Alba, operated the SEM at the laboratory of the Direction of Laboratories and Academic Support of INAH, and Dr. Demetrio Mendoza of the National Institute for Nuclear Research (ININ), provided his support in analyzing the samples in the SEM.

Emiliano Melgar Tisoc advised the project "Materiales conquiológicos del Complejo Calica. Un análisis morfofuncional".

## BIBLIOGRAPHY

1. L.A. Martos López, "Proyecto arqueológico Calica 1992-1999", INAH-DEA, México.
2. L.A. Martos López, *Por las Tierras Mayas de Oriente. Arqueología en el área de Calica Quintana Roo*, CONACULTA-INAH, CALICA, México, 2003.
3. A. Velázquez Castro, "La Investigación de la tecnología de elaboración de los objetos de concha a través de la Arqueología experimental" en *Actualidades arqueológicas* Año 0 No 3 (2005-2006) 1-11.
4. A. Velázquez Castro, *La producción especializada de los objetos de concha del Templo Mayor de Tenochtitlán*, Colección científica No. 159 INAH, México 2007.
5. A. Velázquez Castro, L.S. Lowe, *Los moluscos Arqueológicos. Una visión del mundo maya*. Cuadernos del Centro de Estudios Mayas No. 34 UNAM (2007).

## Manufacturing Techniques of the *Pinctada mazatlanica* Objects in Tula, Hidalgo, México

R. B. Solís Ciriaco<sup>1</sup> and O. Sterpone Canuto<sup>2</sup>

<sup>1</sup> Museo del Templo Mayor, Instituto Nacional de Antropología e Historia, MEXICO.

e-mail: reynabsolis@hotmail.com

<sup>2</sup> Centro INAH-Hidalgo, MEXICO.

**Abstract.** In the archaeological site of Tula (AD 700-1200), located in the Southeast part of the state of Hidalgo, Mexico, about 400 shell objects made of the Pacific Ocean species *Pinctada mazatlanica*, have been recovered. This material appears in different phases of the productive process, and it has been associated to ceremonial structures, burials, and domestic areas. The context that presents the biggest quantity of the evidences of production of these goods is the Boulevard, an area defined as a “group of houses”. There, at least three domestic households with a courtyard and a temple were constructed during the early Tollan phase (850-950 AD) and explored archaeologically in 1986 by a group directed by Osvaldo Sterpone. Trough the use of experimental archaeology and the observation of the various modifications with optical microscopy (OM) and scanning electron microscope (SEM), it was possible to deduce the techniques and tools used for its production, which should have been concentrated in one or in a few workshops controlled by the rulers of the site.

**Keywords:** shells, manufacture, technology, Toltecs, SEM.

### INTRODUCTION

Since earlier times and in different parts of the world, a power source for prestige and social hierarchy were prestige goods. Most of them are characterized for being exotic or restricted circulation materials, although they could be products of external trade which worked as status symbols for the elite [1].

One of the raw materials employed as prestige goods was the shell objects. Due to its foreign origin and scarcity, especially at inland sites far away from the coasts, this material has been employed to justify hierarchy, power and status.

An example of this prestige and power justification can be found in the Toltec capital of Tula (AD 700-1200), a hilltop site located in the Southeast part of the state of Hidalgo, México (Figure 1). There, the archaeologists found about 400 shell objects made of

the Pacific Ocean species *Pinctada mazatlanica* in several contexts.



FIGURE 1. Geographical location of Tula, Hidalgo.

It is interesting that the biggest quantity of the unworked shells (Figure 2) and the pieces in different stages of the productive process (Figure 3) were concentrated in the Boulevard (Figure 4), a group of at least three domestic households with a courtyard and a temple that were constructed during the early Tollan phase (AD 850-950) [2-3]. In contrast, the majority of the finished objects (Figure 5) were deposited inside offerings and burials at the principal structures, palaces and plazas in the Tula Grande area (AD 700-1200) (Figure 6), where the elite members and priests of the Toltecs lived and performed ceremonies [4].



FIGURE 2. Unworked shell of *Pinctada mazatlanica*.



FIGURE 3. Pieces in different stages of production.



FIGURE 4. The aerial view of the Boulevard [3].



FIGURE 5. Finished object: a zoomorphic pendant.



FIGURE 6. View of the Temple of Tlahuizcalpantecuhtli (in background) from the Burned Palace (El Palacio Quemado) in Tula Grande.

Based on their patterns of distribution, the aim of this article is the identification of the tools and techniques employed in the production of these objects, and the technological comparison between the pieces from the Boulevard and Tula Grande to distinguish which of them could be produced locally.

## TECHNOLOGICAL ANALYSIS

We analyzed the *Pinctada mazatlanica* pieces with experimental archaeology and the characterization of their traces of manufacture. In the first case, we used the database of more than 600 experiments of the Project “Manufacturing Techniques of the Shell Objects from Pre-Columbian Mexico”, coordinated by A. Velázquez Castro [4], using tools and techniques (Figure 7) reported in the historical sources [5] and the archaeological contexts [6-7].

To analyze the experimental and archaeological traces, we followed the methodology proposed by Velázquez [4], using Optic Microscopy (OM) at 10x, 30x, and 63x, and Scanning Electron Microscopy (SEM) at 100x, 300x, 600x, and 1000x. The last one in High Vacuum Mode (HV), with the same parameters:

Secondary electrons signal (SEI), electron beam of 20 kV of energy, 42 of spotsize, and 10 mm of work distance from the sample surface.



**FIGURE 7.** Experimental archaeology on shells: abrading of *Pinctada mazatlanica* with andesite.

Also, it is important to highlight that the SEM analysis allowed us to identify with great accuracy the tools and techniques employed in the production of this objects.

## RESULTS

The micrographic analysis of the experimental modifications and its comparison with the archaeological ones, allowed us to identify the tools and techniques used in the production of the shell objects at Tula:

Andesite stones were used to abrade the surfaces and to regularize the edges (Figures 8-9) while obsidian flakes and blades were used for the incisions and cuts (Figures 10-11).

Finally, chert burins and polishers were used to drill and brighten the pieces (Figures 12-13).

## CONCLUSIONS

The identification of a standardization and technological homogeneity in the production of the *Pinctada mazatlanica* objects from all of the contexts of Tula, allowed us to infer that the manufacture of these objects was locally and could be controlled and regulated by the elite, which concentrated the artisans in the Boulevard and monopolizing the production, distribution and consumption of these goods at Tula Grande.

This specialized production is located at domestic units, and the prestige goods were consumed at the ceremonial areas, palaces, burials and tombs, as symbols of power and richness of the elite members and priests of Tula.



**FIGURE 8.** Archaeological surface with scars of the abrading with andesite at 30x.

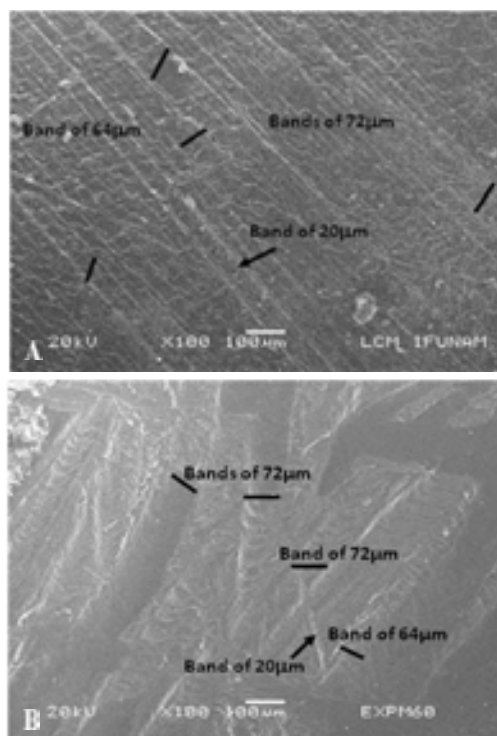


**FIGURE 9.** Analysis of surfaces: archaeological pendant (A) and experimental abrading with andesite (B), both at 100x.

## ACKNOWLEDGMENTS

Authors thank J. Arenas and J. A. Alva for the SEM images, E. Melgar for the photos of the objects and the optical microscopy images, A. Velázquez and his team for the experiments and the use of the database for the technological analysis, and the field workers at the Boulevard.



FIGURE 10. Archaeological edge of a pendant at 30x.



FIGURE 12. Archaeological polishing at 30x.

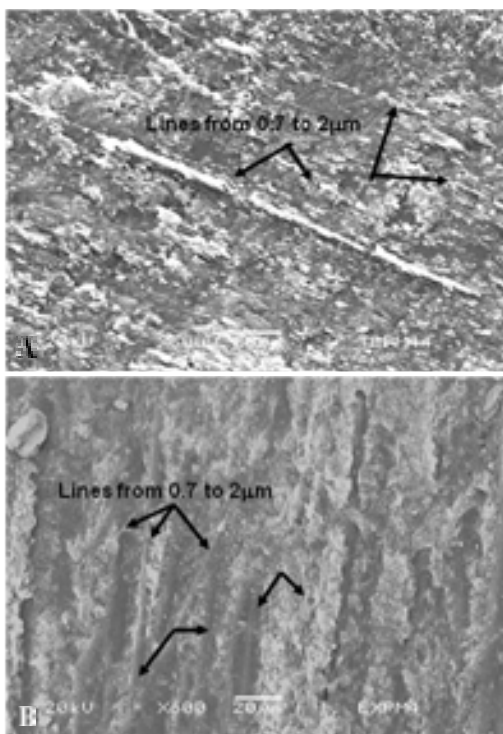


FIGURE 11. Analysis of edges: archaeological pendant (A) and experimental cutting with obsidian flakes (B), both at 600x.

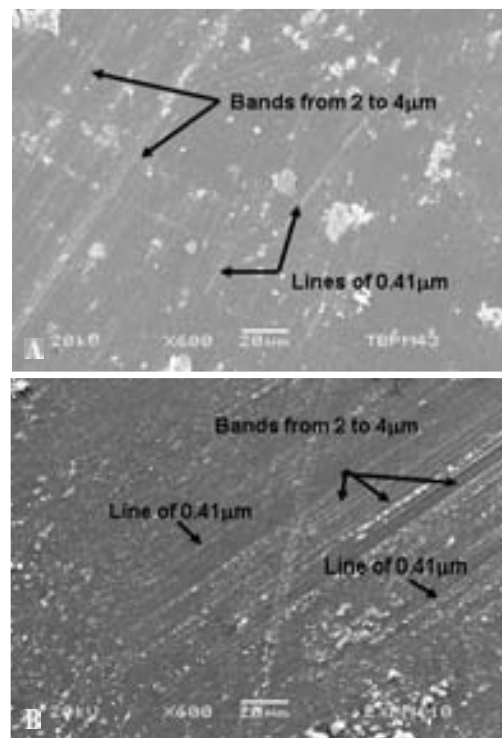


FIGURE 13. Analysis of brightening: archaeological pendant (A) and experimental abrading with andesite and polishing with chert nodules (B), both at 600x.

## REFERENCES

1. P. Drucker, "On the Nature of Olmec Polity", in *The Olmec and Their Neighbors, Essays in Memory of Matthew W. Stirling*, E. P. Benson, (ed.), Dumbarton Oaks Research Library and Collections, Trustees for Harvard University, Washington, D.C. 1981, pp. 29-48.
2. M. R. Guevara Chumacero, "Buscando el Origen del Estado Tollan. La Formación de organizaciones Estatales Secundarias", Masters Thesis, Facultad de Filosofía y Letras-Instituto de Investigaciones Antropológicas, UNAM, México 2003.
3. M. R. Guevara Chumacero, *Dimensión Antropológica* 29 (2003) 7-32.
4. O. Sterpone Canuto, *Tollan a 65 años de Jorge R. Acosta*, Universidad Autónoma del Estado de Hidalgo, INAH, México, 2007.
5. A. Velázquez Castro, *La producción especializada de los objetos de concha del Templo Mayor de Tenochtitlan*, INAH, México, 2007.
6. B. de Sahagún, *Historia General de las Cosas de la Nueva España*, Porrúa, México, 1956, 4 vols.
7. L. Suárez Díez, *Técnicas Prehispánicas en los Objetos de Concha*, INAH, México, 1974.
8. E. R. Melgar Tisoc, "La producción especializada de objetos de concha en Xochicalco", Masters Thesis, Facultad de Filosofía y Letras-Instituto de Investigaciones Antropológicas, UNAM, México, 2009.

# Manufacturing Techniques of the Turquoise Mosaics from the Great Temple of Tenochtitlan, Mexico

E. R. Melgar Tísoc and R. B. Solís Ciriaco

<sup>1</sup> *Museo del Templo Mayor, Instituto Nacional de Antropología e Historia, INAH. Seminario 8, Centro Histórico, México D.F. 06060, MEXICO. e-mail: anubismarino@gmail.com*

**Abstract.** In the offerings of the Great Temple of the Aztecs, the archaeologists found thousands of turquoise inlays from different stages of this building. Some of them could be restored as disks, and others are parts of knives and figurines. With the information obtained by non-destructive techniques like X-Ray Fluorescence (XRF) and Ultra Violet Fluorescence (UVF), we know that they mixed pieces from different mines, and more interesting, not all of them are “chemical” or real turquoise from the South-Western United States. Also, we applied the technological analysis of these pieces with experimental archaeology and the characterization of their manufacturing traces. As results, we identified different tools employed in the mosaics from the earlier stages, which contrast with the great standardisation of the pieces from the later stages. So, the aim of this paper is to show the technological analysis applied on these objects and discuss their place or workshop of origin.

**Keywords:** Turquoise, manufacture, technology, Tenochtitlan, SEM.

## INTRODUCTION

In the offerings of the Great Temple of Tenochtitlan in the Basin of Mexico, the archaeologists found thousands of objects that were made on different raw materials, some of them from local sourcing areas (like basalt, andesite, and obsidian), and other were exotic (as jadeite, serpentinite, travertine, chert, shell, and turquoise). Also, it is interesting that the presence and quantity of these pieces changed among the seven different stages of construction of this building, some of them corresponding to the reign of the Mexican rulers or *tlatoque* [1].

Unfortunately, it is common that the research of these objects were restricted to the provenance of the raw material, and the typological classification [2-3]. In contrast, their technological analyses were scarce [4]. Consequently, it is difficult to identify which pieces came to the Aztec capital as raw materials and which came already manufactured.

To solve this problem, we chose the turquoise to compare their origin with the production characteristics of the inlays and mosaics that were buried in Tenochtitlan.

**TABLE 1.** Construction Stages and Rulers of Tenochtitlan

Stage	Period	Rulers ( <i>Tlatoque</i> )
I	AD 1325-1375	Tenochtitlan Foundation
II	AD 1375-1427	Acamapichtli, Huizilhuilitl and Chimalpopoca
III	AD 1427-1440	Itzcóatl
IVa	AD 1440-1469	Moctezuma I
IVb	AD 1469-1481	Axayácatl
V	AD 1481-1486	Tízoc
VI	AD 1486-1502	Ahuízotl
VII	AD 1502-1520	Moctezuma II

For their provenance, in previous studies it was characterized the chemical composition of these objects (Figures 1 to 3), using X-Ray Fluorescence (XRF), Ultra Violet Fluorescence (UVF), Infra-Red Imaging (IRI), and PIXE [5-6].



FIGURE 1. XRF analysis on turquoise mosaics.

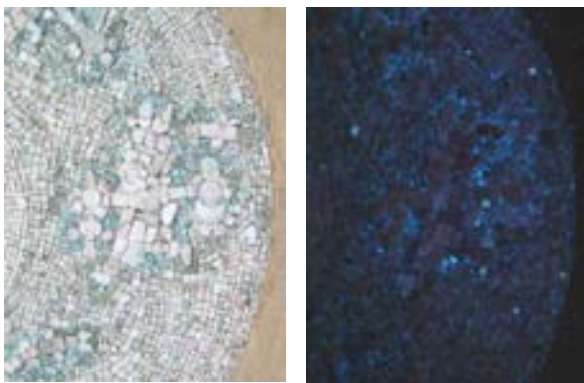


FIGURE 1. XRF and UVF analyses of turquoise mosaics.

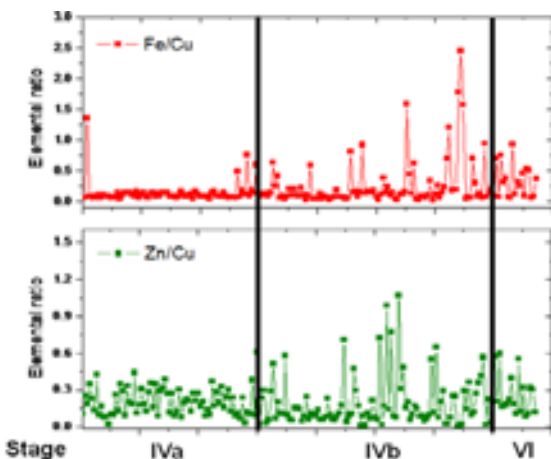


FIGURE 3. Comparison between XRF measures by stages.

In these analyses “chemical” turquoise from the Southwestern United States was identified, most of them from New Mexico and Arizona, in the later offerings from the Stages IVb and VII, but, in the

earlier offerings from the Stage IVa, they were mixed with other greenish and bluish stones, some of them known as “cultural” turquoise like crisocole, azurite, malaquite, and cuprite.

Because of their foreign origin as raw materials, we want to know if these two patterns could show different technology, and if we could identify their place of production by comparing their traces of manufacture with the pieces from the few turquoise workshops known archaeologically: Chalchihuites in Zacatecas [7] and Pueblo Bonito in New Mexico [8].

### ANALYZED SAMPLES

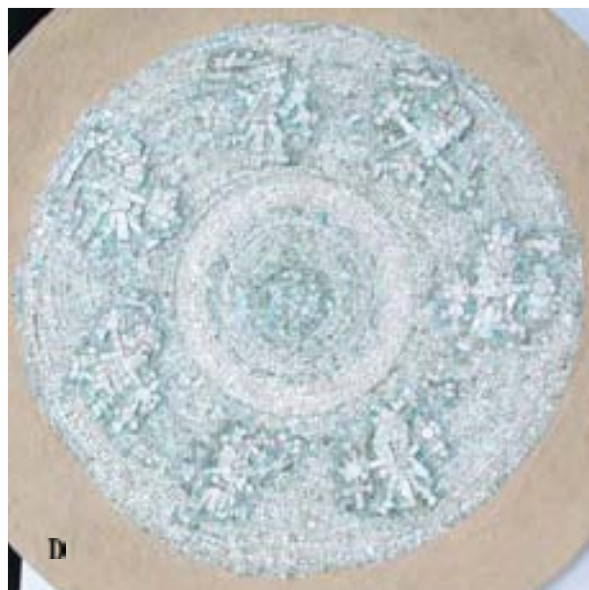
In this study, more than 30,000 turquoise inlays from the offerings of the Great Temple of Tenochtitlan were analyzed. The artifacts have been chosen from different offerings that belong to the construction stages IVa, IVb, V, VI and VII. The pieces are mainly geometrical inlays, and some of them were restored as mosaics and disks (Figures 4).



FIGURE 4a. Turquoise mosaics from Stage IVa.



FIGURE 4b-4c. Turquoise mosaics from Stage IVb.



**FIGURE 4d.** Turquoise mosaics from Stage VI.

### TECHNOLOGICAL ANALYSIS

We analyzed the turquoise pieces with experimental archaeology and the characterization of their traces of manufacture. In the first case, we used the database of more than 250 experiments of the Project “The lapidary objects of the Great Temple: styles and technological traditions”, using tools and techniques (Figure 5) reported in the historical sources [9] and the archaeological contexts [7-8]. To analyze the experimental and archaeological traces, we followed the methodology proposed by A. Velázquez [4] on shell pieces, but applied on lapidary objects [10]. Based on it, we employed Optic Microscopy (OM) at 10x and 30x, and Scanning Electron Microscopy (SEM) at 100x, 300x, 600x, and 1000x. The last one in High Vacuum Mode (HV), with the same parameters: secondary electrons signal (SEI), 20 kV of energy, 42 of spotsize, and 10 mm of work distance.

### RESULTS

We identified two patterns of manufacture:

The first one corresponds to Stage IVa, when the “chemical” turquoise was mixed with other stones (Figure 6). In the offerings of this stage, the inlays showed abrading with sandstone (Figure 7), and cutting with obsidian flakes (Figure 8).



**FIGURE 5.** Experimental archaeology on turquoise: abrading with andesite (A) and cutting with obsidian blades (B).



**FIGURE 6.** “Cultural” turquoise inlays in Chamber III (Stage IVa) at 30x.

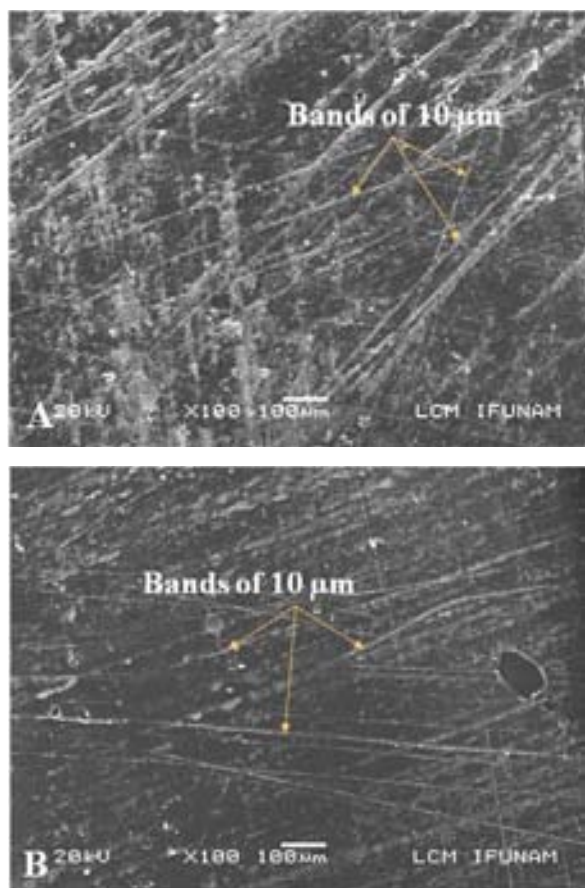


**FIGURE 7.** Analysis of surfaces: archaeological inlay from Stage IVa (A) and experimental abrading with sandstone (B), both at 100x.

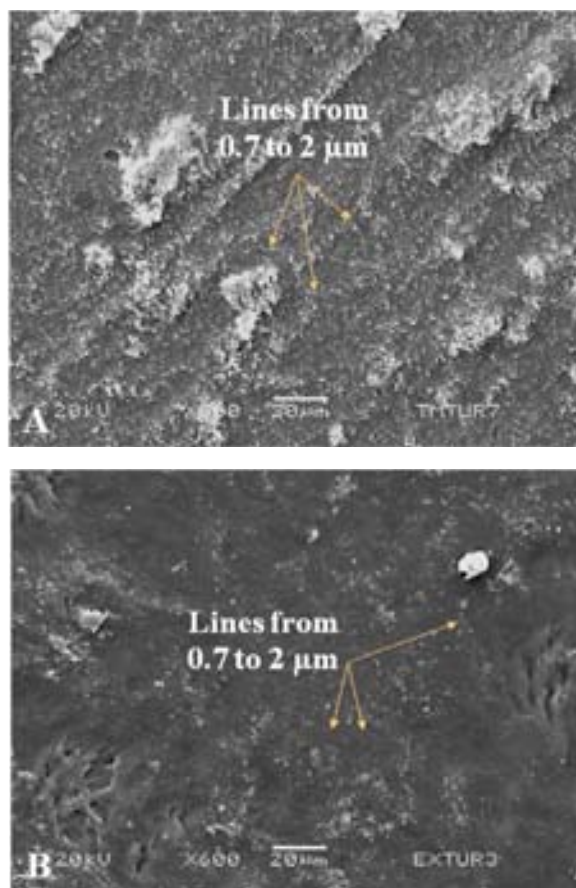


**FIGURE 8.** Analysis of edges: archaeological inlay from Stage IVa (A) and experimental cutting with obsidian flakes (B), both at 600x.

The second pattern corresponds to Stages IVb to VII, when the “chemical” turquoise appeared unmixed (Figure 9). In these offerings, the inlays showed abrading with basalt (Figure 10), cutting with obsidian flakes (Figure 11), and brightening with leather. It has the same traces of experimental cutting with obsidian flakes as seen in Figure 5B, both at 600x. Also, it is different compared with the experimental cutting with chert flakes as seen in Figure 12.

## DISCUSSION AND CONCLUSIONS

The turquoise found in the offerings of the earlier stages (IVa) of the Great Temple of Tenochtitlan appeared mixed with other greenish and bluish stones from different sources. In contrast, in the later stages (IVb to VII), the turquoise came principally from Arizona and New Mexico [5,6].

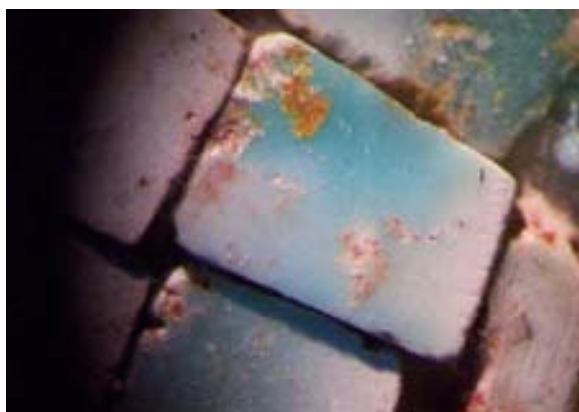


**FIGURE 9.** “Chemical” turquoise inlays in Offering 99 (Stage VI) at 30x

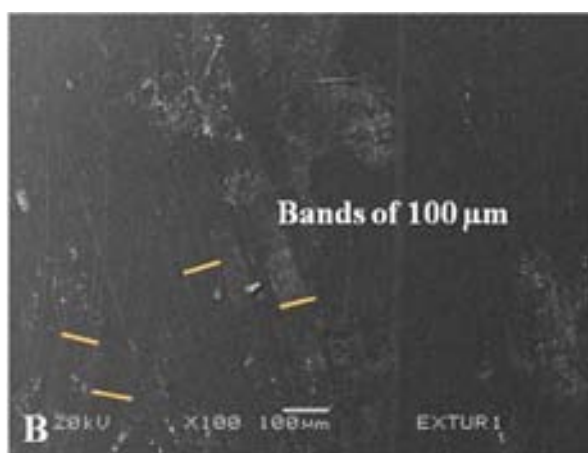
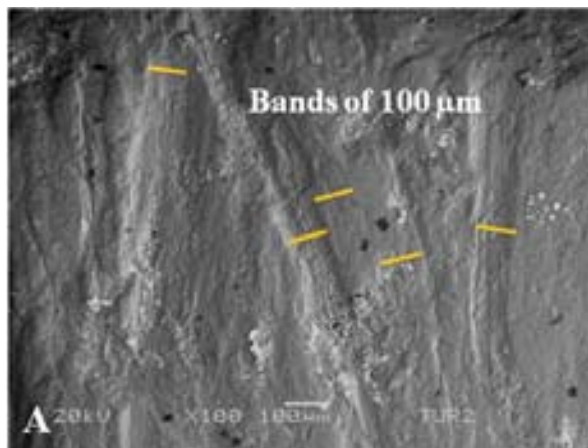


**FIGURE 10.** Analysis of surfaces: archaeological inlay from Stage VI (A) and experimental abrading with basalt (B), both at 100x.

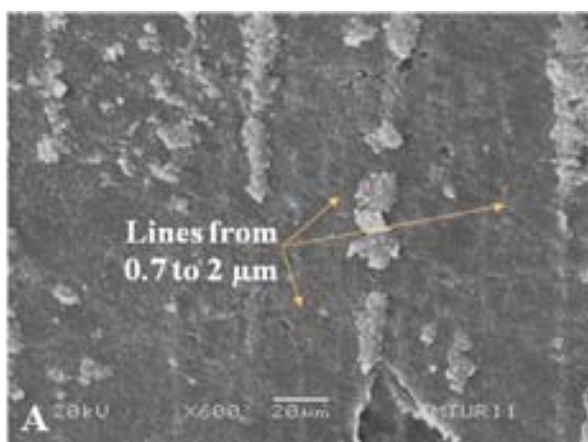


**FIGURE 11.** Analysis of edges: archaeological inlay from Stage VI. 600x

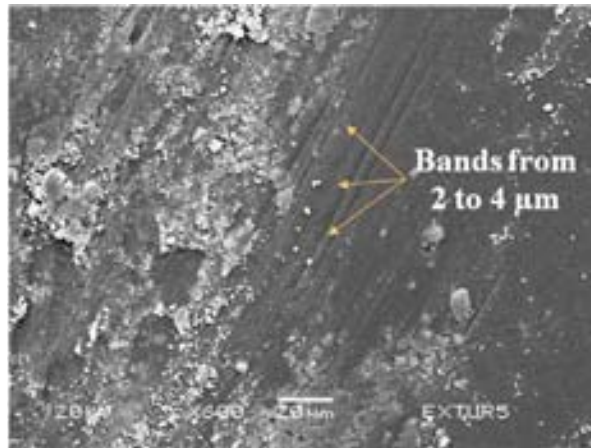


**FIGURE 12.** Analysis of edges: Experimental cutting with chert flakes at 600x.

Comparing the technological analysis with the provenance of these inlays, we identified two patterns of manufacture based on the different abrading tools employed:

The sandstone of the earlier one (Stage IVa) is not common in the lapidary objects of Central Mexico [10] and it matches with the tools reported in the turquoise workshops at the Chaco Canyon [8]. So, these inlays could be produced in that area and came to Tenochtitlan as finished objects by long distance trade.

The basalt of the later one (Stages IVb to VII) shares the same tool employed in other lapidary objects of the Late Postclassic in Central Mexico [10] and matches with the “Mexican style” that Adrián Velázquez and Emiliano Melgar identified on shell, obsidian, and travertine [4,10]. Probably, the turquoise of these pieces came to Tenochtitlan as raw materials by commerce and tribute and local artisans worked them in the workshops located inside the palaces of the Aztec rulers [9].

Perhaps these two technological patterns reflect the different sociopolitical conditions of the Aztecs, because the earlier one characterized by the mixed pieces with foreign manufacture corresponds with the period when they were under the control of the Tecpaneca of Azcapotzalco and they do not have the power and economy to maintain artisans. In the later one that shares the manufacturing techniques and tools applied on other Mexican objects, this period starts with the rebellion commanded by the Aztecs and the development of the Triple Alliance of Tenochtitlan, Texcoco and Tlacopan. At this time, they conquest other territories and obtained resources by tribute and commerce that allowed them to support artisans, some of them living inside the palaces [9].

## ACKNOWLEDGMENTS

Authors thank J.L. Ruvalcaba, T. Calligaro, J. Curado, K. Laclaventine, K. López and F. Jaimes for the PIXE, XRF, IRF and UVF analyses; J. Arenas and J. A. Alva for the SEM images; A. Velázquez for teaching us the technological analysis; and F. Carrizosa for the facilities to analyze the pieces at the Great Temple Museum, INAH.

## REFERENCES

1. E. Matos Moctezuma, *The Great Temple of the Aztecs. Treasures of Tenochtitlan*, Thames & Hudson Ltd., London 1988.
2. I. Athié Islas, “La obsidiana del Templo Mayor de Tenochtitlan”, Bach. Archaeology Thesis, ENAH, 2001.
3. C. J. González González and B. Olmedo Vera, *Esculturas Mezcala en el Templo Mayor*, INAH, México 1990.
4. A. Velázquez Castro, *La producción especializada de los objetos de concha del Templo Mayor de Tenochtitlan*, INAH, México 2007.
5. J. L. Ruvalcaba, K. Laclaventine and E. Melgar “Non-Destructive Characterization of Turquoise Artifacts from Offerings from Templo Mayor, Tenochtitlan, México”, paper presented in XVII IMRC, Academia Mexicana de Ciencia de Materiales, Cancún 2008.
6. K. Laclaventine, “Caracterisation Non-Destructive In situ de Turquoises d’Offrandes du Templo Mayor de Mexico-Tenochtitlan - Etude de provenance de turquoises par analyses de Fluorescence de Rayons X (XRF)”, Master Thesis in Archaeomaterials, Université Bordeaux IV, 2008, France.
7. A. Maldonado Reséndiz, “La lapidaria en turquesa de Chalchihuites”, paper presented in 6º Ciclo de Conferencias del Templo Mayor y Tlatelolco en voz de sus investigadores, Museo del Templo Mayor, México 2007.
8. J. E. Neitzel, “Elite Styles in Hierarchically Organized Societies. The Chacoan Regional System”, in *Style, Society, and Person. Archaeological and Ethnological Perspectives*, C. Carr y J. E. Neitzel (eds.), Plenum Press, New York 1995, pp. 393-417.
9. B. de Sahagún, *Historia General de las Cosas de la Nueva España*, Porrúa, México 1956, 4 vols.
10. E. Melgar Tisoc, “La lapidaria del Templo Mayor: estilos y tradiciones tecnológicas”, Archivo del Templo Mayor, INAH, México 2004-2009.

## **Analysis of Modified Osseous Remains from Monte Alban, Oaxaca, Mexico**

N. Valentín Maldonado<sup>1</sup> and G. Pérez Roldán<sup>2</sup>

<sup>1</sup>*Subdirección de Laboratorios y Apoyo Académico, Instituto Nacional de Antropología e Historia  
Moneda 16, Centro, México, D.F. CP. 06060, MEXICO. e-mail: nvalentinm@hotmail.com*

<sup>2</sup>*Escuela Nacional de Antropología e Historia, Instituto Nacional de Antropología e Historia  
Periferico Sur y Zapote, S/número Col. Isidro Fabela, México, D.F. CP. 14030, MEXICO.  
e-mail: gilgertions@yahoo.com.mx*

**Abstract.** The present work is about the biological identification, typology and analysis of the manufacturing traces on the osseous remains from the archaeological site of Monte Alban, Oaxaca, México, that were sent to the Subdepartment of Laboratories and Academic Support, INAH. The osseous material consists of 74 remains (100%) of four zoological groups: Chondrichthyes Class (shark) (5%), Actinopterygii Class (fishes) (5%), Birds Class (27%), and Mammalia Class (63%). The mammals are the most present with 47 pieces; of these the more abundant belong to *Odocoileus virginianus* (White-tailed deer) with 32 elements, followed by the birds remains, *Meleagris gallopavo* (turkey), with 20 remains. Of the 74 remains, 65 have traces of manufacture and modifications for the elaboration of different tools, like drills, spatulas, needles, pins, beads, pendants and debitage. The traces of manufacture were analyzed with an Optic Microscope (10X, 20X, 30X, 40X) and with an Scanning Electron Microscope (MEB) (100X, 300X, 600X y 1000X).

**Key words:** Bone, animal, Monte Alban, Oaxaca, technology.

### **INTRODUCTION**

The archaeozoology is the discipline that studies the faunal remains found in the archaeological contexts [1-2]. These studies give the opportunity to know the relationship established amongst the ancient human settlements with the animals and their environment, allowing the discovery of the biological and cultural aspects of these relationship.

The proper identification of the species found in archaeological contexts provides the biological information known about them; like geographic distribution, habitat, ecological requirements, size, shape, and color, to mention a few [1-4]. From the cultural point of view, it is possible to obtain information about the use they had for the animals, which parts of them were most exploited, methods and

techniques for obtaining them and the processes and practices to cut, abrade, and polish, among others [5].

There are other tools that provide more archaeozoological information. One of them is the taphonomy, which states that a group of physical, chemical, biological and/or cultural processes act on the bones after an animal dies, changing its natural structure leaving characteristic modifications [6-7].

From other characteristics it could be possible to infer different human activities; for example, the blackening of the specimens could be evidence of its exposure to fire for eating purposes, or the employment of bones as tools, or the initial processes of the manufacture of tools. Based on the analysis of this kind of evidences, it is possible to know the different environments that were exploited by human groups, the use they gave to the resources, the degree

of specialization that they had and the relationships they established with distant places.

## MATERIALS AND METHODS

The osseous material from Monte Alban, Oaxaca, was sent already clean and separated by bag number. It came from different excavation units, where the more abundant are the ones from the different excavated areas at the N platform of Monte Alban. Because of that, each piece is analyzed without making a stratigraphic correlation, or an element association.

Of the 74 remains, 65 showed manufacturing traces and modifications for the elaboration of different tools, like drills, spatulas, needles and ornaments among others. These cultural modifications complicate the identification of the remains because they lost diagnostic characteristics to recognize them. Also, in some cases it was only possible the identification of the genus and in others the class level.

The identification was made basically by direct comparison with modern specimens from the reference osteological collection of the Archaeozoology Laboratory “Ticul Álvarez Solórzano”, and the proper bibliography for each group.

## OBJECTIVE

The main objectives of the present work are the identification of the species used in Monte Alban and to establish the manufacturing techniques of the elements made on bones from the more representative organisms: deer (*Odocoileus virginianus*), turkey (*Meleagris gallopavo*), rabbit (*Sylvilagus cunicularius*) and canids (*Canis familiaris* and *Urocyon cinereuargenteus*).

## IDENTIFICATION

### Phylum Chordata :

**Class Chondrichthyes** (sharks). Only one tooth was found. It came from the Tomb 7, from a looting trench; it is a pendant (H125).

**Class Actinopterygii** (fishes). Three bones were separated from the fish remains, but it was not possible to identify them at species level; they do not have cultural modifications (H7 and H57).

### Class Birds, Family Phasianidae.

*Gallus gallus*.- Domestic bird, commonly known as hen, it was introduced to our continent with the Spaniards arrival. This osseous remain has traces of been cooked and its presence suggests a postconquest intrusion (H47).

*Meleagris gallipavo*.- Commonly known as turkey, formerly of wide distribution in Mexico. It used to live in the mountains, mainly in the pine - olm oak zone,

and near the coast plains. This species was domesticated and widely used since Early Formative until nowadays. Its utilization has been integral, basically used as eating source, for feathered crafts, and as raw material for the fabrication of different objects.

Of this bird 20 objects were analyzed: two beads (H86 and H231), two tubes (H35B and H 169), a whistle (H182b), a spatula (H171), a drill (H187), an undefined piece (H109, H54), 11 debitage materials (H95, H176, H183, H170, H166, H111, H163, H155, H250, H192, and H125).

**Class Mammalia.** Of this class two worked objects were separated, but its high degree of modification did not leave any diagnostic parts: the first one is a diaphysis bone that was used to elaborate an anthropomorphic figurine (H156), the second remain is a tip fragment of a burned needle-drill (H36).

**Family Hominidae.** *Homo sapiens*.- superior left side incisive tooth that shows evidence of dental mutilation (F4 type or B2).

**Family Leporidae.** Known as rabbits and hares, they have numerous species in Mexico. A fragment of the long diaphysis bone was analyzed, forming part of a spatula, but the species could not be determined because it lost diagnostic parts (H180).

*Sylvilagus cunicularius*.- Known as Mexican rabbit, of big size; its distribution area covers the semi-arid tropics of south and center Mexico, spreading in some places to the pine-olm oak zone [8]. Two remains were studied, one worked object that function as a whistle made over the femur diaphysis (H222), and other unmodified, a radio diaphysis (H4A), which presented cook marks.

**Family Canidae.** *Urocyon cinereuargenteus*.- The gray fox exists thorough the whole Mexican Republic, its presence is variable according to the vegetation. The more abundant populations live in semi-arid scrublands in both temperate and tropical zones. A left ulna was modified to form a drill that was burned for a possible ritual use (H202).

*Canis* sp. - Dogs, wolves and coyotes belong to this genre, and they have wide distribution. The analysis of the only identified piece was an incisive tooth, so the species could not be identified (H25).

*Canis familiaris*.- This species was introduced alongside the first settlers of the American continent. It is a domestic animal whose distribution it is related to the human population.

Of the identified remains we have seven osseous pieces, one of them has no modification ( superior premolar tooth H10), while the other six had the next uses: three pendants, two of them are canines with a biconic drill hole (H45 and H210) and the other one it is an ulna fragment from a young dog with the same drill hole (H252). A dipstick elaborated with a tibia diaphysis (H35A). A jaw with a cross section in the anterior region (H204) could be a votive object

because it is related to a funerary context (Tomb 14). And the last piece is a tibia fragment with a cross section which could be a preform (H179).

**Family Tayassuidae.** *Dicotyles tajacu*.- Commonly known as collared peccary, it is widely distributed throughout the whole Mexican Republic, especially in tropical forests and along both seashores. There is an incisive tooth with a conic drill hole that we classified as a pendant (H27).

**Family Cervidae.** *Odocoileus virginianus*.- The white tailed deer is widely distributed throughout the whole Mexican territory in both temperate and tropical zones. The exploitation of this species has been recorded since ancient times until today.

A huge amount of the analyzed materials can be considered as white tailed deer although its specific osseous characteristics that help with its identification are altered, therefore this species was assigned to the modified materials, as only this species could be identified within the collection.

Of the more abundant objects made with this raw material there are 15 of which the next could be distinguished: eleven needles (H94, H50, H143, H146, H154, H107, H193, H48, H249, H174 and H126); three drills (H172, H131 and H249); two dipsticks (H160 and H102), two hollow earflares (H, H83 and H249), two spatulas (H145 and H158), one automorphic object (H178), one needle-earflare (H14), one chisel (H163), one tube (H44a), and one fragment of a finished object whose function could not be determined. The objects that were disposed with manufacturing traces were three, one uterus with handcraft traces and one molar fragment (H25, H181, H168, H23 and H34).

## TYPOLIGICAL ANALYSIS

The typological work was carried out according to Pérez proposal [9], who divides its usage in three, depending on the artifact function: a) practical, b) ornamental and c) votive.

### *a) Practical usage*

The practical usage refers to the objects that had a tool function and in the analysis showed wear traces. Inside the collection we found sharp, beveled edge, blunt and musical objects.

### *Sharp objects*

*(Needle or bodkin).* - Pointed osseous tool which proximal extremity is drilled. Needles are of variable length and section, usually circular, oval or flat. In the analyzed material 12 were identified, 11 of which are from deer and one mammal needle-perforator, all of them correspond to practical objects.

*(Pins or skewers).* - Pointed objects of similar morphology as the needle and identical section, but which proximal extremity is not drilled and it is usually more bulged than the distal. The object in this collection may have had two practical functions (needle-earflare), and it was made in deer bone.

*(Awls, punches and drills).*- These kind of artifacts have an universal function; they can be used in rituals, like tools for different handcrafts; given the wide range of employment they have, their function were established according to the context where they were found, along with their wear traces.

In the collection six objects were analyzed, four of them are of practical usage (one of turkey and three of deer bones), while two are of votive usage (one form grey fox and the other one of deer).

### *Beveled edge objects*

*(Chisel).*- It is a sturdy utensil that has an active part made by a simple or double beveled edge, generally obtained with sawing. The description and definition of chisel can be found without distinction in the literature related to artifacts like straighteners and gouges. The wear traces of this practical instrument can be found in the proximal extremity; the mark leaved by the hammer is the splintering (sharding) and in the distal extremity which usage trace is the blunting and/or the shotting, which is distinctive of this tool. Of the samples it was studied a chisel made of deer bone and its use was practical.

### *Blunt objects*

Primary group defined by a distal extremity obtained through a sewing cross section or through usage, causing bluntness and the regularization of the cutting edge of the piece (10).

*(Spatula, gouge and scrapers).*- Consists of an osseous object that presents both blunt extremities and a long body, but with constant thickness. The artifacts with this morphology have been associated with functions that include from spoons to fur work but they do not have an exact function for which in the typology were denominated like spatulated objects. In the collection four objects were analyzed, one made of a turkey, another from a rabbit and two others from a deer.

*(Dipstick).*- This instrument has an active blunt part or lightly pointed, with its medial part lengthened and plain, similar to that of the needles, employed as pinned hair, cloth or other decoration forms. This name is also applied to the objects obtained from the production of needles and pins. In the typology three dipsticks were studied, one from dog bone and two of deer bone (the first one has a practical usage and the other two are debitage).

### ***Hollow objects***

(*Tube*).- They are lengthened morphology pieces with an annulus section, they are obtained by the adjustment of bird or mammal bones. In the analyzed material three tubes were identified, two made from turkey and one from deer. The function of these is unknown [10].

### ***Musical Objects***

(*Whistle*).- The morphology corresponds to that of the hollow objects, but they always present one or more perforations along the shaft and sometimes they have a semi rectangular piercing. In the collection two whistles were determined, one from turkey bone and other from rabbit which only presented piercing.

### ***b) Ornamental usage***

They are those that decorate different objects, like clothes, feathers, threads, among others [11-13]. Pendants, beads and earflares are also part of this category, for that reason they have the function of decorating the human body.

(*Pendant*).- The so-called ornamental pieces that present one or more drill holes in order to be suspended with a thread or cord, and without a radial symmetry between the objects [13]. In the studied samples five perforated teeth were identified, three of them were from a dog, one from a shark and the last one from a peccary.

(*Bead*).- It is an object that has a drill hole and serves as radial symmetry, generally appearing, although not in every case, grouped in strings [13]. In the Monte Alban collection two tubular beads were found, both made from long turkey bones.

(*Earflare*).- The earflare made on bone is hollow. It is generally made with femurs using the transversal circular section of some even-toed ungulates. For its elaboration the artisan makes two cross sections; then with some abrasive and polishing the medial part of the piece is abraded in both sides (internal and external), until the desired form is obtained. The objects in this site were two hollow earflares made from deer bones.

### ***c) Votive usage***

This use is assigned to those archaeological pieces that were found in offerings, hiding places, or burial associated elements; in other words, there would be those artifacts made to be placed in some of these events or artifacts that were used by the individuals and were buried with them.

(*Figurine*).- There are carved or molded objects, that represent human beings generally made from long

bones. In this typology a figurine representing a man with religious clothing was analyzed and was made from a long deer bone.

## **TECHNOLOGICAL ANALYSIS**

The technological analysis of Monte Alban's bone objects was made according to the methodology proposed by Velázquez [14] and developed within the "Manufacturing Techniques of Shell Objects from Prehispanic Mexico" project. Based on the common lack of the so-called direct production indicators, in this project the technology is studied through experimental archaeology. Following this project, the modifications (abrading, cutting, drilling, piercing, incising, polishing and brightening) made in Prehispanic times are replicated using the bones of modern specimens of the different identified species. The purpose of this is to employ the different materials and tools that according to diverse sources (archaeological contexts, historical sources and studies made by other researchers) can be assumed were used in the past.

To pass over the purely speculative level and in order to propose with major security the tools and techniques employed, the experimental manufacturing traces are characterized and compared with the present traces on the archaeological pieces. This comparison was made in three levels of analysis: macroscopic, optic microscopy at low amplifications (10X, 30X and 63X) and scanning electron microscopy (MEB) (100X, 300X, 600X and 1000X). The latter is the technique that has achieved the best results, and it is suitable in the studies of the superficial characteristics of the materials.

For the technological analysis of the bone objects from Monte Alban, 23 samples with polymer replicating tape were obtained, including pieces of the different identified taxa, as well as the diverse modifications, such as surfaces, edges, drill holes, incised designs and abradings. These samples were covered with gold ions and observed on high vacuum mode, with 20 kV of ray energy, spotsize of 42, a work distance of 10 mm, with a secondary electrons signal (SEI). Four amplifications of each polymer were obtained (100X, 300X, 600X and 1000X). Later, these micrographies were compared with experimental ones on modern material made with the tools that the analyzed traces indicated and with the micrographic database of "The manufacturing techniques of shell objects from Pre-Hispanic Mexico" project directed by Dr. Adrián Velázquez Castro, obtaining the following results:

### Surfaces

Nine polymers of surfaces from the following pieces were examined: a whistle, a bead and one debitage, all from turkey bones (*Meleagris gallopavo*); one pendant from domestic dog (*Canis familiaris*); a pin, a needle, a dipstick, and a chisel from white tailed deer bones (*Odocoileus virginianus*) and one needle-drill of an unidentified bone.

### Incisions

Two incised designs were studied; one in a turkey bone whistle (*Meleagris gallopavo*) and one of the anthropomorphic figurine made from white tailed deer bone (*Odocoileus virginianus*).

### Edges

Nine edges were analyzed: a whistle, a bead, and debitage of turkey bones; one incisive pendant and one dog jaw; a pin, a dipstick and an anthropomorphic figurine made from deer bone.

### Drill holes

Two drills were examined: one from a dog bone pendant and another one from a deer bone needle.

Piercings.- one was examined in a rabbit bone whistle (*Sylvilagus cunicularius*).

The results suggest the following tools:

a) *Surfaces*.- In all the cases it was possible to appreciate straight lines of 3 and 4  $\mu\text{m}$  of width, that are intercrossed producing a rough surface. This traces matches with the experimental abrading with sandstone. Over these features there are thinner lines from 1 and 2  $\mu\text{m}$  (figure 1 and 2).

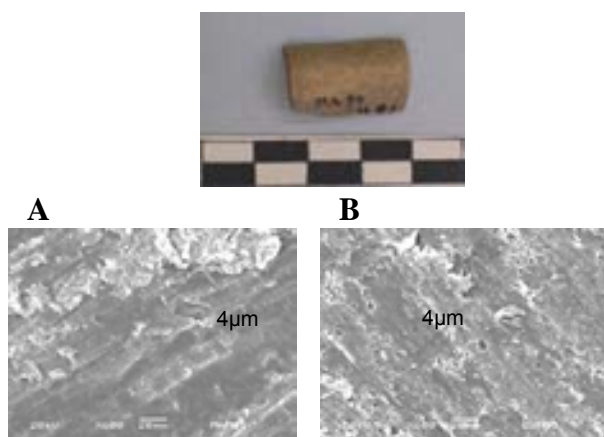


**FIGURE 1.** Bead from *Meleagris gallopavo*, abraded with sandstone, A: archaeological and B: experimental.

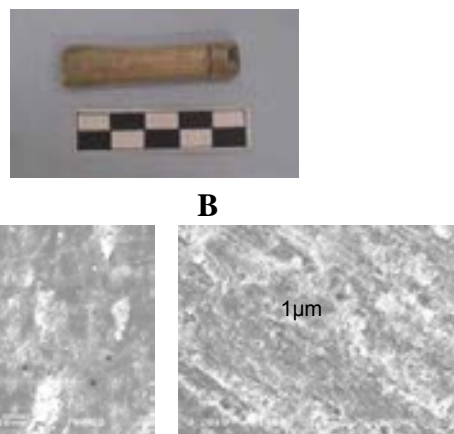


**FIGURE 2.** Whistle from *Meleagris gallopavo*, polished with chert nodule, A: archaeological and B: experimental.

b) *Edges and incised designs*.- In this modifications there are groups of thin lines from 0.6 to 0.8  $\mu\text{m}$  of width, coinciding with the traces produced by cuts or incisions made with obsidian edges or pointy objects (figure 3).

c) *Drill holes*.- On their inner walls, there are intercrossed bands of 3 and 4  $\mu\text{m}$  of width, forming rough surfaces, or joint together in bigger bands, in which interior thin lines can be observed (figure 4).

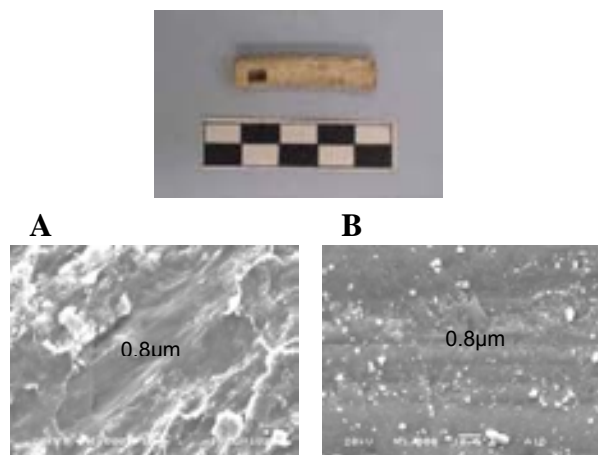


**FIGURE 3.** Whistle from *Sylvilagus cunicularius*, drilled with obsidian. A: archaeological and B: experimental.

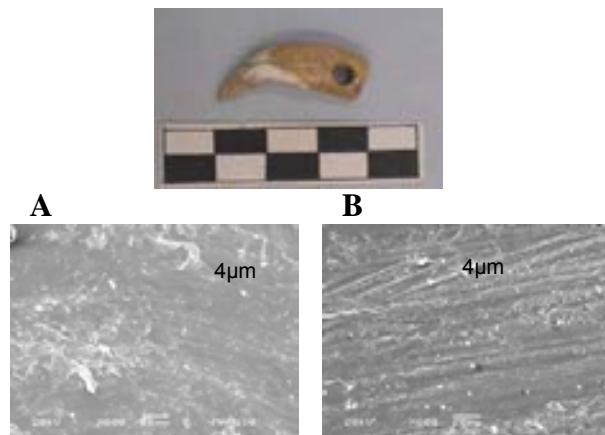


**FIGURE 4.** Pendant from *Canis familiaris*, drilled with chert tool, A: archaeological and B: experimental.

## RESULTS AND DISCUSSION

The obtained results show the whole employment of the fauna at the site, specially the turkey and the deer. There are many evidences that they had been widely used for eating and for the production of different objects and tools, as the studied samples shows. Because from 74 osseous remains identified, the most abundant were from the white tailed deer (63%) and the turkey (27%). Of these samples, only 65 have manufacturing traces and modifications for the elaboration of different tools; the most abundant are the needles (12), drills (4), spatulas (4), and pendants (5). The technological analysis of the different observed elements with the Scanning Electron Microscope showed us that the abrading was made with sandstone, the drilling, piercing and cutting were made with obsidian, and that the polished pieces were made with chert nodules. Only one drill hole was made with a chert burin, a pendant elaborated from a *Canis familiaris* canine.

The amount of debitage elements, joined with the uniformity within the lithic material used for the objects manufacture allowed us to propose that these tools were elaborated in the city of Monte Alban, they are local productions.

## ACKNOWLEDGEMENTS

We thank Dr. Marcus Winter from Oaxaca INAH Center, for providing the analysis material; Dr. Adrián Velázquez from the Templo Mayor Museum, INAH, for his advisory assistance in the manufacturing traces analysis, and Dr. Demetrio Mendoza from the National

Institute of Nuclear Investigations, for his technical support.

## REFERENCES

1. A.T. Clason, A. T. *Helenium*, v. 12, (1972) 139-153.
2. J.S. Davis, *La arqueología de los animales*, Bellaterra, S. A. Barcelona, 1989.
3. R.G. Klein, R. Cruz-Urbe, *The analysis of animal bones from archaeological sites. Prehistoric archaeology and ecology series*, Chicago, Karl W. Búster and Leslie G. Freeman (eds.), University of Chicago Press, Chicago, 1984.
4. O.J. Polaco, "La fauna en el Templo Mayor, una aproximación metodológica", en *La fauna del Templo Mayor*, Oscar J. Polaco (coord.), Colección Divulgación, INAH, México, 1991, pp. 15-31.
5. L.R. Binford, L.R., *Bones: Ancient men and modern myths*. Academia Press New York. New York, 1981.
6. A. K. Behrensmeyer, "Taphonomy and the fossil record", en *The complex processes that preserve organic remains in rocks also leave their own trace, adding another dimension of information to fossil sample*, *American Scientist* **72** (1984) 558-566.
7. A.K. Behrensmeyer, A. P. Hill, *Fossil in the making vertebrate taphonomy and paleoecology*, The University of Chicago Press, Chicago, 1988.
8. L. Starker, *Fauna silvestre de México. Aves y mamíferos de caza*. Instituto Mexicano de Recursos Naturales Renovables, México, 1965.
9. G. Pérez, Gilberto, *El estudio de la industria del hueso trabajado. Xalla, un caso teotihuacano*. Tesis de Licenciatura en Arqueología, ENAH, México, 2005.
10. A. Álvarez, Gema, *De la Caza al Útil. La industria ósea del Tardiglacial en Asturias*, Gobierno del Principado de Asturias, Consejera de Cultura, 1997.
11. L. Suárez, *Técnicas prehispánicas en los objetos de concha*. Colección Científica 14, INAH, México. 1974.
12. L. Suárez, *Tipología de los objetos prehispánicos de la concha*, Colección Científica 54, INAH, México, 1977.
13. A. Velázquez Castro, *Tipología de los objetos de concha del Templo Mayor de Tenochtitlan*, Colección Científica 392, INAH, México, 1999.
14. A. Velázquez Castro, *La producción especializada de los objetos de concha del Templo Mayor de Tenochtitlan*. Colección Científica 519, INAH, México, 2007.

## Objects Made of Copal, A Glance through the Time

Naoli Victoria Lona

*Posgrado en Antropología, Facultad de Filosofía y Letras/Instituto de Investigaciones Antropológicas  
Universidad Nacional Autónoma de México.  
Circuito Exterior s/n, Ciudad Universitaria, México DF C.P. 04510, MEXICO..  
e-mail: naoliv@hotmail.com.*

**Abstract.** Since pre-Hispanic times, copal (resin of *Bursera bipinnata*) has been used for different purposes: medicinal, ritual or religious, which has prompted its transportation from Guerrero state to Mexico City (pre-Hispanic Tenochtitlan), as verified by ethnographic studies in Guerrero, Morelos, Puebla and Mexico City. The resin was brought to Tenochtitlan where it was transformed into different objects like bars, spheres, conglomerates, bases of sacrificial knives, anthropomorphic figurines and diverse amorphous fragments. The macroscopic and microscopic study of more than 300 objects of copal from the offerings of the Archaeological Zone the Great Temple (Templo Mayor), permitted the establishment of a constant in the processes of manufacture of several formal groups, which were then subjected to corroboration by Computerized Axial Tomography (CAT). This radiological technique, created for the study of live human organisms, is very effective in archaeological applications since it is not invasive but still allows observation of the surface of an object as well as its interior by means of virtual slices. In addition, it allows detection of the densities of the components of the object, thus the possibility of establishing different materials of its composition.

**Keywords:** Copal, Templo Mayor Tenochtitlan, Computerized Axial Tomography (CAT), resin, offerings.

### INTRODUCTION

Copal is one of the vegetal resins most frequently used in Mesoamerica since pre-Hispanic times, not only for its medicinal properties, but also for its ceremonial attributes expressed in its peculiar odor and its white smoke when burned, that is believed to facilitate the communication between the humans and their deities gods that govern the earthly order.

This study is based on copal found in Mexica archaeological contexts of the Great Temple of Tenochtitlan (Late Postclassic period, AD 1325 - 1521). But, in order to understand the ancient role of copal, it was also important to consider its modern production, in an interdisciplinary perspective with archaeological, historical, botanical and ethnographic aspects, including physical, chemical and radiological

analyses, such as Computerized Axial Tomography (CAT).

Historical sources and material evidence shows that copal (*Bursera bipinnata* for Mesoamerica), in addition to being burned in ceremonies, was deposited in the offerings to the gods in different forms, classified in general as geometric, anthropomorphic and amorphous objects.

The same tree produces two types of copal: gum, stone or wild and the "saint" (*santa*), white or "penca" (leaf of *Agave*). The first appears naturally on the surface of the trunk like in little mostly grayish. A curved knife is used to scratch the surface of the trunk and branches, separating the fragments of fresh copal, with a gumlike consistency, but like small stones.

White copal is obtained by diagonal cuts in the trunk or branches provoking the emanation of the

semi-liquid milky sap of the tree, which accumulates in *Agave* leaves placed by the “copaleros”. As the substance hardens, it takes the form of its container, resulting in bars of white copal. This is the most common form in which this type of resin has been transported since pre-Hispanic times from the provinces Tlachco and Tepecuacuilco to Tenochtitlan as tribute every 80 days: 8000 packages of wild copal wrapped in maize leaves and 400 baskets of white copal in bars [5, 10].

## EXPERIMENTAL DETAILS

### Formal groups of objects of copal

The archaeological collection (of over 300 elements of copal found in 61 offerings) has been classified in six formal groups: bars, spheres, conglomerates, bases of sacrificial knives, anthropomorphic figurines, and miscellaneous fragments recovered from the Great Temple of Tenochtitlan and adjacent buildings.

The manufacturing process was established based on a detailed description of every object in the archaeological collection considering, and an analysis of the process of deterioration.

Different stages of conservation allowed to establish the stages of the process on having reverted the action of the deterioration, being complemented by analyses of radiological type that corroborated some of the hypotheses developed as result of the first stage of the study.

### Physical principles of Computerized Axial Tomography (CAT)

CAT is a method of sectional imaging which shows the structures in axial or transverse plane, without overlapping, considering the density of the materials in a system of units called Hounsfield Units [2]. Although this technique was developed for use in the study of the relative density of human organs, because it is non-invasive, it has a number of potential applications in archaeology (Figure 1).

Analysis of the density of human organs generated basic information with values that identify water as 0(zero) Hounsfield Units; muscles and organs with an average value of 80; calcium and bone, 400; metal, 2000; fat, -40; and air, -1500.

Some of these measures were useful to identify materials in the interior of the pieces of copal, for example, stucco compared with calcium, and air that indicated spaces within the object. To complement the basic information for the study of copal, modern and ancient resin was subjected the tomography, revealing densities between -80 and -50, regardless of the age of the material. Other elements mixed in the copal objects

were also measured, such as small stones and straw with a density of 30 and 60 Hounsfield Units.

The same procedure used for humans was applied to the archaeological material; the piece was placed on the table that slides towards the gantry to take the images, to measure densities, and to generate three-dimensional images.

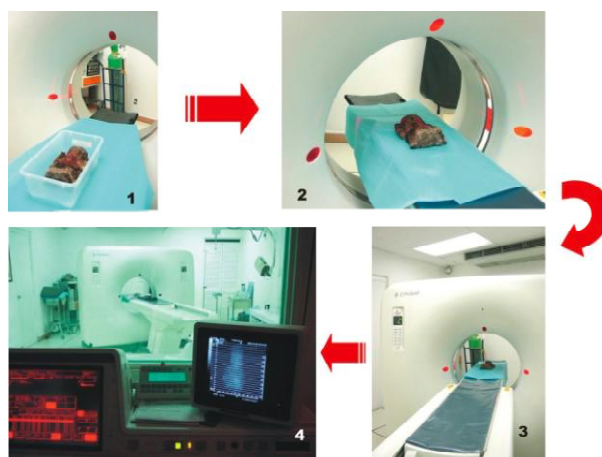


**FIGURE 1.** Process of the analysis of the archaeological pieces with CT (Photography by author).

To be able to work the resin, in any of its presentations, heat is necessary to smooth and shape it like clay. Different evidence indicates the application of direct and indirect heat on the vegetal material, such as crystallized areas and stains on one hand, and fingerprints from shaping the resin or warming the resin in pots on the other [10].

This latter procedure is suggested by Fray Bernardino de Sahagún, who describes how copal and other substances like the “chapopotli” (tar) and the “ulli” (rubber), were crumbled to melt them in pots that were placed on embers to make medicinal ointments or a kind of cream [8], and it is possible that the copal resin was warmed in the same way to manufacture the objects.

## RESULTS

### Bars of white copal

The ethnographic study of copal helped significantly to understand the manufacture of the bars, because as previously mentioned, the fresh resin takes the shape of the *Agave* leaf used like a mold and the consequent marks are visible on the surface. In general, when the *Agave* leaf is filled with copal, it is replaced by another one, but sometimes the resin spills, and the drops are called “lágrimas” (tears) because of their shape and origin; these are used just like the rest of the copal, although they are less

expensive. These elements, similar to stalactites, could be the small leaves or flakes of white copal found in archaeological contexts (Figure 2).

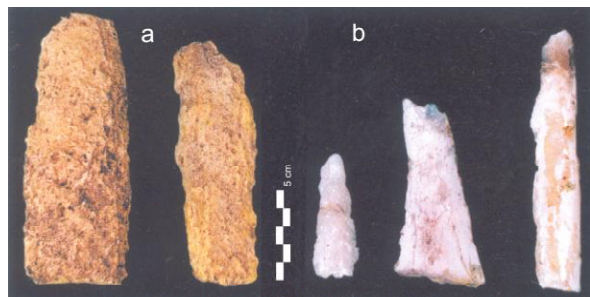


**FIGURE 2.** Pre-Hispanic (a) and modern (b) copal bars (Photography by author).

### Spheres and conglomerates of gum and white copal

These objects were asymmetrical but with a clear general shape, with small visible depressions possibly caused by the pressure made with the fingers, and in

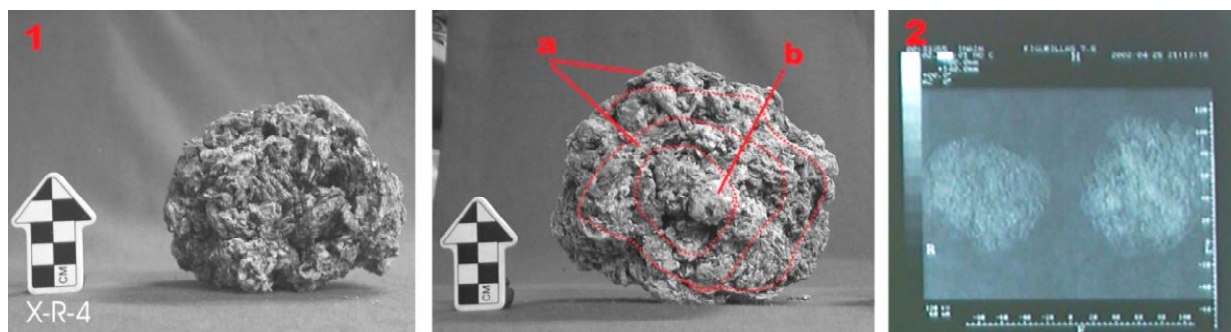


**FIGURE 1.** Spheres of gum copal (offering X). The images (1, 2) shows that they were shaped (a) in concentric layers since (b) a central sphere (Photography by author).



**FIGURE 2.** Sacrifice knives of flint with bases of white and gum copal: (a) White copal (offering 11); (b) white copal (offering 6); (c) Gum copal (offering 6) (Photography by author).

other cases marks resulting from smoothing or polishing (Figure 3).

The process of manufacture starts by joining fragments of the resin to make a spherical nucleus. On its surface, concentric layers are added until the desired form and size is obtained, leaving spaces between every layer and fragments of copal adhered.

The external layer of the object was smoothed or polished, and subjected to heat to enhance the adhesive properties of the resin and to assure the consolidation of the piece.

### Bases of sacrificial knives of gum and white copal

The principle is similar to the spheres and conglomerates, the difference being that the fragments of copal do not stick to a nucleus of resin, but to the proximal section of the knife starting with the flat faces, and later, the lateral ones. The object is then smoothed or polished fire or heat is possibly applied to possible to consolidate the components (Figure 4).

### Anthropomorphic figurines of white copal

The process of manufacture of anthropomorphic figurines was established on the basis of the analysis of 80 pieces of this group, comprised of 19 female figurines, 53 male figurines and 8 of indeterminate genre as a result of poor conservation.

A nucleus of copal is evident, with specific facial and corporal characteristics, made by joining fragments of resin in a mold until it is filled (Figure 5). The nucleus is then covered with a layer of stucco, using a double mold where the representation of facial and corporal features is evident, such as apparel [10].

Finally the figurines are decorated by pigments and garments made of paper, and occasionally complementary elements like flags (Figure 6).

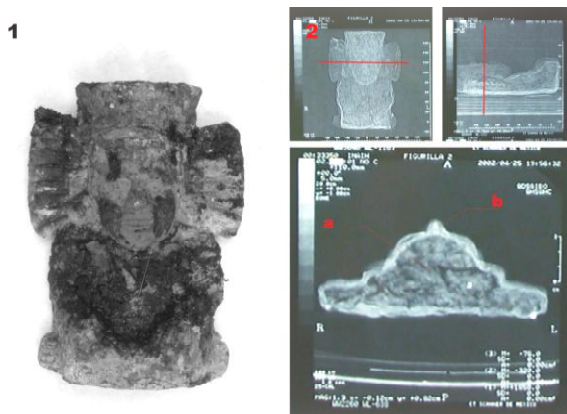


**FIGURE 3.** The tomography (2) of figurine of copal (1) shows clearly the copal nucleus (a) wrapped by the stucco layer (b) (Photography by author).

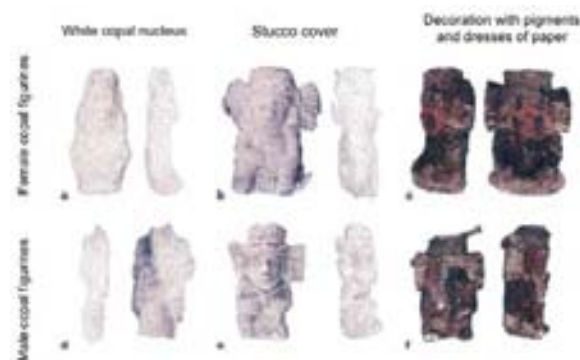


**FIGURE 4.** The nucleus of copal (a, d) is covered by a stucco layer (b, e) on which it was decorated with pigments and garments of paper (c, f) (Photography by author).

## DISCUSSION

Copal is a resin used since pre-Hispanic times, with both curative and religious uses that was burned and buried in diverse forms. There are two kinds of copal: gum and white, which can be observed in mass and in small leaves or flakes.

The formal classification for the collection of copal objects from the Great Temple is: bars, spheres, conglomerates, bases of sacrificial knives, anthropomorphic figurines and diverse fragments specified as miscellany.

For the successful manufacture of copal objects, it is necessary to soften the resin, so the application of heat is an essential part of the process.

The adhesion of fragments of resin was common to obtain the desired forms, the surface of which was smoothed to give the appearance of a single unit.

Figurines were elaborated by shaping a nucleus of copal and stucco covering, over which the decoration is placed.

The process of deterioration is useful to rebuild the process of manufacture of the copal objects.

## CONCLUSIONS

The macroscopic analysis of more than 300 objects provides an important base to propose and to corroborate manufacture hypothesis.

Working with the analytic tools of different disciplines, such as the invaluable contribution of the Computerized Axial Tomography, is important because it allowed us to corroborate the macroscopic observations, thus providing more information about the technical process of manufacture, such as the materials used in the manufacture of the objects without destroying the archaeological pieces, because it is a non-invasive and very exact tool.

## ACKNOWLEDGMENTS

Author acknowledges the support of Dr. José Luis Criales, director of CT Scanner de México, Dr. Leonardo López Luján from Museo Templo Mayor - INAH, Mtro. Adrián Benítez, and thanks the enthusiasm of all those that contributed and supported this research.

## REFERENCES

1. F.F. Berdan, P. Rieff Anawalt, *The Essential Codex Mendoza*. University of California Press, Berkeley, 1997.
2. J.L. Criales, personal communication (2004).
3. D.C. Harwood-Nash, *Journal of Computer Assisted Tomography* **3** (1979) 768-773.
4. J.K. Lee, S.S. Sagel, R.J. Stanley, *Computed Tomography*. Raven Press. New York; 1983, 1-5.
5. *Matrícula de Tributos*, interpretation of Víctor M. Castillo & Ma. Teresa Sepúlveda. Edición facsimilar de la Secretaría de Hacienda y Crédito Público. México, 1991, p. 31; Láminas. 16r, 17r.
6. R.L. Moodie, *Roentgenologic Studies of Egyptian and Peruvian Mummies*. Chicago Field Museum of Natural History, Chicago, 1931.
7. WMF Petrie (Deshaced, 1987).
8. B. de Sahagún, *Historia General de las cosas de Nueva España*. **3**, 1126. Cien de México / CONACULTA. México, 2000.
9. *The Codex Mendoza*, Frances F. Berdan y Patricia Rieff Anawalt (eds.). University of California Press, Los Angeles, 1992, Láminas. 38r, 39r .
10. N. Victoria Lona, *El copal en las ofrendas del Templo Mayor de Tenochtitlan*, Dissertation thesis in Archaeology, Escuela Nacional de Antropología e Historia, INAH, México, 2004 (in press).

## **ICP-MS Analysis for the Characterization of Obsidian Sub-Sources in Sierra de Pachuca Region, Hidalgo, Mexico**

Denisse Argote Espino<sup>1</sup>, Jesús Solé Viñas<sup>1</sup>, Osvaldo Sterpone Canuto<sup>2</sup>  
and Pedro López García<sup>3</sup>

<sup>1</sup> *Instituto de Geología, Universidad Nacional Autónoma de México, MEXICO. e-mail: jsole@geologia.unam.mx*

<sup>2</sup> *Centro INAH-Pachuca, Instituto Nacional de Antropología e Historia, MEXICO.*

<sup>3</sup> *Escuela Nacional de Antropología e Historia, Instituto Nacional de Antropología e Historia, MEXICO.*

**Abstract.** Central Mexico contains several of the most important obsidian sources in Mesoamerican lithic industry. Numerous archaeological investigations suggested that economical and political expansion of some of the major Mesoamerican societies were linked to the control of the obsidian sources and its distribution. Sierra de Pachuca still is one of the most important sources of raw material and has several mines spread around the region. Some of the main quarries in Sierra de Pachuca in pre-Hispanic times were: Cruz del Milagro, El Durazno (El Nopalillo), Sembo and Oyametal. Each sub-source suffers a preferential exploitation by particular cultures. For example, Teotihuacan is generally correlated to Cruz del Milagro peak and probably Zembo quarry, while El Durazno one is associated with Tenochtitlan's control. A geochemical characterization of each sub-source would be of great importance in the identification of obsidian artifacts found in diverse archaeological settlements giving a direct connection to influence zones of the culture associated with the control of each specific mine. Although X-ray Fluorescence (XRF) analysis of major and minor chemical elements has proved to be inconclusive, trace elements in ppb or ppt, including rare earths, could give us a better clue. Having this purpose in mind, an Inductively Coupled Plasma Mass Spectrometer (ICP-MS) was applied to analyze 12 obsidian samples collected from these four sub-source locations at Sierra de las Navajas, followed by several statistical analysis (discriminant, fuzzy cluster, among others). This study shows the importance of accurate characterization of obsidian raw material when attempting to define sub-source usage.

**Keywords:** Obsidian, Sierra de Pachuca, Mesoamerica, ICP-MS, Multiple-Discriminant Analysis

### **INTRODUCTION**

Obsidian is usually a siliceous volcanic glass, widely used by Mesoamerican people to make tools, ornaments and weapons since prehistoric times. This natural resource was so valuable during the pre-Hispanic period that large commercial networks developed in order to distribute it through out Mesoamerica. Thus, provenance studies of obsidian are important indicators of economical and cultural interaction between ancient civilizations.

For long time, archaeologists have relied on obsidian artifacts and raw materials analysis based on their external optical characteristics to identify their sources. Nowadays, artifact's chemical analysis plays an important role in provenance studies. Obsidian is a suitable archaeological material for this kind of research, when compared to organic or ceramics materials, because the internal composition of an obsidian source is usually very homogeneous exhibiting little variability, although differences between sources are much larger. Therefore the use of a high precision chemical technique will lead to the

identification of sources with a high degree of certainty. Multi-element trace analysis applied to obsidian archaeological samples can discover distinctive trends or patterns traceable to their natural sources. Several studies on this topic have already been published and the reader can follow the researches undertaken by Carballo, Cobean, Glascock, Healan, Neff, Neivens, Smith, Spence, Vogt, Weigand [1-5,7,10-11,14-15].

Pachuca obsidian source, known to archaeologists as Sierra de las Navajas, has been a major obsidian source for Mesoamerican societies for more than 3000 years, producing fine unique green obsidian. This obsidian is known for its clean conchoidal fracture and almost complete lack of crystals, making it ideal for tool manufacture and projectile points. This primary obsidian source was the economic backbone of major sociopolitical centers in the central Mexican highlands like Teotihuacan, Tula and Tenochtitlan, and established the basis for local and long distance consumption and trade. Pachuca's obsidian has been found as far to the South as Honduras and El Salvador [2], and in Oklahoma to the North of Mesoamerica [1]. However, the amount of Pachuca's obsidian found in archaeological sites decreases as distance increases from the source.

Sierra de Las Navajas obsidian exploitation, carried out during thousands of years, resulted in a very complex mining enterprise, generating thousands of quarries and human settlements. Among the important mining areas in Las Navajas there were: Cruz del Milagro, El Durazno, Sembo, Rancho Guajolote and Oyametl. Traditionally these locations have been associated to production by different peoples and cultures, for example, Teotihuacan is generally said to have mined the Cruz del Milagro peak, including the Sembo location, while El Durazno quarry is associated with Aztec Tenochtitlan's control. Nevertheless, according to local people accounts, there are still more obsidian mines along the slopes of Las Navajas that have yet to be discovered, described and stratigraphically explored, including mines along the central and western ridges [9]. Research undertaken by Pastrana since 1987 in the Durazno area has discovered settlements and housings, activity areas related to obsidian mining and tool transformation processes from Classic (200 A.D.) to Postclassic periods (1520 A.D.) [13].

## GEOLOGICAL SETTING

Sierra Las Navajas is an extinct peralkaline rhyolitic volcanic center located on the northern edge of the Trans-Mexican Volcanic Belt, south of the Sierra Madre Oriental, between the cities of Pachuca and Tulancingo, Hidalgo, Mexico. Las Navajas volcanic deposits cover approximately 250 km<sup>2</sup> and consist primarily of pyroclastic and rhyolite lava flows

with numerous basaltic cinder cones and flows along the flanks. Two principal geological moments formed this region: its Eastern portion is conformed by volcanic cones and domes of the Late Pliocenic age with a composition ranging from andesite to rhyolite; the Western portion belongs to the Pleistocene, when the largest volcanic structures formed, and its composition ranges from andesite to dacite [10]. Four distinct flow complexes are present, each one is composed of one or more lava flows tapping the same magma chamber. In all cases the obsidian appears to have been emplaced as continuous bands within a larger flow. These obsidian bands originally alternated with bands of pumiceous or crystalline rhyolite, which have since weathered to aluminum-rich clay. The volume change associated with this alteration resulted in breaking the brittle obsidian into easily mined blocks [9].

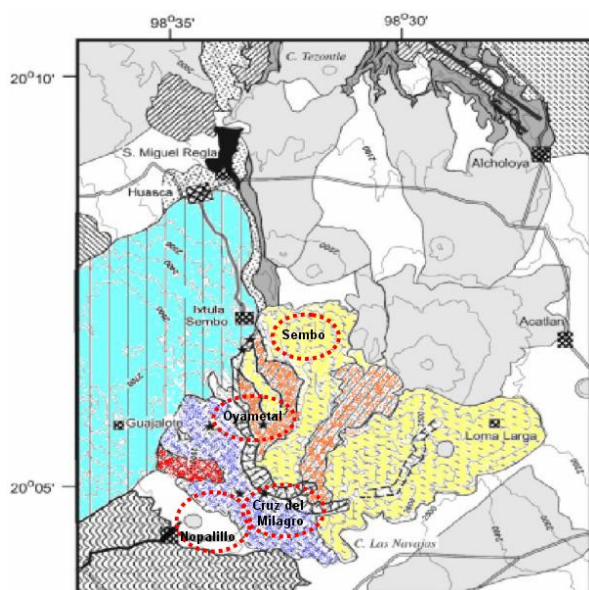


**FIGURE 1.** Sierra de Pachuca geology [9] denoting the four principle obsidian flow complexes: (red) Guajolote, (purple) Las Minas, (orange) Ixatla, (yellow) El Horcón.

The geology indicates a long and varied volcanic history at Las Navajas. The first major obsidian-bearing lava flow were the minimally exposed Guajolote flows to the Southwest, followed by the best known Las Minas flows to the West and South. Later, the collapse of the Northern side of the volcano produced a catastrophic debris avalanche that apparently exposed the magma chamber, causing explosive eruptions. <sup>40</sup>Ar/<sup>39</sup>Ar geochronology of the basalts immediately underlying and overlying the debris avalanche deposit give an approximate date for the avalanche of 2 My [9]. The southern and central Ixatla post-avalanche flow complex fills part of the collapsed amphitheater, and it is associated with a

banded-gray obsidian not as prolifically mined as the clear green Las Minas obsidian.

El Horcon final eruptive complex (composed of rhyolites and obsidians) filled the collapsed amphitheater and overflowed its Eastern and Western walls, forming all of the major peaks of Las Navajas. and El Horcon Flow to the East and North. El Horcon final eruptive complex (composed of rhyolites and obsidians) filled the collapsed amphitheater and overflowed its Eastern and Western walls, forming all of the major peaks of Las Navajas. The North and East flanks of Sierra Las Navajas are also covered with post-avalanche El Horcon flows. El Horcon flows bear crystal-rich grey or brown obsidian unsuitable for use.

The obsidian is found in two forms: as part of a lava flow (several occurred in the Pliocene) or in blocks carried down the cliffs. Except from the peak of Cerro del Milagro, where the obsidian can be outcropped, blocks of obsidian in a loose matrix are routinely mined or excavated from the surface, but mostly have been obtained through deep shaft mines with horizontal tunnels branching out to optimize the richest subsurface layers [12].

## METHODOLOGY

Following Lighthart [9] observations on the obsidian emplacement as part of an original flow and not as debris dragged by a lahar [12], and knowing the existence of four different volcanic flows in the region with distinctive geochemical patterns, we intended to demonstrate the hypothesis that diverse important mining areas were not related to the same flow. So, if sub-sourcing interpretations are correct, this will enable us to identify some mining processes and obsidian extraction and subsequently determine who were the actors exploiting it or controlling these processes in pre-Hispanic times.

The linkage between quarry production and obsidian products in a regional exchange context requires accurate characterization of lithic artifacts. Lithic sources with multiple loci of raw material often present difficulty in determining these loci once the material has been transported to distant sites. Sub-source characterization, compared to source characterization, can be used to trace artifacts back to a specific quarry location [2,15]. Previous X-ray Fluorescence (XRF) experiments with raw material collected in the area were not conclusive as to determine whether there were different groups within the same major source. Classification of major and minor elements did not give out accurate results. So, an ICP-MS analysis was applied in order to define key trace elements capable of accurately discriminate between the different sub-sources.

Induced Couple Plasma Mass Spectrometry was developed in 1980's decade. It combines the ICP technology with the accuracy and the low limit

detection of a mass spectrometer, making easier the introduction of samples and a faster analysis [8]. The following steps provide a brief overview of how the ICP-MS analyzes the sample. First, the sample solution is pumped into the inlet system, where is nebulized, forming a fine sample aerosol. The aerosol is then carried into a high temperature argon plasma, which atomizes and ionizes the sample to produce a cloud of positively charged ions. The sample ions are extracted from the plasma into a vacuum system containing a quadrupole analyzer or mass filter. The analyzer can scan the mass range very quickly, so multi element analysis can be performed on the sample. The ions are focused into the analyzer, where they are separated by their mass to charge ratio ( $m/z$ ). The ion concentration of a specific mass to charge ratio is measured by an electron multiplier detector. The count rate obtained for a particular ion is compared with a calibration plot to give the concentration for that element in the sample (for quantitative analysis).

Carballo et al. [3] showed that the cost per sample using ICP-MS is much lower than INAA analysis and that a sample size of one to eight for ICP-MS is comparable to the analysis of over 30 quarry samples with INAA. In this basis, we analyzed a total of 12 obsidian samples collected from four of the principal sub source locations at Sierra de Pachuca (Cruz del Milagro, Nopalillo, Sembo and Oyamental), followed by several statistical analysis (discriminant, fuzzy cluster, between others). An Agilent 7500 ICP-MS model was employed. After the determination of trace elements and rare earth composition of the samples, we proceed to explore the data with statistical software applying a Multivariate Discriminant Analysis. We chose this technique among others because of the type of variables we are managing (one dependent categorical and several independent numerical), and because it analyzes all the data at once, determining the variables that contribute the most to the classification model [6], avoiding the trail-error part of the traditional bivariate plotting.

## RESULTS

In the rare earths normalized plot, the patterns of the four sub-sources show the same trend and can not be tell apart. When we applied the Discriminant Analysis, we recognize that the variables that contribute the most to the model are Cd and Ba, principally, and U and Sc with less importance (Table 1). The classification matrix shows us a 100 % certainty classification for Oyamental, Sembo and Durazno sub-sources, and a 66% for Cruz del Milagro quarry. One of the samples of Cruz del Milagro is classified as part of Sembo sub-source.

When plotting the first two discriminant functions, those that contain most of the information, we see that the samples for each sub-source are contained in a different quadrant with one exception only. An Oyametal sample is drawn in the quadrant containing the El Durazno samples.

TABLE 1. Summary of the discriminant analysis of the ICP-MS results for Sierra de Pachuca samples

Variables in the model					
	Wilks' Partial L	F-remove	p-level	Toler.	1-Toler.
Cd	0.023512	89.2201	0.00017	0.01811	0.98389
Ba	0.109644	13.5339	0.00778	0.03349	0.96650
U	0.217163	6.00807	0.04113	0.07639	0.92360
Sc	0.34217	3.20421	0.12114	0.69145	0.30854

Classification Matrix					
Rows: Observed classifications					
Columns: Predicted classifications					
	Percent	Durazno	Sembo	Cruz	Oy
Durazno	100.00	3	0	0	0
Sembo	100.00	0	3	0	0
Cruz	66.667		1	2	0
Oy	100.00	0	0	0	3
Total	91.667	3	4	2	3

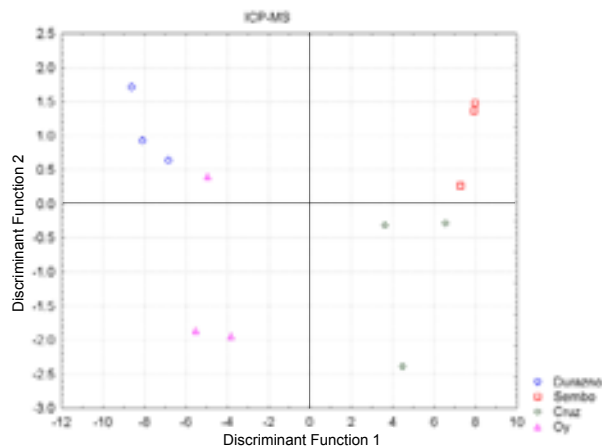


FIGURE 2. Plot of the first two discriminant functions.

### CONCLUSIONS

The Sierra de Pachuca obsidian represented one of the principal pillars in the economical and cultural structures of Mesoamerican civilizations.

This work shows part of the great potential of analytical methods in the chemical characterization of obsidian sources and the identification of the provenance of archaeological material. As Neivens et

al.[11] wrote: “Micro-sourcing offers the archaeologist a tool for looking beyond the trade routes and into the processes of economic and social order”.

Although data is not totally conclusive, certain degree of sub-sources classification was shown. Further studies are still been applied (for example, geochronology and artifact analysis) to obtain a more complete knowledge of the region geology that could indicate us valuable differences between the sub-sources. Nevertheless, the ICP-MS combined with the application of a Multivariate Discriminant Analysis gives a good approximation of sub-source differentiation in Sierra de Pachuca region.

### ACKNOWLEDGMENTS

This research has been supported by PAPIIT-UNAM Mexico project IN118809. Authors thank Patricia Girón, Elena Lounejeva and Juan Pablo Bernal for the great and patient assistance in the instrumental analysis.

### REFERENCES

1. A.W. Barker, C.E. Skinne, S. Shackley, M.D. Glascock, M.D., J.D. Rogers, *American Antiquity* 67 (2002) 103–108.
2. G.E. Braswell, E.W. Andrews, M.D. Glascock, *Ancient Mesoamerica* 5 (1994) 173–192.
3. D.M. Carballo, J. Carballo, H. Neff, *Latin American Antiquity* 18 (2007) 27-43.
4. R.H. Cobean, *A world of obsidian: the mining and trade of a volcanic glass in ancient Mexico*. INAH- Pittsburgh University, Mexico, 2002.
5. M. Glascock, G.E. Braswell, R. Cobean, “A systematic approach to obsidian source characterization” in *Archaeological Obsidian Studies*, S. Shackley (Ed.), Plenum Press, New York, 1998, pp. 15-66.
6. J.F. Hair, R.E. Anderson, R.L. Tatham, W.C. Black, *Multivariate Data Analysis with Readings*, Macmillan Publishing Co., Toronto, 1992.
7. D.M. Healan, *Ancient Mesoamerica* 8 (1997) 77-100.
8. K.E. Jarvis, A.L. Gray, R.S. Houk, *Handbook of inductively coupled plasma mass spectrometry*. Blackie Academic & Professional, London, 1996.
9. A. Lighthart, *Geoarchaeology* 19 (2004) 71-91.
10. F. López, R. Nieto, R. Cobean, “La producción de obsidiana en la Sierra Las Navajas, Hgo.”, in: *La obsidiana en Mesoamérica*, M. Gaxiola y J.E. Clark (eds.), Serie Arqueología, Instituto Nacional de Antropología e Historia, Mexico, 1989, pp. 193-197.
11. M. Neivens, G. Harbottle, K. Kimberlin, “Some geochemical characteristics of the Pachuca obsidian region: a strategy for interpreting artifact groups”, in: *La obsidiana en Mesoamérica*, M. Gaxiola y J.E. Clark (eds.), Serie Arqueología, Instituto Nacional de Antropología e Historia, Mexico, 1989, pp. 51-58.
12. A.R. Pastrana Cruz, *La explotación azteca de la obsidiana en la Sierra de las Navajas*, Serie

- Arqueología, Instituto Nacional de Antropología e Historia, Mexico, 1998.
13. A.R. Pastrana Cruz, *La secuencia de explotación de la obsidiana de La Sierra de Las Navajas, Hidalgo, México*, UAH, México, 2008.
  14. M.E. Smith, A. Burke, T. S. Hare, M. D. Glascock, *Latin American Antiquity* 18 (2007) 429-450.
  15. M.W. Spence, J. Kimberlin, G. Harbottle, "State-controlled procurement and the obsidian workshops at Teotihuacán, Mexico", in: *Prehistoric quarries and lithic production*, J.E. Ericson & B.A. Purdy (eds.), Cambridge University Press, Cambridge, 1984, pp. 97-105.

## Plumbate Technology Revisited

H. Neff

*Institute for Integrated Research in Materials, Environments, and Society, California State University, Long Beach, 1250 Bellflower Blvd., Long Beach, CA 90840, USA. e-mail: hneff@csulb.edu*

**Abstract.** Plumbate ware is unique in pre-Hispanic Mesoamerica for several reasons, chief among them being the extremely hard, lustrous, glazed surface. Creating a surface with these properties certainly required a unique combination of raw materials and technological practices. Half of this formula has been solved by the recent demonstration that the Plumbate source zone lies on the Pacific coast near the border between Chiapas and Guatemala. The next step is to unravel the technological process that turned the raw clays of this region into Plumbate. In this paper, I present new hypotheses and analytical results bearing on Plumbate raw-material preparation and pyrotechnology.

**Keywords:** Plumbate, glaze, alkali, pottery, laser ablation-ICP-MS

### INTRODUCTION

Plumbate is distinguished by a highly lustrous, extremely hard surface that varies in color from orange to olive green and gray. Anna Shepard [1] demonstrated that the surface is, in fact, vitrified, making it the only pre-Hispanic glazed ware from Mesoamerica. Although archaeologists and explorers have long been fascinated by its wide distribution and unusual technological qualities [2], it was not until the 1950s and 1960s that archaeologists correctly inferred that Plumbate was produced on the Pacific coast, in the vicinity of the Chiapas-Guatemala border. Coincident with Shepard's ceramic technological work, archaeological surveys by Edwin Shook [3], Philip Drucker [4], and Gareth Lowe [5] and excavations by Bertha Dutton [6] showed that Plumbate peaks in frequency in this region.

Shepard [1] had used petrographic analysis to identify two paste types, which were both typologically distinct and, apparently, chronologically successive. My dissertation research [7] established that the petrographic paste types are also distinct chemically, but based on analyses from the likely production region, the stylistically simpler, presumed earlier (San Juan) vessels were made of both pastes rather than just one, as Shepard had concluded. This evidence accorded with the hypothesis that the fancy,

decorated vessels (Tohil) originated in this region, despite their comparative rarity in sherd collections.

I originally investigated the evolution of Plumbate pottery production as a Ph.D. dissertation project and have conducted related work more recently [8, 9]. The more recent work included a survey of clay and tempering materials on the coastal plain on both sides of the Mexico-Guatemala border. Analysis of these materials and comparison to Plumbate reference groups identified the source of San Juan Plumbate as the coastal plain along the lower Rio Naranjo region in Guatemala and the source of Tohil Plumbate as the lower Rio Cahuacan in adjacent Chiapas, Mexico (Figure 1).

Field observations in 2004 within the mangrove zone of the Estero Ponce, near the mouth of the Rio Cahuacan, further strengthen the hypothesis that this region is where Tohil Plumbate was produced. Robert Rosenswig [10] had identified a number of mounds within the mangrove forest, some of which have extremely dense concentrations of Plumbate sherds. During our visit in 2004, Rosenswig and I found fired, red earthen features eroding out of the edges of several of these mounds. A clay sample collected near these mounds, like the lower-Cahuacan clays collected earlier [8], matches the elemental profile of Tohil Plumbate. The co-occurrence of matching raw materials, dense sherd (waster?) concentrations, and kiln or open-pit firing remains implies very strongly

that the Estero Ponce is where Tohil Plumbate was produced.

Thus, a wealth of evidence indicates that Plumbate was produced within the littoral zone or on the lower coastal plain. Was Plumbate production actually *confined* to the lower coast (as opposed to being practiced there as well as other locations), such that its appearance at inland locations such as Izapa reflects economic exchange? While the available chemical compositional evidence favors this interpretation, a technological hypothesis pointing to the same conclusion can also be proposed.

There are relatively few possible explanations for the hard, vitrified surface of Plumbate. Shepard [1] suggested that reduced iron, FeO (in a reducing atmosphere), acted as a flux, which promoted vitrification of a high-alumina slip at temperatures around 950° C. There is no analogue for such a process, however, and this explanation leaves the lustrousness of orange (oxidized) surfaces unexplained. On the other hand, there are many examples of alkaline glazes, including "salt-glazing." All alkaline glazes are produced by the fluxing action of alkali metals such as sodium or potassium when mixed with silica and alumina (both of which would be present in a slip clay). In "salt glazing," sodium gas produced by throwing rock salt into a hot kiln fluxes silica and alumina on the vessel surface, creating vitrified, often crazed, grayish surfaces[11]. Glaze can also be produced by mixing brine into the slip clay. Shepard [1] did not consider the possibility that the unique Plumbate surface was an alkaline glaze of some kind, but the recent evidence that Plumbate was a littoral zone product raises this possibility.

Invention of an alkaline glaze on the lower coast could have been a by-product of pyro-technological practices of lower-coastal populations. Besides pottery production, the other Classic-period economic activity evident at sites within the mangrove-estuary zone is salt production. Oblong ceramic supports and firing features indicate that salt was produced by the "*sal cocida*" technique, in which heat is used to evaporate water from brine in ceramic containers [12,13]. Accidental over-heating and production of sodium gas could have fortuitously caused the fusion of silica on the surface of salt-making vessels.

Wood can contain up to 15% potash, and mangroves concentrate salt in old tissues, so wood ash from mangroves could have enriched both potash and soda in the slip clay. This expectation is, in fact, borne out in analysis of mangrove wood ash from Nigeria [14]. Slip clays might also have been prepared with saline or brackish water, which would have both promoted deflocculation of clay particles and furnished the sodium that volatilized during firing and acted as a flux.

Another route to invention of an alkaline glaze could have involved accidental or purposeful (perhaps

to promote deflocculation) mixing of mangrove-wood ash, a by-product of salt production, with slip clay.

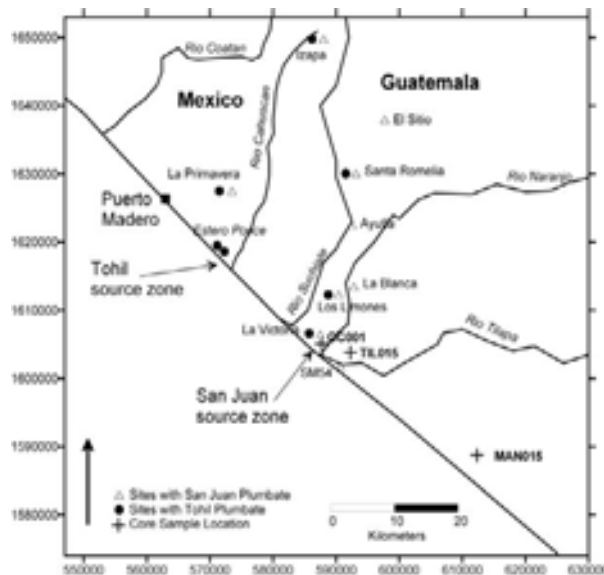


FIGURE 1. Map of eastern Soconusco showing locations mentioned in the text.

## NEW EVIDENCE ON THE NATURE OF PLUMBATE GLAZE

Evidence pertinent to the alkaline-glaze hypothesis has been generated recently through several kinds of analysis of Plumbate surfaces. First, the assumption that slip and body clay are different components, the slip having been enriched in alkaline fluxes, implies (1) that the slip should be enriched in sodium, potassium, and possibly other fluxes relative to the body, and (2) there should be little or no correlation between levels of fluxes in the slip and body. In addition, vitrification of the surface should produce some element mobility within the surface layer, so that there should be a clear depth-related gradient through the surface layer.

The first set of predictions can be tested by comparing INAA data on Plumbate pastes vs. XRF data on Plumbate surfaces. Since the latter analyses were done on intact surfaces, some of the fluorescent x-rays will come from the underlying paste, but the data should be dominated by the surface, which is estimated to be about 50 micrometers thick. As shown in Figure 2, the predicted enrichment in one key alkali, potassium, is borne out across a substantial number of San Juan, Tohil, and unassigned Plumbate sherds. XRF determinations on the surface are two to five times the concentrations measured on the underlying pastes. Although there may be some systematic bias between measurements made using the two different techniques, the XRF calibration for potassium was

developed carefully because it is used for potassium determination in luminescence dating dosimetry. On powdered specimens, the XRF values compare favorably with INAA values.

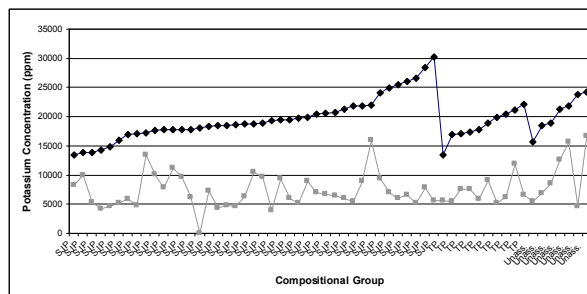


**FIGURE 2.** Potassium concentrations in surfaces (diamonds) and paste (squares) of San Juan, Tohil, and Unassigned Plumbate sherds, arranged in increasing order of surface concentration.

Figure 2 also suggests a distinct lack of correlation between surface and paste potassium concentrations, with the possible exception of the unassigned Plumbate. The positive correlation of 0.51 for the six unassigned specimens may be explainable in part by the fact that they are not Plumbate and/or are not exemplary of Plumbate technology. Overall, however, the comparison of surface and paste potassium concentrations accord with the hypothesis that the two are different components, the surface being enriched by technological practices rather than simply being a reflection of underlying paste variation.

EDS electron-microprobe provides useful information about the distribution of alkalis and iron within the slip and body of Plumbate sherds. In most samples, the depth of the very-dense surface layer is about 40 – 70 micrometers (Figure 3). Although sodium was below detection at most spots with the EDS, potassium shows clear enrichment at the surface and drops below detection at the bottom of the slip layer before rising again in the paste, perhaps reflecting the presence of potassium-feldspars and other materials in the paste (Figure 6). Calcium shows a similar pattern, although I have omitted one data point in the paste with >4% calcium presumably on or close to a feldspar grain. Finally, iron rises to a peak around 10 – 30 micrometers below the surface and then declines to about half the surface concentration within the paste.

EDS data are limited because of poor sensitivity to many elements of interest and because of highly localized effects such as the feldspar grain just mentioned. Laser ablation-ICP-MS circumvents both problems. First, sensitivity is in the sub-ppm range for most elements. Second, laser ablation along a line removes a sample of approximately uniform thickness with each pass, so analyzing the ablated material from

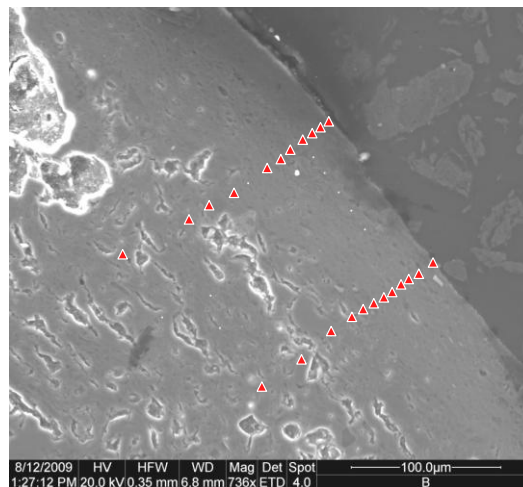


**FIGURE 3.** SEM image showing locations analyzed by EDS.

individual successive passes generates a more-representative average composition for a given depth. Successive passes are essentially a depth profile that shows how composition of the glaze/ceramic changes with depth. Four samples were analyzed this way, one gray and one orange example of sherds determined by paste analysis to belong to Tohil and San Juan Plumbate compositional groups. Twelve passes were collected on each sherd, so each cross section represents approximately 70 micrometers that begins at the surface and ends in the uppermost part of the

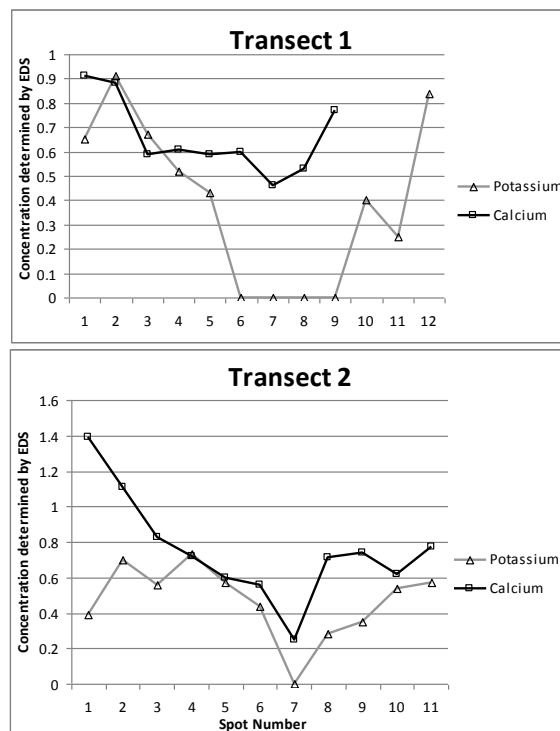


**FIGURE 4.** EDS depth profiles of potassium and calcium concentrations from the two transects shown in Figure 3.

body paste (Figure 5). Of particular interest are the changes in alkalis and other potential fluxes through the Plumbate surface layer.

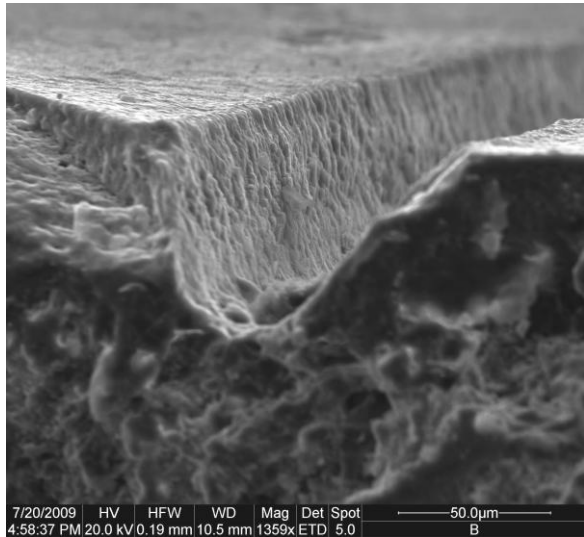


FIGURE 5. SEM image of trench created on Plumbate sherd surface by 12 laser ablation passes.

Principal components analysis (PCA) was used to investigate patterns of variation of possible fluxes and other major and minor elements within each analyzed sample. In Tohil sherds, both orange and gray, potassium, rubidium, cesium, copper, and zinc are the main determinants of scores on Principal Component 1, while sodium also contributes on the gray sample. Iron, interestingly, is almost completely uncorrelated with the major determinants of PC1, and in fact variation in iron is very poorly represented by the first two components. The orange and gray San Juan Plumbate sherds show a pattern of elemental variation across the surface layer much like Tohil Plumbate. Again, potassium rubidium, cesium, copper, and zinc are major contributors to PC1 in both cases, and sodium is an additional important contributor in the case of the gray San Juan sample. Again, iron is poorly represented on the first two components and uncorrelated with the elements that contribute most strongly to PC1. Plotting Component 1 scores for the four Plumbate types against depth clearly shows the pattern of decreasing scores down to about 30 – 40 micrometers, after which they level out (Figure 6). Thus, the PCA indicates that Plumbate slips are zoned, with enriched alkalis, copper, and zinc in the uppermost 30 - 50 micrometers.

The zonation suggested by PCA is confirmed by examination of elemental variation with depth across the slip. Of the major alkali fluxes, soda and potash, soda concentrations are highest in Tohil Plumbate, with values ranging from one to three percent, while potash is highest in San Juan Plumbate, with surface

concentrations between three and 6.5 percent. Total soda and potash measured at the surface ranges from 3.5 to 7 percent (Figure 7).

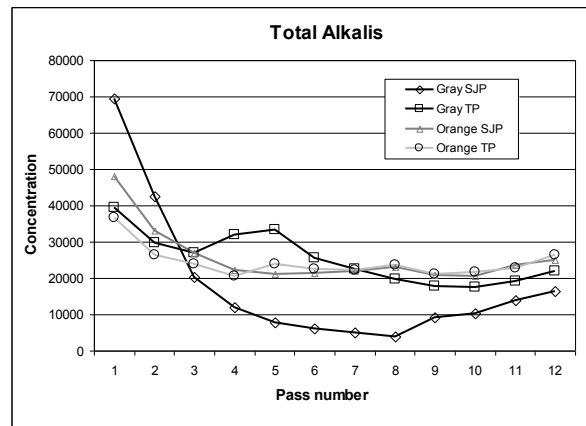


FIGURE 6. Scores on Principal Component 1 obtained from PCA using Na, Mg, K, Ca, Fe, Cu, Zn, Rb, Sr, Cs, and Ba 12 on successive laser ablation passes over four Plumbate sherds.

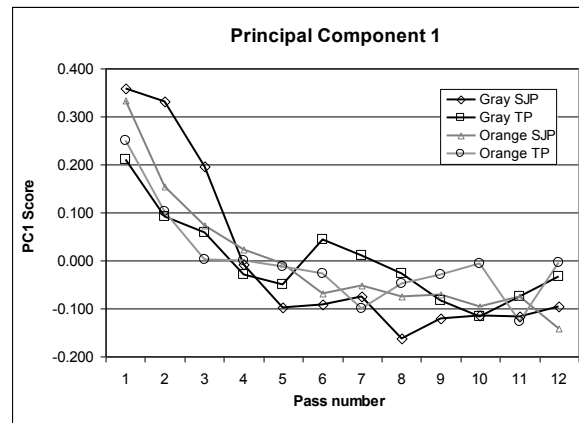
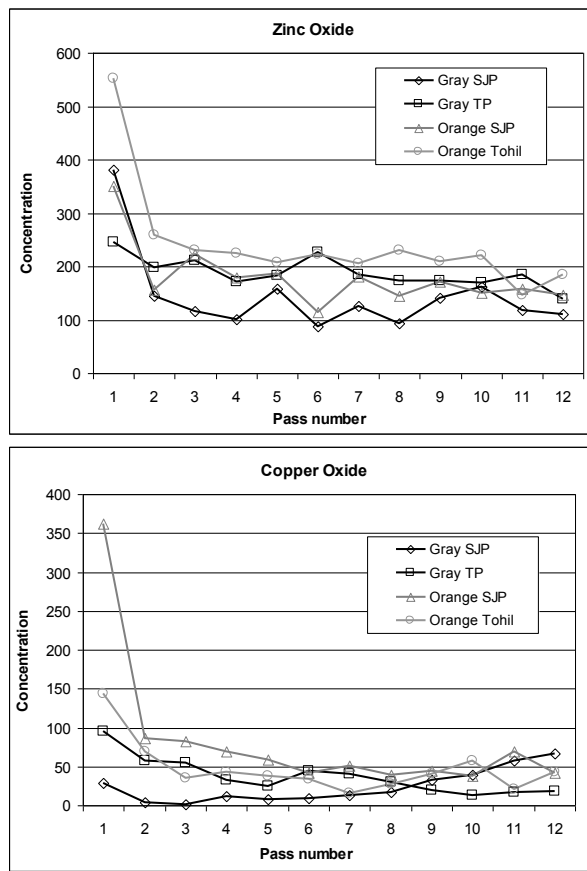


FIGURE 7. Total alkali concentration ( $K_2O + Na_2O$ ) plotted against depth in four Plumbate sherds

Copper and zinc also contribute very strongly to Component 1 scores, and it is clear that both elements are highly enriched in the uppermost layers, down to about 20 – 30 micrometers (Figure 8). This enrichment is most pronounced in the oxidized, orange surfaces. Although total zinc and copper oxide concentrations are below 0.01%, it is worth noting that these values are substantially higher than in any natural clays sampled anywhere on the southern Mesoamerican Pacific coast. Thus, their enrichment is a technological property, not a property of raw materials alone. Very small quantities of zinc are used in modern pottery as auxiliary fluxes fired up to about 1050° C [15]. It is worth noting that both copper and zinc are commonly used colorants in modern glazes as well; the deep red



**FIGURE 8.** Copper oxide and zinc oxide concentrations plotted against depth in four Plumbate sherds.

colors of some Plumbate may be created partially by reduced copper.

Finally, while iron does not show the same pattern of enrichment within the surface layer as the alkalis (Figure 9), copper, and zinc, it is clearly enriched in the slip material compared to the paste. Concentrations of about 8 – 11% in the slip are comparable with EDS determinations. The LA-ICP-MS results show more clearly, however, that the visible surface is relatively diluted in iron compared to deeper slip layers, while, again, the visible surface is distinguished by high alkalis, copper, and zinc.

## CONCLUSIONS

The analyses reported here are not definitive, but they do allow a refinement of hypotheses about the nature of Plumbate technology. There is, as predicted, an enrichment of alkalis in the visible surface layer. Although the actual concentrations are only in the 3.5 – 7% range, we can hypothesize that they were sufficient to promote fusion at the temperatures achieved by Plumbate potters, given the other compositional characteristics of Plumbate slip (high alumina, high iron). The enriched soda and potash did

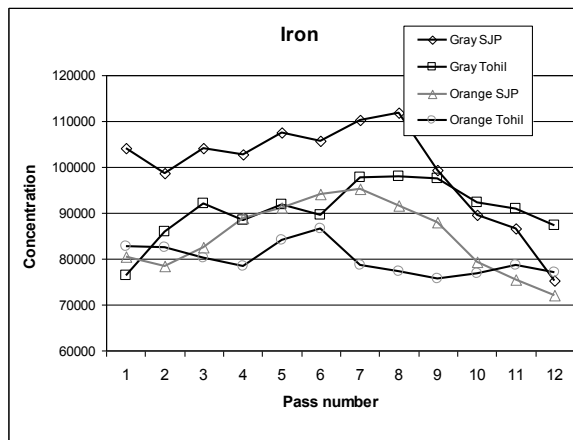


**FIGURE 9.** Iron concentrations plotted against depth in four Plumbate sherds.

not come only from the Plumbate slip clays, but rather are a technological addition, possibly related to preparation of the slip with mangrove ash (a source of potash) and brine.

Copper and zinc are also enriched in the visible surface layer, and, while present in low total amounts, are much higher than in natural clays of the region. Interestingly, mangroves are known to take up zinc in environments subject to heavy-metal contamination, and it is worth hypothesizing that mangrove ash might also be the source of enriched copper and zinc, which were pulled from the littoral zone sediments into the mangrove tissues. Their presence in the surface layer may have both contributed to fusion of the surface and to the unusual color properties, such as deep reds and iridescence, seen on some Plumbate vessels.

Iron is the most enriched potential flux in the surface layer. It is known to act as a flux, however, only in its reduced form, FeO, so that it would only have contributed to fusion in the reducing atmospheres in which the gray vessels were fired. Recalling Shepard's (1948) observations, it can be hypothesized that the greater hardness of gray vessels is created by the fluxing action of FeO in the subsurface slip layer.

If this unique glazing technology was discovered once, it can be discovered again. Thus, I suggest that definitive tests of hypotheses about the nature of Plumbate technology will come from replication experiments in the littoral zone of southern Pacific Chiapas, using the slip clays, brine, and mangrove wood that would have been available to Plumbate potters. If similar visual qualities can be achieved, the microstructure and chemistry of the replicates can then be compared to ancient Plumbate surfaces in order to fine-tune the recipe and pyrotechnology. These experiments would replicate the evolutionary process through which Plumbate technology was discovered and refined by the evolutionary processes that shaped the choices of Late and Terminal Classic potters.

## ACKNOWLEDGMENTS

This research was supported in part by Grant No. BCS-0604712 from the US National Science Foundation. The Foundation for the Advancement of Mesoamerican Studies, Inc. supported fieldwork.

## REFERENCES

1. A. O. Shepard *Plumbate: A Mesoamerican Trade Ware*. Carnegie Institution of Washington, Publication 573 Washington, D.C., 1948.
2. B. P. Dutton, *A History of Plumbate Ware*. Papers of the School of American Research, no. 31. School of American Research, Santa Fe, 1943.
3. E. M. Shook, "Archaeological survey of the Pacific coast of Guatemala." In *Handbook of Middle American Indians*, G. R. Willey, ed., vol. II, University of Texas Press, Austin, 1965, pp. 180-194.
4. P. Drucker, *Preliminary Notes on an Archaeological Survey of the Chiapas Coast*. Tulane University, Middle American Records, vol. 1, no. 11, 1948.
5. G. W. Lowe, and J. A. Mason, "Archaeological survey of the Chiapas coast, highlands, and upper Grijalva Basin" in *Handbook of Middle American Indians*, G. R. Willey, Ed., vol II. University of Texas Press, Austin, 1965, pp. 195-236.
6. B. P. Dutton and H. R. Hobbs, *Excavations at Tajumulco, Guatemala*, Monographs of the School of American Research, no. 9. School of American Research, Santa Fe, 1943.
7. H. Neff *Developmental History of the Plumbate Pottery Industry in the Eastern Soconusco Region, A.D. 600-A.D. 1250*. Unpublished Ph.D. Dissertation, University of California Santa Barbara, 1984.
8. H. Neff Sources of raw material used in Plumbate pottery. In *Incidents of Archaeology in Central America and Yucatan*, M. Love, M. P. Hatch, and H. Escobedo, eds., 2002. pp 217-231, University Press of America, Lanham, MD.
9. H. Neff, *Journal of Archaeological Science* **30** (2003) 21-35.
10. Rosenswig, Robert "Informe Técnico Parcial del Proyecto Formativo Soconusco." Report submitted to the Instituto Nacional de Antropología e Historia, Mexico, DF, 2001.
11. P. M. Rice *Pottery Analysis: A Sourcebook*. University of Chicago Press, Chicago, 1987.
12. A. P. Andrews *Maya Salt Production and Trade*. University of Arizona Press, Tucson, 1983.
13. H. McKillop *White Gold of the Ancient Maya*. University Press of Florida, Gainesville, 2002.
14. C. A. Loto, and O. A. Fakankum Characterization of the ashes of Nigerian red and white mangrove woods. *Wood Science and Technology* **23** (1989) 357-360.
15. J. R. Taylor and J. C. Bull *Ceramic Glaze Technology*, Pergamon, New York, 1986.

## **Characterization of Slates from Teotihuacan using XRD, PIXE and Ionoluminescence**

J. M. López Juárez<sup>1</sup>, J. L. Ruvalcaba-Sil<sup>2</sup> and M. Aguilar Franco<sup>2</sup>

<sup>1</sup>*Posgrado en Estudios Mesoamericanos, Facultad de Filosofía y Letras,*

*Universidad Nacional Autónoma de México; MEXICO. e-mail: xulieta.lopez@gmail.com*

<sup>2</sup>*Instituto de Física, Universidad Nacional Autónoma de México, MEXICO. e-mail: sil@fisica.unam.mx*

**Abstract.** Slate is a metamorphic rock of extremely thin grain, its origins are sedimentary clays that been transformed due to the pressure and / or moderate heat give a laminate texture. In Teotihuacan, an important amount of slates objects of all kind are found in ceremonial areas as well as habitation units, nevertheless, these materials have never been analyzed before. This research is focused on the analysis of a set of slates artifacts discovered during the excavations of the Moon Pyramid carried out by Sugiyama & Cabrera in Teotihuacan, Mexico. The studied pieces are from the burials 2, 3, 5 and 6 and they correspond to the Miccaotli phase (100-200 A.D.). Because of Teotihuacan's geology, it is evident that the raw material was imported; the slate sources that possibly supplied Teotihuacan could be inside the actual states of Guerrero, Morelos, Michoacán, Estado de Mexico, Puebla, Veracruz and Oaxaca. The aim of this research is to determine the material features, technological and manufacturing aspects as well as the religious and social implications for the slate. In this first work, we present a methodology for the characterization of the archaeological slates. X-ray diffraction provides information about the mineral crystalline phases. On the other hand, PIXE is used for the measurement of the elemental contents, including trace elements while the Ionoluminescence may be used for the identification of specific mineral phases in the material, such as calcite in the slate. To show the feasibility of the slate characterization and its provenance, the archaeological data are compared with the results of the analysis of slates from several geological sources.

**Keywords:** Slate, Teotihuacan, XRD, PIXE, Ionoluminescence, geological sources.

### **INTRODUCTION**

Slate is a metamorphic rock of extremely thin grain, its origins from sedimentary clays that been transformed due to the pressure and / or moderate heat give a laminate texture [1]. Then it is possible to produce large and thin rock sheets to manufacture objects. The color of slate usually varies from gray to black, but it can be greenish, yellowish, and reddish brown. Slate can be rich in clays, and calcareous or bituminous when abundant in calcium carbonate or hydrocarbons [2, 3]. The composition of slate ranges for the most usual oxides ranges for SiO<sub>2</sub> = 22-46%, Al<sub>2</sub>O<sub>3</sub> = 2-18%, CaO = 20-39%, and FeO = 1-10%.

Slate is a very usual and abundant material in the archaeological excavations in Teotihuacan. It can be found in funerary contexts and burials, as filling material in the buildings structures as well in the ceremonial area and in the domestics regions of the ancient Mesoamerican city mainly for the Terminal Formative and Classic Horizon (100 to 650 A.D.) [4-5]. This material may be related to other objects or materials used only for the social hierarchies as green stone, obsidians, pyrite items and mollusks [6].

From the geological characteristics of the Teotihuacan region, it is clear that this material must be imported from other close areas of central Mesoamerica (Figure 1).

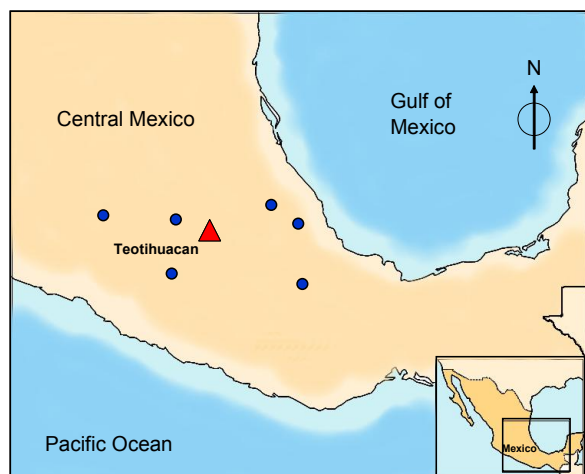


**FIGURE 1.** Map of localization of Teotihuacan and the closer slate sources in central Mesoamerica - blue circles.

In a first stage our research has been focused in the study of 131 slate artifacts discovered in the Moon Pyramid project excavations [7, 8]. This is one of the most important and known architectonic structures of the north ceremonial area of Teotihuacán (Figure 2).



**FIGURE 2.** Moon pyramid of Teotihuacan.

The objective of this first analysis has been to establish and test a general methodology for the characterization of archaeological slates objects and lithic materials with a meta-sedimentary origin. At the same time, several geological samples from various formations in Guerrero, Morelos and Michoacán states of Mexico has been selected considering the geographic proximity and their geology. For composition comparison purposes, some samples from

the Fontanelli quarry in Italy, were included in the study.

In this work, the methodological proposals as well as the first results of the analysis for the characterization of the material and its provenance are presented. The techniques involved were X-ray Diffraction (XRD) for mineralogical analysis and Ion beam base techniques, mainly Proton Induced X-ray Emission (PIXE) and Ionoluminescence (IOL) for elemental analysis and specific mineral identification from light emission.

## ARTIFACTS & GEOLOGICAL SAMPLES

The objects are discs, decorated flat pieces, small anthropomorphic figures, beads, pendants and small instruments. Some of the selected objects are shown in Figure 3. The selection criteria also considered conservation conditions since slate artifacts may be significantly deteriorated at the surface. The main set of the objects were discovered in burials 2, 3, 5, and 6 in the Moon pyramid (118 pieces), but 13 objects from the filling materials of the stage building 1, one of the oldest in Teotihuacán were included. The geological samples (7 pieces) were collected from Tlalpujahuá in Michoacán, Pachivía and Iguala in Guerrero as well in an area of highway to Acapulco; and in the Morelos region, and Valle de Bravo and Tejupilco regions of the México state.



**FIGURE 3.** Some representative slate objects discovered in the Moon pyramid offerings.

## METHODOLOGY

Depending on its size and shape, some artifacts were analyzed by X-ray diffraction (XRD) on flat areas- without sampling and powdering. A special sample holder for this purpose was used in a Bruker AXS diffractometer model D8 Advanced with a Linx eye detector. The XRD patterns were identified using the JCPDF database.

On the other hand, PIXE and Ionoluminescence (also called Ion Beam Induced Luminescence IBIL) were applied to contribute to the mineral identification and to determine the elemental concentrations in order to establish probable provenance of the pieces by comparison to geological samples. An external proton beam of 3 MeV was used to irradiate an area of 1.5 mm diameter on the artifact surface [9]. Characteristic X-rays and induced luminescence by the proton beam were simultaneously detected by two X-ray detectors (light and heavier trace elements). A He jet improves the detection of low energy X-rays. For heavier elements detection, a LGe detector with a 80 μm Al filter was used. IOL was performed by an Ocean Optics USB2000 spectrometer connected to an optic fiber to cover a light wavelength range from 300 to 1000 nm with higher efficiency in visible-near infrared region. The experimental setup is shown in figure 4.

Archaeological artifacts and geological samples were analyzed under the same conditions in two regions. Additionally, for elemental analysis a set of standard reference materials from NIST (SRM2704, SRM 2711, SRM1880a) were also irradiated. Then AXIL code and the PIXEINT program were used for quantitative analysis. Figure 4 shows the experimental device and the irradiation of one of the artifacts.

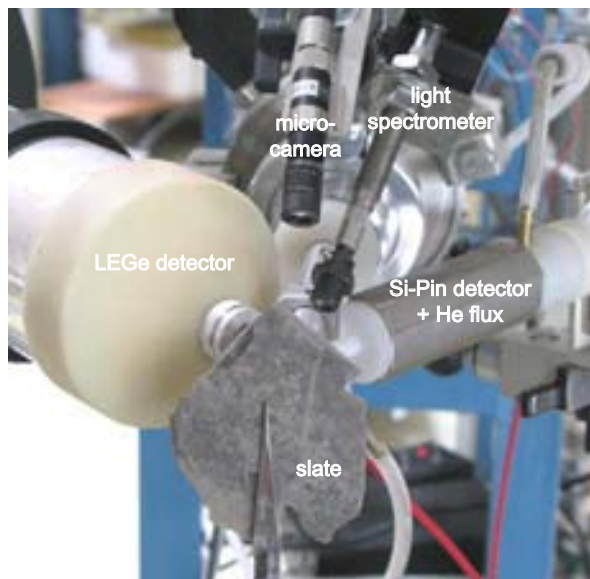


**FIGURE 4.** PIXE-IOL external beam setup of the Pelletron IF-UNAM accelerator.

## RESULTS AND DISCUSSION

### X-Ray Diffraction

About 30 samples were analyzed by XRD. The XRD analysis results of the geological samples are shown in figure 5. Several crystalline minerals are identified: Quartz ( $\text{SiO}_2$ ) and Calcite ( $\text{CaCO}_3$ ), Muscovite ( $\text{KAl}_2(\text{AlSi}_3\text{O}_{10})(\text{F},\text{OH})_2$ ) can be considered the main mineral phases while the secondary phases are Montmorillonite ( $\text{Al}_2\text{O}_5 \cdot 4\text{SiO}_2 \cdot 4\text{H}_2\text{O}$ ) and Clinocllore ( $\text{Mg}_5\text{Al}(\text{AlSi}_3\text{O}_{10})(\text{OH})_8$ ) that are present only in the Tejupilco sample quarry.

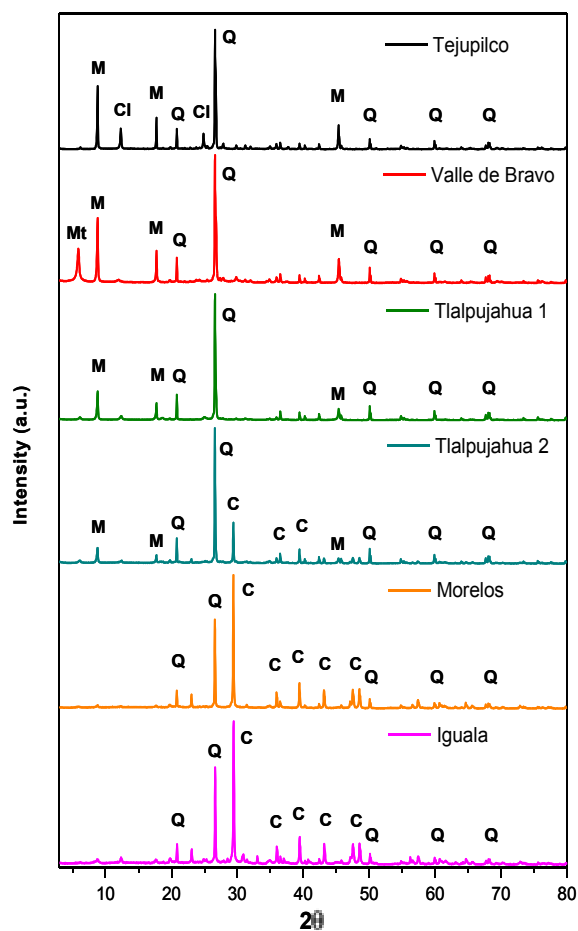


**FIGURE 5.** XRD spectra for the geological slate samples. C: calcite, Q: quartz, M: muscovite, Mt: Montmorillonite, Cl: clinocllore.

Quartz is always present in all the quarries but calcite appears only for the Morelos, Iguala and Tlalpujahuá samples while Muscovite was observed in Tejupilco, Valle de Bravo and one Tlalpujahuá samples. Thus we can observe two groups of slate mineralogical composition. The first one composed by

Quartz and Montmorrillonite with, in some cases Montmorrillonite and Clinocllore, and a second group composed by quartz and calcite. Calcite content can varies in significantly since sometimes it can be higher than the quartz amount. Tlalpujahua may be the intersection of both groups as a function of its calcite content.

The archaeological slate results present similar features than the geological samples (Figure 6). There are pieces with a high content of quartz and calcite may be present in variable amounts, sometimes as the main mineral phase. Muscovite has been observed as a secondary phase in few cases. These results indicate that in the archaeological items, we may expect two groups, one rich in quartz and another one rich in calcite. The rich quartz and rich calcite groups may be related to Tejupilco, Valle de Bravo and Iguala and Morelos, respectively.

Then, base on the previous results, if the minerals matrix of the slate artifacts are very different, XRD data may provide a first insight about their probable provenance.

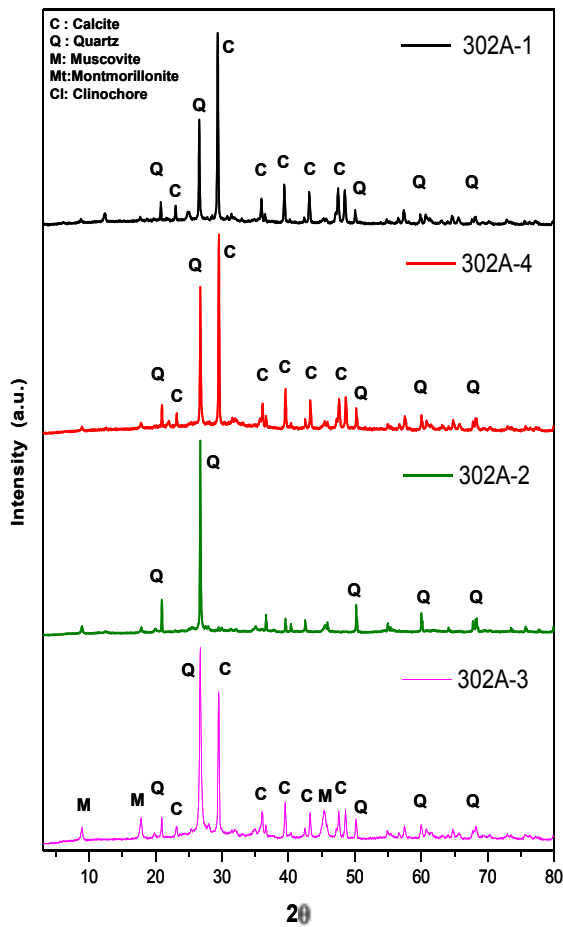


FIGURE 6. XRD spectra for the archaeological slate artifacts. C: calcite, Q: quartz, M: muscovite, Mt: Montmorrillonite, Cl: clinocllore.

### IOL and PIXE

The Ionoluminescence phenomena were observed only in a set of slate pieces. The emitted light was always red and a comparison with minerals of quartz and calcite IOL spectra and spectra databases [10] it is possible to identify the mineral phase and its impurities responsible of the light emission. The clays are usually not luminescent.

Figure 7 shows the typical IOL spectra for the geological samples, archaeological items and a calcite reference measured with our external beam setup.

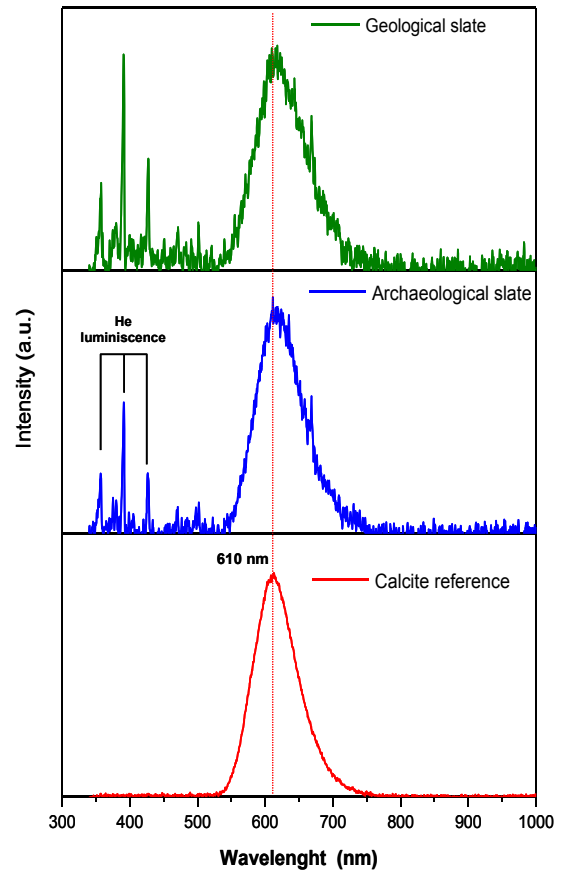


FIGURE 7. Typical IOL spectra of slate materials.

The IOL spectra comparison allows the identification of calcite as the main luminescent phase. Thus, the measurement of the red light emission intensity at 610 nm provides a quick measure of the calcite content in the slate artifacts and when no light emission is detected; it corresponds to a rich quartz matrix. Since the IOL measurements required one to few seconds, this non-destructive analysis can be use for a quick discrimination of the composition in different regions of the archaeological slate artifacts. The Helium luminescence induced at 400 nm by the proton beam on the helium flux for the light elements detection can be used to normalize the intensity of the

610 nm emission in order to compare the emission of different pieces or samples. These results show the power of this method for specific identification of minerals with a high sensibility.

On the other hand, in PIXE spectra of the archaeological pieces and mineral samples, about 20 elements were detected (Mg, Al, Si, P, S, Cl, K, Ca, Ti, Cr, Mn, Fe, Co, Ni, Cu, Zn, Ga, As, Rb, Sr, Zr). Figure 8 shows the typical PIXE spectra of both, light and heavier elements using the Si-PIN and LEGE detectors respectively.

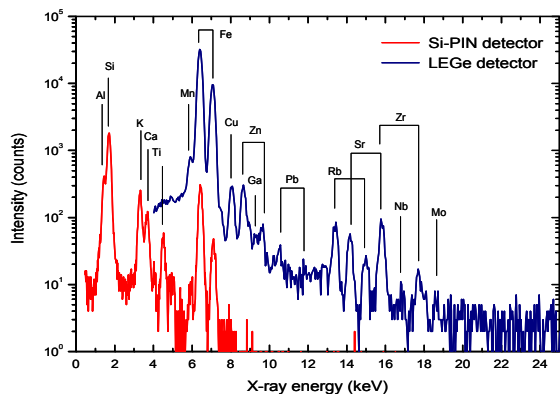


FIGURE 8. Typical PIXE spectra of slate.

After the measurement of the elemental concentrations, a cluster analysis was carried out for a first grouping. Afterwards, a main factor analysis can be applied for a more detailed statistical analysis. In Figure 9, it is presented the dendrogram obtained from a cluster analysis for some of the geological samples and archaeological items presented in the figures 5 and 6 with the XRD results. Weighted group average and Euclidian distances were considered for cluster analysis.

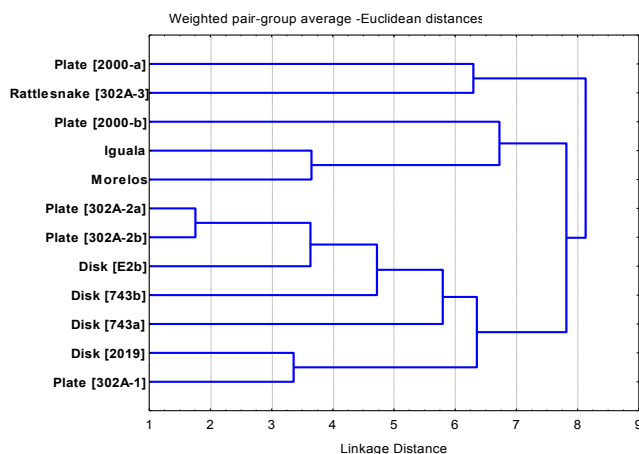


FIGURE 9. Cluster analysis from PIXE measurements of archaeological artifacts and geological slates.

In figure 9 we can observe that the clustering agrees the previous result of XRD and a rich calcium group is clustered with Iguala and Morelos geological samples. Also the rich quartz matrix items form a small group. From the analysis of PIXE data, Si and Ca concentrations as well as Fe and Ti contents explains the main distribution observed in the dendrogram of figure 9. Of course, Ca and Si are related to calcite and quartz contents, and Fe and Ti are minor elements for discrimination of the subgroups. Further analyses are in progress on the all set of artifacts and additional geological sources.

## CONCLUSIONS

XRD and PIXE combined with Ionoluminescence have shown to be complementary and suitable techniques for the study of the archaeological and geological artifacts of slate without sampling or powdering. It has been possible to identify specific mineral phases as well as major and minor elements, which can be related to their sources. This may help us to identify the slate deposits that may supply Teotihuacan.

Iguala and Morelos geological samples are alike between them and they are the most similar from mineralogical point of view to the archaeological pieces. These sources present higher contents of quartz (Si) and calcite (Ca). Other archaeological pieces present different contents of montmorillonite and clinocllore. This indicates another unknown source.

Ionoluminescence signals from calcite agree with the mineral identification and the calcite luminescence intensity is related to the amount of this mineral in the slate.

PIXE results agree with XRD and IOL grouping but the elemental concentrations can discriminate secondary groups and the use of unknown or non identified sources of slate.

Further analyses using this methodology are in progress on a large amount of archaeological samples from the Moon pyramid offerings and other areas of Teotihuacan. More field work is in progress in order to obtain more samples from other slate sources.

## ACKNOWLEDGMENTS

Authors thank K. López and J. Beristain for Pelletron acelerator operation and J.C. Pineda and J.G. Morales for their technical support. Also, we thank Dr. Saburo Sugiyama Director of Project Pyramid of the Moon for the access to the archaeological artifacts. This research has been support by grants CONACyT U-49839-R and PAPIIT UNAM IN403210.

## REFERENCES

1. A. Bussbey, *Rocas y fósiles*, Ed. Planeta, Madrid España 1994.
2. M. Iriondo, *Introducción a la Geología*, Ediciones el Río 1985.
3. A. Kopf, *Field Guide to North American Rocks and Minerals*, National Audubon Society, New York, 1979.
4. L.R. Manzanilla Naím, *Metrópolis prehispánicas e impacto ambiental. El caso de Teotihuacán a través del tiempo*; El Colegio Nacional, México, 2008, 357-410.
5. T. Murakami, "Power relations and urban landscape formation: A study of construction labor and resources at Teotihuacan; Dissertation of the requirement for the Degree Doctor of Philosophy; Arizona State University, 2010.
6. J. M. López Juárez; *La pizarra de la antigua ciudad de Teotihuacan. Tipología e interpretación*; Tesis de Licenciatura en Arqueología, ENAH-INAH, 2006.
7. S. Sugiyama, R. Cabrera, "El Proyecto Pirámide de La Luna 1998-2004: Conclusiones preliminares", in: *Sacrificios de consagración en la Pirámide de La Luna*; 2006, 11-24.
8. S. Sugiyama, L. López Luján; Sacrificios de consagración en la Pirámide de La Luna, Teotihuacan en: *Sacrificios de consagración en la Pirámide de La Luna*, 2006, 25-52.
9. Ciliberto E. y Spoto G. eds., *Modern Analytical Methods in Art and Archaeology*, Chemical Analysis, Series of Monographs on Analytical Chemistry and its Applications, Vol. 155, J.D. Winefordner Series Ed., John Wiley and Sons, N.Y., 2000.
10. J.L. Ruvalcaba Sil, L. Manzanilla, E.R. Melgar Tisoc, Ru. Lozano Santa Cruz, *X-ray Spectrometry* **37** (2008) 96-99.
11. H. Calvo, J.L. Ruvalcaba-Sil, T. Calderón. *Journal of Analytical and Bioanalytical Chemistry* **387** (2007) 869-878.
12. S. Calusi, E. Colombo, L. Giuntini, A. Lo Giudice, C. Manfredotti, M. Massi, G. Pratesi, E. Vittone, *Nuclear Instruments and Methods B* **266** (2008) 2306-2310.
13. E. Colombo, S. Calusi, R. Cossio, L. Giuntini, A. Lo Giudice, P.A. Mandò, C. Manfredotti, M. Massi, F.A. Mirto, E. Vittone, *Nuclear Instruments and Methods B* **266** (2008) 1527-1532.

# Dating Techniques through the Characterization of Materials. XVI Century South Sardinian Coast Defense Towers

C. Giannattasio<sup>1</sup> and S.M. Grillo<sup>2</sup>

<sup>1</sup> Faculty of Architecture, Department of Architecture, Cagliari, ITALY. e-mail: cgiannatt@unica.it.

<sup>2</sup> Faculty of Architecture, Department of Geo-engineering and Environmental Technologies Cagliari, ITALY.

**Abstract.** The object of this study are some towers situated in the area of Cagliari, belonging to the Sardinia coast defense system realized between the Sixteenth and the beginning of the Seventeenth century. This architectural assembly, very rich and articulated, is full of historical and cultural significance, being the expression of traditional human activities. Having lost the role in our society since the XIX century, it is actually in a progressive state of degradation. Starting by this preamble with the purpose of warranting a better preservation and management of similar cultural heritage examples, the contribution illustrates the methodology adopted which follows an interdisciplinary approach, integrating historical-archaeometrical and scientific tools. On one hand, the constructions have been explored from an architectural point of view, using the chrono-typological analysis of masonries by showing their structural aspects and the executive modalities for their setup. Metric and photographic surveys supported by drawings highlighted the constructive peculiarities of the masonries analyzed. On the other hand, they have been studied through mineralogical-petrographic and geochemical methods for the characterization of stone materials used, and by the analysis of plasters and mortars, to define their main features and to try to identify the provenance area of the materials used. This contribution is part of a more comprehensive study and it refers especially to the Su Perdusemi tower, situated in Cagliari.

**Keywords:** masonries, stratigraphy, chronology, building stones, mortar petrography, weathering.

## INTRODUCTION

This study is part of an extensive research concerning the coast defense system realized in Cagliari's district (Sardinia, Italy), during the 16<sup>th</sup> and 17<sup>th</sup> century [1-2].

Unfortunately, these structures are suffering from rapid deterioration of their stone fabric as a result of disuse and abandonment since the 19<sup>th</sup> century, after they had lost their original function.

The investigation intends to record and evaluate the traditional building techniques used for the

construction of their masonries. Specifically the three principal objectives of this study are:

1. The record through visual observation of any particular building techniques that differentiate these constructions from other ones of the same period.
2. The description of the construction systems used and the report of the deterioration that may be observed, to enable future appropriate interventions for their conservation.
3. To find evidence to facilitate the dating of other contemporary edifices, especially of vernacular architecture ('minor' buildings).



**FIGURE 1.** Cagliari, Su Perdusemini tower and its context.

## HISTORICAL REFERENCES

As we said before, the coast defense tower investigated dates back to the 16<sup>th</sup>-17<sup>th</sup> century, under the rule of Spain.

This period is very important for the development of the protection system, because the island represented a strategic ambit at that time, by a commercial and political point of view [3-7].

During the second half of the 16<sup>th</sup> century Marco Antonio Camós [8-10] was instructed by the viceroy Juan Coloma d'Elba to quantify the existing towers and to register their conditions. The viceroy's aim was to convince the authority to ameliorate the defense system, in order to protect Sardinia as well as Spain.

This process continued until 1587, when the dominator decided to institute an Administration for the towers, starting up a concrete development process, the defense system of the Kingdom of Naples serving as example.

These towers had basically the role of a lookout point, therefore they were always located on rocky promontories (Figure 1). In other words, their position was imposed by the existence of obtaining a good visibility level towards the sea, as well as of the neighboring coastal area.

Prevalently these constructions show a circular plan (Figure 2), with a cylindrical or a cut-off conical façade [11-12], still in coherence with the past catalane culture, even if in the same years in the other Italian contexts the military engineering praxis focused on the realization of quadrilateral buildings.

Usually a vaulted system covered the building. The dimensions of these towers are small, presenting a diameter included between 5 and 12 m, with a masonry section of 1 m and an height of 8-10 m.



**FIGURE 2.** Cagliari, Su Perdusemini tower. The image shows the small quarry where the building materials were excavated.

The fronts show a very simple drawing, devoid of any decoration element.

The openings too are very simple, with access doors situated some meters above the ground, accessible through a mobile wooden stair.

Presently these structures are completely abandoned and they lost their function after the Unity of Italy.

## THE METHODOLOGY ADOPTED

With reference to the investigated buildings, the study carried out is based on the use of an archaeological method, consisting in the sampling and the classification of the masonries, through a photographical, architectural, metrical and material survey, concerning the structures, the stones and the mortars used for their construction.

Specifically, stones and mortars have been examined by a morphological, metrological, lithological and petrographical point of view, obtaining chronological series, referred to the 16<sup>th</sup>-17<sup>th</sup> centuries.

The sampling has been supported by the use of a database and a catalogue schedules, containing all the registered data, concerning the typology of each tower and the traditional construction techniques.

The drawing of each tower (Figure 3), with the annotation of their structural and material based conditions, was very useful for the understanding of the dimensional and technical characteristics.



**FIGURE 3.** Cagliari, Su Perdusemmini tower. The building archaeological survey (drawing by M. Porcu).

### The masonries sampling

This mode of investigation allowed to define the constructive techniques usually used for the realization of this kind of buildings during the XVI<sup>th</sup> and XVII<sup>th</sup> century, yet precisely dated through archive and cartographic documentation [13-14].

The masonry technique used was ‘a cantieri’ (Figures 4 to 6). This practice, deriving by the roman *opus incertum*, consisted in the preparation of two or three courses of rubbles, rough-hewed just in the external and support faces. The result was an irregular, coarse opus, with horizontal linings generally distanced 50-60 cm, characterized by thick joints between one another, with mortar of poor quality, sometimes signed by not slaked lime nodules. Very often the assembly of the rubble stony elements took place without paying attention to the stagger of vertical joints.

Notwithstanding the above mentioned characteristics, this typology was the outcome of an ingenious device, conditioned by economical reasons, i.e. by the aim of making the most of the available stones of different size, accurately dressing external angles and using horizontal elements with stabilizing function thus warranting structural solidity.

As we will specify after, all the examples investigated used local material directly extracted from the subsoil or taken from neighboring quarries (sandstone, limestone, granite, etc.). They demonstrate the use of rubble pieces or regular ashlar of variable

size and of various manufacturing processes. Numerous small rock pieces left over from hewing bigger blocks have been applied to fill empty spaces.

Between two courses one can find tiny squaring materials, together with a double mortar layer, highlighting the passing from one another, i.e. the closing of a module of the masonry and the following restarting of the new one.



**FIGURE 4.** Cagliari, Su Perdusemmini tower. The picture shows the ‘cantieri’ masonry technique used.



**FIGURE 5.** Cagliari, Su Perdusemmini tower. Vertical section of the masonry.

Sometimes planking holes can be found, distanced both horizontally and vertically about 1.70 m. Generally it can be observed that for practical reasons, they are always aligned with the superior limit of the ‘cantiere’.

Interstices are filled with plentiful gross mortar, characterized by numerous components of unslaked lime nodules.

The stones composing the ‘cantiere’ show different sizes, 15-20 cm high and 15-22 cm wide. In each ‘cantiere’ the dimension of stony elements decreases from the bottom to the top of the tower, evidently for stability reasons.

### Lithological and petrographical analysis

Together with the exam of masonries by a technical point of view, the study included mineralogical characterization of the masonry samples and mortars. Specifically, it was carried out both X-Ray diffraction and optical microscope polarized light microscopy (OM) on the thin section.

Trough this study, as well as through the on site surveys, it emerged that the historical towers were built using materials of local provenance and the use of different stones was conditioned by their availability.

The investigation of the towers very close to the Cagliari city shows that for their realization carbonatic rocks have been used. In fact in this area it occurs a formations of calcareous arenaceous argillitic series of Oligocene-Miocene-Holocene sequences [15].

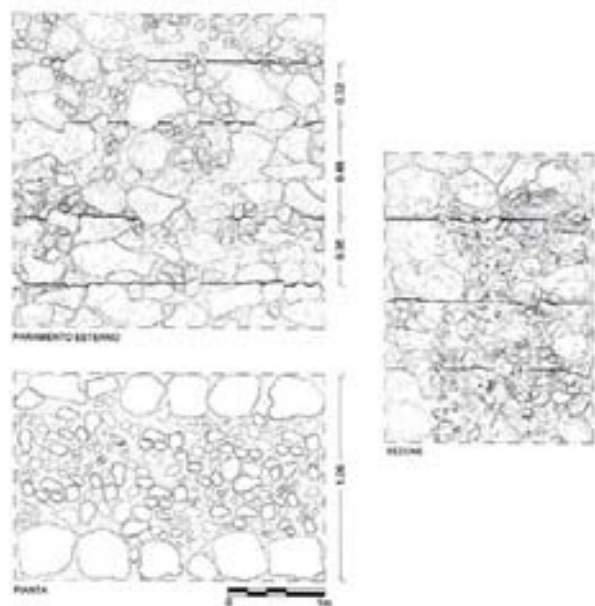


**FIGURE 6.** Cagliari, Su Perdusemini tower. Front, plan and vertical section masonry detail (drawing by V. Pintus).

The more important lithotypes used for building and construction purposes are usually Miocene rocks of calcareous nature.

The stratigraphic sequence of this area from bottom to top comprises a soft marly arenaceous limestone (Pietra Cantone). On top of that a more or less marly calcarenite (Tramezzario) can be found; finally at the uppermost top there is a hard compact organogenic limestone occurs (Pietra Forte) with good mechanical properties and very low porosity and permeability [16].

The important quarrying activities of the calcareous strata illustrate the use of this material in ancient times within close vicinity of the city of Cagliari. The immediate availability of this calcareous strata within close proximity of historic settlements allowed it to be applied for various purposes and used for the construction of the coastal towers near the city.

The other towers present in the Cagliari gulf were built using different stones as granitoids rocks, metamorphic rocks, sandstones, material from the river, always following the criteria of local provenance.

Generally the geology of this area is dominated by granitoids, volcanic and sedimentary rocks. The presence of several pits and mining traces testifies old historic quarry activity.

Also the aggregates of mortar and plaster are generally realized with sand of the close beach, while the binder is composed by a carbonatic lime.

## A CASE STUDY: SU PERDUSEMINI TOWER

### The site

Su Perdusemini tower is situated in Sant’Elia, a small quarter very close to the city and to the sea.

The building was built on the outcrop of limestone (Pietra Forte) and the ashlar blocks used for the construction of the tower came from a small quarries present close to it (Figure 2), maybe used as kiln too.

### The building

The tower shows a light cut-off conical shape. Its dimensions are little, because of its position on top of a rock. The walls are 1,00 m thick, while the height is about 10 m with a diameter of 6 m.

The architectural composition is very simple, without any decoration elements. Only the window positioned on the top is realized with monoliths in calcareous squared stone. It represents a rare case, in which the window shows a block of stone frame and the door is accessible by the ground level.

## Mineralogical analysis of materials

The optical study of the aggregates and binder composition shows two types of mortars. Both mortars consist of sandy aggregates made mainly of fossil and lithic calcareous fragments with single crystal quartz grains and very few feldspar (Figure 7). This composition together with the granulometric and the morphometric characteristic of the aggregate grains are similar to those of the marine beach sand.

The two mortars differ especially in the binder/aggregate ratios and in a higher content of the crystal quartz in the mortar used as plaster and for the realization of the masonry joints. The lime binder consists of micro to cryptocrystalline carbonates and sometimes it shows a non-homogeneous texture due to the presence of lumps (Figure 8). A rim of reaction with formation of cryptocrystalline carbonate is often present around aggregate grains. The principle stone used for this tower is Pietra Forte, a limestone white, massive, frequently bioclastic organogenic (Figures 9-10), followed by few ashlar of Pietra Cantone.

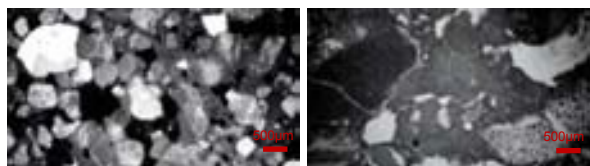


**FIGURE 7.** Cagliari, Su Perdusemi tower. Thin-section photomicrographs (crossed polarizer) of plaster mortar with coarse grained quartz-feldspar and fossil carbonate aggregates (a). Micrite binder with lumps and cryptocrystalline reaction rims around fossil fragments (b).

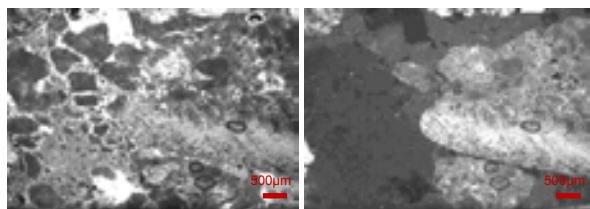


**FIGURE 8.** Cagliari, Su Perdusemi tower. Thin-section photomicrographs (crossed polarizer) of white mortar with fossil and lithic fragments. Micrite binder with CaO nodules.

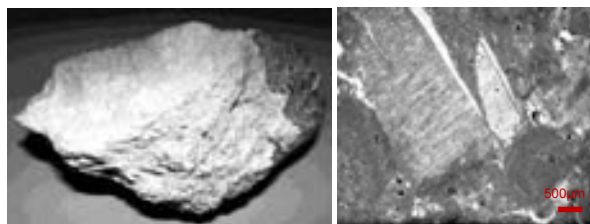


**FIGURE 9.** Cagliari, Su Perdusemi tower. Pietra Forte: hand samples with black patinas and thin-section photomicrographs (crossed polarized).

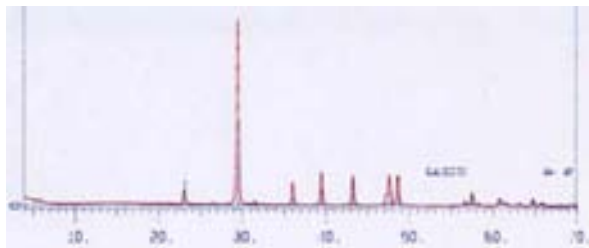


**FIGURE 10.** Cagliari, Su Perdusemi tower. X-Ray diffraction.

## The masonry technique

The masonry, in calcareous rubble stones, is realized with ‘cantieri’ high about 38 cm, composed by a different number of layers, in relation to the size of the stones used (Figures 4-6).

They prevalently are about 13 cm high, with a maximum dimension of 20 cm and a minimum one of 3 cm.

The little pieces are used to fill the holes resulting from the use of very heterogeneous rock employed to build the wall, especially in the inner part of it, i.e. the nucleus of the section (Figure 5).

The irregularity of elements dictates the size of the joints, with large quantities of mortar. Sometimes the mortar layers include nonslaked lime modules.

## Deterioration conditions

Today the building is in a critical stage of deterioration. In fact it has a lot of cracks and the stony elements delimiting the door and the window are dismembering (Figure 11). Besides, the plaster in a great extent is peeling off the walls. Where it is still present, erosion by wind action and weathering generally results in a deep deterioration (Figure 12).

In some parts of the tower, wind erosion caused the decay of the external section of the wall, so that the inner structure is exposed (Figure 5).

But much of the weathering damage observed in the stones and in the mortar of tower is associated to marine aerosols due to diffusion and crystallization of soluble salts of marine origin especially in combination with direct solar radiation [17]. This process is testified by the presence of exfoliation, disintegration, loss of strength, alveolation, consistent black patinas (Figure 13) of stones and mortar [18].

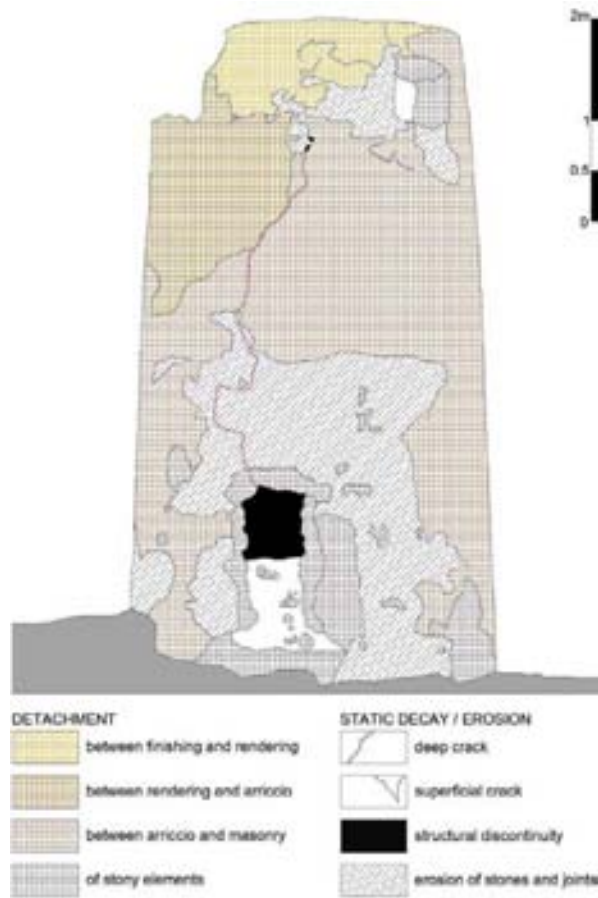


FIGURE 11. Cagliari, Su Perdusemini tower. Deterioration mapping (drawing by M. Porcu).

## CONCLUSIONS

This study, based on an interdisciplinary approach using the knowledge of the construction techniques together with the physical-chemical analysis of the materials, aims to provide a chronological *datum* that can be applied to identify and date masonry structures, previously anonymous constructions which mostly consists of vernacular architecture without formal architectural features. It allows us to reevaluate our architectural heritage and to recognise the wider sense of the word ‘monument’, that may now be seen to also include traditional historic urban fabric. In other words, even if the study is not exhaustive, it offers a sampling that can represent an useful point of reference for recognizing historical manufacture, at disposal of insiders.

Besides the deep knowledge of the constructive characteristics (from a structural, lithological, petrographical and mineralogical point of view), is the only preliminary remark to plan a conservation project, with respect of material and figurative consistence of

architectural heritage. The decay conditions of similar historical structures highlight the need for a restoration strategy that will ensure their preservation and management.



FIGURE 12. Cagliari, Su Perdusemini tower. Deterioration of the external plaster.



FIGURE 13. Cagliari, Su Perdusemini tower. Black patinas of the stones.

## REFERENCES

1. C. Giannattasio, “Les tours côtières du sud de la Sardaigne. Techniques de construction et problématiques de conservation”, in *Actes de la Deuxième Rencontre Internationale sur le Patrimoine Architectural Méditerranéen - RIPAM2* (Marrakech, 24-26 octobre 2007), Marrakech, 2009.
2. C. Giannattasio, S.M. Grillo, “The Mezzaspiaggia tower (Cagliari-Italy): the dating of structures by the metrological-chronological analysis of masonry and the petro-geochemical stratigraphy of building materials”, in *Proceedings of the 37° International Symposium on Archaeometry* (Siena, 12-16 maggio 2008), I. Turbanti-Memmi ed., Springer, 2010, 489-494.
3. D. Scano, *La Sardegna, e le lotte mediterranee nel XVI secolo*, in “Archivio Storico Sardo”, XX, 1-2, 1936, pp. 32-36;
4. S. Casu, A. Dessi, R. Turtas, “Il «disegno di Jacopo Palearo Fratino per il sistema fortificato di Cagliari (1563-1579)»”, in *Arte e cultura del ‘600 e del ‘700 in Sardegna* T. Kirova ed., Congress Proceedings, Cagliari-

- Sassari 1983), Edizioni Scientifiche Italiane, Napoli 1984, pp. 69-88.
5. S. Casu, A. Dessì, R. Turtas, “La difesa del Regno: le fortificazioni”, in F. Manconi (edited by), *La società sarda in età spagnola*, Musumeci Editore, Aosta 1992, pp. 64-73;
  6. F. Russo, *La difesa costiera del Regno di Sardegna dal XVI al XIX secolo*, Roma, 1992, pp. 26-42.
  7. M. Rassu, *Baluardi di pietra. Storia delle fortificazioni di Cagliari*, Cagliari 2003.
  8. E. Pillosu, *Le torri litoranee in Sardegna*, La Cartotecnica, Cagliari, 1957.
  9. E. Pillosu, *Un inedito rapporto cinquecentesco sulla difesa costiera della Sardegna di Marco Antonio Camo*, in “*Nuovo Bollettino Bibliografico Sardo*”, 1959-60, 21, pp. 3-10, 22, pp. 7-12, 23, pp. 3-8, 24, pp. 3-11, 25, pp. 5-9.
  10. P. Castelli, “La progettazione del sistema territoriale di difesa”, in *Arte e cultura del ‘600 e del ‘700 in Sardegna* T. Kirova ed., Congress Proceedings, Cagliari-Sassari 1983, Edizioni Scientifiche Italiane, Napoli, 1984, pp. 54-59.
  11. F. Fois, *Torri spagnole e forti piemontesi in Sardegna*, La Voce Sarda Editrice, Cagliari 1981, pp. 12-13.
  12. G. Mele, *Torri e cannoni. La difesa costiera in Sardegna nell’età moderna*, EDES Editrice, Sassari 2000, p. 101.
  13. Archivio di Stato di Cagliari, Antico Archivio Regio and Fondo Amministrazione delle Torri; L. Piloni, *Carte geografiche della Sardegna*, Editrice Sarda Fossataro, Cagliari 1974.
  14. I. Zedda Macciò, “Genesi di una forma cartografica: dall’idea all’esperienza”, in A. Asole (scientific direction), *Sardegna. L’uomo e le coste*, Banco di Sardegna, Sassari 1983, pp.13-26.
  15. G. Barroccu, T. Crespellani, A. Loi, *Rivista Italiana di Geotecnica* 2 (1979), a. XV, 98-144.
  16. J.J. Hermann, N. Herz, R. Newman, *Interdisciplinary studies on ancient stone*, “ASMOSIA”, 5 (2002).
  17. P. Prokos, Equilibrium conditions of marine originated salt mixture: an ECOS application at archaeological site of Delos, Greece, in *Salt weathering on buildings*, Copenhagen, 2008, pp. 139-149.
  18. J. Èlsen, A. Brutsaert, M. Deckers, R. Brulet, *Materials Characterization* 53 (2004), 289-295.

## **Dating Tests, Mineralogical Analysis and Technological Characterization on Building Materials from Archaeological Excavations in Urban Historical Sites**

L.P. Traversa<sup>1</sup>, M.I. Casadas<sup>2</sup>, M.E. Peltzer<sup>2</sup>, F. Iloro<sup>1</sup> and A. M. Cesio<sup>3</sup>

<sup>1</sup>*Laboratorio de Entrenamiento Multidisciplinario para la Investigación Tecnológica (LEMIT), La Plata, ARGENTINA.*

<sup>2</sup>*Instituto Cultural de la Provincia de Buenos Aires, ARGENTINA.*

*e-mail: mariacasadas@yahoo.com.ar or mepeltzer@yahoo.com.ar*

<sup>3</sup>*Centro de Tecnología de Recursos Minerales y Cerámicos (CETMIC), ARGENTINA.*

**Abstract.** This paper presents three types of comparative technical testing on floor tiles, common ceramic bricks and earthenware used in archaeological buildings in two historical sites of Buenos Aires Province, Argentina. These sites, named “La Tablada” and “Casa Vicente Casco”, are placed in the urban area of Ensenada and Chascomús cities, respectively. They were studied during the archaeological excavations from 2007 to 2008 by the Instituto Cultural de la Provincia de Buenos Aires. The techniques for dating were developed and applied in the LEMIT laboratories, where the technological study of the bricks was also done. This methodology is also suitable for pottery dating. The technique lies on the observation that these materials expand by ageing. A set of measurements as a function of the temperature indicates that the contraction of a brick is a function of its age. Other building materials were also analyzed by CETMIC, the results of the mineralogical study by XRD are presented as well.

**Keywords:** dating test, building materials, ceramic bricks ceramic, earthenware, floor tiles.

### **INTRODUCTION**

The present work shows on the one hand the results of the characterization of common ceramic bricks from two archaeological sites in the Province of Buenos Aires, that are: Casa Vicente Casco, area Chascomús, and the bases of Paraje La Tablada, area Ensenada. Both sites are located in urban areas, then it was possible to study the behavior of building materials that are exposed to similar environmental and climatic characteristics. From the performed studies it was possible to obtain two types of information: a) Technological, chemical and mineralogical comparison between the different samples and b) Comparison of the behavior of

materials in front of the different techniques used for building, such as absorption, porosity, density and compressive strength.

On the other hand it was applied a dating method on bricks from such sites, which is interesting for dating ceramic pieces, based on the observation that ceramic materials expand as they grow older; then, running various tests on them at different temperatures it was observed that a greater contraction of bricks corresponds to the older materials [1].

The building materials from different sectors of the sites have been analyzed by LEMIT as institutional partnership in the archaeological studies conducted from Dirección Provincial de Patrimonio Cultural

(DPPC) of the Instituto Cultural de la Provincia de Buenos Aires (ICPBS).

Thus this work is the result of a joint intervention of two institutions carrying out research with the common purpose of providing contributions, from different perspectives, to scientific knowledge [2].

## ARCHAEOLOGICAL EXCAVATIONS IN URBAN HISTORICAL SITES

### Casa Vicente Casco

It is located opposite the Plaza San Martín, Chascomús, and it was constructed between the nineteenth and twentieth centuries.

Named after Don Vicente Casco who was born in Asunción, Paraguay in 1776, arrived in Buenos Aires in 1809 and settled in Chascomús, a village at that time. The original house was purchased in 1825 to the Andrade family. In 1831 began its expansion, making it more protected from the indian raids. It was the first multi-storey housing and at the same time one of the oldest in Chascomús, which appears on the measurement plans of 1826 [3]. (Figures 1 and 2).



FIGURE 1. Casa Vicente Casco.

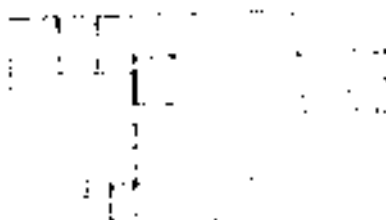


FIGURE 2. Plan of Casa Vicente Casco

After the death of the couple in 1979 his descendants Casco donate the property to the City on the condition that it hosted the "Chascomús Historiographical Institute". Despite it, nowadays operates in the site the "Casa de Cultura de la Municipalidad" (Culture House of the Town).

Today it is an area devoted to culture and history of the city and the region through the development of social activities and cultural life through exhibitions and permanent and temporary exhibitions, lectures and seminars given and other cultural events.

The first courtyard (Figures 3 and 4) has a floor consisting of three levels. The lower one corresponds to the original brick floor, the following is made of Sacoman tiles and the upper is formed by tiles of the late twentieth century. This floor was replaced by the current brick deck with the aim of its restoration.



FIGURE 3. Entrance to 1<sup>st</sup> courtyard.



FIGURE 4. 1<sup>st</sup> courtyard restored.

The second courtyard (Figure 5) was built afterwards. At first it was a large plot containing the "matera" (a place for preparing and drinking "mate").



FIGURE 5. 2<sup>nd</sup> courtyard.

*Overview of the archaeological test drillings:* five test drillings were performed in order to observe the behavior, similarity, continuity and characteristics of the bases, and to obtain samples for analysis.

All drillings were conducted in the second courtyard (Figure 5) except the excavation beneath the floor of the library, identified as S5.

The test drillings for the second courtyard were identified as S1 (Figures 6 and 7).



FIGURE 6.



FIGURE 7. Test drilling 1 (S1)

*Test drilling 1:* Located in the back door of the bathroom, intersection with the outer wall of the dining room.

It as drawn up a grid of 1 x 1 m excavated in flour levels of 0.20 m. each. On it, the bases of the bathroom and those of the lateral posterior wall of the house were cleared. These bases were cleared for visualization and measurement, obtaining samples for different analysis and testing proposed to CETMIC.

The base of housing is continuous, 0.70 m. depth consisting of 8 brick rows, joined with mudmortar.

That corresponding to bathroom shows 4 continuous upper rows and 4 lower projecting rows, also bound with mudmortar.

The fill context occurs up to 65 cm depth, from which the sterile clay sediment begins.

*Test Drilling 2:* Locate in the inner sidewalk of second court yard. It was opened a grid of 1.00 x 1.00 m in order to discover the back base of the house, determine its continuity and the type of mortar used.

The results showed the presence of 8 rows of continuous brick joined with mud mortar.

*Test drilling 3:* Located in sector inner sidewalk of the second courtyard. It was performed a grid of 0.50 x 0.50 m in which the same characteristics of the drilling 2 were observed.

*Test drilling 4:* Located in west angle of "La Matera" of second courtyard. It was performed a grid of 0.30 x 0.30 m in which there was a base composed by 4 brick rows held together with mud mortar.

*Test drilling 5:* Excavated under the floor of the library. It was conducted a grid of 0.50 x 0.50 m in which there were 8 rows of bricks joined with mud mortar. [3]

Among the found materials there were those classified as bone (Figure 8), earthenware, , iron, metal, roof tiles, glass, among others.



**FIGURE 8.** Bone materials.

## Site "La Tablada"

Today the archaeological site "La Tablada" (Figure 9) is in the area of Ensenada, Provincia de Buenos Aires.

"La Tablada" was a place where a post operated from 1873 for meeting and recognition of cattle that were destined to slaughter [4]. On that place, it was overseen the introduction of cattle to salting, compliance with the hygiene conditions and payment of taxes assessed by the state.

It was a big farm of 41 hectares, donated by the town, and its operations started in August 1873 [5]. On it, administrative offices were built for cattle control and some relays or supply posts.



**FIGURE 9.** Site "La Tablada" (bases of the place).

It was established in the middle of the "southern road" between Buenos Aires and Magdalena, at the intersection of the road leading to the saltings of Ensenada and Berisso. The "Camino Real" (Royal Road) of Virreinato del Río de la Plata had two main routes: one towards north reaching Peru and the second to the west that led to Cuyo, penetrating to Chile through the Andes. Subsequently the Camino Real del Sur was extended from Buenos Aires to Magdalena. Along the entire route of Camino Real there was established a relay ("postas") service at intervals between 30 and 50 km. The postas provided the traveler a change of riding horses and carthorse, and a postilion with a remuneration fixed by the State, taking a further obligation to provide him accommodation [6].

*Archaeological research:* This work was performed as urban archaeological recovery, framed by the Archaeological Research Project in military settlements: guards, forts, "fortines" (small forts) and "postas" (relays). Foundation and development of villages in the area of natural boundary of Rio Salado.

The origin of the tasks performed by the Cultural Institute was a ground-leveling work, where the neighbors observed the existence of brick structures joined with mud mortar, which probably would correspond to the relay La Tablada.

A surface of 63 meters square by 0.30 m deep was excavated, in which 3.000 historical archaeological materials were recovered. On them it was carried out a first typological classification based on the raw materials that constitute them, such as skeletal elements (Figure 10) of mammals, fish and birds, earthenware (Figure 11), domestic and playful, metals (Figure 12) such as coins, screws, pins, plates, jewelry and cutlery, glasses (Figure 13), bottles, cups, marble (Figure 14), coal, leather, stone, roof tiles and bricks, among others (Figure 15).

Samples were taken from bricks and mortar for the “posta” structures, which were sent to LEMIT to carry out technological analysis and their probable dating by a method in experimentation.



FIGURE 10. Bones.



FIGURE 11. Earthenware.



FIGURE 12. Metals.



FIGURE 13. Glasses.

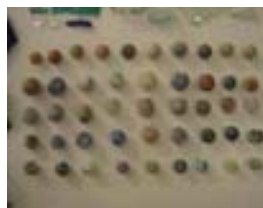


FIGURE 14. Marble.

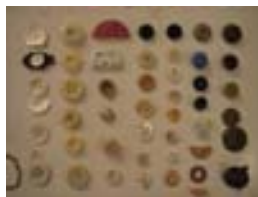


FIGURE 15. Buttons.

## ANALYSIS OF MATERIALS

### Mineralogical Analysis of Materials from Casa Vicente Casco

CETMIC performed mineralogical studies by X-ray diffraction on bricks, mud mortars and floor tiles.

*Bricks analysis:* the studied samples were identified as L1 and L2, corresponding to first courtyard and warehouse floor respectively.

The components of sample L1 were mostly quartz ( $\text{SiO}_2$ ), and feldspar ( $(\text{Ca},\text{Na})(\text{Al},\text{Si})_2\text{Si}_2\text{O}_8$ ), and scarce cristobalite ( $\text{SiO}_2$ ) and hematite ( $\text{Fe}_2\text{O}_3$ ) (Figure 16).

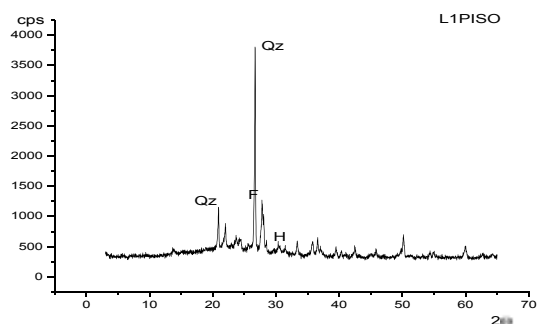


FIGURE 16. Diffractogram of sample L1.

The components of sample L2 were mostly quartz ( $\text{SiO}_2$ ), feldspar ( $(\text{Ca},\text{Na})(\text{Al},\text{Si})_2\text{Si}_2\text{O}_8$ ) and iron oxide (hematite,  $\text{Fe}_2\text{O}_3$ ), and in a small proportion carbonated material  $\text{Ca}(\text{Mg},\text{Mn})(\text{CO}_3)$  and components such as chlorite, smectite, illite, montmorrillonite (Figure 17).

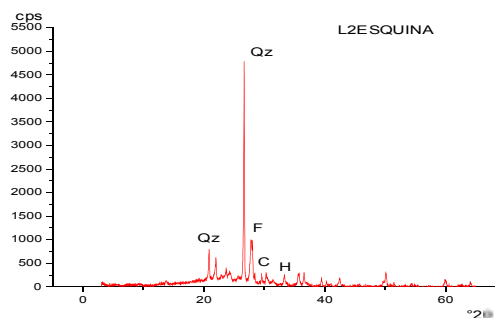


FIGURE 17. Diffractogram of sample L2.

*Analysis on mud mortars:* conducted on samples obtained from drilling 1; the results showed a higher proportion of quartz and feldspar components, with a lower proportion of cristobalite ( $\text{SiO}_2$ ) and hematite ( $\text{Fe}_2\text{O}_3$ ) (Figure 18).

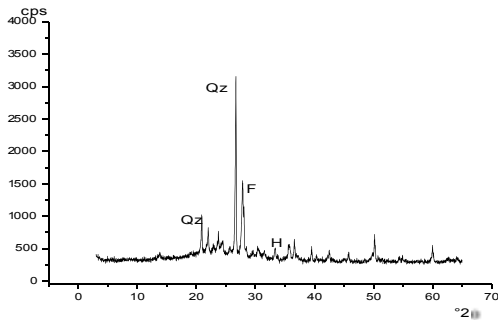


FIGURE 18. Diffractogram of mortar from test drilling 1.

*Studies on floor tiles:* the analyzed sample corresponds to a tile taken from the first courtyard, whose analysis yielded a composition of sodium feldspar ( $\text{Na Al Si}_3\text{O}_8$ ) and Calco-Sodium ( $\text{Na Ca}(\text{Al Si})_2\text{Si}_2\text{O}_8$ ), with hematite and quartz. It could also contain carbonated material type  $\text{Ca}(\text{Mg},\text{Mn})(\text{CO}_3)$  and some gypsum ( $\text{CaSO}_4 \cdot 2\text{H}_2\text{O}$ ) (Figure 19).

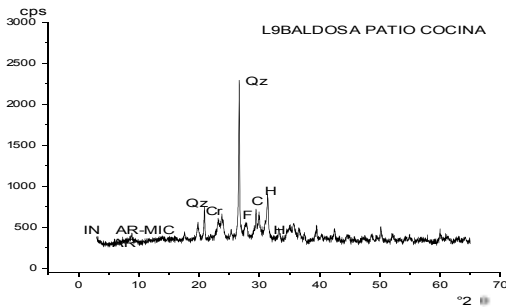


FIGURE 19. diffractogram of tile sample.

### Comparative Technological Analysis of Bricks from “Casa Vicente Casco” and site “La Tablada”

Physical-mechanical tests were performed in order to characterize, on samples of common ceramic bricks, the following parameters:

*Porosity (p):* is given by the ratio between the amount of water absorbed by immersion during 24 hours and the volume of the sample.

*Density (ρ):* is given by the ratio between the weight of saturated surface dry sample and its volume

obtained by weight difference in the air and underwater.

*Absorption (abs 24 h):* the ability of water absorption by immersion for 24 hours.

*Compressive Strength (f'c):* it is linked to its ability to withstand the efforts.

TABLE 1. Results of average product of three determinations on each case.

Site	p (%)	ρ g/cm <sup>3</sup>	abs. 24 h (%)	f'c (mpa)
Casa Casco	20.9	1.63	24.7	6.0
La Tablada	19.0	1.73	23.0	7.3

Table 1 shows a high absorption in the samples, which shows a direct relationship between porosity and low resistance

### DATING OF BRICKS

LEMIT continues to undergo experiences based on a technique for dating of bricks, according to m. a. Wilson *et al.*, 2003 [1]. after these studies all fired clay ceramic materials (bricks, tiles and pottery) are expanded with age, a process linked to the slow uptake of water due to the phenomenon of absorption.

These materials then subjected to a drying cycle at 450 ° C reacquire its original size.

The result of the experiments performed was that the increasing of linear expansion of ceramic materials by moisture in the long term depends on an exponential function of time ( $t^{1/4}$ ) and on the mineralogy of the material used on the bricks.

In the experiments carried out with english bricks, it appears that the variation in length in the thermal cycle takes the following expression:

$$\delta = k \times 10^{-5} (t)^{0.24}$$

where:

- δ = mean length change
- k = correlation coefficient
- t = time (days) [1]

In previous experiments conducted in the LEMIT, bricks samples of different ages were used (1, 70, 110, 120 years) made with materials of similar mineralogical characteristics, which is the condition of the dating method [2].

Dating experiments were also performed with brick samples from sites casa casco and la tablada, but because of the scarce number of available samples and their small dimensions, it was impossible to make a number of determinations and to put metal pins in the ends. only the edges were sawed to level them and allow for proper placement in the length measuring instrument (Figure 20).



FIGURE 20. Length measuring instrument

The test specimens were 164 x 40 x 50 mm, subjected to a thermal cycle of 450° C for 2 hours, after which the values of  $\delta$  (%) were obtained for each case. the results were about 0.299 mm and 0.185 mm for casa casco and la tablada respectively. These values are average of two determinations and it is possible to pose that the bricks are older than 170 years by making a comparison with data from other experiences and assuming that the material is similar.

## CONCLUSIONS

In mineralogical studies the samples from Casa Vicente Casco have similar mineralogical characteristics on bricks and mortar. This may be because the bricks are made from raw materials obtained in the vicinity of the site locations of buildings, since they correspond to the soils used for settlement mixtures. It is not so in the case of tiles,

which would indicate their different origin or manufacture place.

In technological characterization, the comparison between bricks from urban historical sites (Casa Vicente Casco and La Tablada) shows a high absorption in the samples, which shows a direct relationship between porosity and low resistance.

With respect to the method of dating: dating is interesting for ceramic pieces, since from the analysis of the results it appears that the contraction measured in the thermal cycle (450° C for 2 hours) can be considered as a function of the age of the brick. But due to the dispersion found in the values obtained from a single sample, for the future tests the number of determinations will be higher for a better approximation in estimating the age of the materials under study.

## REFERENCES

1. M. A. Wilson, W. Hoff, Ch. Hall, B. Mc Kay, A. Hiley, "Kinetics of Moisture Expansion in Fired Clay Ceramics: A (Time)<sup>1/4</sup> Law" Ed. Sociedad Física Americana, Ridge, New York, 1958, Revue. *Physical Review Letters* **90** no. 12 (2003).
2. L. P. Traversa, M. I. Casadas, M. E. Peltzer and F. Iloro, "Caracterización Tecnológica y Presentación de un Método de Datación en Ladrillos Cerámicos Comunes Procedentes de Sitios Arqueológicos Históricos Rurales", in *Actas del V Congreso de Arqueología de la Región Pampeana Argentina CARPA*, La Pampa, Argentina, 15 á 18 de Septiembre de 2008. Ed. Universidad Nacional de Luján, en prensa.
3. M. I. Casadas, M. E. Peltzer, "Investigaciones Arqueológicas en la Casa Vicente Casco de la Ciudad de Chascomús, Provincia de Buenos Aires", in Congreso Nacional de Arqueología Argentina, Jujuy 2007, Tomo II, pp.12 - 20.
4. Z. Quatrín y O. Otero, "Investigación Arqueológica Tablada de la Ensenada". Informe Técnico CIC-LEMIT, Buenos Aires 2000.
5. AHPBA 1870-72 carpeta 682. Nota del Ministerio de Hacienda del 13 de diciembre de 1872.
6. R. Napp, "La República Argentina", Editorial Sociedad Anónima, 1876, p.p. 314, anexo & mapas.
7. R. Fort., M.J. Varas, E. Pérez-Monserrat, J. Luque, M. Alvarez de Buergo, C. Vazquez-Calvo, *Boletín de la Sociedad Española de Cerámica y Vidrio*, **46** (2007) 145-152.
8. T. González Limón, M. Alvarez de Buergo. "Manual de diagnosis y tratamiento de materiales pétreos y cerámicos". Colegio de Aparejadores y Arquitectos Técnicos de Barcelona. Colección Manuales de Diagnosis Vol 5, 1997, 89-106.

# **Diagnosis of State of Preservation and Quantification of Trace Elements in Ancient Bones from La Laguna, Tlaxcala Mexico**

L.R. Couoh<sup>1</sup>, J.L. Ruvalcaba<sup>2</sup>, L. Bucio<sup>2</sup> and J. Arenas<sup>2</sup>

<sup>1</sup>*Posgrado en Antropología, Facultad de Filosofía y Letras, Instituto de Investigaciones Antropológicas,  
Universidad Nacional Autónoma de México, MEXICO. e-mail: loucouoh@gmail.com*

<sup>2</sup>*Instituto de Física, Universidad Nacional Autónoma de México, MEXICO.*

**Abstract.** To carry out the quantification of the trace elements of bone – to determine tendencies in diet – it is fundamental to know the state of the preservation of bone tissue. In this research, the procedure to examine the diagenetic damage of bone was addressed in two ways: 1) Detection and quantification of the presence of collagen and the analysis of the structure of the Haversian systems. 2) Identification of the exogenous elements incorporated onto the biogenic hydroxyapatite, measurements of the changes in the major mineral components (Ca and P) and the calculation of the crystallinity of the bone. The set of techniques employed were: Differential Scanning Calorimetry (DSC), Fourier Transform Infrared Spectroscopy (FTIR) and Ionoluminescence (IOL) to detect and quantify the presence of collagen; X-Ray Diffraction (XRD), Particle Induced X-Ray Emission Spectrometry (PIXE) and Transmission Electron Microscopy (TEM) to analyze crystallinity and elemental composition; and Scanning Electron Microscopy (LV SEM) was used to determine the degradation of bone microstructure. With regard to trace elements, measurements were done with PIXE and two trace elements were quantified first, the concentration of strontium (Sr) – as the representative of vegetal ingesta – and zinc (Zn) – indicative of the level of animal protein present. The results demonstrated a correlation between the state of preservation and the antiquity of the samples, that is, the older sample was more degraded than the more recent. An order of collagenic degradation to all of the samples was established; likewise the analytical results of the mineral part of bone also matched the same order. We concluded that the diagenetic damage was not significant enough to affect the elemental biogenic contained in each sample. Therefore the reliability in the biogenic signals of the trace elements was high. According to the “herbivorism index” the samples showed a similar pattern of concentrations found in an herbivorous animal, which we also analyzed. So, this suggests a predominantly vegetal diet. Furthermore, the reduced values of Zn and Fe could be indicative of a low consumption of animal protein and because of that, we suggest that our findings corroborated the visual signs on the skeletons of poor nutrition and health.

**Keywords:** Ancient Bone, Diagenesis, Collagen, Hydroxyapatite, Trace Elements, Paleodiet

## **INTRODUCTION**

After an individual dies, the bone tissue experiences physical and chemical changes determined

by the context in which they are located and by the time that they have been buried. Therefore the organic (collagen) and the mineral constituents (hydroxyapatite) of the bone suffer change. The dynamic process of change and modification of the composite of the bone is what is known as diagenesis.

On the bones' surfaces there can be changes like fractures, differences in coloration, disintegration – partial or even total. In the internal structure, the spongy bone is more susceptible to alteration than the compact bone. In its microstructure, the diagenesis can affect the Haversian systems through an increase in the porosity that leads to the destruction of the tissue. In the nanostructure, the structural and elemental arrangement of the mineral phase can suffer an increase or dissolution of the crystals and incorporation of exogenous elements. Also, a manifestation of diagenesis is the decrease or the increase of major constituents of the mineral part of the bone, the Ca and P. Any alteration in the Ca/P ratio indicates dissolution or recrystallization through the action of the mineral carbonation. On the other hand, the collagen, as the principal organic component, can be lost by the acceleration of the diagenesis process and by time. The knowledge of the state of preservation allows us to validate our findings of the trace elements which are related directly to the tendency in diet.

A trace element is any number of elements required by living organisms, in small amount, to ensure normal growth, development, and maintenance. And because of the physico-chemical properties of the hydroxyapatite, the trace element can be incorporated into the bone tissue [1]. In particular, strontium and zinc are used as indicators for varied diets. The reconstruction of nutrition is based on the process of physiological bio-purification of calcium in food chains by discriminating against the strontium and zinc. The elemental analysis of human bone is often used in paleoanthropology for dietary and environment reconstruction, as well as in the assessment of the social and economic status of human groups.

## SAMPLES AND METHODS

The collection of bones recovered at the site “La Laguna” belonged to in the Formative and Epiclassic period. This site in the present city of Apizaco, in the North East of the state of Tlaxcala, México.

From nine skeletons, samples of compact bone were taken for the different experiments. The region of interest was the mid-shaft of the diaphysis of long bone (Table 1). A sample of a deer bone from the same site was analysed with PIXE as herbivore reference in the trace element analysis.

### Differential Scanning Calorimetry (DSC)

The powdered samples of bone were analyzed in SDT/Q600 TA Instruments®. For the DSC measurements, the heating rate was constant at 10°C/min in an air atmosphere. The sample amount used was 10 mg of bone. The software TA Universal Analysis was used to calculate the enthalpy ( $\Delta H$ ) of the organic material. This technique has been proved to be very sensitive in the quantification of protein remains in bone [2, 3].

### X-Ray Diffraction (XRD)

This experiment was performed in Bragg-Brentano geometry by the Bruker D8 Advance diffractometer using Cu-K $\alpha$  radiation ( $\lambda = 1.5416 \text{ \AA}$ ) at 40kV and 30mA. Data were collected using a  $2\theta$  range of 3°-110° with step size of 0.05. The bone powder was set on a diffractometer fitted with a rotating sample-holder. For the qualitative phase analysis the database ICDD (International Centre of Diffraction Data) was used and the Crystallinity Index (CI) was determined [4].

### Fourier Transform Infrared Spectroscopy (FTIR)

The FTIR analysis was carried out by using Nicolet Nexus 670 FTIR and Bruker Vector 33 FTIR equipment. The bone powder was mixed with KBr powder (100:1 ratio) and compressed to form pellets. All measurements are made from 4000 to 400 cm<sup>-1</sup>. This experiment was to identify the presence of collagen and to assess its state of preservation.

TABLE 1. Chronology and burial context of the samples.

Chronology	Burial context	Sample	Bone
Late Formative (600-350 BC)	Bell-shape pit F46	F46-1	Right tibia
Late Formative (600-350 BC)	Bell-shape pit F46	F46-2	Right femur
Late Formative (600-350 BC)	Bell-shape pit F46	F46-3	Right femur
Late Formative (600-350 BC)	Bell-shape pit F43	F43	Right femur
Late Formative (600-350 BC)	Pit	B63	Left femur
Late Formative (600-350 BC)	Pit	F83	Left femur
Terminal Formative (100 BC-AD100/150)	Surphase –no pit	I129	Left femur
Terminal Formative (100 BC-AD100/150)	Pit	H142	Left femur
Epiclassic (750-900 AD)	Pit	H149	Right tibia
Formative (600 BC-AD100/150)	Surphase –no pit	Deer	Left femur

### Particle Induced X-Ray Emission Spectrometry (PIXE)

To characterize the exogenous elements and trace elements in the bone matrix, analysis by PIXE was used. Two procedures to prepare the samples were followed. The first consisted of a cross-section cut of the bone to be irradiated with the beam in the central zone of the bone (between the periosteum and endosteum). The second was the chemical cleaning treatment [5]. This experiment was performed using the external beam of the Pelletron IF-UNAM accelerator, 3 MeV proton beam, two X-ray detectors (Si-PIN and LEGe with He flux and 80um Al filter, respectively) and 12 nA current on the sample for 5 min. NIST SRM 1400 (bone ash) reference material was irradiated under the same conditions for quantitative analysis. For elemental concentration, AXIL and PIXEINT programs were used.

### Ionoluminescence (IOL)

The objective of IOL analysis was to detect Mn<sup>2+</sup> impurities and organic material. The Spectrometer Ocean Optic UV-VIS-NIR (200-1000nm) was attached to the external device of the Pelletron Accelerator. The 74 UV Ocean Optic lens was placed at a 45° angle in front of the beam exit. The cross-section samples were placed in front of the beam, which was a 1.3 MeV. Each sample was irradiated at the periosteum and endosteum zone. To improve the measurements of luminiscence a portable dark room was used to cover the experimental device.

### Scanning Electron Microscopy (LV SEM) and Transmission Electron Microscopy (TEM)

Thin plates (2mm thickness) of bone were used to analyze the state of the Haversian systems. Each

sample was hand ground with sandpaper of different degrees of roughness (400, 1200, 1500, 2000, 4000) lubricated with distilled water, followed by 3 minutes of ultrasonic cleaning. The microscope employed was JEOL JSM 5600 LV SEM. To assess the state of degradation, the Oxford Histological Index (OHI) [6, 7] was used.

To isolate the hydroxyapatite crystals from the amorphous material (collagen) and characterize its morphology the procedure of the reference was followed [8]. JEM-2010F FAS TEM was used. The images were analyzed with Digital Micrograph software. Only three samples were analyzed with this technique (I129, F83, F46-2). A typological classification for the crystals in ancient bone was employed [9].

### Soil analysis

The pH of the soil samples was analyzed according to standard procedure [10]. Only five samples of burial soil were available for analysis by PIXE, the reference materials NIST SRM 2704 and SRM 2711 were irradiated under the same conditions for quantitative analysis.

## RESULTS

### Diagnosis of the State of Preservation

The set of techniques applied made possible the measurement of the quality and the quantity of collagen and biogenic apatite (Tables 2 and 3).

With respect to the organic phase, the DSC results show an exothermic process of the combustion of the collagen. This begins at 207°C, presents a maximum peak at 350°C and ends at 550°C. All the samples show different values of  $\Delta H$  and, considering that the degradation of the protein responds to different factors

**TABLE 2.** Results of all the samples in order to more and less degradation (E=Epiclasic; LF= Late Formative; TF= Terminal Formative). The luminescence band of the organic material is 496nm<sup>(a)</sup> and the Mn:Hap is 580nm<sup>(b)</sup>.

Sample	DSC ( $\Delta H$ ) J/g	FTIR				IOL				SEM OHI	XRD CI	pH Soil
		Amide I	Amide II	Amide III	Proline peak	Endosteum Organic <sup>(a)</sup> Mn:Hap <sup>(b)</sup>	Periosteum Organic Mn:Hap					
H149 (E)	2623	5	3.3	1.6	3.8	24.8	0	18.5	18.4	5	1.2	6.3
F43 (LF)	1903	3.7	3.1	1.8	3.7	27.4	0	6.61	18.6	4	2.6	6.6
B63 (LF)	1847	1.3	1	0.6	2	33.1	20.7	0	241.7	3	5	7
F46-2 (LF)	1554	1.3	0.9	0	1.8	10.2	0	11.5	61.6	3	3.5	8.3
I129 (TF)	1474	1.6	1.2	1.2	2.4	17.6	10.8	0	215	3	3	6.2
F83 (LF)	1223	1.4	1.1	0.5	2.2	20.0	0	8.1	42.1	2	5.3	7.3
H142(TF)	1196	1.6	1.3	1	2.3	8.2	0	23.6	27.1	3	2	6.2
F46-1 (LF)	966.6	0.9	0.9	0	1.9	11.5	0	7.5	29.2	2	5.1	8.3
F46-3 (LF)	861.8	1	0.7	0	2	16.3	0	5.2	7	1	5	8.3

mainly time, it is interesting to note that the sample from the Epiclassic (H149) presents the highest value of  $\Delta H$  in contrast to the, presumably, older sample, the F46-3 from the Late Formative. Nevertheless, the  $\Delta H$  values of the samples from the Terminal Formative overlap with some of the Late Formative.

The intensities of FTIR bands (amide I, II, III and proline peak) of collagen decrease with the increase of the degradation of the bone. Considering that the energy bond of amide III (292kJ/mol) is smaller than the amide II (391kJ/mol) and I (725kJ/mol) [11], the FTIR spectra of the samples show that the amide III present the lower intensity and in three cases this signal is absent. Conversely, the proline peak shows stability. This is because the proline – also the hydroxyproline – is a quarter or greater of the total of the complex molecules that constitute the collagen. To understand the state of preservation of the functional groups, the relative heights of the amides and proline peak with respect to the band of the phosphate group ( $PO_4^{3-}$ ) at  $1035\text{cm}^{-1}$  was calculated. The sample H149 presents the highest transmittance values, which means a better state of preservation. This also matches with the results of DSC, whereas the F46-1 and F46-3 are at the lowest levels.

In respect of IOL experiment, all the samples manifest luminescence in two specific bands: the

496nm and the 580nm. The first corresponds to the activation of the organic material, and the second to the  $Mn^{2+}$  ions on HAp [12-14]. The results show that in general the area of the endosteum contains most of the organic material. This was expected because the periosteum is the zone which is in direct contact to the soil. Likewise, the periosteum presents strongest luminescence intensity of the  $Mn^{2+}$ , which means more diagenetic alteration, as in the samples B63 and I129. Remarkable is the lower intensity of luminescence of  $Mn^{2+}$  in the endosteum.

To assess the level of destruction of the microstructure, the Histological Index of Oxford (HIO) was employed [6, 7]. In this index 5 points to good histological preservation and 0 indicates that any histological structure was preserved. The results corroborate the good state of preservation of the Epiclassic sample. The F43 also shows a good state but it should be appreciated that there are signs of thermic alteration which the body had received in a probable post-mortem ritual. This case is interesting because, when a body suffers a thermic alteration the chance of DNA and collagen surviving is greater [15]. The rest of the samples show different forms of destruction caused by bacteria and fungus, which resulted in micro and macro porosity. The sample with the worst preservation in its microstructure is the F46-

**TABLE 3 .** Results of the elemental analysis of the bone samples ( with and without chemical cleaning) and the associated soil of some of them (E=Epiclassic; LF= Late Formative; TF= Terminal Formative)

Sample	Al (%)	Si (%)	Mn ( $\mu\text{g/g}$ )	Fe ( $\mu\text{g/g}$ )	P (%)	Ca (%)	Ca/P	Zn ( $\mu\text{g/g}$ )	Sr ( $\mu\text{g/g}$ )
Bone ash SRM 1400	6.53	30.44	0	660	17.9	38.18	2.13	181	249
H149 (E)	0	0	13	116	22.2	48.6	2.18	80	219
Chemical cleaning/ H149 (E)	0	0	14	79	23.2	47.1	2.03	137	292
F43 (LF)	0	0	0	0	19.4	48.2	2.48	93	801
Chemical cleaning/ F43 (LF)	0	0	22	46	22.1	45.2	2.04	214	539
Soil of F43(LF)	7.06	19.5	0.08	4.02	0	1.49	x	76	339
B63 (LF)	0	0	28	22	20.8	45.1	2.16	120	766
Chemical cleaning/ B63 (LF)	0	0	47	72	19.5	41.5	2.12	356	677
F46-2 (LF)	0	0	0	68	20.6	45.2	2.19	144	666
Chemical cleaning/ F46-2 (LF)	0	0	26	53	22.2	46.3	2.08	159	655
Soil of F46-2 (LF)	4.77	15.0	0.09	4.25	0	1.01	x	77	361
I129 (TF)	0	0	25	32	20	44.8	2.24	101	926
Chemical cleaning/ I129 (TF)	0	0	34	157	19.8	43.3	2.18	208	816
F83 (LF)	0	0	0	29	20	46.0	2.3	147	746
Chemical cleaning/ F83 (LF)	0	0	24	51	21.6	44.5	2.06	258	499
Soil of F83 (LF)	9.40	28.8	0.07	3.59	0	2.37	x	59	420
H142(TF)	0	0	43	19	19.6	44.4	2.26	90	1037
Chemical cleaning/ H142(TF)	0	0	34	101	22	45.4	2.06	125	633
F46-1 (LF)	0	0	18	34	20.5	46.7	2.27	110	972
Chemical cleaning/ F46-1 (LF)	0	0	26	175	20.2	42.3	2.09	192	802
Soil of F46-1 (LF)	5.43	16.2	0.08	4.18	0	1.27	x	77	343
F46-3 (LF)	0	0	0	58	18.2	44.2	2.42	127	1322
Chemical cleaning/ F46-3 (LF)	0	0	21	136	20.5	45.1	2.04	142	884
Soil of F46-3 (LF)	5.29	16.0	0.08	4.19	0	1.37	x	67	494
Chemical cleaning/ Deer	0	0	39	63	19.9	41.1	2.06	161	1188

3, which is also the one with less collagen ( $\Delta H$ ).

With respect to the mineral phase, with XRD, the reflections registered correspond to the apatite signal ( $25.5^\circ$ ,  $31^\circ$  and  $34^\circ \theta$ ). For this reason the apatite is the majority mineral fraction in all the samples. When the bone is buried the crystals increase in size or change its morphology. If the organic phase is removed the apatite crystals suffers dissolution and the biggest crystal increase their size at the expense of the smaller. Furthermore, these changes can be accelerated during and after the organic material decomposition. It is important to measure the pH of the burial soil because it has a direct effect on crystallinity of bone, either to increase or decrease it. Collagen is better preserved in a ground that is alkaline or neutral. If the pH is acid, the crystals can be dissolved quickly [16].

The scale of Crystallinity Index (CI) ranges from 0 to 10 [4]; in a fresh bone the CI is close to 0. The samples show values from 1 to 5. The ones with greater CI have an alkaline pH burial soil.

The morphology of the crystals analyzed by TEM is type II, which is in form of needles with an arrangement in parallel with each other [9]. This is because of the dissolution or demineralization of some crystals and the crystallization of others. It is possible that there is an association between the crystals shape and its CI but more experiments are needed.

We put much care to eliminate the exogenous elements from the surface of the mineral bone by chemical cleaning, which seems to be effective. The results by PIXE show a reasonable measurement of what the biogenic bone's elements can be expected. On the other hand, the elemental analysis of burial soil allowed us to approach to determine how much of the elements lost by chemical cleaning came directly from the soil, and how much of the soil could remain in the bone's matrix.

Chemical cleaning had the effect of decreasing Sr in the samples and the improvement of measurements of Zn. In the case of the Fe we are sure that the nature of this element is biogenic because in the soil its concentration is very low. Elements such as K, Si, Fe, Al and Mn are common in the soil and for this reason are considered as the main contaminants of the matrix of the bone. It is interesting to note that there is no record of K, Al or Si in any sample, but surprisingly the Mn had remained. This suggests its incorporation into the bone's mineral structure.

The two main components of the mineral phase had an increase in their percentages, up to 5% in P and 8% in Ca. Therefore the Ca/P ratio in the samples did not change significantly. A bone with typical diagenesis shows Ca/P ratio of 2.5 [17]. The sample B63 has the closest ratio to the reference (SRM 1400) and, at the same time presents the highest concentration of Mn, which is in concordance with the result of IOL. Likewise the rest of the samples show the presence of Mn. Only this element was not removed completely

with the chemical cleaning. Nevertheless, we know by IOL data that this element affects mainly the periosteum zone.

As a result of all the data presented we determine that the effects of the diagenetic alterations, over the samples of bone tissue, did not interfere significantly in the preservation of the composite of the bone. Time played a fundamental role in the deterioration of the collagen in conjunction with the action of bacteria and fungus, which modified the structural arrangement of the collagen fibers without causing their total destruction. Therefore, we rely in the use of the elemental analysis as the biogenic signals of the trace elements.

## Trace elements

To know the predominant tendency in diet – herbivore or carnivore – of the ancient inhabitants from “La Laguna”, the presence of Sr is used as indicator of vegetal consumption, and Zn of animal protein. All samples show high levels of Sr, in the trophic chain, remarkably close to the level of Sr in deer (Figure 1). There is no doubt that the higher level of Sr (over the standard value – SRM 1400) is as a result of the absorption and deposit into the mineral matrix because of the diet. The general omnivorous nature of the human being is corroborated because, even though the concentration of Sr is high, it will never reach the level of the herbivorous (deer).

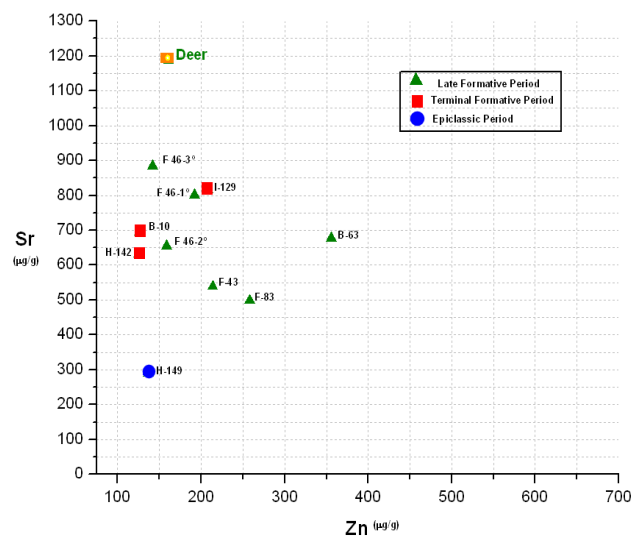


**FIGURE 1.** Sr/Zn ratios. The tendency of the group pointed to the trophic level of the herbivorous.

On the contrary, the concentration of Zn is considerably low. In some cases this is lower than the standard value. This is opposite of our expectations because the human being, in his omnivorous condition,

has different sources to get this mineral: animal protein, grains and cereals. Of the total of the Zn consumption, 20% is accumulated into the mineral matrix of bone [18] and part of this is associated with the collagen. According to the results in this study the consumption of proteins in the diet was not enough to supply the appropriate contribution of Zn to the normal physiology of the organism.

In this sense, it is known that Fe does not have a mechanism of fixation into the bone matrix, and because of that becomes one of the most vulnerable elements in the diagenetic processes. However, in this study the results of the set of experiments indicate that the concentration of Fe belongs to the biogenic composition of the bone and is not a consequence of the diagenetic process. Furthermore, the low level of Fe matches with some stress indicators – owing mainly to the lack of iron because of poor nutrition– found in the skeletons (from where the samples were taken) such as porotic hyperostosis, infectious process, enamel hypoplasia and periodontal disease[19].

The Sr/Zn ratio matches with the deer's ("herbivorous index") (Figure 1). This means that the typical herbivorous animal has the highest content of Sr and the lowest of Zn. Using the Sr/Zn ratio, the trophic level of any human population can be measured against this index [5]. In this respect, no difference was found between the samples from the Formative and the Epiclassic period.

## CONCLUSIONS

To understand the diagenetic processes, it is essential to consider the reciprocal relationship between the mineral and organic phase, because any signal of deterioration in one will cause a repercussion in the other.

The guiding parameter used to diagnose the state of preservation of bone was the presence of collagen, because in relation to the mineral compound, its life span is shorter and its vulnerability to suffer greater diagenetic processes. The state of preservation of the microstructure, the structure of the functional groups of the protein, as well as the collagen contents – measured by  $\Delta H$  – match with the analytical results of the mineral phase. Therefore the intrinsic relationship between the collagen and the hydroxyapatite was confirmed.

The order of degradation showed the sample H149 from the Epiclassic as the best preserved and, the F46-3 from the Late Formative as the least. The difference in the state of preservation of the samples is due mainly to the time that they had been in the ground. Because all the samples came from the same area we assume that the diagenetic factors worked in a similar way on the bones from both periods.

The chemical cleaning showed its effectiveness to reach a total quantification of the elemental biogenic

contents in each sample. In this way the exogenous elements attached to the mineral surface were eliminated, surprisingly, with the exception of Mn. We found that the location of this exogenous element is more prevalent in the periosteum, which leads us to consider the endosteum as a better area to apply analysis in future researches.

Finally, the reliability in the biogenic signals of trace elements is high. According to the "herbivorous index" the samples showed a tendency towards the Sr/Zn ratio of the deer. In conclusion we suggest that the vegetal ingesta was the principal source of nutrition in the ancient population of "La Laguna".

## ACKNOWLEDGMENTS

This research has been partially supported by UNAM grants DGAPA PAPIIT IN113-109-2, IN403210 and CONACyT Mexico grants 81700 and U49839-R. Authors thank K. López and J. Beristain for Pelletron Accelerator operation; J. Cañetas, L. Rendón, R. Hernández and D.A. Quintero from the Central Laboratory of Microscopy, IFUNAM; J.O. Flores and H. Sánchez for FT-IR experiments at The Center for Applied Science and Technological Development (CCADET-UNAM); E.M. Rivera for the FT-IR at the Applied Physics and Advanced Technology Centre (CFATA-UNAM). To the archaeologists: A. Borejsza, D. Carballo and R. Lesure from UCLA.

## REFERENCES

1. J.H. Beattie, A. Avenell, *Nutr Res Rev*, **5** (1992) 167.
2. L.F. Lozano, M.A. Peña, A. Heredia, J.O. Flores, A. Gómez, R. Velázquez, I.A. Belío, L. Bucio, *J. Mat. Sci.*, **38** (2003) 4777-4782.
3. L.R. Couoh, J.L. Ruvalcaba, "Characterization of bone remains for deterioration and dating studies". Symposium of Archaeological and Arts Issues in Materials Science, XVI IMRC 2007 Cancún, Quintana Roo.
4. A. Bartsiokas, A.P. Middleton, *J. Archaeolog. Sci.*, **19** (1992) 63-72.
5. R. Rodríguez, *Paleonutrición de poblaciones extinguidas en Mesoamérica y las Antillas: Xcaret y el Occidente de Cuba*, Ph.D. Thesis, Escuela Nacional de Antropología e Historia INAH, Mexico, 2004.
6. R.E.M., Hedges, A.R. Millard, A.W.G. Pike, *J. Archaeolog. Sci.*, **22** (1995) 201-209.
7. A.R. Millard, "Deterioration of bone" in *Handbook of archaeological Sciences*, D.R. Brothwell, A.M.

- Pollard (eds), WileyBlackwell, Great Britain (2001) 633-643.
8. X.W. Su, F.Z. Cui, *Mat. Sci. Engin. C*, **7** (1999) 19-29.
  9. I. Reiche, C. Vignaud, M. Menu, *Archaeometry*, **44**, 3 (2002) 447-459.
  10. NOM-021-SEMARNAT-2000, *Diario Oficial de la Federación*, Mexico, 2003, **23 de abril**.
  11. L. Pauling, *General Chemistry*, 1st ed. Dover, New York, 1970.
  12. H. Calvo del Castillo, J.L. Ruvalcaba, T. Calderon, *Anal. Bioanal. Chem*, **387** (2007) 869-878.
  13. D. Spermann, St. Jankuhn, J. Vogt, T. Butz, *Nucl. Instr. and Meth. In Phys. Res. B*, **161-163** (2000) 867-871.
  14. A.A. Bettiol, C. Yang, G.P. Hawkes, D.N. Jamieson, K.G. Malmqvist, R.W. Day, . *In Phys. Res. B*, **158** (1999) 299-305.
  15. K.A. Brown, K. O'Donoghue, T.A. Brown, *Inter. J. Osteoarch*, **5** (1995)181-187.
  16. F. Berna, A. Matthews, S. Weiner, *J. Archaeol. Sci*, **31**(2004)867-882.
  17. A.A. Hassan and D.J. Ortner, *Archaeometry*, **19** (1977) 131-135.
  18. J.E. Buikstra, S. Frankenberg, J. Lambert, L. Xue, "Multiple elements: multiple expectations" in *The chemistry of prehistoric human bone*, T.D. Price (ed), Cambridge University Press (1989)155-210.
  19. L.R. Cough, *De la hidroxiapatita al entierro*, M. A. Thesis, Facultad de Filosofía y Letras – Instituto de Investigaciones Antropológicas UNAM, México, 2009.

## **Basalt Chemical Weathering at Puebla Historical Buildings**

M. Teutli<sup>1</sup>, E. León<sup>2</sup>, J. Cerna<sup>3</sup> and A.C. Ruíz<sup>3</sup>

<sup>1</sup> *Facultad de Ingeniería, Benemérita Universidad Autónoma de Puebla, MEXICO. e-mail: teutli23@hotmail.com*

<sup>2</sup> *Facultad de Arquitectura, Benemérita Universidad Autónoma de Puebla, MEXICO.*

<sup>3</sup> *Facultad de Ciencias Químicas, Benemérita Universidad Autónoma de Puebla, MEXICO.*

**Abstract.** This work presents an approach for diagnosis of basalt weathering damage based on chemical anion detection. An effort of correlating chemical properties with typical acid rain urban pollutants goes from a chemical analysis of an unweathered sample collected at the Belem Hill quarry, and those obtained from a XVI century catholic temple facade. Taking as reference the unweathered stone, collected damaged samples show an increase of up to 32 times in sulfate, 16 times in carbonate, and 105 times in nitrate.

**Keywords:** basalt, weathering, historical buildings, atmospheric pollutants.

### **INTRODUCTION**

Materials exposed to open air undergo several forms of weathering due to microbial activity and atmospheric pollution.

Many air pollutants are released through industrial activity, consumption of fossil fuels and motor vehicle traffic. Catalyzed by nitrogen oxides gaseous SO<sub>2</sub> undergoes oxidation and turns into H<sub>2</sub>SO<sub>4</sub>. Also, NO reacts producing NO<sub>2</sub>, and both of them react with air humidity to form HNO<sub>3</sub>, which is a powerful acid and a detrimental factor for stone materials [1]. Dry deposition of sulfur and nitrogen oxides plays a primary role in the chemical weathering of carbonate building stones, laboratory experiments have shown that sulfite is the main product when SO<sub>2</sub> is alone, while sulfate is produced if SO<sub>2</sub> is in presence of NO<sub>2</sub> in a 1:6 ratio of SO<sub>2</sub>/NO<sub>2</sub> [2].

Main anions in urban rainwater can be attributed to urban pollutants like SO<sub>4</sub><sup>-2</sup>, NO<sub>3</sub><sup>-</sup>, CO<sub>3</sub><sup>-2</sup>, while main alkaline cations come from the coarse fraction of the atmospheric aerosol, since Ca<sup>+2</sup> and Mg<sup>+2</sup> are common constituents of soil [3].

Historical buildings, having exposed areas of stone elements, are candidates to exhibit weathering damage due to sunlight, wind, rain and air pollutants. All mentioned factors can be a source of chemical damage which became evident through signs like

scaling and flaking [4]. It is known that stone decay is a function of the amount and source of moisture, as well as its chemical content.

The atmosphere at Puebla Historical Center has shown a rise in pollutant concentration during the last decades; therefore weathering processes have affected buildings having basalt stone facades. The environmental damage becomes evident through surface appearance changes, which inherently imply both chemical and structural affectation.

This work presents an approach to estimate basalt stone damage, by analysis of incorporated anions which usually are present in acid rain; chemical analysis have been limited to detection of pH, conductivity, sulfate, chloride, nitrate phosphate and carbonate.

### **ANALYTICAL APPROACH**

Four samples of exposed damaged basalt were collected from a facade of a catholic temple from the XVI century which is located in a zone of heavy vehicular traffic at downtown Puebla, samples are designated as Ext East (5 South street), Ext North (3 West Av), Interior 1 (North yard), Interior 2 (Main entrance at the East side). Also for comparison, a reference sample was obtained from an inner part of a rock, which was collected at Belem Hill quarry one of

the main Puebla basalt providers during the XVI and XVII century. All samples were grinded to a size of 100 mesh; the analytical sample was prepared according to the ASTM C 114. Chemical analysis were done by gravimetric and colorimetric techniques.

## RESULTS

### Reference characterization

The reference sample has the following characteristics: pH=8.62, sulfate= 15 ppm, carbonate=1.12%, nitrate 0.8 ppm, phosphate 0.23 ppm, density=2040 kg m<sup>-3</sup>, porosity 0.5%, in order to classify this sample, results are compared with the ones reported in [5] as it is shown in Table 1. From this comparison it is possible to say that the reference sample can be considered an unweathered basalt.

Considering that urban environment generate conditions of acid rain, which eventually fall on the exposed stones, then ions present in the weathered basalt must be related to acid rain. In the literature there are references of corrosion studies using simulated acid rain, chemical composition of the one reported by [6], is shown in Table 2.

Authors also mention that solution pH has been adjusted with sulfuric acid or potassium hydroxide. In order to compare the acid rain composition referred by [6] with the rain in Puebla, 23 samples were collected in the period of 4 months in the rainy season 2009, containers were located on the roofs of the catholic temple. Samples have been analyzed for pH, conductivity, sulfate, nitrate, phosphate, chloride, total alkalinity, total hardness, calcium and magnesium content. Results are reported in Table 3.

From comparison of data in Table 2 and 3, it can be observed that main ions follow the order of SO<sub>4</sub><sup>-2</sup>>NO<sub>3</sub><sup>-</sup>>NH<sub>4</sub><sup>+</sup>>Cl<sup>-</sup>; therefore, an approach to estimate weathering can be done through detection of these ions in the stone. In Table 3, it becomes evident that rain in Puebla does not correspond to the synthetic acid rain, since the main anions exhibit a different order of importance: CO<sub>3</sub><sup>-2</sup>>Cl<sup>-</sup>>SO<sub>4</sub><sup>-2</sup>>NO<sub>3</sub><sup>-</sup>>PO<sub>4</sub><sup>-3</sup>; also it is observed that average values for Ca<sup>+2</sup> and Mg<sup>+2</sup> are not so close or low like the ones considered in [6].

Although, it is important to quote that for assessing weathering of stones, it is important to report rain ion concentrations based on m<sup>2</sup>, since exposed surface damage for any stone will be increased as long as the amount of rain is high enough to favor the contact rain-stone surface for long periods of time, even though ion concentration is low; the opposite case is when ion concentration is high enough but the amount of rain is quite low, since the contact time will be short and not enough to favor ion penetration into the stone. Therefore, based on the amount of rainwater that has

fallen in the place (1 m<sup>-2</sup> = mm of rain) concentrations should be reported as mg m<sup>-2</sup>, rather than mg l<sup>-1</sup>. In Table 4 are reported the values of main ions expressed in mg m<sup>-2</sup>, as can be observed these values are quite different from those in Table 3.

Although some values are different, the order of importance prevails the same: CO<sub>3</sub><sup>-2</sup>>Cl<sup>-</sup>>SO<sub>4</sub><sup>-2</sup>>NO<sub>3</sub><sup>-</sup>>PO<sub>4</sub><sup>-3</sup>. Then, the chemical analysis of weathered stone samples will be focused on these ions, values are reported in ppm (mg l<sup>-1</sup>) since these ions correspond to those that can be solubilized in distilled water. Results of chemical analysis for chloride, sulfate, nitrate, phosphate and carbonate content for the reference and the four weathered samples are reported in Table 5.

Ammoniacal nitrogen was not analyzed since it is assumed that in the exposed face of the stone an aerobic conversion will take place leading to the conversion of NH<sub>4</sub><sup>+</sup> to NO<sub>2</sub><sup>-</sup> and finally to NO<sub>3</sub><sup>-</sup> [7]. In respect to the unweathered sample, anion concentration have been increased in important amounts since sulfate goes from 6 to 33 times, nitrate goes from 26 to 105 times, and carbonate content have increased from 11 to 16 times. Chloride is an special case, since it is absent in the unweathered sample. From data in Table 4 and 5, it can be observed that main weathering ions in Puebla atmosphere are represented by carbonate, chloride and sulfate. Also it can be mention that stone pH diminishes when the ratio of Cl<sup>-</sup>/SO<sub>4</sub><sup>-2</sup> is less than 0.3, while a ratio of Cl<sup>-</sup>/SO<sub>4</sub><sup>-2</sup>>0.3 corresponds to an increase in pH.

Therefore, in order to assess how easily ions come incorporated into the stone, small samples of unweathered basalt were immersed into concentrated solutions of the following salts: MgSO<sub>4</sub>, (NH<sub>4</sub>)<sub>2</sub>SO<sub>4</sub>, NaCl, NH<sub>4</sub>Cl, MgCl<sub>2</sub>. After 20 days samples were extracted and dried a room temperature by 24 hrs, followed by 4 hrs of stove drying; after weighting and grounding, an analytical sample was prepared and analyzed for sulfate and chloride, results are shown in table 6.

From data in Table 6, it is seen that sulfate in a weathered stone could come either from an organic or an inorganic form since their soluble concentration are very close (72 and 51 ppm), something similar happens to the chloride ions (35.98 and 30.84 ppm), but for this last, the amount associated to divalent metals cannot be neglected since the chloride associated with Mg is about 40% of the one associated to Na.

In weathered samples a chemical analysis cannot be helpful in defining if the anion was associated with ammonium or with a metal. Then, it is proposed to add the anion concentrations registered in Table 6 and get a fraction that will represent the amount associated to ammonium and the one associated to metal. Factors for sulfate are reported in table 7, and those for chloride are reported in Table 8.

Then considering the above reported factors for sulfate and chloride, it is possible to split the registered concentrations for weathered samples, into

contributions based on the amounts determined with each type of salt. Results are reported in Table 9.

**TABLE 1.** Reference characterization.

Parameter	Fresh basalt	Slightly weathered basalt	Reference sample
pH	>8	5<pH<8	8.62
Dry density (kg m <sup>-3</sup> )	2811±48	2116±241	2047
Porosity	0.32±13	7.96±3.98	0.5
Water content (%)	0	29±9	2

**TABLE 2.** Composition of simulated acid rain, pH=3.5 [6].

Ion	Concentration, ppm
F <sup>-</sup>	0.0098
Cl <sup>-</sup>	1.0
NO <sub>3</sub> <sup>-</sup>	7.1
SO <sub>4</sub> <sup>-2</sup>	11.1
NH <sub>4</sub> <sup>+</sup>	2.3
Na <sup>+</sup>	0.42
K <sup>+</sup>	0.11
Ca <sup>+2</sup>	0.049
Mg <sup>+2</sup>	0.045

**TABLE 3.** Chemical composition of 2009 rain season at downtown Puebla.

Parameter	min	max	Average
pH	5.28	7.66	6.29
Conductivity, µS cm <sup>-1</sup>	30.00	340.00	90.00
SO <sub>4</sub> <sup>-2</sup> , ppm	1.00	46.00	10.54
NO <sub>3</sub> <sup>-</sup> , ppm	0	4.98	2.14
PO <sub>4</sub> <sup>-3</sup> , ppm	0	4.36	0.96
Cl <sup>-</sup> , ppm	8.22	88.63	31.15
Total alkalinity (CO <sub>3</sub> ), ppm	5.90	149.47	35.52
Total Hardness (CO <sub>3</sub> ), ppm	68.25	315.00	122.48
Ca <sup>+2</sup> , ppm	4.21	42.05	13.15
Mg <sup>+2</sup> , ppm	14.03	51.02	21.56

**TABLE 4.** Main ions in rainfall during the 2009 season at Puebla.

Parameter	min	max	Average
SO <sub>4</sub> <sup>-2</sup> , mg m <sup>-2</sup>	3.7	200.36	29.32
NO <sub>3</sub> <sup>-</sup> , mg m <sup>-2</sup>	0.00	60.37	12.45
PO <sub>4</sub> <sup>-3</sup> , mg m <sup>-2</sup>	0	47.91	6.11
Cl <sup>-</sup> , mg m <sup>-2</sup>	5.34	879.77	216.40
Total alkalinity (CaCO <sub>3</sub> ), mg m <sup>-2</sup>	3.83	635.99	177.54
Total Hardness (CaCO <sub>3</sub> ), mg m <sup>-2</sup>	76.74	2150.51	588.34
Ca <sup>+2</sup> , mg m <sup>-2</sup>	8.19	181.39	53.69
Mg <sup>+2</sup> , mg m <sup>-2</sup>	12.43	412.48	111.36

**TABLE 5.** Analytical data of basalt samples.

Sample	pH	Conductivity µS cm <sup>-1</sup>	Chloride ppm	Sulfate ppm	Nitrate ppm	Phosphate ppm	Carbonates %
Reference	8.62	80	0	15	0.80	0.23	1.12
Ext East	4.19	1 310	125.42	490	31.50	0.48	14.85
Ext North	9.29	2 910	178.80	94	84.00	0.65	12.43
Interior 1	7.13	770	51.40	190	20.90	1.66	15.28
Interior 2	9.21	3 230	205.61	420	76.00	0.47	17.49

**TABLE 6.** Determination of anion content for unweathered stones immersed into salt solutions.

Salt	Initial weight	Final weight	Anion concentration	mg <sub>anion</sub> kg <sub>sample</sub> <sup>-1</sup>
H <sub>2</sub> O	7.166	9.5978	0	0
MgSO <sub>4</sub>	10.3272	10.3372	51 ppm SO <sub>4</sub> <sup>2-</sup>	0.494
NaCl	10.9698	10.9835	35.98 ppm Cl <sup>-</sup>	0.328
(NH <sub>4</sub> ) <sub>2</sub> SO <sub>4</sub>	9.2266	9.2288	72 ppm SO <sub>4</sub> <sup>2-</sup>	0.780
MgCl <sub>2</sub>	9.1804	9.1950	13.71 ppm Cl <sup>-</sup>	0.149
NH <sub>4</sub> Cl	13.0956	13.0990	30.84 ppm Cl <sup>-</sup>	0.236

**TABLE 7.** Estimated sulfate contributions.

MgSO <sub>4</sub>	(NH <sub>4</sub> ) <sub>2</sub> SO <sub>4</sub>	TOTAL	X (MgSO <sub>4</sub> )	Y((NH <sub>4</sub> ) <sub>2</sub> SO <sub>4</sub> )
51 ppm	72 ppm	123 ppm	0.41	0.59

**TABLE 8.** Estimated chloride contributions.

MgCl <sub>2</sub> , ppm	NH <sub>4</sub> Cl, ppm	NaCl, ppm	TOTAL, ppm	X (MgCl <sub>2</sub> )	Y (NH <sub>4</sub> Cl)	Z(NaCl)
13.71	30.84	35.98	80.171	0.17	0.38	0.45

**TABLE 9.** Ion concentration in weathered stones based on organic and inorganic contributions.

Sample	Mg(SO <sub>4</sub> ) ppm	(NH <sub>4</sub> ) <sub>2</sub> SO <sub>4</sub> ppm	Mg(Cl) <sub>2</sub> ppm	NH <sub>4</sub> Cl, ppm	NaCl, ppm
Reference	6.22	8.78	0	0	0
Ext East	203.17	286.83	21.43	48.25	56.21
Ext North	38.98	55.02	30.56	68.78	80.13
Interior 1	78.78	11.22	8.78	19.77	23.04
Interior 2	174.15	245.85	35.14	79.10	92.15

## CONCLUSIONS

Obtained results show that chemical composition of the weathered samples has been severely affected since their anion content has been significantly raised in respect to the unweathered one, sulfate goes from 6 to 33 times, carbonate from 11 to 16 times, nitrate from 26 to 105 times.

From these data it can be established that incorporation of chloride and sulfate ions into weathered samples modify the pH to acid when the ratio of Cl/SO<sub>4</sub><0.3; while ratios of Cl/SO<sub>4</sub>>0.3 tends to displace pH to alkaline values.

## ACKNOWLEDGMENTS

This research has been partially supported by the School of Engineering, Benemérita Universidad Autónoma de Puebla, Mexico.

## REFERENCES

1. A. Cicek, A. Aslan, K. Yazici, A. Savas Kopal. (2008). Effects of environmental conditions on historical buildings: lichens and NO<sub>x</sub> gases. *Environ Monit Asses.* DOI10.1007/s10661-008-0388-1.
2. B. Moroni, L. Pitzurra, G. Poli, *Environmental geology* **46** (2004) 436-447
3. A.P. Baez, R. Belmont, Comparative study of the chemical composition of rain of three different zones in México. *Contam. Ambient.* **3**, (1987) 25-28.
4. H. Stück, L.Z. Forgó, J. Rüdrieh, S. Siegesmund, A. Török, *Environmental Geology.* **56**, (2008) 699-713.
5. V. Moon, J. Jayawardane, *Engineering Geology* **74**, (2004) 57-72.
6. Y. Shi, Z. Zhang, J. Su, F. Cao, J. Zhang. *Electrochimica Acta* **51**, (2006) 4977-4986.
7. S.E. Manahan, *Environmental Chemistry.* CRC Press LLC, 2000, chapter 6.

## **Biodeterioration of Mineral Materials in Cultural Heritage, Archaeology and Historical Collections**

L.E. Rendon<sup>1</sup>, X. Li<sup>1</sup>, M.E. Lara<sup>2</sup>, M. Rendon<sup>2</sup> and S. K. Rendon<sup>3</sup>

<sup>1</sup> *Instituto Mexicano de Tecnología del Agua, Cuernavaca, MEXICO. e-mail: lerendon@tlaloc.imta.mx*

<sup>2</sup> *Marudecori, Consulting, Cuernavaca, MEXICO.*

<sup>3</sup> *Facultad de Química, Universidad Nacional Autónoma de México, MEXICO.*

**Abstract.** Cultural heritage, archaeology and historical collections are subject to the deterioration and degradation action of the environment and microorganisms. These processes are normally referred to as *weathering*. This propensity (influenced by the climate) results in significant losses of precious cultural heritage in almost every region in Mexico. Indeed, this problem is not limited to humid and warm regions, and extends as far north as 40th parallel and well into the South America. A number of archaeology and historical collections have received some (albeit limited and expensive) provisions to slow the *weathering* process, but most of our cultural heritage (pre-Hispanic as well as modern) have received lesser resources applied to this problem. Clearly, the political conscience does not, and cannot, separate the long-term consequences of neglecting the cultural richness in Mexico. Serious attention and (re)investment in the conservation and reclamation capital will be needed to sustain our cultural heritage.

**Keywords:** Weathering, biodeterioration, mineral materials, archaeology.

### **INTRODUCTION**

Mankind uses rocks, stones, and other natural and manufactured products as construction materials. Both in their natural state and when incorporated into a built structure, they are subject to the deterioration and degradation action of the environment and microorganisms. These processes are normally referred to as *weathering*. It is often difficult to distinguish between no biological and biologically mediated weathering of mineral materials. The two processes can occur concurrently, each contributing to the overall deleterious effects. Mineral materials are used extensively in the construction industry and include a range of familiar building materials such as stone, bricks, roofing tiles and shingles, asbestos,

mineralized felts, fascias (which are often natural stone or ceramic in nature), cement based renderings, plasters and mortars, and adhesives and groutings. Concrete is used as reinforced structural elements and as building blocks.

### **Biofilms and mineral materials**

Biofilms are not confined to solid-liquid interfaces. They can also be found at solid-air interfaces [1]. Almost all surfaces in nature, including mineral materials, may be colonized by microorganisms; this includes buildings [2] and monuments [3, 4]. Microorganisms are able to obtain calcium, aluminum, silicon, iron, and potassium from the substratum by bio-solubilization, a process that involves the

production of various organic and inorganic acids by microorganisms, bacteria, algae, lichens (symbiotic associations between fungi and algae), and fungi. These acids attack and degrade calcareous minerals by the dissolution of calcium ions and lead to the eventual formation of degraded products such as gypsum, calcite, glauconite, dolomite, ettringite, and quartz [5]. In addition to liberating nutrients, the production of acids lowers the pH of the surrounding environment. Microbial colonization of a surface can be associated with the formation of mucilaginous matrices, which may also be involved in degradative processes. Capsules and extracellular polymeric materials are produced by many bacteria and algae, but little attention has been paid to the role of the fungi in the structure or nutrition of biofilms [6]. Fungi have been reported as members of natural biofilms [7] and their participation in these structures on mineral materials deserves more attention.

The processes involved in no microbiological weathering of rocks are better understood than those that occur in the presence of microorganisms.

### NONBIOLOGICAL WEATHERING PROCESSES

Apart from degradation by living organisms, rock, stone, and other constructional materials are weathered, that is, reduced to a more dispersed state, by rain, wind, gravity, ice, temperature change, and reaction with atmospheric gases. There are two general types of weathering: mechanical, involving only physical forces, and chemical, in which the chemical structure of the material is changed. In cold and/or dry climates, mechanical degradation is usually more important, whereas in the humid tropics and semi tropics, chemical degradation is predominant. The products of mechanical weathering include fragments of rock and materials formed by expansion and contraction of the rock, freezing and thawing cycles, and earth movements. Products of chemical weathering include the soil in its many forms; these chemical transformations follow mechanical weathering.

#### Chemical Weathering

Chemical weathering involves the migration of ions within the rock structure and within the surrounding environment. Ions may be mobilized by solution in water, which is enhanced by the presence of inorganic acids such as carbonic acid, sulfurous acid, sulfuric acid, and nitrous acid, and  $\text{HNO}_3$ , derived from the gases carbon dioxide, sulfuric

dioxide, nitrogen monoxide, and nitrogen dioxide, respectively. In the cases of iron and manganese, the chemical elements in the structure can be oxidized by atmospheric oxygen or reduced by volcanic  $\text{H}_2\text{S}$ . Silicate rocks are complex salts of silicic acids. Cations such as magnesium and potassium can be leached from the rock, leaving silica as the final product. Clays result from the weathering of aluminosilicates, and other silicon containing minerals include quartz ( $\text{SiO}_2$ ) and kaolin ( $\text{Al}_4\text{Si}_4\text{O}_{10}(\text{OH})_8$ ). Iron oxides and bauxite are other resistant products of the weathering of siliceous rocks. Limestone and dolomites are degraded by the dissolution of calcium and magnesium carbonates in the structure, leaving behind the less soluble impurities such as clay and quartz (sand).

### BIOLOGICAL WEATHERING BIODETERIORATION AND BIODEGRADATION

Krumbein and Jens [8] quote the Bible as an early publication on the infectious nature of decay in houses [Leviticus XIV, pp. 33–57], which also indicated the difficulty of treatment. Colonization and biodeterioration of building materials are determined by environmental conditions, the most significant being physical parameters (temperature, moisture, light intensity) and the chemical nature of the surface. It is generally accepted that microorganisms do not directly use the mineral components of building materials, but may solubilize them as a result of their normal metabolic activities, allowing the resultant ions to be absorbed by the cells in some cases. It is axiomatic that the only microorganisms able to colonize clean building surfaces are those that do not require organic materials for growth, namely, the autotrophs. These include the photosynthetic algae and cyanobacteria and lithotrophic bacteria. The literature usually cites photosynthetic organisms as the primary colonizers [9, 10, 11], but there is little direct experimentation to provide evidence for this. Most of the information on the biological weathering of minerals comes from the literature on soil formation and describes processes at the soil/rock boundary. Estimates of the rates of weathering of rocks on the continental platforms give half-life values between 30 and 1,800 million years for complete weathering, depending on the site and composition of the rock [12]. This is equivalent to 1 mm/y to 1 mm/1,000 y. Such processes may be of importance in the deterioration of structures built below the ground, but the literature in this respect is mostly restricted to the behavior of metal and concrete pipes. Above the ground, biodeterioration is the result of activities of

superficial (epilithic) and deeper (endolithic) organisms - see Figure 1. Colonizing organisms must be able to withstand dry conditions, the effects of high temperatures and light at the surface. Changes in acidity resulting from anthropogenic and natural inputs are also important. Microorganisms may increase the rate of transformation by their metabolic activities, such as the uptake of ions and the production of acids and chelating agents. They may also alter the water permeability of the minerals by the deposition of polymeric materials and surfactants. Water transport may be increased or decreased, according to the nature of the deposits, leading to localized dissolution or salting [13]. Often, the end result of these processes is a catastrophic failure of the surface layer, known as *spalling*. Until such spalling takes place, the structure appears to be in sound condition, although the superficial rind or patina may hide a deep zone of rotten stone beneath the surface. After the initial catastrophic failure, the degraded mineral layer is subject to rapid and sustained erosion. Once this loose, friable surface is exposed, colonization by higher plants, with their extended root systems, may lead to more rapid deterioration.



**FIGURE 1.** Mayan building in Chichen Itza, Mexico, showing blackening of limestone by epilithic and endolithic fungi and cyanobacteria.

## CONCRETE CORROSION

Microbially induced concrete corrosion (MICC) is an important biological/chemical phenomenon that exerts extreme effects on the mineral materials used extensively in the construction industry and that include a range of familiar building materials such as stone, bricks, roofing tiles and shingles, asbestos, mineralized felts, fascias (which are often concrete made), cement based renderings, plasters and mortars, and adhesives and groutings. This phenomenon is especially important in concrete used as reinforced

structural elements and as building blocks. Three sustained environmental factors -  $H_2S$ ,  $O_2$  and moisture - are required to establish biofilms of sulfur oxidizing microorganism (SOM) on the surface and crack space of buildings and monuments. The growth of these microorganisms results in the production of sulfuric acid, which dissolves calcium from the concrete matrix and often causes extensive damage to the concrete structure system. Biogenic sulfuric acid production in these building structures results in the creation of sinkholes, cracks, dirt outflow, storm and rain water infiltration and the final loss of their structural integrity.

MICC often involves two types of bacteria which are common to many sanitary sewer systems, namely sulfate reducing bacteria (SRB) *Desulfovibrio desulfuricans* and sulfide oxidizing bacteria *Thiobacillus thiooxidans* (also known as 'concretivorous', or 'concrete eater'). Sulfur present in acid rain is transformed into hydrogen sulfide by sulfate reducing bacteria which tend to grow on the wet perimeter of the concrete body. In cracked areas of the concrete surface, the hydrogen sulfide is released into the crack's space. The *Thiobacillus* bacteria, which grow on the cracks usually filled with rain water, convert the hydrogen sulfide to sulfuric acid in presence of oxygen. The chemical reaction associated with production of sulfuric acid is:



A freshly placed concrete has a pH of approximately 11 – 13, depending upon the mix design. This pH is due to the formation of a stable compound, calcium hydroxide  $Ca(OH)_2$ , a common by-product produced during the hydration of cement. This initial high pH on the surface of the concrete will not allow any bacterial growth; however, this high pH state lasts for only a short period of time and the pH level slowly declines over time, due to interaction with carbon dioxide ( $CO_2$ ) and hydrogen sulfide ( $H_2S$ ) gases. These gases form weak acidic solutions when dissolved in water (carbon dioxide forms carbonic acid and hydrogen sulfide forms thiosulfuric acid and polythionic acid), that lower the pH of the concrete surface to 9 or 9.5. *Thiobacillus* bacteria that have a unique ability to convert hydrogen sulfide to sulfuric acid in the presence of oxygen start colonizing at a pH of about 9. The first colony of bacteria reduces the surface pH value from 9 to 6.5 by excreting sulfuric acid. These bacteria will not be able to survive at pH values lower than 6.5, and thus the colony dies and the residence is then taken over by another species that is capable of surviving below a pH of 6.5. This newly formed species of *Thiobacillus* further reduces the pH value

from 6.5 to 4 before dying off. This process of colonizing and dying of bacteria continues, until the pH at the surface of the concrete can be brought to a value as low as 1 or 0.5 [14]. The sulfuric acid produced by the bacteria interacts chemically with the hydration products in the hardened concrete paste. The chemical reactions involved in corrosion of concrete are:

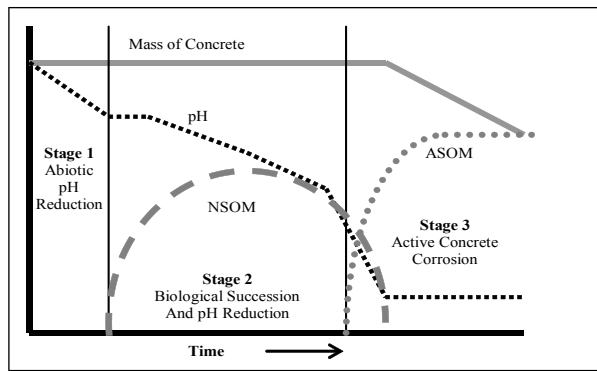
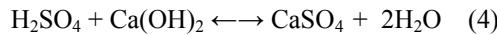
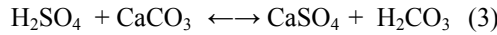
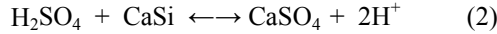


**FIGURE 2.** A conceptualization of concrete surface properties during the onset and progression of microbially induced concrete biodeterioration. NSOM are neutrophilic sulfur oxidizing microorganisms that have H<sub>2</sub>S growth optimum near neutral pH; ASOM are acidophilic sulfur oxidizing microorganisms that have H<sub>2</sub>S growth optimum in acidic pH ranges.

### BACTERIAL GROWTH MODEL

The most common model of bacterial growth is a model based on the limiting amount of substrate in a closed system:

$$\frac{dX}{dt} = \left[ \frac{\mu_m SX}{K_s + S} \right] - bX \quad (5)$$

where S is the concentration of limiting substrate,  $\mu_m$  is the maximum specific growth rate, X is the biomass concentration, K<sub>s</sub> is the half saturation concentration of substrate, and b is the endogenous decay rate. If multiple “substrates” are limiting, the products may describe bacterial growth rates:

$$\frac{dX}{dt} = \frac{\mu_m SX}{K_s + S} \left( \frac{S_2}{K_{S_2} + S_2} \right) - bX \quad (6)$$

In the case of heterotrophs or SOM, S may be an organic substrate or sulfide, while S<sub>2</sub> is the electron acceptor (oxygen). During autotrophic growth, S may be CO<sub>2</sub>, the electron donor, or oxygen.

Substrate removal:

$$\frac{dS}{dt} = -\frac{\mu_m}{Y} \frac{SX}{K_s + S} \left( \frac{S_2}{K_{S_2} + S_2} \right) \quad (7)$$

where  $\mu_m/Y=k$  is the maximum specific substrate utilization rate and Y = true cell yield. To model the formation of metabolism by-products (such as sulfuric acid) an expression similar to Eq. 7 can be used.

Environmental variables such as temperature and pH impact kinetic terms  $\mu_m$ , k, and K<sub>s</sub>. For example,  $\mu_{mT} = \mu_{m20} \theta^{(T-20)}$  is a common expression used to estimate the effect of temperature on the growth of heterotrophic aerobic bacteria degrading organic materials.

### Biogenic Nitric Acid Corrosion

Although thiobacilli are considered to be responsible for the degradation of concrete above ground, two groups of nitrifying bacteria are considered to play a major role in the degradation processes below ground. They are responsible for the oxidation of ammonia via nitrous acid to nitric acid [2]. The first group includes species of *Nitrosomonas* and *Nitrosovibrio*, which oxidize ammonia via hydroxylamine to nitrous acid. The second group that affects the oxidation of nitrous acid to nitric acid includes members of the genera *Nitrobacter* and *Nitrosovibrio* [15]. The action of nitric acid upon the calcareous binding material of concrete results in the production of calcium nitrate. This is a soluble salt that is either lost from the concrete, resulting in the formation of corrosion pits, or remains, thus adding salt to the pore water.

### CONCLUSION

The deterioration of stonework, brickwork, and other mineral materials by microorganisms has an immediate impact on the construction and conservation industries because of the financial implications of remedial treatments. The incidence of lichens, cyanobacteria, algae, and fungi on stonework and monuments is often considered merely to be

aesthetically undesirable, rather than severely damaging to these structures. However, there is little doubt that physical and chemical attack can also occur through the activities of organisms growing on the surface (epilithic) or in deeper layers (endolithic) of rock and stone structures.

The role of bacteria in the breakdown of natural rock and the genesis of soils has long been accepted and the same processes can participate in the biodegradation of stone-built structures. The actinomycetes have recently been highlighted as important bacterial colonizers of rocks and buildings of cultural heritage and future research will certainly focus on the degradative activities of these organisms. Biofilms, as regions where the metabolic activities of microorganisms are concentrated, have been accepted as of major relevance in the biodeterioration of materials, and this is an area of increasing importance in the study and control of biodeterioration of construction materials.

Techniques recently introduced into biofilm research, such as atomic-force microscopy, environmental-scanning electron microscopy, confocal-laser-scanning microscopy, green fluorescent protein, fluorescent in situ hybridization (FISH), denaturing gradient gel electrophoresis (DGGE), and other molecular biology methods, are already being used on artificial and natural mineral materials. Rolleke and coworkers [16] using 16S rDNA analysis, showed the presence of the Archaea genus *Halomonas* on a mural in a German church, confirming the presence of extremophiles (in this case, salt-tolerant bacteria) on buildings. Recently, Saad and coworkers [17] have suggested the use of 17S rDNA analysis by DGGE to identify fungal genera on painted surfaces.

Early results suggest that this is a promising technique for probing building surfaces and identifying changes in fungal biodiversity caused, for example, by the use of biocides. The future will see a huge increase in our knowledge of the types of organisms whose activities are really important in the deterioration and degradation of these structures.

## REFERENCES

1. L. H. G. Morton and S. Surman, *Int. Biodet. Biodeg.* **34** (1994) 203–22.
2. W. Sand and E. Bock, *Geomicrobiol. J.* **9** (1991) 129–138.
3. R. J. Koestler, A. E. Charola, M. Wypyski, and J. J. Lee, in G. Felix ed., *Vth International. Congress in Deterioration & Conservation of Stone*, vol. **2**, Presses Polytechniques Romandes, Lausanne, Switzerland, 1985, pp. 617–626.
4. P. S. Griffin, N. Indictor, and R. J. Koestler, *Int. Biodet.* **28** (1991) 187–207.
5. C. Ascaso, J. Galvan, and C. Rodriguez-Pascual, *Pedobiologia* **24** (1982) 219–229.
6. M. V. Jones, in J. Wimpenny, P. Handley, P. Gilbert, and H. Lappin-Scott, eds., *The Life and Death of Biofilms*, Bioline, Cardiff, 1995, pp. 157–160.
7. M. E. Aktar and W. I. Kelso, *Biol. Fertil. Soils* **16**, (1983) 305–312.
8. W. E. Krumbein and K. Jens, *Oecologia* **50** (1981) 25–38.
9. W. E. Krumbein, *Deutsche Kunst-und Denkmalpflege* **31** (1973) 54–71.
10. C. Grant, *Int. Biodet. Bull.* **18** (1982) 57–65.
11. C. Saiz-Jimenez, in J. Szege, ed., *Soil Biology and Conservation of the Biosphere*, Akademiai Kiado, Budapest, 1984, pp. 757–767.
12. J. Vezier, in A. Lerman, M. Meybeck, eds., *Physical and Chemical Weathering in the Geochemical Cycle*, Kluwer Academic Publishers, Norwell, 1988.
13. W. H. Dukes, *Architects' J.* **156** (1972) 433–438.
14. M. Lara, X. Li, L. Rendon, *Ingeniería Hidráulica en México*, vol. XXIV, num. 2 (2009) 139–146.
15. L. M. Prescott, J. P. Harley, and D. A. Klein, *Microbiology*, 4th International ed., WCB/McGraw Hill, New York, 1999.
16. S. Rolleke et al., *Appl. Environ. Microbiol.* **62** (1996) 2059–2065.
17. D. S. de Sousa Saad et al., in 4 Labs, *Fourth Latin American Biodeterioration and Biodegradation Symposium*, Buenos Aires, 16–20th, April 2001. Published on CD ROM.

## Analysis of Black Crust from a Cuban Historic Building

J. Reyes<sup>1</sup>, F. Corvo<sup>1</sup>, Y. Espinosa-Morales<sup>1</sup>, C. Valdes<sup>2</sup>, P. Bartolo<sup>3</sup>, D. Aguilar<sup>3</sup>, P. Quintana<sup>3</sup>, B. Hermosín<sup>4</sup> and C. Saiz-Jimenez<sup>4</sup>

<sup>1</sup> *Centro de Investigación en Corrosión, Universidad Autónoma de Campeche, MEXICO.  
e-mail: javreyes@uacam.mx*

<sup>2</sup> *Centro Nacional de Investigaciones Científicas, La Habana, CUBA.*

<sup>3</sup> *Centro de Investigación y estudios Avanzados-Unidad Mérida, MEXICO.*

<sup>4</sup> *Instituto de Recursos Naturales y Agrobiología de Sevilla, SPAIN.*

**Abstract.** Atmospheric pollution is the major cause of degradation for historic buildings in urban environments. In this study we analyzed the composition of black crust deposits observed over the walls and façade of the historic San Francisco de Asis Minor Basilica and the Convent (Old Havana City, Cuba). SEM/EDS, DRX and Py-GC/MS techniques were employed to characterize organic and inorganic composition of black crusts samples. SEM/EDS results show the presence of Ca, C, O and Si like predominant elements, reflect of the use of coralline quarry blocks base during erecting of the building. Moreover, high levels of S can be observed into the mineral matrix of the crust. DRX analysis indicated that calcite is the predominant phase contained in limestone with small quantities of gypsum, quartz and magnesium silicates. Nevertheless, those samples collected from walls bordering Oficios Street show gypsum like predominant phase. Gypsum is a primary product of sulfur dioxide reaction in polluted environments. Py-GC/MS analysis indicated the presence of homologous series of *n*-alkanes, *n*-alkenes, and *n*-fatty acids as predominant compounds. Distribution and CPI index for *n*-alkanes series indicated that most of the organic fraction is entrapped in the crust during deposition of atmospheric particles produced by vehicles exhaust.

**Keywords:** black crust, historic building, SEM/EDX, XRD, Py-GC/MS, Old Havana.

### INTRODUCTION

Black crust formed on building stone external surfaces is an undesirable phenomenon that appears in urban environments. It produces aesthetic damage, change on surface properties and affect stone physical and mechanical stability of the building. Also, it is the cause of economic lost due to constant maintenance work in buildings.

In urban environments, the primary sources of degradation of historic building are reactive gases and particles which produce the formation of deposits on the stone surface. Black crust is formed on exposed calcareous material as a result of diverse physical and

chemical processes originated during the interaction of stone surface and environmental agents [1- 3].

In buildings constructed with calcareous materials, the main damage observed is the formation of black crusts. Also black crusts are formed by the deterioration of calcium rich plaster [3].

Black crust is a neo-mineral deposit formed by the reaction of limestone surface with sulfur dioxide (SO<sub>2</sub>), emitted during coal and fuel oil combustion [4, 5]. The black crust also embeds organic substances from atmospheric deposition and microbial biomass of microorganisms that colonize stone surface [6].

The historic area of Havana City is located beside the Havana Bay. Hundreds of historic buildings built

with limestone quarry blocks, and in most of the cases covered with limestone mortar compose the historical area of the City known as Old Havana.



**FIGURE 1.** The portico of San Francisco de Asis Minor Basilica and the Convent. It can be observed the presence of black crusts.

Those building are under the effect of an aggressive tropical-urban environment that causes the apparition of several deterioration pathologies, resulting remarkable the formation of black crust. This is the case of the san Francisco de Asis Minor Basilica and the Convent, located at the Old Havana area (Figure 2)



**FIGURE 2.** In the circle, the location of The San Francisco de Asis Minor Basilica and the Convent at the Havana City. The squares show the location of industrial installation in the area, including an oil refinery.

The Convent was built at the end of the Sixteenth Century and rebuilt in baroque style at the middle of the Eighteenth Century. In the present time, the building houses a museum of religious art, concert, and art exposition hall. The building is located about 200 m from the Bay shoreline. The walls and the main façade of the building bordering the Oficios Street are under the effect of vehicle emissions of private and public cars that daily flow across the street. Also in the neighbor area an intense industrial activity is carried out (Figure 2).

In this study, an analysis of black crust collected from the historic building was carried out. SEM/EDS, DRX and Py-GC/MS were applied in order to determine the chemical composition of the black crust and the role of environmental condition as a key factor in the appearance of black deposits in external structures of San Francisco de Asis Minor Basilica and the Convent.

## MATERIALS AND METHODS

### Sampling

Fragments of black crust were retired from the portico of the main façade of the building. The material was collected by using a scalpel and stored in an inert hermetical recipient until the analysis was carried out.

### SEM/EDS analysis

Fragments about 1 cm<sup>2</sup> of black crust fragments were examined without previous preparation in a scanning electron microscopy (Philips XL30 ESEM) coupled with an X-ray dispersive analytical system. The analysis was carried out under low vacuum at 20 kV, at a working distance of 10 mm and tilt angle of 0°. An X-ray SUTW-Sapphire detector was employed.

### XRD analysis

The samples of black crust previously grinded were introduced in a Bragg-Brentano Geometry X-ray diffractometer (Siemens D5000). The equipment operated with a CuK $\alpha$  radiation ( $\lambda = 1.5416 \text{ \AA}$ ). The operation conditions were the following: 25 mA and 35 kV and a step of size of 2°/2 $\theta$ /min in the 2-60° 2  $\theta$  range.

### Py-GC/MS analysis

A few mg of sample were deposited in a Curie-point small hallow ferromagnetic cylinder (590 °C) and then wetted with 5 ml of tetramethyl ammonium hydroxide (TMAH, 25 % in methanol). The cylinder was lightly dried under nitrogen flow and immediately inserted

under the pyrolyser. The analysis was performed in a GC/MS system (Termoquest Finnigan) coupled to a Curie point pyrolyser (Fischer 0316). The GC oven was programmed from 50 to 280 °C, at rate of 5 °C min<sup>-1</sup>. This temperature was held for 100 min and then raised to 310 °C a 20 °C min<sup>-1</sup> rate. The final temperature was held for 2 min. The mass spectra interpretation was carried out by using the NIST library and by comparison with own made spectra.

## RESULTS

Degradation of historic building is a complex phenomena that involve physical, chemical and biological agents [7]. The particular characteristics of the tropical climate of Havana City, lead to the formation of black crust in limestone building due to two important factors: high relative humidity levels and the presence of atmospheric pollutants like sulfur dioxide [8].

San Francisco de Asis Minor Basilica and the Convent, was built with coralline stone, a highly porous material very susceptible to degradation. Black crust was formed over these material mainly in the lower zone of the main façade, where sun radiation does not impact directly.

Figure 3a shows a fragment of coralline limestone collected from the building showing the presence of black crust. It is a very compact structure firmly attached to the stone matrix. Figure 3b, shows a 4x image of the crust obtained by stereoscopic microscopy. The black crust has a thickness about 1 mm. It has an irregular surface with pitted aspect. Black micro particles, dust deposits and crystals can be observed into their structure.



**FIGURE 3.** (a) Fragments of coralline stone showing the presence of black crust. (b) Stereoscopic image (4x) of black crust sample.

SEM image (20x) reveals the presence of numerous micropores distributed along the irregular surface of the sample (Figure 4). General EDS spectrum obtained from the surface of the crust shows the presence of crustal and contaminant elements. Calcium (Ca), carbon (C), and oxygen (O) are the mayor elements. Also, sulfur (S), silicon (Si),

magnesium (Mg), aluminum (Al), phosphorus (P), chlorine (Cl), sodium (Na), iron (Fe) and potassium (K) were presents.

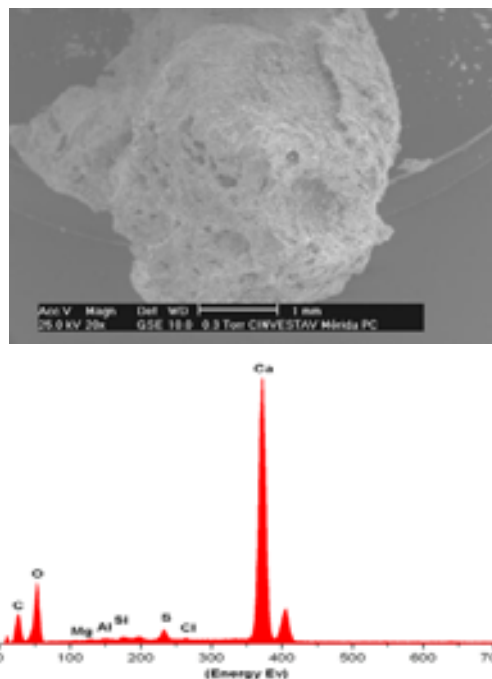


**FIGURE 4.** SEM image (20x) of black crust sample and their respective EDS spectrum.

Two kind of mineral structures can be observed in the black layers: a rich Ca- and rich S- content structures. Figure 5 shows the typical rhombohedral crystal corresponding to the rich calcium carbonate matrix of the coralline limestone used during the construction of San Francisco de Asis Minor Basilica portico. Their respective EDS analysis also indicates the presence of small quantities of S. As it was previously mentioned, S can be originated during vehicle emissions and industrial activities in the neighbor area of the Old Havana [8].

Laminar plaques are the form in which S- rich content structures seem to develop into the black layer of the building. Figure 6 shows a rich S conglomerated structure located inside the plaques, as have been demonstrated by their respective EDS spectrum.

Several authors report that in urban environment, the presence of S is consequence of wet and dry deposition process [2, 3, 9]. The high proportion of Ca and O observed in the same sample, indicate that gypsum matrix is present in the black layer [10].

Crustal elements like Mg, Al, Si, K and Fe, can be present in the natural stone or deposited over the material surface from dust particles [1]. Na and Cl (and also K and Mg in low proportions), are a reflex of the marine character of the atmosphere at Havana City.

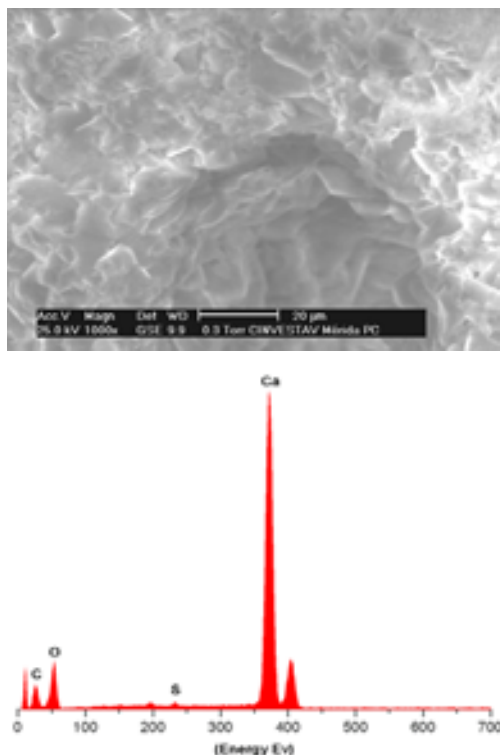


FIGURE 5. Rich Ca- rombohedral crystal observed in black crust samples and their respective spectrum.

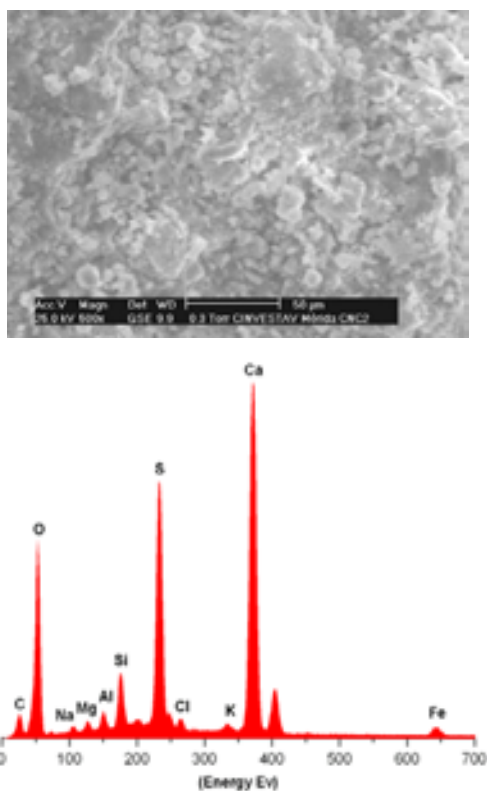
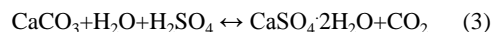
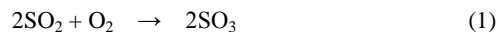


FIGURE 6. Rich S- conglomerated observed in black crust samples and their respective spectrum.

Several hypotheses have been proposed for the formation of the black crust but all of them involved particulate matter, SO<sub>2</sub> and water. The results of the interaction between porous limestone and SO<sub>2</sub> is the formation of gypsum, according the reactions [11]:



The structure of the crust is the result of a continuous dissolution/crystallisation process, which brings about the slow accumulation of particulate matter and/or soot on the surface of the calcareous materials.

This process seems to be occurring in the formation of black crust in the portico of San Francisco de Asis Minor Basilica and the Convent, as has been demonstrated during the DRX analysis. Figure 7 shows two typical diffractograms obtained from the black layer from the building.

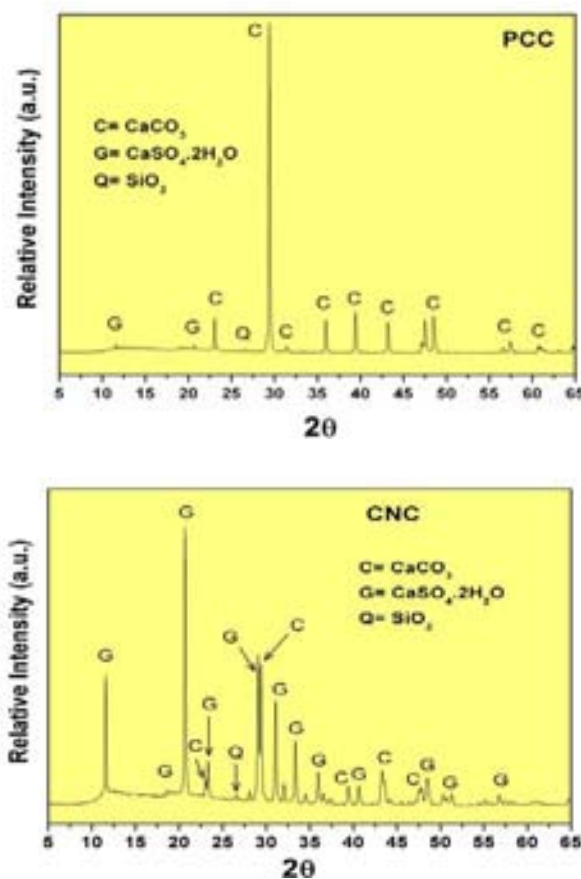


FIGURE 7. Typical XRD diffractograms obtained during the analysis of black crust samples. C, calcite; G, gypsum; Q, quartz.

According to the results, it seems that gypsum is the only one characteristic neo-mineral compound presented in the samples. Moreover, calcium carbonate and quartz are original minerals presents in coralline limestone, the base- stone material construction employed to build the Convent.

The study and characterization of organic compounds deposited into the mineral matrix of black crusts can be used in two ways: as indicator of the influence of organic pollution in the black crust formation and to determine the origin of atmospheric pollutants that cause deterioration of the building [12, 13, 14].

Diagnostic criteria like carbon maximum number ( $C_{MAX}$ ), the Carbon Preference Index (CPI), and the presence of molecular markers; currently used in organic geochemistry and environmental studies result useful for the analysis of organic compounds in black crusts [12, 15, 16].

Figure 8 shows a total ion chromatogram (TIC), obtained from the pyrolysate of black crust sample from the portico of The San Francisco de Asis Minor Basilica. The list of the major compounds identified during the Py-GC/MS analysis is presented in Table 1.

The results indicate that the mineral matrix in the crust contains a complex mixture of organic compounds dominated by *n*-fatty acids ( $C_{12}$ - $C_{26}$ ), *n*-alkanes ( $C_{14}$ - $C_{33}$ ) and *n*-alkenes ( $C_{14:1}$ - $C_{19:1}$ ).

The individual evaluation of the different series of compounds identified in the samples according diagnostic criteria indicate their probably sources. *n*-Fatty acids showed a strong even to odd C-number predominance, with  $C_{MAX}$  at  $C_{16}$ . According to Simoneit [17], it is characteristic of biogenic inputs.

The presence of the  $C_{18:1}$ unsaturated fatty acids have been related with the colonization of stones substrata by phototrophic microorganisms, which have been proved to accumulate lipids [14].

The *n*-alkane series shows a  $C_{MAX}$  at  $C_{24}$  and CPI index of 0.90 (Figure 9). Criteria diagnostics indicate that CPI index closer to 1 are certainly related whit vehicle exhaust emissions [18]. Increase in the CPI value can be related with a major contribution of biogenic source in the final distribution of aliphatic compounds [17].

In this sense, CPI index and  $C_{MAX}$  observed in the crust sample can be considered of anthropogenic origin, as have been reported by Hermosin et al, in a study realized to relate the organic composition of black crust from different European monuments [4].

Figure 10 shows the  $m/z$  95 fragmentogram corresponding to naphthenic fraction. Naphthenics are the unresolved compounds mixture fraction (UCM), considered a typical molecular marker from fossil fuel emissions.

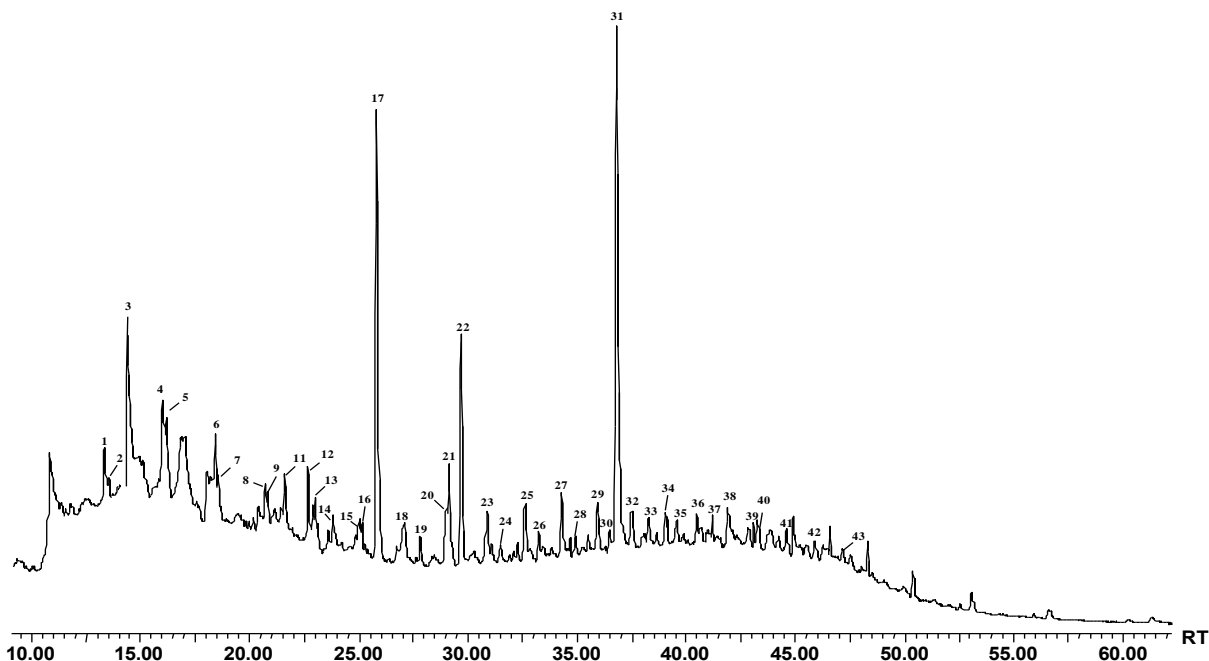


**FIGURE 8.** Total Ion Chromatogram (TIC) from the pyrolysate of San Francisco de Asis Minor Basilica and the Convent. Compound numbers are listed in Table 1. RT, Retention Time.

**TABLE 1.** Major compounds identified in the pyrolysate of black crust of The San Francisco de Asis Minor Basilica and the Convent.

Peak	Compound
1	<i>n</i> -tetradecene
2	<i>n</i> -Tetradecane
3	<i>n</i> -Dodecanoic acid
4	<i>n</i> -Pentadecene
5	<i>n</i> -Pentadecane
6	<i>n</i> -Hexadecene
7	<i>n</i> -Hexadecane
8	<i>n</i> -Tridecanoic acid
9	<i>n</i> -Heptadecene
10	<i>n</i> -Heptadecane
11	<i>n</i> -Tetradecanoic acid
12	<i>n</i> -Octadecene
13	<i>n</i> -Octadecane
14	<i>n</i> -Pentadecanoic acid
15	<i>n</i> -Nonadecene
16	<i>n</i> -Nonadecane
17	<i>n</i> -Hexadecanoic acid
18	<i>n</i> -Eicosane
19	<i>n</i> -Heptadecenoic acid
20	<i>n</i> -Heneicosane
21	<i>n</i> -Octadecenoic acid
22	<i>n</i> -Octadecenoic acid
23	<i>n</i> -Docosane
24	<i>n</i> -Nonadecanoic acid
25	<i>n</i> -Tricosane
26	<i>n</i> -Eicosanoic acid
27	<i>n</i> -Tetracosane
28	<i>n</i> -Heneicosanoic acid
29	<i>n</i> -Pentacosane
30	<i>n</i> -Docosanoic acid
31	Phthalate
32	<i>n</i> -Hexacosane
33	<i>n</i> -Trieicosanoic acid
34	<i>n</i> -Heptacosane
35	<i>n</i> -Tetracosanoic acid
36	<i>n</i> -Octacosane
37	<i>n</i> -Pentacosanoic acid
38	<i>n</i> -Nonacosane
39	<i>n</i> -Hexacosanoic acid
40	<i>n</i> -Triacontane
41	<i>n</i> -Hentriacontane
42	<i>n</i> -Duotriacontane
43	<i>n</i> -Tritriacontane

It manifests into a chromatogram like a hump. Their presence in environmental samples indicates petrogenic inputs in the global composition of organic compound and is unequivocal signal of the influence of organic pollutants in the formation of black crust in the urban environment of Havana City.

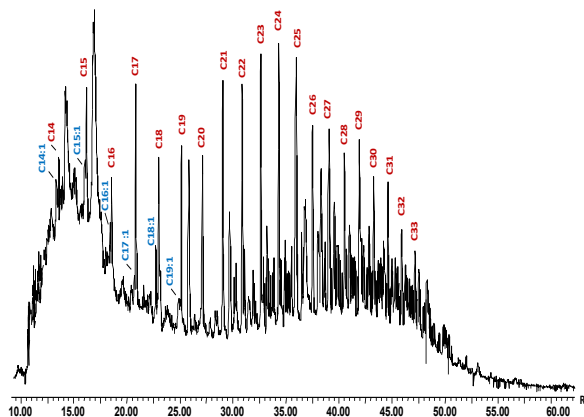


**FIGURE 9.** Mass fragmentogram (m/z 83 +85 ) corresponding to *n*-alkanes and *n*-alkenes series observed in the pyrolysate of black crust samples. RT, Retention Time. C<sub>n:1</sub> indicate an alkene structure.

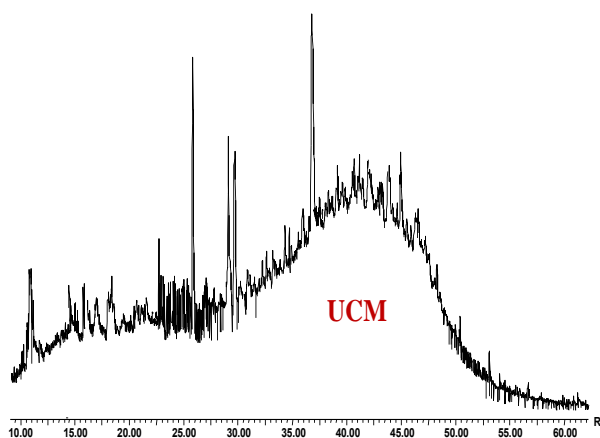


**FIGURE 10.** Mass fragmentogram (m/z 95) corresponding to naphthenic fraction present in the black crust sample RT, Retention Time. UCM. Unresolved compounds mixture.

## CONCLUSIONS

An integral composition analysis of organic and inorganic compounds presented in the black crust formed over the portico of San Francisco de Asis Minor Basilica located in the Old Havana was carried out.

The results indicate that black crust formation is consequence of the interaction of sulfur dioxide with coralline limestone substrata to form neomineral gypsum. Gypsum incorporates into their mineral matrix organic and inorganic compounds, including those emitted during fossil fuel combustion in the neighbor area of the building.

On this way, it is important to note that gypsum sulfated crust and organic and inorganic compounds deposited on their surface or embedded into their

structure can be used as tracers during the study of deterioration process of historic buildings in urban environments.

### ACKNOWLEDGEMENTS

The present study was possible thanks to the support of FOMIX CAMP-2005-C01 project and CONACYT International Cooperation Office-Mexico across coordinated action scheme with CSIC-Spain.

### REFERENCES

1. C. Riotino, C. Sabbioni, N. Ghedini, G. Zappiaa, G. Gobbi, O. Favoni, *Therm. Chim. Acta.* **321** (1998) 215-222
2. A.G. Nord, K. Holenyi, *Water, Air, Soil Poll.* **109** (1999). 147-162.
3. J. Sanjurjo, C. A. S. Alves, J. R. Vidal, D. Fernández. (2009). Origin of gypsum-rich coatings on historic buildings. *Water, air, soil Pollut.* In press.
4. B. Hermosin, M. Gaviño, C. Saiz-Jimenez, "Organic compounds in black crusts from different European monuments: a comparative study" in. *Air pollution and cultural heritage.* (Saiz-Jimenez ed.), Taylor and Francis Group, London, 2004, 47-55.
5. N. Schiavon, G. Chiavari, *Environ. Geol.* **46** (2004). 448-455.
6. C. Saiz-Jimenez., *Sci. Tot. Environ.* **167** (1995) 273-286.
7. D. Camuffo, M. Del Monte, C. Sabbioni. *Water, Air and Soil Pollut.* **19** (1983). 351-359.
8. F. Corvo J. Reyes, C. Valdes, F. Villaseñor, O. Cuesta, D. Aguilar, P. Quintana. *Water, Air, Soil Pollut.* **205** (2010) 359-375.
9. A. Torock, N. Rozgonyi, *Environ. Geol.* **46** (2004) 333-349.
10. P. Maravelaki-Kalaitzaki, G. Biscontin. *Atmos. Environ.* **33** (1999) 1699-1709.
11. Amoroso G., Fassina V. *Stone Decay and Conservation. Atmospheric Pollution, Cleaning, Consolidation and Protection.* Materials Science Monographs. Elsevier, Amsterdam, 1983.
12. C. Saiz-Jimenez, B. Hermosin, J. J. Ortega-Calvo, G. Gomez-Alarcon, *J.Anal. Applied Pyr.* **20** (1991) 239-251.
13. J. Reyes, *Diagnostic criteria for the identification of organic compounds in airborne aerosols emitted by vehicle exhaust and their application to the study of the de deterioration of the Cathedral of Seville.* Ph. Dr. Thesis. Universidad de Sevilla, Spain. 2004. (In Spanish).
14. A. Bonazza, C. Sabbioni, N. Ghedini, B. Hermosin, V. Jurado, J. M. Gonzalez, C. Saiz-Jimenez. *Did smoke from the Kuwait oil well fires affect Iranian archeological Heritage?* *Environ. Sci. Technol.* In press.
15. B. R. T. Simoneit, *App. Geochem.* **17** (2002) 129-162.
16. J. Reyes, B. Hermosin, C. Saiz-Jimenez, *Org. Geochem.* **37** (2005) 2019-2025.
17. B. R. T. Simoneit, *Int. J. Environ. Anal. Chem.* **23** (1986) 207-233.
18. B. R. T. Simoneit, *Int. J. Environ. Anal. Chem.* **22** (1985) 203-233.

## **Laboratory and In Situ Evaluation of Polysiloxane Hidrofuge Product for Protection of Stone at San Francisco de Asis and Basilica Minor in the Old Havana, Cuba.**

C. Valdés Clemente<sup>1</sup>, F. Corvo Pérez<sup>2</sup> and C. Lariot Sánchez<sup>2</sup>

<sup>1</sup> *Centro Nacional de Investigaciones Científicas (CNIC), Ciudad de La Habana, CUBA.  
e-mail: ceclia.valdes@cnic.edu.cu*

<sup>2</sup> *Instituto de Ciencia y Tecnología de Materiales (IMRE), Universidad de la Habana, CUBA.*

**Abstract.** Several and important historical buildings were constructed between XVI and XIX century in Havana City using coralline limestone, original from the Island. Nowadays, these buildings are located in the Historical Center of Havana City. San Francisco de Asis Convent and Basilica Minor building is an example of the use of this type of stone like structural material. This building was built 300 years ago. In the present time, the structure shows deterioration in the stone walls due, mainly, to high humidity. In the present paper, the protective efficiency of a hydrofuge commercial product using petroleum solvent and polysiloxane is evaluated by means of scanning electron microscopy, laboratory and in situ tests. A comparison between the results obtained for polysiloxane hydrofuge product and another silicone commercial hydrofuge is made under laboratory conditions and SEM evaluation. Different laboratory evaluation techniques concerning to the influence of water, such as capillary absorption (in situ), water absorption by partial immersion, water vapour permeability and adsorption isotherms were applied. The sealing and penetration capacity of the hydrofuge products in the porous stone was determined using Microscopy and X-ray distribution by energy dispersive system. Elements localization was also carried out. The capacity of the products to decrease water access inside the stone was confirmed. Polysiloxane hidrofuge product showed better properties than silicone one under laboratory conditions. Surface Mapping of a cross section of the stones showed presence of Si up to more than 60  $\mu\text{m}$  deep for polysiloxane based product. It was not the case for silicone based product. A more homogeneous distribution was also observed for the polysiloxane based product.

**Keywords:** coralline limestone, polysiloxane hydrofuge, silicone hydrofuge.

### **INTRODUCTION**

During the Spanish colony, in the Caribbean region, large settlements were established. These settlements spreaded and became big cities. In Cuba, San Cristobal de La Habana turned into a principal Village. The monumental buildings were built using

coralline stone, original from the Island. Many of these buildings and other works lasted up today.

San Francisco of Asis Convent and Basilica Minor (Fig. 1) is a good example of these monuments. This building was constructed over 300 years ago [1]. At this building focused this work.



**FIGURE 1.** San Francisco of Asis Convent and Basilica Minor.

It is very well known that stone is one of the most widely used construction materials by man. Its durability and stability has been proved over time; however, properties are modified either by the action of the environment (including the influence of air pollutants). With increasing industrialization, urbanization and car traffic pollutant levels in the atmosphere increase continuously, as also their deposition on stone surfaces. It increases deterioration of material [2, 3].

The analysis of the stone degradation mechanisms has led to the conclusion that it is necessary to protect it, particularly from the action of water, which facilitates the entry of pollutants into the limestone, and the growth of biological organisms. Different types of coatings and water repellents have been used [4] to protect limestone.

Hydrophobic products applied (in aqueous or organic solutions) can reduce surface sensibility to water absorption. They must meet the following conditions: no permeability to liquid water, water vapor permeability, chemical and photochemical stability, oil repellence, good optical properties to preserve the original colour, no affecting neither the stone nor the environment [5, 6, 7].

The correct application of synthetic organic chemicals, particularly acrylic and siloxane polymers, silicones, epoxies, acrylics and others guarantees, in general, an effective protection. This application is efficient and economic, avoiding any physical or aesthetic deterioration [5, 6]. Nevertheless, it should always be taken into account before any surface treatment. To attack the problem adequately the collection of information on physical and chemical properties of stone material is required [4, 8].

In the present paper, the protective efficiency of a hydrofuge commercial product based on polysiloxane dissolved in petroleum solvent is

evaluated by means of scanning electron microscopy, laboratory and in situ tests.

A comparison between the results obtained for polysiloxane hydrofuge product and another silicone commercial hydrofuge is made under laboratory conditions and SEM evaluation.

## MATERIALS AND METHODS

Hydrofuge commercial products:

- Sikaguard 700s, polysiloxane base dissolved in organic solvent (applied outdoors).
- Sikagard 702W, silicon base dissolved in aqueous solvent (applied indoor).

### Surface preparation for *in situ* testing:

The selected surfaces were subjected to a water pressure jet cleaning. After this procedure, a drying time of 24 h was established (Figure 2). The polysiloxane-based treatment was applied on one of the columns in the courtyard north of Convento (Figure 2b) and a column of the northern facade of the Basilica (Figure 2c).



**FIGURE 2.** Hydrofuge products application. a) surfaces cleaning; b) column of courtyard north; c) column of northern facade.

### Stone evaluation with and without application of repellent products:

#### *In situ*

The evaluation was carried out after 6 and 18 months of products application. Aspects considered were the following: visual discoloration of the surface, material disintegration, grow of biological organisms and development of a patina or crust.

#### *Capillary-Absorption*

An evaluation of selected sites was carried out using the method known as "Karsten Pipe", particularly suitable for assessing the effectiveness of water repellent treatments [4, 9]. The maximum evaluation time was 30 min. and the adsorption coefficient was calculated according to the ISO 15148 [11].



FIGURE 3. "Karsten Pipe" method.

## Laboratory tests

### *Water absorption by partial immersion*

The partial absorption coefficient was determined according to ISO 15148 [10].

Three octahedral stones samples were used, not treated, treated with polysiloxane hydrofuge product and treated with silicone hydrofuge product. Samples were placed on supports in a vessel according to the procedure established for the test. Samples were submerged 3 mm depth. Time intervals for mass evaluation were: 1, 3, 5, 10, 15, 30, 60, 480 and 1 440 min.

### *Water vapor permeability* [11]

Water vapor permeability of nine cylindrical stone samples was determined: three samples without treatment, three with the application of silicone based treatment and three with the application of polysiloxane-based product. Samples dimensions were: diameter: 37 mm and width: 10 mm. Each cylinder was placed between two plastic foils, one opened by both sides and one closed at the other side and containing inside 15 mL of distilled water. Samples were sealed by an adhesive hydrophobic tape. These samples were weighted during seven days up to constant weight.

### *Adsorption isotherms*

Adsorption isotherms were obtained at room temperature ( $25 \pm 1$  ° C) according to ISO 12751 standard [12]. Nine samples were tested: three samples without treatment, three with silicone-based treatment and three with polysiloxane-based treatment. Samples dimensions were 10 x 3 x 1 cm.

In order to obtain adsorption-desorption curves, samples were exposed to Relative Humidity values of 22, 57, 75, 84 and 97% and maintained in this controlled environment up to constant weight.

## *Scanning Electron Microscopy and EDX.*

Samples surfaces with and without treatment were examined through a scanning electron microscope TESCAM TS 5130 and EDX INCA SB 350. The microscope works at a potential of 10 to 20 KV.

## RESULTS AND DISCUSSION

### *Evaluation of protective products in situ*

The visual assessment was made at two exposure times after the application in selected areas. The results are shown in Table 1. The application of hydrofuge products did not cause any aesthetic change in the stone surfaces. Four months after surface cleaning, in untreated areas, the formation of a dark-coloured biological patina was observed.

### *Absorption capillary (Karsten Pipe)*

According to the values of water absorption coefficient (Table 2) determined in situ at the test site respecting polysiloxane based product, it can be concluded that no significant changes of this parameter occur after 18 months of application. It confirms the results of the visual observation carried out on the treated surfaces.

The absorption coefficient determined on the treated surfaces is considerably lower respecting untreated surfaces, indicating the effectiveness of the repellent product. The values obtained at the same stage in untreated surfaces are different, being higher at the column of the Plaza de San Francisco (more directly submitted to weathering due to wind action, rainfall, solar radiation and air pollutants).

It must be noted that the effectiveness of repellents products directly depends on the material pores size distribution which will allow access to treatment within the rock.

### **Laboratory evaluation of stone "with" and "without" application of hydrofuges products**

#### *Water absorption by partial immersion*

An important property that water repellent products should meet is to create a hydrophobic surface that prevents the persistence and the passage of water over the stone surface to its interior. The assessment results are shown in Figure 4.

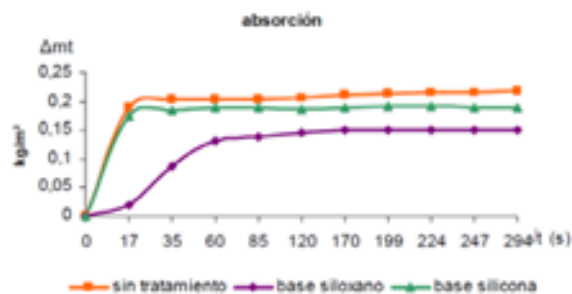


**FIGURE 4.** Graphic water absorption partial immersion test, no treatment –orange-, siloxane base –purple-, silicon base –green-.

The porous stones take water in two successive stages: initially the water rises to the top of the material, which will experience a rapid increase in weight versus time and in the second stage the remaining later fills the pore space. The water content at the inflection point is called St. [13]. It can be seen that the value of St is superior to the basic product polysiloxane, which indicates that it is the one that offers greater resistance to water absorption by capillarity and therefore the one having better water repellent properties.

The analysis of variance (Table 3) confirms this result because there are significant differences between the value of St for the product respecting the stone base polysiloxane and silicone-based product.

#### *Water vapor permeability*

The results of this trial are shown in Figure 5. It is known that water vapor can be absorbed into the pores of the rock and passes through the continuous pores from one side to the other side of the stone.

One of the prerequisites that water repellent treatments must have is to keep the water vapor permeability of the stone material. The results show that both products keep this property in the treated stones.

To evaluate the effectiveness of both treatments a random statistical design was used and a 95% confidence level showing significant differences between the samples treated and untreated rock was obtained (Table 4).

During the first 168 h, silicone base product and stone allow the flow of much water vapor than the siloxane based product, but after 168 h, the behavior of the two products is quite similar to that presented by the stone without implementing them. By statistical analysis (Table 5) using the statistical program Origin 6.0 from 168 h yielded the result showing that no significant differences between the products used and the untreated stone is observed.

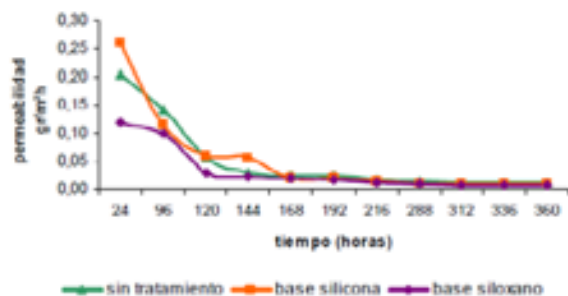


**FIGURE 5.** Water vapor permeability, no treatment –green-, Silicon base –orange-,siloxane base –purple-.

#### *Water vapor adsorption isotherms*

It can be seen (Figure 6) that stones treated with silicone base product presented a higher absorption of moisture, while those treated with polysiloxane base show a similar behavior to untreated stones. This result indicates that the properties of silicone based products are less suitable for the conservation of stone.

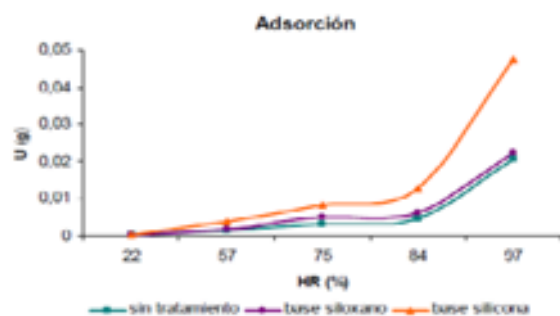


**FIGURE 6.** Adsorption isotherm. no treatment –green-, silicon base –orange-, siloxane base –purple-.

The randomized design (Table 6) made for a 95% confidence level, showed that significant differences exist with respect to the thickness of samples used for each treatment and untreated stone. This result indicates that more or less water vapor adsorption depends not only on the characteristics of the stone, but also is related to the thickness of the stone material to be analyzed.

### **Micrographic characterization and determination of the puntual chemical composition in rock hidrofuge applied products.**

The capacity of the water repellent product and its penetration was analyzed by scanning electron

microscopy. Their constituents were mapped using energy dispersive spectroscopy X-ray.

The layers formed on the samples by the hydrofuge products are very thin and apparently does not alter the surface morphology at the magnifications used in this study (Fig. 7 A, B and C).

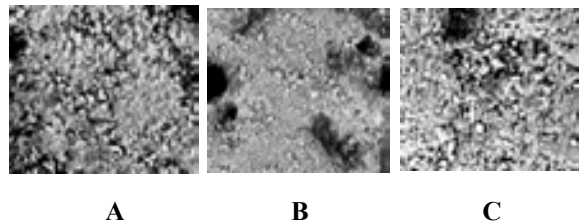


**FIGURE 7.** A) Micrograph (SEM) of untreated shell limestone; B) Limestone treated with silicone base; C) Limestone treated with base polysiloxane.

EDX spectra (Figure 8) indicate the presence of silicon on the surface of the stone; however, there is further evidence about the presence of silica in the stone surfaces treated with polysiloxane base. It is valid to note that on these surfaces, a polyhedra forming a square was observed indicating the application of the product.

Through the mapping of the cross sectional areas of the samples it can be observed the presence of silicon. In the case of samples with polysiloxane base treatment (Figure 9) the presence of silicon was very close to 100  $\mu\text{m}$  deep infiltration capacities denoting the same in the stone. There is much evidence of silicon cavities corresponding to cracks and imperfections of the stone which facilitates infiltration of the product.

Cross-section of the stone base with silicone treatment (Figure 10) bags full of particles can be seen in areas where calcium carbonate is not fully consolidated. These pockets, cracks and other irregularities serve as preferential pathways in the dissemination of waterproofing product into the interior of the stone. The result of the mapping indicates the presence of Si but its distribution is not as homogeneous as seen in the polysiloxane base.

## CONCLUSIONS

The capacity of the polysiloxane product to decrease water access inside the stone was confirmed. Polysiloxane hydrofuge product showed better properties than silicone one in the laboratory. Surface Mapping of a cross section of the stones showed presence of Si up to more than 100  $\mu\text{m}$  deep for polysiloxane based product. That is not the case for silicone based product. A more homogeneous distribution was also observed for the polysiloxane based product.

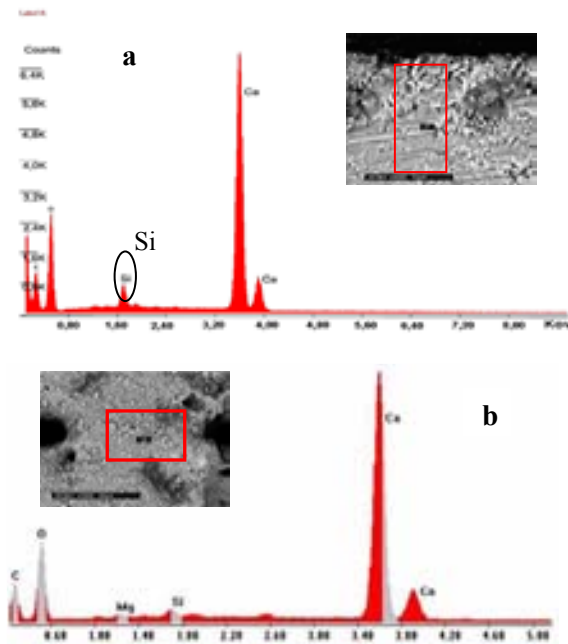


**FIGURE 8.** EDX of the cross section of rock treated: a) polysiloxane base; b) silicone base.

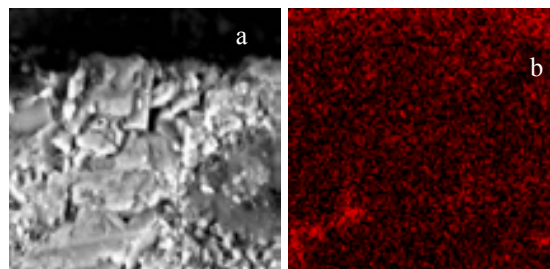


**FIGURE 9.** Stone treated polysiloxane. a) Zone mapping with EDX silicon in cross section, b) mapping of silicon in cross section.

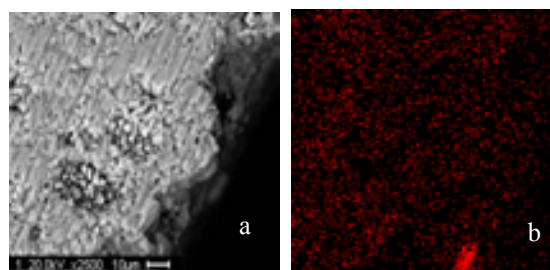


**FIGURE 10.** Stone treated silicone. a) Zone mapping with EDX silicon in cross section, b) mapping of silicon in cross section.

TABLE 1. Visual diagnosis 18 month after treatment.

Hidrofuge	Chances in color		Rugosity		Growth Biological organisms		Crust		Patinas	
	yes	no	yes	yes	yes	no	yes	no	yes	no
Polysiloxane		x		x		x		x		x

TABLE 2. Capillary absorption results test.

Surfaces	Absorption coefficient ( $\text{kg/m}^2\text{s}^{0.5}$ )			
	Yard North		San Francisco Square	
	4 month	18 month	4 month	18 month
Untreated stone	0,162	0,0924	0,202	0,320
Stone treatment with polysiloxane base	0,0046	0,0046	0,0047	0,0046

TABLE 3. Statistic results absorption by partial immersion test.

Systems	Significance level $P < 0,05$	Significant differences
Stone – Silicone Base	$P = 0,45356$	No
Stone – Polysiloxane Base	$P = 0,0089$	Si
Silicone Base – Polysiloxane Base	$P = 0,0353$	Si

TABLE 4. Aleatory statistical design results.

Source	Square sum	g.l	Variance	$R^2$	Fcal.	Ftab
$\alpha$	51,58	2	25,9	0,59	6,61	$F_{\text{tab } 3,4} = 6,59$
$\beta$	19,6	2	9,8	0,22	2,49	$F_{\text{tab } 3,4} = 6,59$
residue	15,7	4	3,92	0,18	-	-
Total	87,1	8	-	-	-	-

TABLE 5. Statistical results obtained.

Systems	Significance level $P < 0,05$	Significant differences
Stone – Silicone Base	$P = 0,06$	No
Stone – Polysiloxane Base	$P = 0,085$	No
Silicone Base – Polysiloxane Base	$P = 0,802$	No

TABLE 6. Aleatory statistical design results.

Source	Square sum	g.l	Variance	$R^2$	Fcal.	Ftab
$\alpha$	101,7	2	50,8	0,69	11,54	$F_{\text{tab } 3,4} = 6,59$
$\beta$	8,8	2	9,15	0,24	2,08	$F_{\text{tab } 3,4} = 6,59$
residue	36,6	4	4,4	0,06		
Total	147,1	8	-	-		

## ACKNOWLEDGMENTS

This work was possible thanks to the cooperation of the Director of the Basilica and Convent of St. Francis of Assisi, Ms. Gertraud Ojeda. We are grateful to technicians and Julia Mellor Eva González Pérez Acosta.

## REFERENCIAS

1. D. Taboada, *El templo encantado*. OPUS HABANA, Vol. III, No. 3-4, 1999, pp. 4-15.
2. N. Schiavon, G. Chiavari. D. Fabbri, *Environmental Geology* **46** (2004) 448-455.
3. F. Monna, et.al., *Atmospheric Environment* **42** (2008) 999 –1011.
4. M. Pérez, *Ensayos y experiencias de alteración en la conservación de obras de piedra de interés histórico artístico*. Centro de Estudios Ramón Araces, Madrid, 1990.
5. P. Maravelaki-Kalaitzaki, et.al., *Progress in inorganic coatings* **57** (2006) 140-148.
6. Tsakalov, P. Manoudis, I. Karapanagiotis, I. Chryssoulakis, C. Panayiotou, *Journal of Cultural Heritage* **8** (2007) 69-72.
7. I. Gorchakov, *Materiales de la construcción*. Ed. Mir, Moscú, 1984.
8. V. Cnudde, et.al., *Engineering Geology* **103** (2008) 84-92.
9. Wagner. *El tubo Karsten un sistema sencillo para determinar la absorción e humedad por parte de los materiales de construcción*. Universidad de Chile, Santiago, 2000.
10. Norma ISO 15148:2002: *Hygrothermal performance of building materials and products- Determination of water absorption coefficient by partial immersion*.
11. Norma ASTM E96. *Test methods for water vapor transmission of materials*.
12. Norma ISO 12571. *Hygrothermal performance of building materials and products- Determination of hygroscopic sorption properties*.
13. P. Coremans, *Clima y microclima. La conservación de los bienes culturales*. UNESCO, 1969.

## **Dissolution of Traditional Mortars under Artificial Rain Conditions: A Laboratory Test.**

J. Reyes<sup>1</sup>, F. Torres<sup>1</sup>, I. Ché<sup>1</sup>, F. Corvo<sup>1</sup>, T. Pérez<sup>1</sup>, H. Bravo<sup>2</sup>, P. Sánchez<sup>2</sup>,  
D. Aguilar<sup>3</sup> and P. Quintana<sup>3</sup>

<sup>1</sup> *Centro de Investigación en Corrosión, Universidad Autónoma de Campeche, MEXICO.  
e-mail: javreyes@uacam.mx*

<sup>2</sup> *Centro de Ciencias de la Atmòsfera, Universidad Nacional Autónoma de México MEXICO.*

<sup>3</sup> *Centro de Investigación y estudios Avanzados-Unidad Mérida, MEXICO.*

**Abstract.** In tropical climates, calcareous materials are very susceptible to dissolution due to the effect of rain. Nevertheless, because of degradation effects are visible after long term periods, there is of particular interest for authorities and conservationist to develop artificial dissolution studies under laboratory conditions to make a fast and comprehensive evaluation of the phenomena. This study focused in determine dissolution rate of calcareous mortar specimens under accelerated conditions. Artificial rain water was prepared based in 1997 wet precipitation data record of San Francisco de Campeche City, simulating pH and ionic composition of more acidic event. Artificial rain was irrigated over 5 x 5 x 1 cm specimens simulating six year of exposure. The dissolution rate was determined by Ca<sup>2+</sup> quantification using High Performance Liquid Chromatography (HPLC) and by gravimetric assay. Mortars formed with slake lime, sand and two types of carbonate clay marls (known as sascab), were tested. Dissolution rate of this material was related to their content of clays and physic-mechanical properties.

**Keywords:** Rain dissolution, colonial buildings, mortar, environmental test.

### **INTRODUCTION**

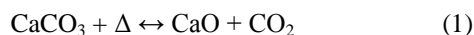
When Spanish arrived to America, calcareous materials were the main construction material systematically used by Mayan architects to erect their majestic cities and ceremonial centers. Spanish used the high availability of these materials to construct civilian, religious and military buildings that remain until now (Figure 1).

In Campeche traditional lime mortar (also called stucco), have been used to join rocks, to construct masonry structures and to cover the walls of the buildings [1].



**FIGURE 1.** Military masonry construction at San Francisco de Campeche City.

The binding material employed during mortar preparation is lime. Lime is produced by calcareous stone burning at the temperature of 900 °C, in the so called lime cycle [2]. During the process, carbon dioxide (CO<sub>2</sub>) and dehydrated lime (CaO) is produced according the next reaction:



Dehydrated lime is constituted by irregular fragments that produce an exothermic reaction when it is mixture with water. As a consequence a white paste with different grade of workability is formed, according the amount of added water. In order to favor best mechanical properties, several aggregates like sand, grinded stone or clays materials like sascab can be used. Sascab is a not consolidate calcareous substrate widely distributed along Yucatan Peninsula. It is a mineral clay marl traditionally employed since pre-Hispanic period in Campeche for building construction due to their high plasticity that gives to the mortar excellent mechanical properties [2]. During the hardness, lime mortar is carbonated by atmospheric CO<sub>2</sub> according to the next reactions:



Carbonation occurs from the surface to inside the mortar structure. It lets the conservation of mortar internal humidity, something that favored a more flexible mechanical performance. At the time, the mortar conform a calcium carbonate crust with similar properties of the original stone [3].

Because of their origin, lime/sascab mortar mixture are susceptible to the same degradation process suffered by limestone. Nevertheless because of their highest porosity it occurs at a shorter time. In tropical climates, the main degradation factor involved in mortar degradation mechanisms is water in form of condensate vapor, rainfall or driven by capillarity [4, 5].

Water penetrates into porous structure dissolving binder compounds, also results an efficient transport medium for salts and atmospheric pollutants that affect the internal structure of mortars. Moreover, when atmospheric water reacts with gases like carbon dioxide (CO<sub>2</sub>), sulfur dioxide (SO<sub>2</sub>), or nitrogen oxides (NO<sub>x</sub>), it acquires acidic properties and form acid rain [6].

Acidic rain is one of the most aggressive degradation factors for calcareous materials as have been observed along the world [6, 7, 8, 9]. Recent studies demonstrate that acid rain is a phenomenon that eventually appears in several sites of Campeche State, including the archeological area of Calakmul

and San Francisco de Campeche City (5, 10). Both places are included by UNESCO into their cultural heritage list.

The effects of rainfall are palpable in long periods, authorities and institutions related with the protection of Campeche's Cultural Heritage, are interested in the development of fast methodologies to study in short time the complex mechanisms of degradation that affect the historic building in the state as a consequence of their interaction with rainfall. In this order, several authors had recommended the use of climatic chamber to obtain recession rate of calcareous material [11, 12, 13].

This study shows the results of lime/sascab mortar coupons recession rate obtained after submitting the coupons to the effect of artificial acid rain prepared according to the pH value observed during the 2007 acid rain campaign carried out at San Francisco de Campeche City.

## MATERIALS AND METHODS

### Sample preparation

Mortar coupons of 5x5x1 cm were made by using four proportion of sascab and slike lime mixture (Table1). Slike lime was fabricated following traditional procedures burning limestone by using tropical woods. Sascab was obtained from two mines located at Pich and Dzibilnocac (DBZ) towns. These locations are the traditional source of sascab used during conservation works of Colonial and pre-Hispanic building at Campeche State. The coupons were coded according their origin: PICH or DBZ followed by the suffix A, B, C or D corresponding to the proportion.

### Mortar samples characterization

Mechanical properties like density, water absorption percentage, porosity and uniaxial compression resistance was measured following standard procedures [14, 15]. On the other hand, mineral composition of sascab was obtained in a Bragg-Brentano Geometry X-ray diffractometer (Siemens D5000). The equipment operated with a CuK $\alpha$  monochromatic radiation ( $\lambda = 1.5416 \text{ \AA}$ ), with operational conditions of 25 mA and 35 kV, step size of 2°/2 $\Theta$ /min in the 2-60° 2 $\Theta$  range.

### Artificial acidic rain water formulation

Artificial acid rain water formulation was prepared considering the ponderated value of pH and the ionic composition of rain water collected by using and automatic dry/wet precipitation collector (Aerochem

Metrics modelo 301) from January to December 2007.

Sampling unity was located at the back roof terrace of INAH-Campeche Center building at the historic area of San Francisco de Campeche City. The analysis of rain samples was carried out by High Performance Liquid Chromatography equipment (HPLC, Waters 515). Water carbonate content was measured according standard procedure [16]. A stoichiometric adjusted was carried out from data record reported in Table 2 in order to determine type and quantity of salts that were included in artificial acid rain formulation. The pH was adjusted until final value of 4.9 by using sulfuric acid (0.1 M).

This value corresponds to the lower pH data registered during the rain water collecting campaign. The resulting solution conductivity was 20  $\mu$ S.

**TABLE 1.** Sascab and slike lime proportion used during mortar preparation.

Code	Slike Lime (g)	Sascab (g)	Proportion
A	375	225	3:2
B	450	150	3:1
C	225	375	2:3
D	150	450	1:3

### Environmental test

The experiment was carried out simulating 6 years of natural exposition. Under test condition a volume of 2.06 L simulate a year of natural exposition, corresponding to the total precipitation obtained during 2007 campaign at San Francisco de Campeche City divided by the exposition area of the coupons (0.0025 m<sup>2</sup>).

Figure 2 shows a scheme of the environmental chamber employed during the study. Medium temperature of 24 °C and relative humidity of 75 % was maintained into the chamber during the test (I and H). Triplicate coupons of each mortar formulation and an acrylic blank was collocated at the sample support (F) and irrigated with artificial acid rain pumped from A to B deposits and then distributed by a manifold (D) until coupons exposition surface area. Water run-off

was collected in a high density polipropilene deposits (G).

The effluent was characterized by pH, conductivity and calcium ion content (Ca<sup>2+</sup>), the last one by using an HPLC equipment. On the other hand, loss mass in mortar samples was determined by gravimetric assays in an electronic balance (Metler Toledo AB204-S/).

## RESULTS

Table 3, shows the results of physical and mechanical properties measured in mortar samples. Figure 3 show the diffractograms corresponding to Pich and Dzibilnocac sascab employed during mortar preparation.

According to the results, mortar samples show low density, high porosity and low mechanical resistance. C formulation (2/3 proportion), shows the better performance: the higher mechanical resistance and the lower water absorption percentage. On the other hand, mortar made with sascab from Dzibilnocac, show the best mechanical resistance.

Many factors like type of aggregate, particle size distribution, type of binder, clay content and drying time, have marked influence in the mechanical performance of the mortars. In this sense, lime particles have high superficial are (about 20 m<sup>2</sup> per gram), then it presents high water absorption capacity.

**TABLE 3.** Physical and mechanical properties of mortar samples.

Sample	Density (g/cm <sup>3</sup> )	Porosity (%)	Water absorption (%)	Uniaxial mechanical compression resistance (Kg/cm <sup>2</sup> )
PICH-C	1.35	49.13	42.12	13.18
PICH-D	1.21	54.44	47.18	11.22
DZM-C	1.38	48.00	31.17	16.25
DZM-D	1.26	52.52	38.12	12.22

**TABLE 2.** Ionic composition of rain water collected at San Francisco de Campeche City during 2007 campaign.

	pH	Na <sup>+</sup> (ppm)	NH <sub>4</sub> <sup>+</sup> (ppm)	K <sup>+</sup> (ppm)	Mg <sup>2+</sup> (ppm)	Ca <sup>2+</sup> (ppm)	Cl <sup>-</sup> (ppm)	NO <sub>3</sub> <sup>-</sup> (ppm)	SO <sub>4</sub> <sup>2-</sup> (ppm)	HCO <sub>3</sub> <sup>-</sup> (ppm)
Ponderated	5.90	1.62	0.10	0.29	0.16	1.09	2.54	0.61	1.72	1.30
Minimun	4.97	0.26	0.01	0.01	0.01	0.31	0.55	0.01	0.01	0.50
Maximun	7.96	18.80	2.09	4.24	3.36	10.882	40.64	3.81	15.12	8.80

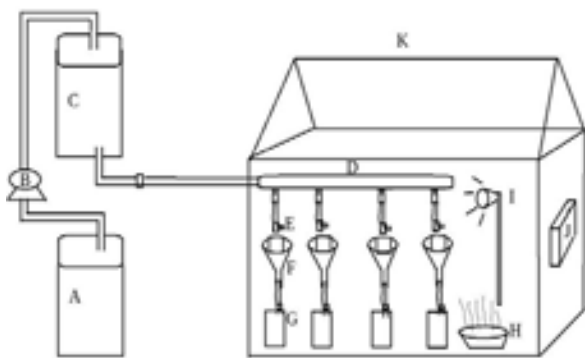


FIGURE 2. Scheme of the environmental chamber employed during the study.

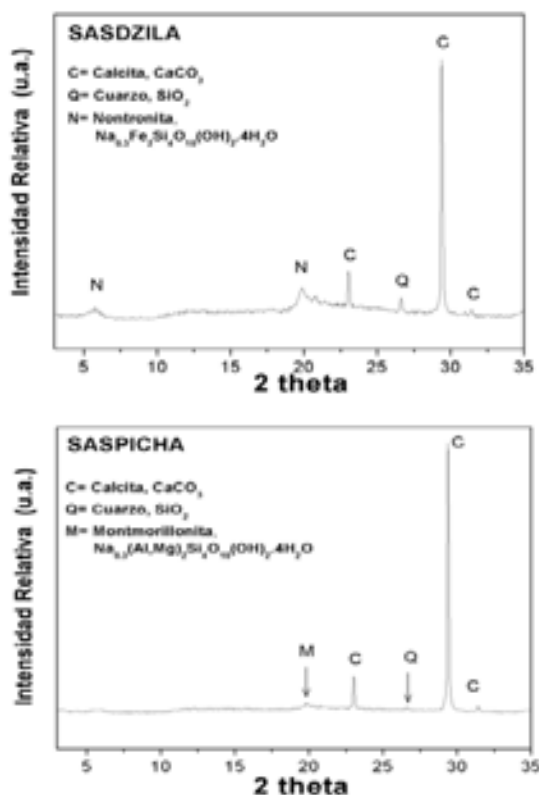


FIGURE 3. XRD spectrum from Dzibilnocac (SASDZILA) and Pich (SASPICHA), sascab type employed during mortar elaboration.

Also, the presence of clays in the mortar cans increase water retention capacity. Winnefeld and Bötger (2006) reports that when water is attracted between laminar surface of clays, it origins an internal pressure that have as a consequence the reduction of material mechanical properties up to 50 % [17].

As XDR analysis indicate, both sascab (the carbonate clay marls used during mortar preparation),

content clays like monmorillonite or nontronite (Figure 3).

The analysis of the effluents from the mortar samples run off indicate an increase in the pH and electric conductivity value in all the samples (Figure 4). The effluents from mortar samples elaborated with sascab from Pich and with D formulation shows the highest increase in these values.

Figure 5 shows the differences in the quantification of the recession rate by  $\text{Ca}^{2+}$  content in the effluent and the gravimetric method after a year of simulated exposition test.

While the tendency in the recession rates is the same, HPLC only quantify soluble  $\text{Ca}^{2+}$ . Gravimetric method measures difference of mass that include soluble  $\text{Ca}^{2+}$  and calcareous particles detached by erosive mechanisms during water flow under mortar surface.

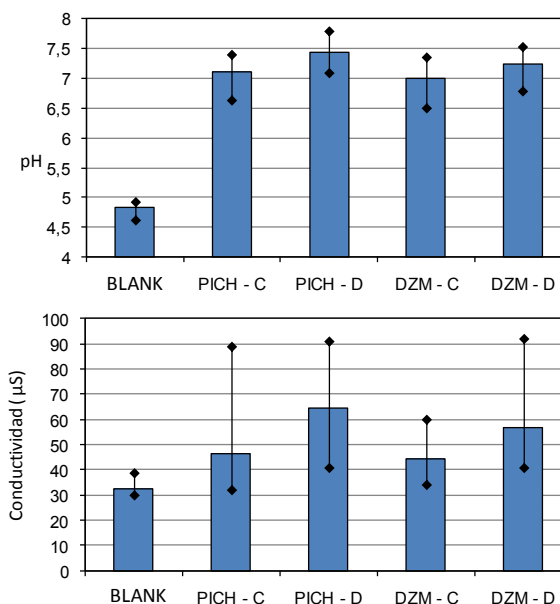


FIGURE 4. Variation of pH and electric conductivity according different mortar formulation.

Table 4 shows the recession rate, after six year of accelerated exposition test under artificial acid rain condition. C type mortar formulation presents lower recession rate than the D type. The highest content on lime in C type is related with these results. Lime contributes to improve the union between aggregate grains.

Other factor involved in highest recession rate of mortar is the clay content of aggregates like sascab [17]. Both sascab types used during this study content clays minerals, nevertheless mortars elaborated with Pich type shows higher recession.

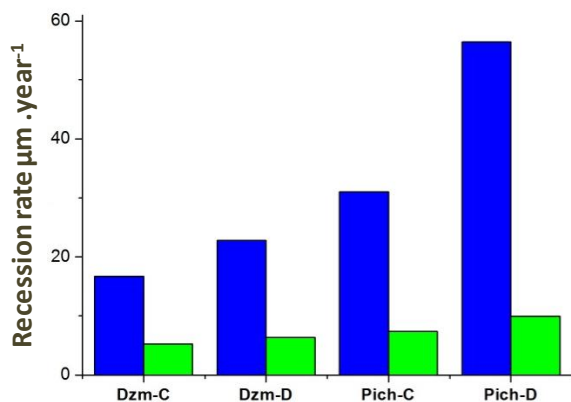
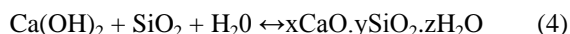


FIGURE 5. Quantification differences between gravimetric mass determination and HPLC analysis of Ca<sup>2+</sup> ion.

TABLE 4. Recession rate obtained after six year of simulated exposition under environmental chamber test conditions.

Sample	Mass loss (mg)	Recession rate µm·year <sup>-1</sup>
PICH - C	277	13.67
PICH - D	885	48.76
DZMC - C	173	9.53
DZM - D	342	18.09

XRD analysis indicates highest quartz content in the sascab from Dzibilnocac. Under certain conditions, quartz gives more durability to the mortar exposed to the environmental condition due to pozzolanic reaction [18]:



This reaction occurs by the dissolution of crystalline silicon compounds with grain size less than 5 µm under alkaline media.

Di- and tricalcic silicates appears similar to those obtained during Portland cement hardening. The benefits of this reaction are: a continue reduction in plasticity and water absorption capacity, effective increasing in grain size, workability, cut resistance and rigidity of the mixture, any way a better mechanical performance.

## CONCLUSIONS

The proportion of the mixtures is determinant in the physical and mechanical properties, like density, porosity, water absorption and compression resistance. Besides, the both bank of materials: Dzibilnocac and Pich showed particular mineral composition that influences the mortar properties.

The clay content in sascab can react as pozzolanic material sealing porosities. It has a determinant role in the durability properties of mortars, resulting mortar prepared with Dzibilnocac type more resistant than Pich ones.

Accelerated essays using simulated conditions provide valuable information about the dissolution of mortars in relatively short time. Also this design let identified the more resistant formulation under environmental chamber experimental conditions. While the experiment proposed in this paper do not represents the real condition of mortar dissolution in natural conditions, the results obtained during the study, can be considered as a first approach to be taken account to the design of strategies for the conservation of built heritage.

## ACKNOWLEDGEMENTS

This research was possible thanks to the support of CONACYT-46434 project and the collaboration of Calakmul Project from Campeche-INAH Center (Mexico). Special thanks to the collaboration of archeologists Omar Rodriguez and Ramón Carrasco .

## REFERENCES

1. C. M. Huitz. *Fortificaciones de San Francisco de Campeche. Arquitectura, usos, arqueología y restauración*. Diario de Campo. 73 (2005) 22-25.
2. H. Ramírez, R. Pérez, H. Díaz, *El cemento y el concreto de los Mayas*. Ciencia Ergo Sum. 6 No. 3 (1999) 275-284.
3. C.G. Solís, P. Quintana, F. Bautista-Zúñiga, F. "La identificación de materiales arcillosos y pétreos utilizados en la manufactura del friso modelado en estuco de la SUBII-C1 de Calakmul, a través de análisis de difracción de rayos X" in *La Ciencia de los Materiales y su Impacto en la Arqueología*, Vol. III, J. Arenas et al. eds., Editorial Lagares, México, 2006, pp. 237-252.
4. J. Reyes, F. Torres, M. Miss, F. Corvo, H. Bravo, P. Bartolo-Pérez, J.A. Azamar-Barrios, Effect of the environment on the degradation of Colonial and Prehispanic buildings in Campeche, Mexico. *Environmental Degradation of Infrastructure and Cultural Heritage in Coastal Tropical Climate*, 2009, 115-142.
5. F. Corvo J. Reyes, C. Valdes, F. Villaseñor, O. Cuesta, D. Aguilar, P. Quintana. *Water, Air, Soil Pollut.* **205** (2010) 359-375.

6. H. Bravo, R. Soto, R. Sosa, P. Sánchez, R. Torres, M. Granada, *Atmos. Environ.* **34** (2000) 1197-1204.
7. P. Baedecker, M. Reddy, K. J. Reimann, C. A. Sciamarella. (1992). *Atmos. Environ.* **26** No. 2 (1992) 147-158.
8. M. Reddy. *Earth Surface and Landforms.* **13** (1988) 335-354.
9. R. A. Livingston. *Graphical methods for examining the effects of acid rain and sulfur dioxide on carbonate stone* in VII International Congress on Deterioration and Conservation of Stone. Lisbon, Portugal, 1992.
10. O. Quirate. *Variaciones de la acidez de lluvia durante 2006 y 2007 en la ciudad de San Francisco de Campeche y la Reserva de la Biosfera de Calakmul (Zona Arqueológica)*. Dissertation work. Facultad de Ciencias Químico Biológicas. Universidad Autónoma de Campeche, Campeche, México, 2009.
- 11 H. Bravo, R. Soto, R. Sosa, P. Sánchez, *Efectos de la lluvia en el material constituyente de monumentos Mayas mexicanos*. Ing. Inv. Tec. (2003) 195-205.
12. F. Lipfert, *Atmos. Environ.* **23** (1989) 425-429.
13. L. Tecer, *Water, Air, Soil Pollut.* **114** (1998) 1-12.
14. ASTM. *Standard method of test for absorption and bulk specific gravity of natural building stone*. American Society for Testing Materials, C97-47, Part XVI, 1985, pp 1-3.
15. NMX-C-164-1986. *Industria de la construcción – agregados – Determinación de la masa específica y absorción de agua del agregado grueso*. Norma Oficial Mexicana, 1986.
16. NMX-AA-036-SCFI-2001. *Análisis de agua - determinación de acidez y alcalinidad en aguas naturales, residuales y residuales tratadas*. Norma Oficial Mexicana, 2001.
17. F. Winnefeld, K. G. Bötger, *Mat. Struct.* **39** (2006) 433-443.
18. E. Quintana. *Relación entre las propiedades geotécnicas y los componentes puzolánicos de los sedimentos pampeanos*. PhD Thesis. Universidad Nacional de Córdoba, Argentina, 2005.



**2nd Latin-American Symposium on Physical  
and Chemical Methods in Archaeology, Art and  
Cultural Heritage Conservation.  
Selected Papers  
Archaeological and Arts Issues in Materials  
Science**

was printed by

González Offset S.A. de C.V.  
Calle 35 No. 244  
Col. Jardines de Santa Clara  
Ecatepec, Edo. de Mex. C.P. 55450  
MEXICO

December 17, 2010

Offset Printing on Bond paper 75 g/m<sup>2</sup>  
Letter size (28 x 21.5 cm)  
Hot melt bound  
Cover printed on coated paper (Couché) 250 g/cm<sup>2</sup>  
plasticized dull

Printing of 200 copies  
more leftovers